HARVARD UNIVERSITY
Graduate School of Arts and Sciences

DISSERTATION ACCEPTANCE CERTIFICATE

The undersigned, appointed by the

Division of Medical Sciences

Committee on Immunology

have examined a dissertation entitled

Neutrophil extracellular traps in thrombosis and inflammation

presented by Kimberly Lindsay Martinod

candidate for the degree of Doctor of Philosophy and hereby certify that it is worthy of acceptance.

Signature: _____

Typed Name: Dr. Harold Dvorak

Signature: _____

Typed Name: Dr. Francis Luscinskas

Signature: _____

Typed Name: Dr. Katya Ravid

_____

Dr. Michael Carroll, Program Head

Date: August 27, 2014

_____

Dr. David Lopes Cardozo, Director of Graduate Studies

Neutrophil extracellular traps in thrombosis and inflammation

A dissertation presented

by

Kimberly Lindsay Martinod

to

The Division of Medical Sciences

in partial fulfillment of the requirements

for the degree of

Doctor of Philosophy

in the subject of

Immunology

Harvard University
Cambridge, Massachusetts

August 2014

Neutrophil extracellular traps in thrombosis and inflammation

Abstract

Neutrophil extracellular traps (NETs), chromatin released by activated neutrophils, were first described for their antimicrobial properties. NETs have a backbone of DNA and histones lined with microbicidal proteins such as neutrophil elastase. NET release has pathological consequences, particularly within blood vessels where NETs can trap red blood cells and platelets, thus contributing to thrombosis (Chapter 1-Overview). NET formation (NETosis) is an active and coordinated biological process involving many enzymatic components. One enzyme in particular, peptidylarginine deiminase 4 (PAD4), citrullinates histones and is required for chromatin decondensation during NETosis. Neutrophils from PAD4-deficient mice are unable to form NETs. We obtained these mice from our collaborator Dr. Yanming Wang, and thus were able to compare $PAD4^{-/-}$ mice to wild-type (WT) mice in mouse models where NETs are formed. These studies have allowed for investigation of the biological relevance of PAD4 and NETs in vivo in thrombotic and/or inflammatory disease.

This dissertation focuses on mouse models of deep vein thrombosis and of sepsis. In venous stenosis, thrombosis is initiated by restricting blood flow in the inferior vena cava (IVC). Here, $PAD4^{-/-}$ mice were greatly protected from thrombus formation (Chapter 2). Leukocyte rolling and platelet plug formation in response to vessel injury were unaffected, indicating that endothelial and platelet activation occurred normally in these mice. The mice did not exhibit any defects

in hemostasis, and could be induced to produce deep vein thrombi by infusion of WT neutrophils that formed NETs as a part of the thrombus scaffold. Because there is potential to develop anti-NET therapies in thrombosis, I investigated if NET-deficiency would render mice immunocompromised (Chapter 3). $PAD4^{-/-}$ mice had similar mortality in the cecal ligation puncture model, and they were protected from shock in an LPS sepsis model where NETs are released in the absence of live bacteria. Therapies aimed at NET prevention or destruction would likely be beneficial without compromising host immunity. Thus, in summary, studying PAD4-deficient mice has revealed the impact of NETs in thrombotic/inflammatory disease and identified PAD4 as an attractive therapeutic target.

TABLE OF CONTENTS

I dedicate this dissertation to my parents, Serge and Sylvie Martinod,

who have encouraged and supported me every step of the way.

Acknowledgements

I met Denisa at one of the first-year Tutorial Dinners, where she talked about this curious phenomenon where neutrophils threw out their DNA like a spider web. From that moment on I was hooked and knew that's what I wanted to study. Most people say that choosing a lab is a tough decision, but for me it was an easy one as I knew I had found a great mentor in Denisa. Thanks for challenging me, giving me independence with my projects, and supporting me throughout the past few years. You truly lead by example, and if I'm able to become even half the scientist you are, I'd consider that a huge success.

One of Denisa's greatest strengths is her ability to hire nice people who are also great scientists. Thanks to all current and former Wagner lab members, in particular Georgette, Melanie, Christine, Simon, Marilena, Carla, Maureen, Naamah, Jaymie, and Steve. Georgette, Melanie, and Christine have been my scientific mentors in the lab and I appreciate their patience talking through pretty much every experiment I've planned and making sure that I didn't get too far off topic. I couldn't have gotten nearly half as much work done without the help of Maureen with her uncanny ability to section tissue at lightning speeds, and her willingness to let me explain the rationale behind the experiments I've done. Thanks most of all to Steve for putting up with me all of these years with my questions, for being able to fix anything at a moment's notice and for keeping the lab running efficiently.

I'm greatly appreciative of Lesley for the countless hours she's spent proofreading pages upon pages of manuscripts, grants, and abstracts and of

Shirley, who is a great listener and is always excited to see images of neutrophils throwing NETs.

I can't thank Charlie Serhan enough, who took a chance hiring an inorganic chemist straight out of undergrad as a lab technician. I couldn't have asked for a better place to see what biomedical research is all about and I would have gone a very different graduate school path if it wasn't for my time in his lab. The rigor with which he approaches science will always be engrained in me.

The fellows in the Serhan lab, Matt, Lisa, Lucy, Nan, and Gabby, now all with their own faculty or industry positions, were always willing to explain what they were working on or what approach they were taking to tackle a question. I'm especially grateful to have met Padmini, Sriram, and Antonio, in addition to being great scientists, have become lifelong friends. Padmini, who deserves a page all to herself, is one of the most amazing and inspiring people that I know. Thanks for just being you.

My first year of graduate school was a tough one, diving into hard-core immunology classes with very little background in biology. I couldn't have made it through all of the material I needed to learn, from the very basic cell biology to cutting edge immunology (I'm still learning all those T cell subsets though…) without the help of my Immunology program classmates. In particular I need to thank Teja, whose positive attitude on research and on life kept me motivated.

I want to thank the members of my DAC for keeping me focused and also pushing me to learn as much as possible in the process, and my Defense Committee for taking the time to review this dissertation. Thanks especially to

Sue Perkins, who keeps the Immunology Program running smoothly, and makes sure we meet all of our deadlines. It was always nice to have a smiling face to turn to all of these years.

I appreciate all of the support I've had from my parents. Although they had some initial reservations when I decided to take 2 years off from school after college to work in a lab, hopefully now they realize that their influence is exactly what led me down this path, to not accept a future doing work I didn't enjoy and to reach for studying what would truly make me happy and keep me challenged. I thank my Dad who has put up with all of my biology questions and my mom who has been there every step of the way, literally, on the phone listening to even the most mundane details of my day. To my sister, Kylie, I'm so glad you're starting on your own path to become a biologist. I have no doubts that you'll be a great scientist.

And last but certainly not least, I'd like to thank Dan who has been by my side for all of my graduate school years. Your encouragement to take a risk and explore a new field when I didn't have a clue what I wanted to do with my life right after graduating from college means so much. I definitely wouldn't be where I am today without your support. Thanks for putting up with all the long hours and always being there to talk things through.

Chapter 1

Overview and Introduction

This chapter contains one published manuscript:

Martinod K and Wagner DD. *Thrombosis: tangled up in NETs*. Blood. 2014 May 1; 123 (18): 2768-76. Epub 2013 Dec 23. PMCID: 4007606.

Section 1.1: Thesis Overview and Attributions

Overview

The original publication observing neutrophil extracellular traps (NETs) came out in *Science* just over 10 years ago, and described a novel antibacterial function of neutrophils[1]. NETs were defined as extracellular DNA strands also staining positive for histones and neutrophil elastase, with an ability to physically trap and kill both Gram-positive and Gram-negative bacteria[1]. These structures were studied extensively in response to many different pathogens, and were later also found to interact with fungi and viruses[2,3]. The process of NET formation after initial stimulation involves the decondensation of chromatin, dissolution of the nuclear membrane, and expulsion of chromatin into the extracellular environment[4]. NETosis is an active, specific cell biological process rather than a passive form of cell death[5] and much remains to be studied about the molecular mechanisms by which NETs occur, as well as the consequences of their release.

Neutrophil hyperactivation has detrimental effects on healthy bystander tissue and thus neutrophils are implicated in many inflammatory disease pathologies[6,7]. As one can imagine, the release of highly charged histones, serine proteases, and myeloperoxidase concentrated on DNA fibers into the extracellular space can contribute to such pathologies. Indeed, aberrant NET production has been implicated in preeclampsia[8], autoimmune disease[9], cancer[10-12], cardiovascular disease[13,14], thrombosis[15,16], sepsis[17], and others[18-21]. Our lab observed that NETs can bind platelets and red blood cells (RBCs) in whole blood and therefore contribute to thrombosis[16]. Since venous thrombi are

RBC rich, the lab looked for and found NETs in a baboon model of deep vein thrombosis[16]. We found similar evidence of NETs being formed in the mouse inferior vena cava (IVC) stenosis model of DVT ([15], Appendix A-3), and found that DNase, which can degrade NETs, prevented thrombus formation. We have since then also identified NETs during in maturing human thrombi in patients suffering from venous thromboembolism ([22], Appendix A-4).

In the same month that our lab's paper defining the role of NETs in thrombosis was published[16], a key study came out in the Journal of Experimental Medicine describing the essential role of the enzyme peptidylarginine deiminase 4 (PAD4) during NET formation[23]. PAD4 acts by deiminating arginine residues to citrulline. This PAD enzyme is unique as it contains a nuclear localization signal and therefore can enter the nucleus and modify histones. The citrullination of histone tails leads to the decondensation of chromatin that occurs extensively in NETosis. Dr. Yanming Wang's group at Pennsylvannia State University generated mice deficient in PAD4, and showed that these mice not only had strongly reduced chromatin decondensation, but also that they were completely unable to release NETs[23]. They were able to elegantly show that NETs could help contain a bacterial infection by using a mutant form of Group A streptococcus which did not secrete a nuclease that would degrade NETs, thus showing a potential role for NETs in vivo. This thus represented the first tool which could be used to specifically study the role of NETs in vivo.

Our lab obtained PAD4$^{-/-}$ mice from Dr. Wang and began studying them in mouse models in which we had evidence of NETs being formed. This genetic

approach therefore allowed us to study the importance of NETs in various disease pathologies. With Melanie Demers in the lab, we developed a microscopy-based approach to quantify NET formation in vitro by isolating peripheral blood neutrophils, stimulating them, and then staining for the histone modification produced by PAD4, citrullinated histone H3 (H3Cit)[10,24]. This method was applied to identify cells that were beginning to undergo NETosis by isolating neutrophils from healthy or tumor-bearing mice, performing cytospins, and immunostaining for H3Cit. I developed an unbiased thresholding method to quantify cells with hypercitrullinated histones using ImageJ, which we now also use routinely to quantify baseline NET-primed cells in whole blood. We optimized this technique further as an immunohistological method of identifying NETs in various tissues, staining for neutrophil membrane markers, H3Cit and DNA in association. This was used to identify NETs in transfusion-related acute lung injury[18], in deep vein thrombi from mice ([15], Appendix A-3, Chapter 2) and humans ([22], Appendix A-4, Chapter 1), as well as in myocardial ischemia/reperfusion injury[14], cancer ([10], Appendix A-5, and unpublished results), and skin wounds (Appendix A-6, and unpublished results), sepsis (Chapter 3). I have also developed a method to detect the presence of NETs in plasma by performing Western blots for H3Cit ([10,11], Chapter 3). These methods were helpful in identifying NETs in mouse models of various inflammatory diseases. We next turned to the PAD4-deficient mice to study the impact of a lack of NET release in these disease models.

There is a growing body of literature that highlights the importance of NETs in pathological thrombosis. In Chapter 1, I provide an overview of what is known about the cell biology of NET production, and how NETs represent an important player in thrombosis. Previous studies using DNase to degrade extracellular DNA showed a highly protective effect of DNase 1 in DVT in mice[15,25]. Chapter 2 shows the phenotype of the PAD4$^{-/-}$ mice in thrombosis models, which nearly completely phenocopies DNase pre-treatment. I therefore proposed that PAD4 is an ideal target for inhibiting NET formation in disease settings, but was wary that such an approach could render subjects more prone to infection. I therefore studied the PAD4-deficient mice in mouse models of sepsis, where the balance between bacterial killing and tissue damage is critical. In Chapter 3, I will describe that NETs are not crucial for host defense in sepsis and may in fact even be detrimental by contributing to endotoxemic shock. This dissertation ends with a discussion section in Chapter 4 providing future directions.

Attributions

I performed and analyzed all experiments presented in this work, unless otherwise noted in the attribution sections of individual chapters. Experiments were designed by my advisor Denisa Wagner and myself with help from Wagner lab members. I wrote the entirety of the main text of the dissertation. Key papers referred to throughout the dissertation, for which I performed experiments and am a co-author, are included in the Appendix of this work for clarity.

Section 1.2.1: Thrombosis: tangled up in NETs

Overview

NETs can entrap platelets and red blood cells, thus contributing to thrombosis. It is now clear that venous thrombi, in addition to known proteinaceous factors such as fibrin, also contain DNA-NETs as an integral component of the thrombus scaffold. This has now been studied in animal models[15,16] and identified to be relevant in human disease[13,22].

After a thorough literature search, Denisa Wagner and I outlined several sections of interest that have either contributed to the lab's 2010 discovery that NETs are important in thrombosis, or resulted from it. There are many aspects of NET formation itself and in the context of thrombosis that remain unknown. We summarize crucial unresolved questions for the field moving forward, and propose how what we've learned could be applied to future therapeutic approaches to either prevent or treat deep vein thrombosis.

Attributions

This was an invited review submitted to Blood in October 2013 and published in December 2013. Denisa Wagner and I reviewed the literature and wrote the manuscript. Figures were reproduced from previously published work from key papers in the field. Figure 1.4 was produced from human thrombus samples generously provided by Richard N. Mitchell, which were immunostained for platelets/neutrophils by Alexander S. Savchenko, and stained for DNA by myself. I took the micrographs and assembled Figure 1.4. Figure 1.5 was kindly

generated by graphic designer Kristin Johnson from a sketch drawn by Denisa Wagner. We thank Siu Ling Wong, Melanie Demers, and Lesley Cowan for careful reading and editing of the manuscript while it was under preparation. We also thank Dr. Paul Kubes and Dr. Charles Esmon for granting us permission to reproduce their figures in our review (Figures 1.1, 1.2).

Section 1.2.2. Thrombosis: Tangled up in NETs

Kimberly Martinod[1,2] and Denisa D. Wagner[2,3,4*]

[1]Immunology Graduate Program, Division of Medical Sciences, Harvard Medical School, Boston, Massachusetts, USA

[2]Program in Cellular and Molecular Medicine, Boston Children's Hospital, Boston, Massachusetts, USA

[3]Department of Pediatrics, Harvard Medical School, Boston, Massachusetts, USA

[4]Division of Hematology/Oncology, Boston Children's Hospital, Boston, Massachusetts, USA

*Correspondence: Denisa D. Wagner, Boston Children's Hospital, 3 Blackfan Circle, Third Floor, Boston, MA, 02115, USA. Ph. 617-713-8300, Fax 617-713-8333, denisa.wagner@childrens.harvard.edu

Abstract

The contributions by blood cells to pathological venous thrombosis were only recently appreciated. Both platelets and neutrophils are now recognized as crucial for thrombus initiation and progression. Here we review the most recent findings regarding the role of neutrophil extracellular traps (NETs) in thrombosis. We describe the biological process of NET formation (NETosis) and how the extracellular release of DNA and protein components of NETs, such as histones and serine proteases, contributes to coagulation and platelet aggregation. Animal models have unveiled conditions in which NETs form and their relation to thrombogenesis. Genetically engineered mice enable further elucidation of the pathways contributing to NETosis at the molecular level. Peptidylarginine deiminase 4 (PAD4), an enzyme that mediates chromatin decondensation, was identified to regulate both NETosis and pathological thrombosis. A growing body of evidence reveals that NETs form in human thrombosis as well and that NET biomarkers in plasma reflect disease activity. The cell biology of NETosis is still being actively characterized and may provide novel insights for the design of specific inhibitory therapeutics. After a review of the relevant literature, we propose new ways to approach thrombolysis and suggest potential prophylactic and therapeutic agents for thrombosis.

Neutrophils are an often underappreciated cell with crucial functions in immunity and injury repair. Because neutrophils are packed with microbicidal proteins and, when activated, generate high concentrations of reactive oxygen species, their ability to kill pathogens comes at a high cost to surrounding tissue. Indeed, when it comes to neutrophils, you certainly can have too much of a good thing. This became even more evident upon the discovery of neutrophil extracellular traps (NETs) by Volker Brinkmann, Arturo Zychlinsky, and colleagues.[1] NETs have been investigated in the context of host defense and also the pathogenesis of several non-infectious diseases. Here we will focus on the role of NETs in thrombosis.

Introduction to NETs

Pathogens can induce neutrophils to release chromatin lined with granular components (such as myeloperoxidase, neutrophil elastase, and Cathepsin G)[1,26], creating fibrous nets with antimicrobial properties, capable of killing both Gram-positive and Gram-negative bacteria.[1] NETs also have the ability to trap and kill fungi[2], are released in viral infections[27], and can sequester viruses.[3] Interestingly, this ability of the host to release extracellular traps in order to protect itself from pathogens is evolutionarily conserved in plants, with root border cells secreting extracellular DNA as part of a defense mechanism against bacterial and fungal infection.[28]

The cell biological mechanisms that allow for NET release are still being characterized. NETosis has been distinguished from apoptosis and necrosis as a

new cell death process.[5] In the Fuchs et al. study, the importance of reactive oxygen species (ROS) via NADPH oxidase was revealed.[5] Because ROS are rapidly cell permeable, addition of exogenous sources of ROS can rescue deficiencies in NADPH oxidase.[5] In the presence of some neutrophil stimuli, ROS may not be needed to form NETs.[29-31] Crucial steps in NETosis were evaluated morphologically in early in vitro studies.[4,5] First, the nucleus loses its characteristic lobular shape and swells. It is now known that the nuclear swelling is due to chromatin decondensation driven by peptidylarginine deiminase 4 (PAD4).[32] PAD4 is a protein citrullinating enzyme that enters the nucleus to modify histones.[32,33] Upon the hypercitrullination of specific arginine residues on histones H3, and H4, there is a loss of positive charge from the transformed arginine residues, and the linker histone H1 and heterochromatin protein 1β dissociate from the nucleosome structure.[33,34] Overexpression of PAD4 results in chromatin decondensation and the release of NET-like structures in cells in vitro that don't normally undergo this form of cell death.[34] Thus, activation of PAD4 is likely the primary driving force in NETosis. Neutrophils from $PAD4^{-/-}$ mice generated by Yanming Wang's group[23] are completely unable to form NETs (Figure 1.1A). Therefore, $PAD4^{-/-}$ mice provide an excellent framework in which to study the role of NETs in vivo.[23,24]

It was proposed that some neutrophil granular enzymes such as neutrophil elastase translocate to the nucleus and help in chromatin decondensation by cleavage of histones.[35] Genetic evidence determining to what

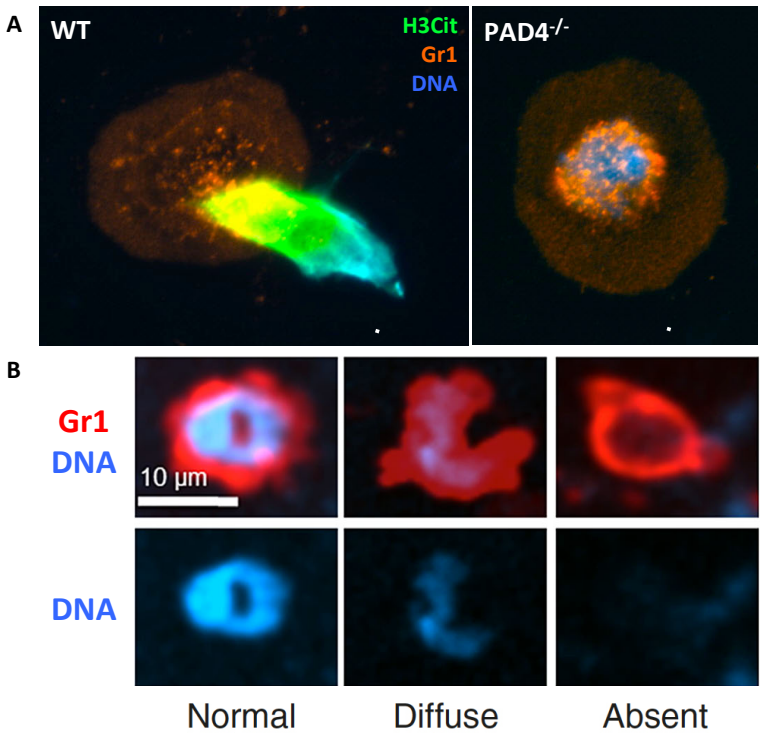

Figure 1.1. NETosis is a regulated process. A. Representative image of a wild-type (WT) or PAD4$^{-/-}$ neutrophil stimulated with calcium ionophore. WT neutrophils undergo histone hypercitrullination (H3Cit, green) and throw NETs, while PAD4$^{-/-}$ neutrophils fail to citrullinate histones, decondense chromatin, or release NETs. Reproduced from Martinod et al. PNAS 2013[24]. Scale bars, 10 µm. B. In response to *Staphylococcus aureus* skin infection, neutrophils can secrete their nuclear contents (right panel) while retaining the ability to crawl and phagocytose, thus "multitasking." Reproduced from Yipp et al. Nat Med 2012 with permission[36].

what extent individual granular proteins contribute to NETosis remains to be established. The serine protease inhibitor Serpin B1 may also regulate NET formation, and it also translocates into the nucleus.[37] The timing of PAD4 activation relative to the above mentioned enzymes' nuclear translocation and its own potential nuclear import still needs to be characterized. Finally, the chromatin network is released into the extracellular milieu.[1,4,5] What happens to the plasma membrane, cytoskeleton, and other organelles during NETosis is not known.

There is likely more than one mechanism of NET release. The process described above takes a fair amount of time (2-4 hours) before NETs are released.[5] Recently, a second mechanism was observed first in vitro and then in vivo using intravital microscopy. Here, the neutrophils rapidly expel NETs (within minutes) in response to live *Staphylococcus aureus*.[36,38] The neutrophil ejects either a portion or all of its decondensed nuclear contents (Figure 1.1B) without releasing the cytoplasmic contents or lysing the plasma membrane[36]. The denucleated neutrophil still retains the ability to crawl and phagocytose bacteria trapped by its own NETs in a highly efficient process called "vital NETosis."[36,39] Large biologically active anuclear fragments of neutrophils were already observed in the 1980s.[40] The mechanism by which nuclear contents are secreted in either process is yet unknown, as are the triggers that induce one form of NETosis over another.

While the beneficial effects of NETs in fighting pathogens were being reported[1,2,41], the pathological nature of NETs rapidly began to emerge. NET

formation was observed in diseases without an obvious microbial trigger such as preeclampsia[8], small vessel vasculitis[42], and systemic lupus erythematosus and its associated nephritis.[43] Defective serum DNases help to drive lupus pathogenesis, resulting in antibody production against self-DNA.[43] Antibodies formed against NET components may promote the pathology of certain autoimmune diseases such as rheumatoid arthritis.[9] In addition, presence of antibodies to neutrophils may induce the formation of NETs such as in transfusion-related acute lung injury.[18]

There could be a benefit of intravascular NET formation in septic conditions where containing an overwhelming bacteremia is likely protective for the host.[41,44] The large quantities of anti-microbial toxic products released with NETs, in particular histones, the main protein component of NETs[26], can contribute to lethality in sepsis.[17] It appears that there is only a fine line between the beneficial and harmful effects of NETs for the infected host.

NETs not only entrap pathogens, they can also bind platelets and red blood cells.[16] Since red blood cell-rich red thrombi are formed in deep veins, it proved fruitful to first look for NETs in deep vein thrombosis (DVT).[16] Indeed, the thrombus experimentally formed in a healthy baboon was full of extracellular DNA (Figure 1.2A). Infection is a risk factor for DVT[45], perhaps through the generation of NETs. The link between NETosis and coagulation was made because of the presence of neutrophil elastase (NE) on NETs. NE inactivates tissue factor pathway inhibitor (TFPI) through cleavage, thus resulting in increased procoagulant activity.[46] Procoagulant activity leads to platelet

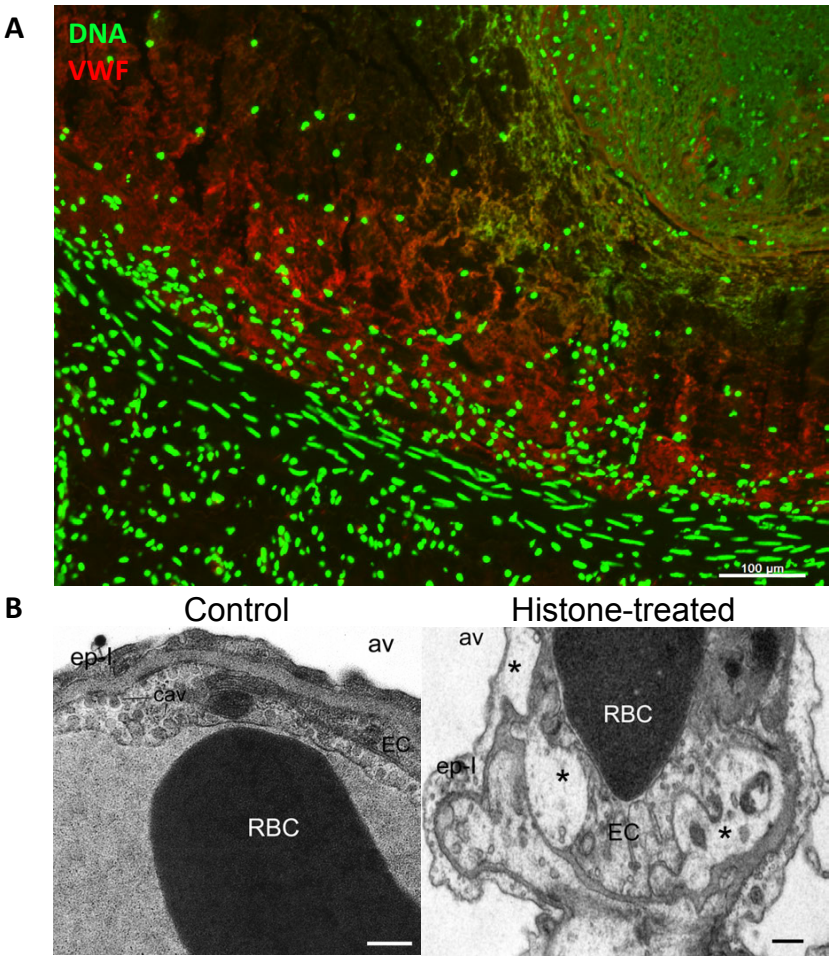

Figure 1.2. NETs are part of deep vein thrombi and histones produce toxicity in vivo. A. A deep vein thrombus was formed in an otherwise healthy baboon by balloon catheterization. The thrombus was excised and analyzed for the presence of extracellular DNA (green) and von Willebrand factor (red), which were found to codistribute. Scale bar, 100 μm. Reproduced from Fuchs et al. PNAS 2010[16]. B. Intravenous histone infusion was detrimental to both endothelium and epithelium, as shown by vacuolization (stars) of these cells in and around the lung capillaries (right). Av, alveolae. Cav, caveolae. Ep-I, type I epithelial cell. EC, endothelial cell. Scale bars, 500 nm. Reproduced from Xu et al. Nat Med 2009 with permission[17].

activation and activated platelets can enhance NET formation[25,41,46], but platelet depletion does not necessarily prevent NETosis.[18]

Nucleic acids, histones and NET enzymes: effects on coagulation

Before the link to NETs was established, nucleic acids and nuclear components were studied individually for their ability to induce coagulation. Nucleic acids activate coagulation[47,48], with RNA binding both Factor XII and XI in the intrinsic pathway. RNA is present in fibrin-rich arterial thrombi,[47] but its origin is not known and whether RNA is released with NETs is still an open question. Also, histones increase thrombin generation[49] in a platelet-dependent manner.[50] Histones activate platelets[16], and platelet activation, in turn, promotes coagulation.[51] Histone infusion leads to formation of platelet-rich microthrombi in a sepsis-like model[17], while also contributing to thrombocytopenia.[52] As noted earlier, infused histones are toxic and lead to endothelial and epithelial cell vacuolization (Figure 1.2B)[17] and cell death[53], and this toxicity is mediated by toll-like receptors 2 and 4.[54] In vivo, histones likely circulate as part of nucleosomes.[17,55] Intact nucleosomes/NETs promote coagulation and increase fibrin deposition.[16,46] In vitro, the addition of DNA and histones in combination results in greater fibrin clot stability than the individual components.[56]

NETs deposition in a flow chamber perfused with blood promotes fibrin deposition and NETs bind plasma proteins important for platelet adhesion and thrombus propagation such as fibronectin and von Willebrand factor (VWF).[16] In

this flow model, RBCs bind to NETs but not collagen.[16] Within thrombi formed in vivo, NETs colocalize with VWF.[16] At times it appears as if VWF connects NETs to the vessel wall (Figure 1.2A). Interaction of NETs with fibrin was also observed after intraperitoneal administration of alum adjuvant resulting in the formation of nodules containing both extracellular DNA and fibrin[31], perhaps trying to encapsulate the foreign substance. Fibrin and NETs likely work together toward immune defense in a process now defined as "immunothrombosis."[57]

NET fibers contain various other factors that can render them procoagulant. As mentioned earlier, serine proteases inhibit TFPI[58], and in addition, tissue factor has been shown to be deposited on NETs.[25,59,60] The source of tissue factor could be from blood[25] or from the vessel wall.[61] Factor XII is present and active on NETs.[25,46] The negatively charged DNA in NETs may provide a scaffold for Factor XII activation which is aided by platelets, but the exact mechanism has not been determined.[25]

NETs in thrombosis: Animal models

Insights from animal models about the presence and role of NETs in thrombosis are extensive.[62-64] The first analysis of baboons with thrombi from balloon catheter-induced DVT revealed the presence of NETs not only within the thrombus (Figure 1.2A) but also their biomarkers in the plasma[16], with their appearance paralleling that of the fibrin degradation product D-dimer.[65] The

mouse models of DVT have allowed for more detailed investigation of the time course of NET formation and the testing of potential therapies.[15,25] Mouse models have also shown a possible role of NETs in arterial thrombosis.[46]

Arterial thrombosis

NETs have been studied in arterial vessel injury induced by ferric chloride application. In this model, the lack of serine proteases in neutrophil elastase/Cathepsin G-deficient mice lessens coagulation via reduced TFPI cleavage.[46] Infusion of the anti-H2A-H2B-DNA antibody[66] that neutralizes histones leads to prolonged time to occlusion as well as lower thrombus stability in the carotid arteries of WT mice, while no effect of antibody infusion is observed in the neutrophil elastase/Cathepsin G-deficient mice.[46] Thus, externalized nucleosomes contribute to thrombogenesis by exposing serine proteases to TFPI. NETs are also present in the carotid lumen in ApoE-deficient mice on high-fat diet, proximal to atherosclerotic lesions[67], supporting the clinical observation that NETs are implicated in coronary atherosclerosis.[13]

Deep vein thrombosis

Platelets and neutrophils are indispensible in the mouse inferior vena cava (IVC) stenosis model of DVT, as well as VWF that might help recruit both of these cell types.[25,68] The release of VWF from Weibel-Palade bodies from endothelial cells is likely driven by hypoxia[69]. Ischemic stroke also elevates plasma nucleosome levels, and systemic hypoxia produced by placing animals in a hypoxic chamber results in release of histone-DNA complexes into circulation.[19] After a day in the hypoxic chamber, mice become highly susceptible

to IVC thrombus formation.[70] Interestingly, hypoxia induces HIF-1α, which is implicated in NETosis.[71] Through their histones, NETs may further enhance endothelial activation as histone infusion in combination with IVC stenosis greatly accelerated thrombus formation.[15] Histone infusion leads to VWF release[15] and signs of microthrombosis in mice.[17] Weibel-Palade body secretion also upregulates endothelial P-selectin, an adhesion receptor for leukocytes.[51] Neutrophils are among the first leukocytes to be recruited to the activated endothelium at the onset of thrombosis and comprise a great majority of the thrombus leukocytes during the early stages of thrombosis.[25,72]

Both the baboon and mouse models show NETs in close association with VWF within thrombi.[15,16] In vitro binding of VWF to NETs is also observed.[16] The interaction of the A1 domain of VWF with histones was originally described[73] long before NETs were discovered and these recent studies help to provide relevance to a phenomenon that was at the time found to have "no conceivable physiological role."[73] Similarly, fibronectin, a molecule important in thrombosis[74,75] contains four DNA-binding domains that also interact with heparin[76], and indeed fibronectin binds to NETs.[16]

While the presence of NETs within deep vein thrombi is undeniable, their importance in DVT pathophysiology is still being actively investigated. Treatment with DNase 1, known to degrade NETs[1], diminishes the frequency of thrombus formation[15,25], indicating that the presence of NETs in DVT is functionally important and that DNase could be therapeutically useful. At earlier time points after IVC stenosis, only a few NETs are present within the forming mouse

thrombus as seen by intravital microscopy, while at later time points NETs are widespread (Figure 1.3A).[25] This was confirmed using citrullinated histone H3 as a marker for NETs[24], revealing an extensive meshwork of NETs throughout the 48-hour-old thrombus (Figure 1.3B). The use of PAD4$^{-/-}$ mice, that cannot undergo the histone modification required for chromatin decondensation in NETosis, demonstrated that NETs are indeed a crucial component of the thrombus scaffold, as the lack of NETs results in fewer thrombi early after IVC stenosis (6 h), with almost no thrombi present after 48 h.[24] In PAD4$^{-/-}$ mice, platelets and leukocytes do accumulate along activated endothelium, and neutrophils are present within the rare thrombi that form[24], showing that NETosis is the critical function of neutrophils in thrombosis. CXCL7 released from platelets in thrombi may generate the chemotactic gradient that directs leukocytes within thrombi[77], and platelets also promote NETosis[25] through a mechanism that is not completely elucidated.[25,41,46]

Venous injury

There may be a difference between arterial and venous responses to injury with respect to NETs. In contrast to the arterial injury model, in venous ferric chloride injury there is no delay in time to occlusive thrombus formation in PAD4$^{-/-}$ mice where NETosis is inhibited.[24] Alternatively, the importance of NETs may depend on vessel size. Arterial injury was examined in the carotid artery[25], which takes longer to occlude than injury of small veins[24] and thus NETs have the time to be produced. In large arteries, NETs may be necessary in addition to

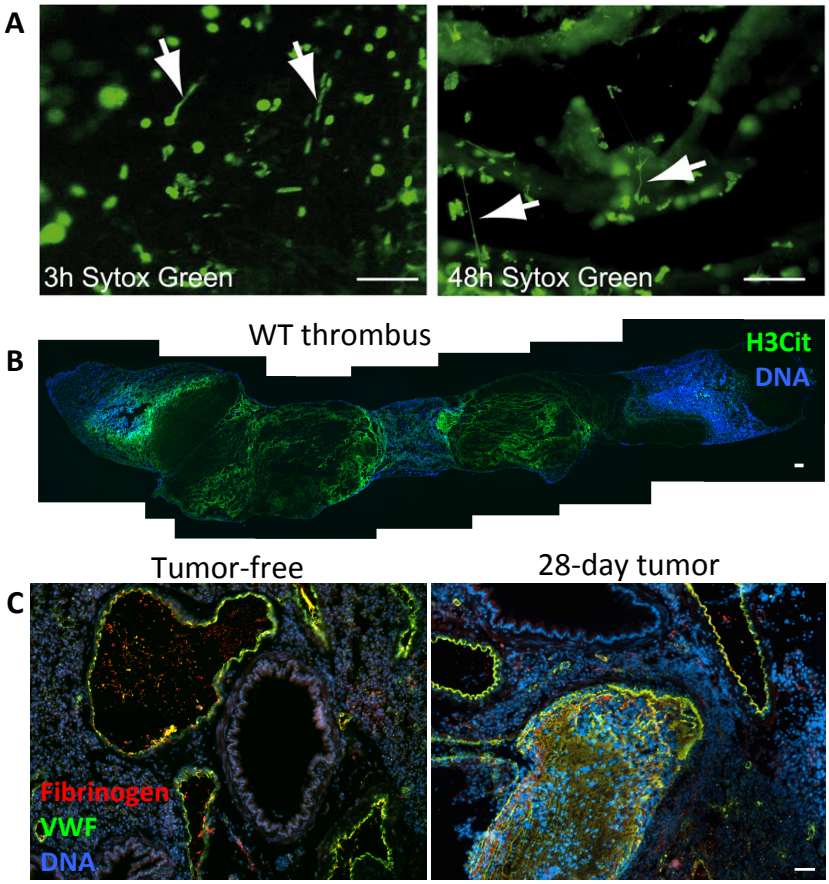

Figure 1.3. NETs form in mouse models of thrombosis and cancer.

A. Intravital microscopy of developing thrombi shows the release of NETs early (3h) and more prominently in occlusive thrombi (48h). Arrows indicate NETs. Sytox Green, DNA. Scale bars, 50 μm. Reproduced from von Bruhl et al. JEM 2012[25]. B. Composite image of a thrombus formed in a WT mouse 48h after IVC stenosis. Mosaic generated using MosaicJ plug-in for ImageJ software[78]. Citrullinated histone H3 (H3Cit) staining (green) shows evidence of a NET meshwork throughout the red portion of the thrombus. Scale bar, 100 μm. C. Mice bearing a mammary carcinoma develop spontaneous thrombi in the lung (right) after 28 days, a time point when NETs are spontaneously generated in these mice. This does not occur in tumor-free mice (left). VWF, green. Fibrinogen, red. DNA, blue. Scale bar, 50 μm. Reproduced from Demers et al. PNAS 2012.[10,42]

fibrin to stabilize the thrombus against arterial shear. Importantly, the PAD4$^{-/-}$ mice retain normal tail bleeding time. Therefore, NETs may not play a critical role in platelet plug formation in response to a small injury. They could, however, provide long-term stability of thrombi in large wounds but this is yet to be investigated. Targeting PAD4 may be beneficial in pathological venous thrombosis because it will not cause spontaneous hemorrhaging or have drastic consequences on physiological hemostasis.

Cancer-associated thrombosis

A high percentage of cancer patients both with and without chemotherapy experience lethal thrombotic complications.[79] Cell-free DNA increases transiently during the course of chemotherapy in patients and in a mouse model.[80] Adding cell-free DNA isolated from in vitro chemotherapy-treated blood to recalcified plasma increases thrombin generation due to contact pathway activation.[80] Mice bearing solid tumors develop an accompanied neutrophilia during tumor progression. In mammary carcinoma and Lewis lung carcinoma, this is associated with increasing plasma DNA levels.[10] Of note, when cancer patients develop neutrophilia, this is usually a sign of poor prognosis.[81] Isolated neutrophils from tumor-bearing mice are primed to undergo NETosis.[10] It is thought that tumors secrete cytokines, such as G-CSF, that systemically prime the neutrophils.[10,11] The elevated DNA and propensity of neutrophils to throw NETs provides a new explanation for cancer-associated thrombosis, as mice with high levels of NET biomarkers, such as plasma H3Cit, show spontaneous thrombosis (Figure 1.3C).[10]

NETs in human thrombosis

While NETs were initially described as occurring within tissues[1,8,82], subsequent work has shown they can form within vasculature.[16,41,46] This may increase the ability to measure certain biomarkers of NETs in plasma. Indeed, DNA[83] and nucleosomes[84] are elevated in septic patients, and cell-free DNA levels were a better predictor of progression to sepsis after traumatic injury than IL-6 or CRP, markers of inflammation.[85] MPO-DNA complexes are elevated specifically during active disease in patients with small-vessel vasculitis[42], when their thrombotic risk is the highest.[86] Also, a case study in a patient with ANCA-positive microscopic polyangiitis showed NETs within a venous thrombus.[87] Thrombotic risk is elevated in other chronic diseases in which NETs form, including cancer, colitis, and rheumatoid arthritis.

The interplay of inflammation and thrombosis is well established. In coronary artery disease, MPO-DNA complexes are elevated in the more severe cases, positively associated with elevated thrombin levels, and robustly predict adverse cardiac events.[13] DNA, nucleosome, and MPO levels correlate with disease state in patients with thrombotic microangiopathies (TMAs), including thrombotic thrombocytopenic purpura (TTP), hemolytic uremic syndrome, and malignant tumor-induced TMA.[20] In TTP characterized by low ADAMTS13 (A disintegrin-like and metalloproteinase with thrombospondin type-1 motifs 13), NETs biomarkers are elevated during acute TTP compared to the same patients in remission (Figure 1.4C)[20], making it a possibility that the disease could be

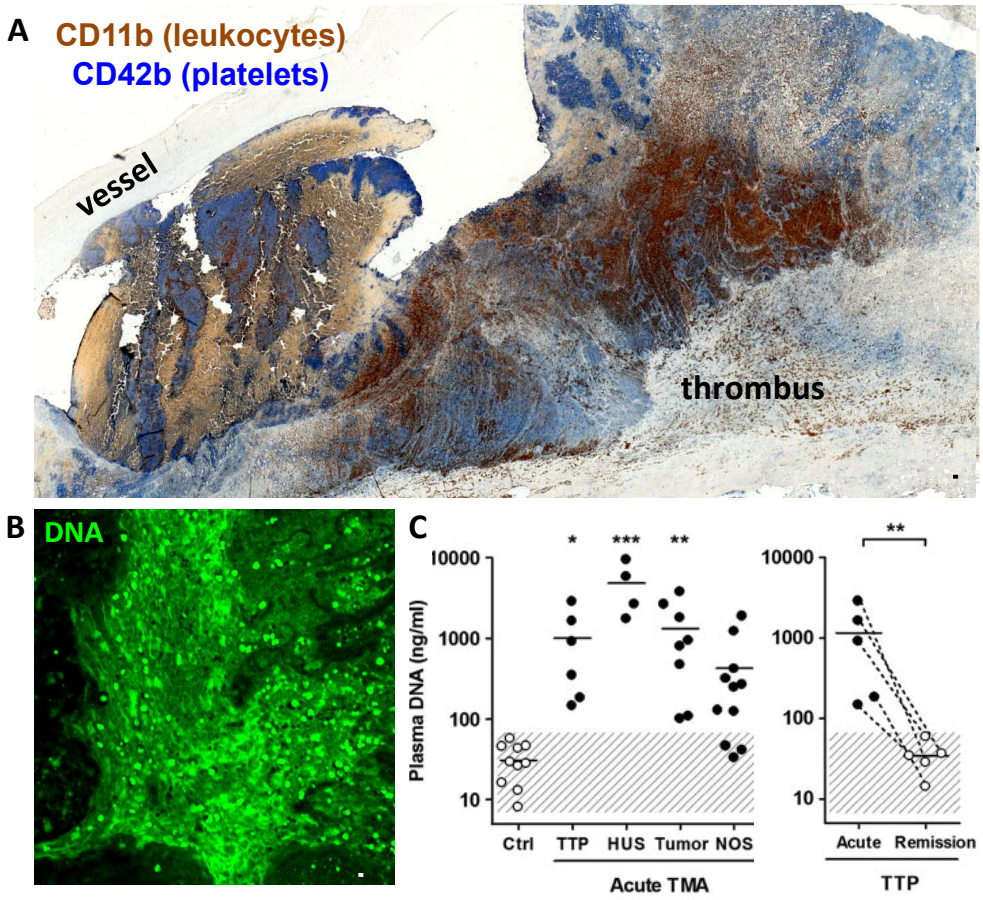

Figure 1.4. Evidence of NETs in human pathological thrombosis. A. Composite image of a human pulmonary embolism specimen obtained surgically and stained by immunohistochemistry for platelets (blue) and leukocytes (brown) showing that areas of the thrombus are rich in both cell types. Scale bar, 100 μm. Mosaic generated using MosaicJ plug-in for ImageJ[78]. Immunohistochemical analysis by Alexander Savchenko. B. Representative image of diffuse extracellular DNA staining (green) present in a surgically-harvested pulmonary embolism patient specimen. Green, DNA. Scale bar, 20 μm. Anonymous specimens in A and B kindly provided by Richard Mitchell. C. Cell-free DNA, a plasma biomarker of NETs, is elevated in patients with thrombotic microangiopathies (left): thrombotic thrombocytopenic purpura (TTP), hemolytic uremic syndrome (HUS), malignancies (tumor) and non-specified cases (NOS). Patients suffering from acute TTP present significantly elevated plasma DNA compared to when in remission (right). This research was originally published in *Blood*. Fuchs TA et al. Circulating DNA and myeloperoxidase indicate disease activity in patients with thrombotic microangiopathies. *Blood*. 2012;120:1157-1164. © American Society of Hematology.

precipitated by an infection or other stimulus that induces NETosis. Circulating NET levels can be used to predict which patients will develop TMAs after bone marrow transplant.[88] Blood products may also contain NETs if not leukodepleted prior to transfusion.[21] These infused NETs could be toxic after transfusion and may possibly contribute to thrombotic events in hospitalized patients.

Risk factors for DVT include trauma, surgery, infection, immobilization and hypoxia[45,89,90], several of which are associated with NET formation. Deep vein thrombi and pulmonary emboli have regions of platelet and leukocyte accumulation (Figure 1.4A) and unpublished observations from our laboratory show that these are also rich in extracellular DNA (Figure 1.4B). Establishing suitable biomarkers for DVT diagnosis is of interest, because for now ultrasound remains the best diagnostic method but is not always reliable.[91] Circulating nucleosomes and markers of neutrophil activation (elastase-α1-antitrypsin, MPO) are significantly increased in persons with DVT, compared to patients with symptoms but lack of confirmed DVT diagnosis.[92,93] Plasma DNA positively correlates with VWF and negatively correlates with levels of ADAMTS13[93], supporting a relationship between NETs and VWF in DVT. In fact, the ratio of ADAMTS13:VWF is the lowest in DVT patients.[93]

Extracellular histone/DNA complexes have also been identified in arterial thrombi following thrombectomy[56,94] obtained from abdominal aortic aneurism patients.[94] The codistribution of fibrin and NETs is apparent in arterial thrombi.[56] Combination therapies digesting fibrin and DNA may be needed for efficient thrombolysis[16] (Figure 1.5) as will be discussed below.

New possibilities to prevent thrombosis and improve thrombolysis

Thrombus development involves an ongoing process of maturation.[95] Animal models of DVT have established a time course of initial neutrophil and platelet recruitment followed by monocyte infiltration and eventual thrombus resolution.[25,68,96,97] There are several potential new targets for either the prevention of thrombosis or enhancement of thrombolysis (Figure 1.5). Platelets and platelet adhesion to VWF are essential to thrombus generation[25,68], and two recent clinical trials showed that aspirin, long regarded as an antiplatelet therapy, prevents venous thromboembolism recurrence.[98,99] Interestingly, aspirin can also inhibit NETosis in vitro.[100] Preventing Weibel-Palade body release, for example with agents that increase nitric oxide generation[101] or otherwise interfere with endothelial VWF/P-selectin secretion[102], or targeting platelet-VWF interactions would both prevent platelets and neutrophils from tethering onto the vessel wall, and their possible recruitment of other platelets and neutrophils upon activation. The A1 domain of VWF binds to glycoprotein 1β on platelets, promoting their adhesion. In vivo, inhibition of this interaction targeting the VWF A1 domain by antibodies or aptamers (reviewed in[103,104]) greatly reduces thrombus formation in arteries and veins.[68,104] Inhibiting VWF would prevent PSGL-1-mediated leukocyte rolling and also firm adhesion via β2 integrins such as Mac1.[105] ADAMTS13, a protease that specifically cleaves VWF[106], can be administered in vivo to reduce thrombosis[107] and to aid in thrombolysis of thrombi in venules.[108] Recombinant ADAMTS13 (rADAMTS13) can prevent

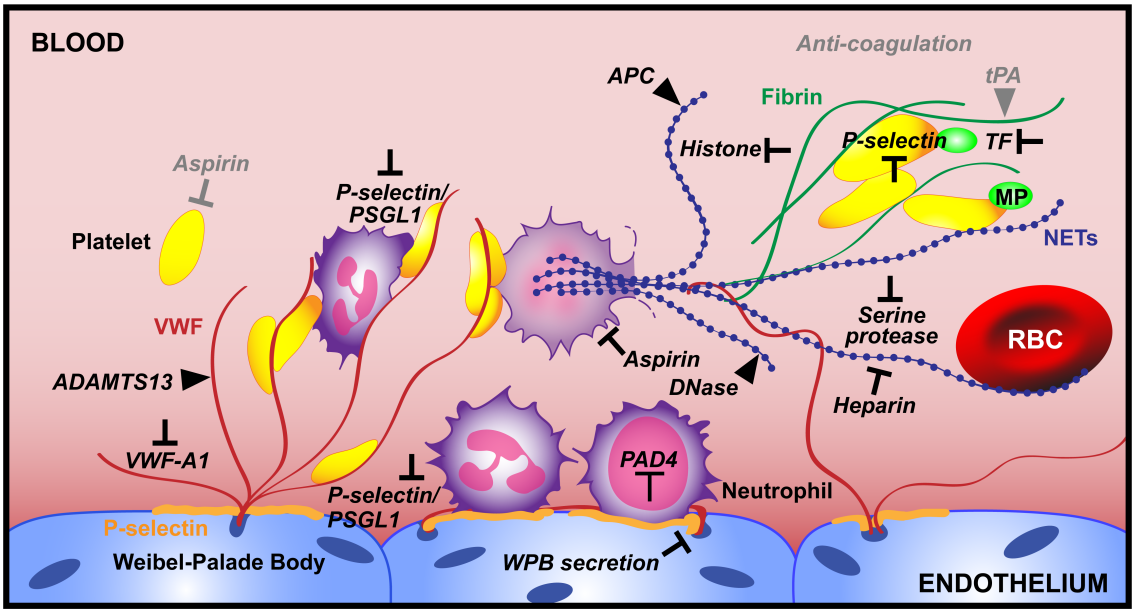

Figure 1.5. Emerging targets for thrombus prevention and thrombolysis. Here we summarize advances in the field of thrombosis with respect to neutrophil recruitment and NETosis and pinpoint targets that should be investigated as potential therapeutics (black). Existing treatments are in gray. We propose PAD4 inhibition as a way to prevent NET release. For thrombi that have already formed, neutralizing the toxic components of NETs is key. Thrombolytic strategies should involve the targeting of both DNA (blue) and the protein elements (red and green) of the thrombus scaffold.

microthrombosis such as in ischemia reperfusion injury occurring in myocardial infarction or stroke.[109,110] rADAMTS13 could also be used in DVT prophylaxis by reducing initial platelet accumulation and neutrophil recruitment, as well as in aiding thrombolysis in combination with fibrinolytic or NET-degrading therapies. Some improvement after combining ADAMTS13 and DNase 1 was observed in a murine myocardial ischemia/reperfusion model.[14] It is of interest to note that polymorphisms in both ADAMTS13 and DNase 1 linked to reduced activity are associated with myocardial infarction in humans.[111,112]

Targeting P-selectin, the other important component of Weibel-Palade bodies and α-granules, is triply beneficial, as it reduces neutrophil recruitment, the activating interaction between neutrophils and platelets, and the generation of TF-containing microparticles.[51] P-selectin inhibition is protective in DVT animal models[25,65,72,113], significantly reducing neutrophil recruitment to the vessel wall[25,72], NET generation[25], and reducing the procoagulant activity of P-selectin.[113,114] The ideal antithrombotic agent will prevent pathological thrombosis with minimal impact on hemostasis. In this respect, neutrophils are such a target. Neutrophil depletion was reported to reduce thrombus size in mouse DVT[25] and this is likely due to their ability to make NETs through the action of PAD4.[24] PAD4 inhibitors would prevent NETs from being formed, while DNases could be used to degrade NETs that are already present (Figure 1.5). A variety of nucleases could be tested for thrombolysis, perhaps even ones of bacterial origin as streptokinase effectively digests fibrin.

Central to the feasibility of NETs degradation is their structure: they are strands of highly decondensed chromatin exposed to the extracellular environment and thus accessible to DNases.[1,26] Certain pathogens produce nucleases that allow them to evade capture and killing by NETs.[82,115,116] Such nucleases may be good candidates to improve thrombolysis. Administration of DNase I has a protective effect in vivo in murine models of ischemic stroke[19], myocardial infarction[14] and deep vein thrombosis.[15,25] Combination therapies including DNase with ADAMTS13 and/or tissue plasminogen activator (tPA) could allow for more complete penetration of thrombolytic agents within large thrombi. Current therapies are centered on anticoagulation and fibrinolysis[117] that, with the exception of heparin (see below), are unlikely to dismantle or degrade the NET component of the venous thrombus scaffold. Indeed, clots produced with NETosing neutrophils could only be degraded with a combination of tPA and DNase I.[16] Similarly, addition of histones and DNA to fibrin clots in vitro makes them more resistant to fibrinolysis.[56]

Interestingly, the widely used anticoagulant heparin dismantles NETs[16] and prevents histone-platelet interactions[52], thus likely decreasing NET-driven thrombosis. DNase I activity on chromatin is enhanced in vitro by the presence of serine proteases, and this can be mimicked by heparin as it dislodges histones from chromatin and allows for greater accessibility for the enzyme.[118] Combining DNase 1 with heparin could further reduce the risk of future thrombotic events.

Neutralizing the toxic components of NETs provides another possible strategy to prevent endothelial injury and thrombosis. Activated protein C

degrades histones and prevents histone-associated lethality.[17] In mice, infusion of histones precipitates DVT[15] and exacerbates ischemic stroke.[19] Inhibiting the serine proteases on NETs could allow for TFPI activity and decreased TF-promoted coagulation.[46] TF is found on NETs[25], and it is likely that TF-containing microparticles are recruited to NETs or NET-associated platelets. Reducing these procoagulant factors would mitigate the damaging effects of NETs until their eventual clearance.

It is likely that macrophages infiltrating the thrombus can act as an endogenous clearance mechanism of NETs during thrombus resolution. Macrophages are able to phagocytose NETs and degrade them with their high lysosomal DNase II contents.[119] In vitro, DNase I preliminary digestion aids the clearance of NETs by macrophages.[119] Addition of exogenous DNase 1 could enhance the accessibility of macrophages to NETs and the removal of fragmented NETs. Monocytes/macrophages also provide plasminogen activator[120] thus helping fibrinolysis. Any potential anti-thrombotic should not negatively impact macrophage function as this could potentially impede thrombus resolution and result in pathologies from excess NETs products.

Questions for the future

From the observations described above, it is clear that inhibiting NETosis would be beneficial to prevent toxic side effects of NETs in inflammation and

reduce occurrence of pathological thrombosis. However, *the importance of NETs in preventing infection* cannot be neglected and needs more thorough evaluation. NETs alone[44] or together with fibrin[46] may wall off local infections and prevent dissemination[57] which could be promoted by DNase/fibrinolysis. Since PAD4-deficient neutrophils are competent in phagocytosis, ROS generation and recruitment to inflammatory sites[23] (K.M. and D.D.W. unpublished data 2013), it is possible that only an overwhelming infection would be problematic when NETosis is inhibited. Although PAD4$^{-/-}$ mice were more susceptible to a mutant Group A streptococcal infection (unable to secrete a nuclease), PAD4$^{-/-}$ mice did not fare worse in necrotizing fasciitis induced by the DNase-secreting Group A Streptococcus.[23] Also, PAD4$^{-/-}$ mice were similar to WT in influenza infection.[121] We thus do not anticipate major problems in treating an uninfected host. Antibiotics could be administered together with the NETosis inhibitors when needed.

Assuming NET inhibition is safe, it will be important to examine at which step NETosis is best arrested. *The original stimulus and the signaling mechanisms leading to chromatin release* during thrombosis need to be uncovered. Hypoxia and its activation of the transcription factor HIF1α were implicated in NETosis[71] and ROS generation could also be important. Whether DVT is modified in mice deficient in HIF1α and mutants that overproduce or underproduce ROS should be evaluated. Interaction of platelets with neutrophils promotes NETosis, and there may be an enhancing effect by the forming clot itself. Fibronectin, present in clots, was shown to have such an effect.[30] We noted

that NETs were mostly present in the RBC-rich (red) portion of the clot.[15] RBCs may not only be recruited by NETs, but may also enhance their production. Whether inhibition of any of these interactions would reduce NETosis remains to be seen.

Little is known about the signaling inside the cell that leads to chromatin release. Raf/MEK/ERK[122], Rac2[123], and NADPH oxidase[5] can participate. Which of these are implicated in pathological thrombosis such as DVT should be determined and tested with available inhibitors. What are the signals that direct neutrophils to either release only nuclear components or the entire cell contents? Which of these NETosis mechanisms is more common in thrombosis? Are the neutrophils within thrombi that have formed NETs dead or do they retain function? Does partial chromatin release[36] occur during thrombosis, serving to enhance neutrophil adhesion to other cells within thrombi? Most importantly, learning more about PAD4, a key therapeutic target candidate, its intracellular substrates other than histones, and how it is activated or translocated to the nucleus may help to design inhibitors with high specificity.

It will be instructive to determine the *implications of NET formation on thrombotic disease progression* and as a biomarker of disease activity. What is the exact role of NETs in thrombosis? Do they contribute to thrombus stability like fibrin[74]? Are they implicated in post-thrombotic syndrome? NETs may play a role in vessel wall injury and recruitment of new cell types into the thrombus, including endothelial cells for thrombus vascularization. During thrombosis, NETs fragments appear in circulation.[15,16] These may be useful biomarkers of active

thrombotic disease[16,92,93] and should be studied carefully as they may reveal more about the process of NETs generation and degradation. Furthermore, it will be critical to know how long these NETs fragments retain pro-coagulant activity and how this depends on their size or composition. We know that NETs generation in diseases such as cancer has a systemic effect on the host[10] and the pro-coagulant activity generated by NETs could promote cancer growth as is the case with thrombin.[124]

It will be important to learn *how NETs and their fragments are naturally cleared.* Animal studies indicate that it would be therapeutically beneficial to clear NETs from the circulation and away from vessel walls. Is VWF implicated in anchoring NETs to the vessel wall, and would ADAMTS13 free the NETs? VWF and DNA plasma levels seem to correlate in human thrombosis.[93] Except for macrophages, with their intracellular DNase II[119], and dendritic cells[125-127], no other cell type has been implicated in NET clearance. The role of platelets and RBCs that bind NETs should be evaluated. DNase I is elevated after ischemia[128] and also early in sepsis[129]: is this to reduce the risk of thrombosis? DNase $I^{-/-}$ mice should be studied to further examine the enzyme's role in NET clearance[119] and as a natural thrombolytic.

In conclusion, we have learned a lot about NETs activity in thrombotic disease since the first observation in 2010 of their presence in a deep vein thrombus. There is certainly plenty more to investigate. Now is the time to test the effect of NET inhibition in DVT prophylaxis and of combination therapies in

thrombolysis, therapies that not only cleave the proteinaceous components of thrombi, but also attack the nucleic acid backbone.

We just saw it from a different point of view

Tangled up in blue[130]

Acknowledgments

We thank Melanie Demers and Siu Ling Wong for helpful discussions, Richard N. Mitchell for providing human pulmonary embolism specimens and Alexander S. Savchenko for immunohistochemical analysis of human samples. We also thank Lesley Cowan for assistance in manuscript preparation and Kristin Johnson for graphic design of Figure 1.5.

Section 1.3: Bibliography

1. Brinkmann V, Reichard U, Goosmann C, et al. Neutrophil extracellular traps kill bacteria. *Science*. 2004;303(5663):1532-1535.

2. Urban CF, Reichard U, Brinkmann V, Zychlinsky A. Neutrophil extracellular traps capture and kill Candida albicans yeast and hyphal forms. *Cell Microbiol*. 2006;8(4):668-676.

3. Saitoh T, Komano J, Saitoh Y, et al. Neutrophil extracellular traps mediate a host defense response to human immunodeficiency virus-1. *Cell Host Microbe*. 2012;12(1):109-116.

4. Brinkmann V, Zychlinsky A. Beneficial suicide: why neutrophils die to make NETs. *Nat Rev Microbiol*. 2007;5(8):577-582.

5. Fuchs TA, Abed U, Goosmann C, et al. Novel cell death program leads to neutrophil extracellular traps. *J Cell Biol*. 2007;176(2):231-241.

6. Kolaczkowska E, Kubes P. Neutrophil recruitment and function in health and inflammation. *Nat Rev Immunol*. 2013;13(3):159-175.

7. Mayadas TN, Cullere X, Lowell CA. The multifaceted functions of neutrophils. *Ann Rev Pathol*. 2014;9:181-218.

8. Gupta AK, Hasler P, Holzgreve W, Gebhardt S, Hahn S. Induction of neutrophil extracellular DNA lattices by placental microparticles and IL-8 and their presence in preeclampsia. *Hum Immunol*. 2005;66(11):1146-1154.

9. Dwivedi N, Upadhyay J, Neeli I, et al. Felty's syndrome autoantibodies bind to deiminated histones and neutrophil extracellular chromatin traps. *Arthritis Rheum*. 2012;64(4):982-992.

10. Demers M, Krause DS, Schatzberg D, et al. Cancers predispose neutrophils to release extracellular DNA traps that contribute to cancer-associated thrombosis. *Proc Natl Acad Sci U S A*. 2012;109(32):13076-13081.

11. Demers M, Wagner DD. Neutrophil extracellular traps: A new link to cancer-associated thrombosis and potential implications for tumor progression. *Oncoimmunology*. 2013;2(2):e22946.

12. Cools-Lartigue J, Spicer J, McDonald B, et al. Neutrophil extracellular traps sequester circulating tumor cells and promote metastasis. *J Clin Invest*. 2013.

13. Borissoff JI, Joosen IA, Versteylen MO, et al. Elevated levels of circulating DNA and chromatin are independently associated with severe coronary

atherosclerosis and a prothrombotic state. *Arterioscler Thromb Vasc Biol*. 2013;33(8):2032-2040.

14. Savchenko AS, Borissoff JI, Martinod K, et al. VWF-mediated leukocyte recruitment with chromatin decondensation by PAD4 increases myocardial ischemia/reperfusion injury in mice. *Blood*. 2014;123(1):141-148.

15. Brill A, Fuchs TA, Savchenko AS, et al. Neutrophil extracellular traps promote deep vein thrombosis in mice. *J Thromb Haemost*. 2012;10(1):136-144.

16. Fuchs TA, Brill A, Duerschmied D, et al. Extracellular DNA traps promote thrombosis. *Proc Natl Acad Sci U S A*. 2010;107(36):15880-15885.

17. Xu J, Zhang X, Pelayo R, et al. Extracellular histones are major mediators of death in sepsis. *Nat Med*. 2009;15(11):1318-1321.

18. Thomas GM, Carbo C, Curtis BR, et al. Extracellular DNA traps are associated with the pathogenesis of TRALI in humans and mice. *Blood*. 2012;119(26):6335-6343.

19. De Meyer SF, Suidan GL, Fuchs TA, Monestier M, Wagner DD. Extracellular chromatin is an important mediator of ischemic stroke in mice. *Arterioscl Thromb Vasc Biol*. 2012;32(8):1884-1891.

20. Fuchs TA, Kremer Hovinga JA, Schatzberg D, Wagner DD, Lammle B. Circulating DNA and myeloperoxidase indicate disease activity in patients with thrombotic microangiopathies. *Blood*. 2012;120(6):1157-1164.

21. Fuchs TA, Alvarez JJ, Martinod K, Bhandari AA, Kaufman RM, Wagner DD. Neutrophils release extracellular DNA traps during storage of red blood cell units. *Transfusion*. 2013.

22. Savchenko AS, Martinod K, Seidman MA, et al. Neutrophil extracellular traps form predominantly during the organizing stage of human venous thromboembolism development. *J Thromb Haemost*. 2014.

23. Li P, Li M, Lindberg MR, Kennett MJ, Xiong N, Wang Y. PAD4 is essential for antibacterial innate immunity mediated by neutrophil extracellular traps. *J Exp Med*. 2010;207(9):1853-1862.

24. Martinod K, Demers M, Fuchs TA, et al. Neutrophil histone modification by peptidylarginine deiminase 4 is critical for deep vein thrombosis in mice. *Proc Natl Acad Sci U S A*. 2013;110(21):8674-8679.

25. von Bruhl ML, Stark K, Steinhart A, et al. Monocytes, neutrophils, and platelets cooperate to initiate and propagate venous thrombosis in mice in vivo. *J Exp Med*. 2012;209(4):819-835.

26. Urban CF, Ermert D, Schmid M, et al. Neutrophil extracellular traps contain calprotectin, a cytosolic protein complex involved in host defense against Candida albicans. *PLoS Path*. 2009;5(10):e1000639.

27. Narasaraju T, Yang E, Samy RP, et al. Excessive neutrophils and neutrophil extracellular traps contribute to acute lung injury of influenza pneumonitis. *Am J Pathol*. 2011;179(1):199-210.

28. Hawes MC, Curlango-Rivera G, Wen F, White GJ, Vanetten HD, Xiong Z. Extracellular DNA: the tip of root defenses? *Plant Sci*. 2011;180(6):741-745.

29. Chen K, Nishi H, Travers R, et al. Endocytosis of soluble immune complexes leads to their clearance by FcgammaRIIIB but induces neutrophil extracellular traps via FcgammaRIIA in vivo. *Blood*. 2012;120(22):4421-4431.

30. Byrd AS, O'Brien XM, Johnson CM, Lavigne LM, Reichner JS. An extracellular matrix-based mechanism of rapid neutrophil extracellular trap formation in response to Candida albicans. *J Immunol*. 2013;190(8):4136-4148.

31. Munks MW, McKee AS, Macleod MK, et al. Aluminum adjuvants elicit fibrin-dependent extracellular traps in vivo. *Blood*. 2010;116(24):5191-5199.

32. Wang Y, Li M, Stadler S, et al. Histone hypercitrullination mediates chromatin decondensation and neutrophil extracellular trap formation. *J Cell Biol*. 2009;184(2):205-213.

33. Wang Y, Wysocka J, Sayegh J, et al. Human PAD4 regulates histone arginine methylation levels via demethylimination. *Science*. 2004;306(5694):279-283.

34. Leshner M, Wang S, Lewis C, et al. PAD4 mediated histone hypercitrullination induces heterochromatin decondensation and chromatin unfolding to form neutrophil extracellular trap-like structures. *Front Immunol*. 2012;3:307.

35. Papayannopoulos V, Metzler KD, Hakkim A, Zychlinsky A. Neutrophil elastase and myeloperoxidase regulate the formation of neutrophil extracellular traps. *J Cell Biol*. 2010;191(3):677-691.

36. Yipp BG, Petri B, Salina D, et al. Infection-induced NETosis is a dynamic process involving neutrophil multitasking in vivo. *Nat Med*. 2012;18(9):1386-1393.

37. Farley K, Stolley JM, Zhao P, Cooley J, Remold-O'Donnell E. A serpinB1 regulatory mechanism is essential for restricting neutrophil extracellular trap generation. *J Immunol*. 2012;189(9):4574-4581.

38. Pilsczek FH, Salina D, Poon KK, et al. A novel mechanism of rapid nuclear neutrophil extracellular trap formation in response to Staphylococcus aureus. *J Immunol*. 2010;185(12):7413-7425.

39. Yipp BG, Kubes P. NETosis: how vital is it? *Blood*. 2013;122(16):2784-2794.

40. Malawista SE, De Boisfleury Chevance A. The cytokineplast: purified, stable, and functional motile machinery from human blood polymorphonuclear leukocytes. *J Cell Biol*. 1982;95(3):960-973.

41. Clark SR, Ma AC, Tavener SA, et al. Platelet TLR4 activates neutrophil extracellular traps to ensnare bacteria in septic blood. *Nat Med*. 2007;13(4):463-469.

42. Kessenbrock K, Krumbholz M, Schonermarck U, et al. Netting neutrophils in autoimmune small-vessel vasculitis. *Nat Med*. 2009;15(6):623-625.

43. Hakkim A, Furnrohr BG, Amann K, et al. Impairment of neutrophil extracellular trap degradation is associated with lupus nephritis. *Proc Natl Acad Sci U S A*. 2010;107(21):9813-9818.

44. McDonald B, Urrutia R, Yipp BG, Jenne CN, Kubes P. Intravascular neutrophil extracellular traps capture bacteria from the bloodstream during sepsis. *Cell Host Microbe*. 2012;12(3):324-333.

45. Smeeth L, Cook C, Thomas S, Hall AJ, Hubbard R, Vallance P. Risk of deep vein thrombosis and pulmonary embolism after acute infection in a community setting. *Lancet*. 2006;367(9516):1075-1079.

46. Massberg S, Grahl L, von Bruehl ML, et al. Reciprocal coupling of coagulation and innate immunity via neutrophil serine proteases. *Nat Med*. 2010;16(8):887-896.

47. Kannemeier C, Shibamiya A, Nakazawa F, et al. Extracellular RNA constitutes a natural procoagulant cofactor in blood coagulation. *Proc Natl Acad Sci U S A*. 2007;104(15):6388-6393.

48. Altincicek B, Stotzel S, Wygrecka M, Preissner KT, Vilcinskas A. Host-derived extracellular nucleic acids enhance innate immune responses, induce coagulation, and prolong survival upon infection in insects. *J Immunol*. 2008;181(4):2705-2712.

49. Ammollo CT, Semeraro F, Xu J, Esmon NL, Esmon CT. Extracellular histones increase plasma thrombin generation by impairing thrombomodulin-dependent protein C activation. *J Thromb Haemost*. 2011;9(9):1795-1803.

50. Semeraro F, Ammollo CT, Morrissey JH, et al. Extracellular histones promote thrombin generation through platelet-dependent mechanisms: involvement of platelet TLR2 and TLR4. *Blood*. 2011;118(7):1952-1961.

51. Wagner DD, Frenette PS. The vessel wall and its interactions. *Blood*. 2008;111(11):5271-5281.

52. Fuchs TA, Bhandari AA, Wagner DD. Histones induce rapid and profound thrombocytopenia in mice. *Blood*. 2011;118(13):3708-3714.

53. Saffarzadeh M, Juenemann C, Queisser MA, et al. Neutrophil extracellular traps directly induce epithelial and endothelial cell death: a predominant role of histones. *PloS One*. 2012;7(2):e32366.

54. Xu J, Zhang X, Monestier M, Esmon NL, Esmon CT. Extracellular histones are mediators of death through TLR2 and TLR4 in mouse fatal liver injury. *J Immunol*. 2011;187(5):2626-2631.

55. Esmon CT. Molecular circuits in thrombosis and inflammation. *Thromb Haemost*. 2013;109(3):416-420.

56. Longstaff C, Varju I, Sotonyi P, et al. Mechanical stability and fibrinolytic resistance of clots containing fibrin, DNA, and histones. *J Biol Chem*. 2013;288(10):6946-6956.

57. Engelmann B, Massberg S. Thrombosis as an intravascular effector of innate immunity. *Nat Rev Immunol*. 2013;13(1):34-45.

58. Petersen LC, Bjorn SE, Nordfang O. Effect of leukocyte proteinases on tissue factor pathway inhibitor. *Thromb Haemost*. 1992;67(5):537-541.

59. Kambas K, Chrysanthopoulou A, Vassilopoulos D, et al. Tissue factor expression in neutrophil extracellular traps and neutrophil derived microparticles in antineutrophil cytoplasmic antibody associated vasculitis may promote thromboinflammation and the thrombophilic state associated with the disease. *Ann Rheum Dis*. 2013.

60. Kambas K, Mitroulis I, Apostolidou E, et al. Autophagy mediates the delivery of thrombogenic tissue factor to neutrophil extracellular traps in human sepsis. *PloS One*. 2012;7(9):e45427.

61. Hampton AL, Diaz JA, Hawley AE, et al. Myeloid cell tissue factor does not contribute to venous thrombogenesis in an electrolytic injury model. *Thromb Res*. 2012;130(4):640-645.

62. Fuchs TA, Brill A, Wagner DD. Neutrophil extracellular trap (NET) impact on deep vein thrombosis. *Arterioscl Thromb Vasc Biol*. 2012;32(8):1777-1783.

63. Gardiner EE, Andrews RK. Neutrophil extracellular traps (NETs) and infection-related vascular dysfunction. *Blood Rev*. 2012;26(6):255-259.

64. Lester PA, Diaz JA, Shuster KA, Henke PK, Wakefield TW, Myers DD. Inflammation and thrombosis: new insights. *Front Biosci (Schol Ed)*. 2012;4:620-638.

65. Meier TR, Myers DD, Jr., Wrobleski SK, et al. Prophylactic P-selectin inhibition with PSI-421 promotes resolution of venous thrombosis without anticoagulation. *Thromb Haemost*. 2008;99(2):343-351.

66. Losman MJ, Fasy TM, Novick KE, Monestier M. Monoclonal autoantibodies to subnucleosomes from a MRL/Mp(-)+/+ mouse. Oligoclonality of the antibody response and recognition of a determinant composed of histones H2A, H2B, and DNA. *J Immunol*. 1992;148(5):1561-1569.

67. Megens RT, Vijayan S, Lievens D, et al. Presence of luminal neutrophil extracellular traps in atherosclerosis. *Thromb Haemost*. 2012;107(3):597-598.

68. Brill A, Fuchs TA, Chauhan AK, et al. von Willebrand factor-mediated platelet adhesion is critical for deep vein thrombosis in mouse models. *Blood*. 2011;117(4):1400-1407.

69. Pinsky DJ, Naka Y, Liao H, et al. Hypoxia-induced exocytosis of endothelial cell Weibel-Palade bodies. A mechanism for rapid neutrophil recruitment after cardiac preservation. *J Clin Invest*. 1996;97(2):493-500.

70. Brill A, Suidan GL, Wagner DD. Hypoxia, such as encountered at high altitude, promotes deep vein thrombosis in mice. *J Thromb Haemost*. 2013;11(9):1773-1775.

71. McInturff AM, Cody MJ, Elliott EA, et al. Mammalian target of rapamycin regulates neutrophil extracellular trap formation via induction of hypoxia-inducible factor 1 alpha. *Blood*. 2012;120(15):3118-3125.

72. Downing LJ, Strieter RM, Kadell AM, et al. Neutrophils are the initial cell type identified in deep venous thrombosis induced vein wall inflammation. *Asaio J*. 1996;42(5):M677-682.

73. Ward CM, Tetaz TJ, Andrews RK, Berndt MC. Binding of the von Willebrand factor A1 domain to histone. *Thromb Res*. 1997;86(6):469-477.

74. Ni H, Yuen PS, Papalia JM, et al. Plasma fibronectin promotes thrombus growth and stability in injured arterioles. *Proc Natl Acad Sci U S A*. 2003;100(5):2415-2419.

75. Matuskova J, Chauhan AK, Cambien B, et al. Decreased plasma fibronectin leads to delayed thrombus growth in injured arterioles. *Arterioscler Thromb Vasc Biol*. 2006;26(6):1391-1396.

76. Siri A, Balza E, Carnemolla B, Castellani P, Borsi L, Zardi L. DNA-binding domains of human plasma fibronectin. pH and calcium ion modulation of fibronectin binding to DNA and heparin. *Eur J Biochem*. 1986;154(3):533-538.

77. Ghasemzadeh M, Kaplan ZS, Alwis I, et al. The CXCR1/2 ligand NAP-2 promotes directed intravascular leukocyte migration through platelet thrombi. *Blood*. 2013;121(22):4555-4566.

78. Thevenaz P, Unser M. User-friendly semiautomated assembly of accurate image mosaics in microscopy. *Microsc Res Tech*. 2007;70(2):135-146.

79. Connolly GC, Khorana AA, Kuderer NM, Culakova E, Francis CW, Lyman GH. Leukocytosis, thrombosis and early mortality in cancer patients initiating chemotherapy. *Thromb Res*. 2010;126(2):113-118.

80. Swystun LL, Mukherjee S, Liaw PC. Breast cancer chemotherapy induces the release of cell-free DNA, a novel procoagulant stimulus. *J Thromb Haemost*. 2011;9(11):2313-2321.

81. Donskov F. Immunomonitoring and prognostic relevance of neutrophils in clinical trials. *Semin Cancer Biol*. 2013;23(3):200-207.

82. Sumby P, Barbian KD, Gardner DJ, et al. Extracellular deoxyribonuclease made by group A Streptococcus assists pathogenesis by enhancing evasion of the innate immune response. *Proc Natl Acad Sci U S A*. 2005;102(5):1679-1684.

83. Martins GA, Kawamura MT, Carvalho Mda G. Detection of DNA in the plasma of septic patients. *Ann N Y Acad Sci*. 2000;906:134-140.

84. Zeerleder S, Zwart B, Wuillemin WA, et al. Elevated nucleosome levels in systemic inflammation and sepsis. *Crit Care Med*. 2003;31(7):1947-1951.

85. Margraf S, Logters T, Reipen J, Altrichter J, Scholz M, Windolf J. Neutrophil-derived circulating free DNA (cf-DNA/NETs): a potential prognostic marker for posttraumatic development of inflammatory second hit and sepsis. *Shock*. 2008;30(4):352-358.

86. Stassen PM, Derks RP, Kallenberg CG, Stegeman CA. Venous thromboembolism in ANCA-associated vasculitis--incidence and risk factors. *Rheumatology (Oxford)*. 2008;47(4):530-534.

87. Nakazawa D, Tomaru U, Yamamoto C, Jodo S, Ishizu A. Abundant neutrophil extracellular traps in thrombus of patient with microscopic polyangiitis. *Front Immunol*. 2012;3:333.

88. Arai Y, Yamashita K, Mizugishi K, et al. Serum Neutrophil Extracellular Trap Levels Predict Thrombotic Microangiopathy after Allogeneic Stem Cell Transplantation. *Biol Blood Marrow Transplant*. 2013.

89. Bovill EG, van der Vliet A. Venous valvular stasis-associated hypoxia and thrombosis: what is the link? *Annu Rev Physiol*. 2011;73:527-545.

90. Heit JA. Venous thromboembolism: disease burden, outcomes and risk factors. *J Thromb Haemost*. 2005;3(8):1611-1617.

91. Coleman DM, Wakefield TW. Biomarkers for the diagnosis of deep vein thrombosis. *Expert Opin Med Diagn*. 2012;6(4):253-257.

92. van Montfoort ML, Stephan F, Lauw MN, et al. Circulating nucleosomes and neutrophil activation as risk factors for deep vein thrombosis. *Arterioscler Thromb Vasc Biol*. 2013;33(1):147-151.

93. Diaz JA, Fuchs TA, Jackson TO, et al. Plasma DNA is Elevated in Patients with Deep Vein Thrombosis. *J Vasc Surg: Ven Lymph Dis*. 2013;1(4).

94. Oklu R, Albadawi H, Watkins MT, Monestier M, Sillesen M, Wicky S. Detection of extracellular genomic DNA scaffold in human thrombus: implications for the use of deoxyribonuclease enzymes in thrombolysis. *J Vasc Interv Radiol*. 2012;23(5):712-718.

95. Seidman MA MR. Surgical pathology of small- and medium-sized vessels. *Surgical Pathology Clinics*. 2012;5(2):435-451.

96. Wakefield TW, Henke PK. The role of inflammation in early and late venous thrombosis: Are there clinical implications? *Sem Vasc Surg*. 2005;18(3):118-129.

97. Diaz JA, Hawley AE, Alvarado CM, et al. Thrombogenesis with continuous blood flow in the inferior vena cava. A novel mouse model. *Thromb Haemost*. 2010;104(2):366-375.

98. Becattini C, Agnelli G, Schenone A, et al. Aspirin for preventing the recurrence of venous thromboembolism. *New Engl J Med*. 2012;366(21):1959-1967.

99. Brighton TA, Eikelboom JW, Mann K, et al. Low-dose aspirin for preventing recurrent venous thromboembolism. *New Engl J Med*. 2012;367(21):1979-1987.

100. Lapponi MJ, Carestia A, Landoni VI, et al. Regulation of neutrophil extracellular trap formation by anti-inflammatory drugs. *J Pharmacol Exp Ther*. 2013;345(3):430-437.

101. Matsushita K, Morrell CN, Cambien B, et al. Nitric oxide regulates exocytosis by S-nitrosylation of N-ethylmaleimide-sensitive factor. *Cell*. 2003;115(2):139-150.

102. Torisu T, Torisu K, Lee IH, et al. Autophagy regulates endothelial cell processing, maturation and secretion of von Willebrand factor. *Nat Med*. 2013;19(10):1281-1287.

103. De Meyer SF, Stoll G, Wagner DD, Kleinschnitz C. von Willebrand factor: an emerging target in stroke therapy. *Stroke*. 2012;43(2):599-606.

104. Bonnefoy A, Vermylen J, Hoylaerts MF. Inhibition of von Willebrand factor-GPIb/IX/V interactions as a strategy to prevent arterial thrombosis. *Expert Rev Cardiovasc Ther*. 2003;1(2):257-269.

105. Pendu R, Terraube V, Christophe OD, et al. P-selectin glycoprotein ligand 1 and beta2-integrins cooperate in the adhesion of leukocytes to von Willebrand factor. *Blood*. 2006;108(12):3746-3752.

106. Furlan M, Robles R, Lammle B. Partial purification and characterization of a protease from human plasma cleaving von Willebrand factor to fragments produced by in vivo proteolysis. *Blood*. 1996;87(10):4223-4234.

107. Chauhan AK, Motto DG, Lamb CB, et al. Systemic antithrombotic effects of ADAMTS13. *J Exp Med*. 2006;203(3):767-776.

108. Crescente M, Thomas GM, Demers M, et al. ADAMTS13 exerts a thrombolytic effect in microcirculation. *Thromb Haemost*. 2012;108(3):527-532.

109. De Meyer SF, Savchenko AS, Haas MS, et al. Protective anti-inflammatory effect of ADAMTS13 on myocardial ischemia/reperfusion injury in mice. *Blood*. 2012;120(26):5217-5223.

110. Zhao BQ, Chauhan AK, Canault M, et al. von Willebrand factor-cleaving protease ADAMTS13 reduces ischemic brain injury in experimental stroke. *Blood*. 2009;114(15):3329-3334.

111. Schettert IT, Pereira AC, Lopes NH, Hueb WA, Krieger JE. Association between ADAMTS13 polymorphisms and risk of cardiovascular events in chronic coronary disease. *Thromb Res*. 2010;125(1):61-66.

112. Fujihara J, Takatsuka H, Kataoka K, Xue Y, Takeshita H. Two deoxyribonuclease I gene polymorphisms and correlation between genotype and its activity in Japanese population. *Leg Med (Tokyo)*. 2007;9(5):233-236.

113. Myers DD, Jr., Rectenwald JE, Bedard PW, et al. Decreased venous thrombosis with an oral inhibitor of P selectin. *J Vasc Surg*. 2005;42(2):329-336.

114. Andre P, Hartwell D, Hrachovinova I, Saffaripour S, Wagner DD. Pro-coagulant state resulting from high levels of soluble P-selectin in blood. *Proc Natl Acad Sci U S A*. 2000;97(25):13835-13840.

115. Buchanan JT, Simpson AJ, Aziz RK, et al. DNase expression allows the pathogen group A Streptococcus to escape killing in neutrophil extracellular traps. *Curr Biol*. 2006;16(4):396-400.

116. Beiter K, Wartha F, Albiger B, Normark S, Zychlinsky A, Henriques-Normark B. An endonuclease allows Streptococcus pneumoniae to escape from neutrophil extracellular traps. *Curr Biol*. 2006;16(4):401-407.

117. Comerota AJ. Thrombolysis for deep venous thrombosis. *J Vasc Surg*. 2012;55(2):607-611.

118. Napirei M, Ludwig S, Mezrhab J, Klockl T, Mannherz HG. Murine serum nucleases--contrasting effects of plasmin and heparin on the activities of DNase1 and DNase1-like 3 (DNase1l3). *Febs J*. 2009;276(4):1059-1073.

119. Farrera C, Fadeel B. Macrophage clearance of neutrophil extracellular traps is a silent process. *J Immunol*. 2013;191(5):2647-2656.

120. Soo KS, Northeast AD, Happerfield LC, Burnand KG, Bobrow LG. Tissue plasminogen activator production by monocytes in venous thrombolysis. *J Pathol*. 1996;178(2):190-194.

121. Hemmers S, Teijaro JR, Arandjelovic S, Mowen KA. PAD4-mediated neutrophil extracellular trap formation is not required for immunity against influenza infection. *PloS One*. 2011;6(7):e22043.

122. Hakkim A, Fuchs TA, Martinez NE, et al. Activation of the Raf-MEK-ERK pathway is required for neutrophil extracellular trap formation. *Nat Chem Biol*. 2011;7(2):75-77.

123. Lim MB, Kuiper JW, Katchky A, Goldberg H, Glogauer M. Rac2 is required for the formation of neutrophil extracellular traps. *J Leukoc Biol*. 2011;90(4):771-776.

124. Green D, Karpatkin S. Role of thrombin as a tumor growth factor. *Cell Cycle*. 2010;9(4):656-661.

125. Lande R, Ganguly D, Facchinetti V, et al. Neutrophils activate plasmacytoid dendritic cells by releasing self-DNA-peptide complexes in systemic lupus erythematosus. *Sci Transl Med*. 2011;3(73):73ra19.

126. Garcia-Romo GS, Caielli S, Vega B, et al. Netting neutrophils are major inducers of type I IFN production in pediatric systemic lupus erythematosus. *Sci Transl Med*. 2011;3(73):73ra20.

127. Sangaletti S, Tripodo C, Chiodoni C, et al. Neutrophil extracellular traps mediate transfer of cytoplasmic neutrophil antigens to myeloid dendritic cells toward ANCA induction and associated autoimmunity. *Blood*. 2012;120(15):3007-3018.

128. Yasuda T, Iida R, Kawai Y, et al. Serum deoxyribonuclease I can be used as a useful marker for diagnosis of death due to ischemic heart disease. *Leg Med (Tokyo)*. 2009;11 Suppl 1:S213-215.

129. Meng W, Paunel-Gorgulu A, Flohe S, et al. Deoxyribonuclease is a potential counter regulator of aberrant neutrophil extracellular traps formation after major trauma. *Mediators Inflam*. 2012;2012:149560.

130. Dylan B. Blood on the tracks. New York: Columbia,; 1975.

Chapter 2

Neutrophil histone modification by peptidylarginine deiminase 4 is critical for deep vein thrombosis in mice

This chapter contains one published manuscript:

Martinod K, Demers M, Fuchs TA, Wong SL, Brill A, Gallant M, Hu J, Wang Y, Wagner DD. *Neutrophil histone modification by peptidylarginine deiminase 4 is critical for deep vein thrombosis in mice*. Proc Natl Acad Sci. 2013 May 21; 110 (21): 8674-9. Epub 2013 May 6. PMCID: 3666755.

Section 2.1: Overview and Attributions

Overview

As discussed in the previous chapter, NETs are found in various thrombotic settings, including deep vein thrombi which are platelet, leukocyte, and red blood cell-rich. The lab routinely studies genetically modified animals in the IVC stenosis model of DVT. This model activates the endothelium directly distal to the ligation to release the contents of Weibel-Palade bodies in the absence of endothelial cell injury. Thrombi that form are morphologically similar to those found in human venous thromboembolism patients, and therefore this model is highly relevant. In the Brill et al. study[1] (Appendix A-3), it was shown that infusion of DNase prior to IVC ligation rendered mice highly protected from forming thrombi. Also, neutrophil depletion was shown to greatly decrease the size of thrombi that form in WT mice[2]. We aimed to study the $PAD4^{-/-}$ mice because of their complete inability to form NETs, and therefore subjected them to the IVC stenosis model. We were surprised by how strong the phenotype was, and therefore we investigated to see if the mice had any inherent defects in endothelial, leukocyte, or platelet activation. In all respects other than NETosis and thrombus initiation, the mice responded normally. Also, mice were able to form platelet plugs in response to vessel injury, and therefore NETs are not highly contributing to basic hemostasis.

Supplemental figures are provided in Appendix A-1.

Attributions

For this chapter, I performed all deep vein thrombosis surgeries and analyses related to the inferior vena cava (IVC) stenosis model, and was responsible for breeding PAD4$^{-/-}$ animals to establish and maintain a colony fully backcrossed to the C57Bl/6J background. Melanie Demers taught me how to properly isolate platelets for platelet aggregation studies. She also taught me how to prepare animals for intravital microscopy, used for the ferric chloride mesenteric venule injury and to measure leukocyte rolling after infusion of activated platelets. We performed all intravital microscopy experiments together and I analyzed the results independently. I learned from Tobias Fuchs how to harvest IVCs after stenosis to visualize leukocyte/platelet aggregates along the vessel wall. He quantified the number of leukocytes adherent in WT vs PAD4$^{-/-}$ animals. Siu Ling Wong performed hematoxylin and eosin staining of thrombus sections and showed me how to identify extracellular DNA patterns using this technique which she had previously developed to look at NETs in skin wounds. Maureen Gallant isolated bone marrow neutrophils for infusion into mice with DVT surgery and helped to prepare cryosections of thrombi for immunostaining. Yanming Wang at Pennsylvania State University kindly provided the *PAD4*$^{-/-}$ mice his lab generated for us to establish our colony, and provided helpful advice. His graduate student, Jing Hu, performed 2 generations of the backcross prior to their arrival in our lab. Denisa Wagner supervised the study, designed experiments, and we wrote the paper together.

I thank Tanya N. Mayadas for helpful discussions and for the method of neutrophil infusion, Stephen M. Cifuni for irradiating mice for bone marrow chimera generation, and Lesley Cowan for assistance in manuscript preparation.

Section 2.2: Neutrophil histone modification by peptidylarginine deiminase 4 is critical for deep vein thrombosis in mice

Kimberly Martinod[1,2], Melanie Demers[2,3], Tobias A. Fuchs[2,3], Siu Ling Wong[2,3], Alexander Brill[2,3], Maureen Gallant[2], Jing Hu[4], Yanming Wang[4], Denisa D. Wagner[2,3,5*]

[1]Immunology Graduate Program, Division of Medical Sciences, Harvard Medical School, Boston, Massachusetts, USA

[2]Program in Cellular and Molecular Medicine, Boston Children's Hospital, Boston, Massachusetts, USA

[3]Department of Pediatrics, Harvard Medical School, Boston, Massachusetts, USA

[4]Center for Eukaryotic Gene Regulation, Department of Biochemistry and Molecular Biology, Pennsylvania State University, University Park, Pennsylvania, USA

[5]Division of Hematology/Oncology, Boston Children's Hospital, Boston, Massachusetts, USA

*Correspondence: Denisa D. Wagner, Boston Children's Hospital, 3 Blackfan Circle, Third Floor, Boston, MA, 02115, USA. Ph. 617-713-8300, Fax 617-713-8333, denisa.wagner@childrens.harvard.edu

Abstract:

Deep vein thrombosis and pulmonary embolism are a major health problem associated with high mortality. Recently, DNA-based neutrophil extracellular traps (NETs) resulting from the release of decondensed chromatin were found to be part of the thrombus scaffold and to promote coagulation. However, the significance of nuclear decondensation and NET generation in thrombosis is largely unknown. To address this, we adopted a stenosis model of deep vein thrombosis and analyzed venous thrombi in peptidylarginine deiminase 4 (PAD4) -deficient mice that cannot citrullinate histones, a process required for chromatin decondensation and NET formation. Intriguingly, less than 10% of $PAD4^{-/-}$ mice produced a thrombus 48 hours after inferior vena cava stenosis whereas 90% of wild-type mice did. Neutrophils were abundantly present in thrombi formed in both groups, while extracellular citrullinated histones were seen only in thrombi from wild-type mice. Bone marrow chimera experiments indicated that PAD4 in hematopoietic cells was the source of the prothrombotic effect in deep vein thrombosis. Thrombosis could be rescued by infusion of wild-type neutrophils suggesting that neutrophil PAD4 was important and sufficient. Endothelial activation and platelet aggregation were normal in $PAD4^{-/-}$ mice, as was hemostatic potential determined by bleeding time and platelet plug formation after venous injury. Our results show that PAD4-mediated chromatin decondensation in the neutrophil is crucial for pathological venous thrombosis and unveil neutrophil activation and PAD4 as potential drug targets for deep vein thrombosis.

Introduction

Venous thromboembolism is associated with high mortality, with approximately 300,000 deaths resulting from an estimated 900,000 cases in the US annually[3]. Neutrophil extracellular traps (NETs) are produced by a novel cell death pathway shown to be important in innate immunity against microbes[4-7]. Recently, NETs were also shown to be involved in thrombosis by binding erythrocytes and platelets[8], and in promoting coagulation by degrading tissue factor pathway inhibitor[9]. Coagulation, platelets, neutrophils and NETs have all been implicated in thrombus generation in mouse models of deep vein thrombosis (DVT)[1,2,10]. Also, certain cancers associated with neutrophilia result in an increased propensity of circulating neutrophils to form NETs and spontaneous thrombosis [11]. NETs are comprised of decondensed chromatin fibers lined with antimicrobial proteins such as neutrophil elastase and myeloperoxidase[4]. A proteomic analysis identified histones as the major protein component of NETs[12]. Histones are highly cytotoxic to the surrounding environment into which NETs are released[13,14], and can enhance thrombin generation[15]. Histone infusion leads to rapid Weibel-Palade body (WPB) secretion from endothelial cells, promoting platelet and leukocyte adhesion and leading to accelerated thrombus generation[1]. Pretreatment with DNase 1, which can degrade NETs, reduces thrombus incidence in wild-type (WT) mice[1,2]. Neutrophils play an important role, as neutrophil depletion greatly reduces thrombus weight in this model[2]. Whether NETs are involved in the pathogenesis of DVT or whether they are merely a

consequence of leukocyte recruitment to the thrombus is unknown. Similarly, the role of NETs in normal platelet plug formation in response to injury, where their presence was also observed[9], remains to be addressed.

While the cellular changes occurring in the neutrophil during NETosis have been well described, the molecular players and processes leading to NET formation are incompletely defined. A critical step in NET formation is the decondensation of chromatin that occurs in the nucleus. Peptidylarginine deiminase 4 (PAD4) is a nuclear enzyme that converts specific arginine residues to citrulline on histone tails. Upon PAD4 activation, histones can become hypercitrullinated at histone H3Arg-8 and -17 or histone H4Arg3 residues, resulting in the extensive chromatin decondensation that leads to nuclear delobulation and swelling during NETosis[16,17]. PAD4-deficient mice are incapable of decondensing chromatin or forming NETs[18], while overexpression of PAD4 is sufficient to drive chromatin decondensation to form NET-like structures in cells that normally do not form NETs[19]. Since NETs are present in pathological thrombi and their dissolution by DNase 1 reduced the frequency of DVT, it was important to address the role of histone modification by PAD4 in the process of NET formation and its involvement in thrombosis.

Results

PAD4$^{-/-}$ neutrophils fail to produce NETs in response to LPS or ionomycin

PAD4 is a calcium-dependent enzyme with a nuclear localization signal that distinguishes it from other PAD family members[20,21]. The enzyme is

activated by Ca^{2+} [17], therefore the calcium ionophore ionomycin was used to induce histone hypercitrullination in isolated peripheral blood murine neutrophils (Fig. 2.1*A*). This led to NET formation in WT and $PAD4^{+/-}$ neutrophils, whereas $PAD4^{-/-}$ neutrophils did not citrullinate histone H3 or form NETs (Fig. 2.1*A*, 2.1*B*). Lipopolysaccharide (LPS) from *Klebsiella pneumoniae* was also unable to induce histone citrullination or NETs in $PAD4^{-/-}$ neutrophils, whereas it is a potent inducer of NETosis in WT neutrophils (Fig. 2.1*A*, 2.1*B*). Moreover, immunostaining showed H3Cit-positive NETs being released from WT neutrophils, while in $PAD4^{-/-}$ neutrophils H3Cit staining was absent (Fig. 2.1*C*). Although $PAD4^{-/-}$ nuclei lost their lobulated shape characteristic of neutrophils, they did not swell, indicating that nuclear decondensation is not occurring in $PAD4^{-/-}$ mice and confirming that other PAD enzymes do not compensate for PAD4 deficiency *in vitro.* Ionomycin-induced NETosis has been shown to be independent of reactive oxygen species[22] and here we show that it is dependent on PAD4. Thus, $PAD4^{-/-}$ neutrophils have shown a complete inability to produce NETs[18] (Fig. 2.1*B*).

$PAD4^{-/-}$ mice are protected in the venous stenosis model of DVT

Biomarkers of NETs are abundant in baboon[8] and mouse DVT[1]. We performed the venous stenosis model of DVT in mice[10]. Briefly, the inferior vena cava (IVC) is ligated to induce a 90% restriction in blood flow. This results in the formation of a thrombus that is macroscopically similar to human deep vein thrombi. It contains a platelet-rich white portion (distal to the ligation site) and an

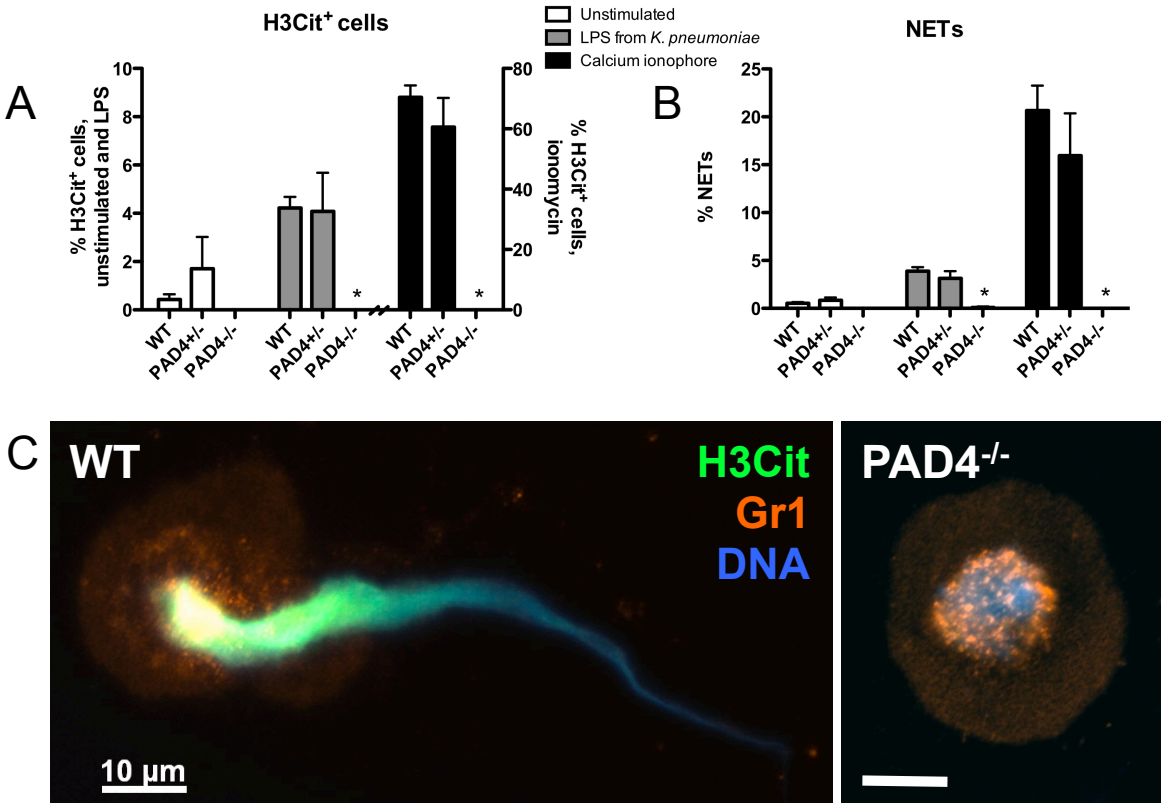

Figure 2.1. PAD4 is necessary for NET formation in response to Ca^{2+} ionophore and LPS from *Klebsiella pneumoniae*. A, B. Neutrophils isolated from WT and $PAD4^{+/-}$ mice became hypercitrullinated at histone H3 (A) and form NETs (B) in response to stimulation with LPS or ionomycin for 2 h. Stimulated $PAD4^{-/-}$ neutrophils were negatively stained by an antibody recognizing histone H3 citrullination at residues 2, 8, and 17 and did not form NETs. C. Representative micrographs of ionomycin stimulated cells showing an H3Cit-positive NET emerging from a WT neutrophil and a condensed, delobulated nucleus in a $PAD4^{-/-}$ neutrophil. H3Cit staining was absent in $PAD4^{-/-}$ neutrophils. H3Cit, green; Gr1 antigen on plasma membrane, orange; DNA, blue. Representative of n=4, scale bar, 10 µm. *$p<0.05$

erythrocyte-rich red portion (proximal to the ligation site). Since PAD4-deficient mice do not form NETs *in vitro*, we hypothesized that NET formation would be greatly impaired in these mice during thrombosis and this may affect thrombus formation and/or stability. PAD4$^{-/-}$ mice were partially protected from producing venous thrombi early after stenosis, with only 28.6% of PAD4$^{-/-}$ mice forming thrombi at 6 h compared to 66.7% of WT mice (p=0.04, Fig. 2.2*A*). Thrombi that formed in PAD4$^{-/-}$ mice were similar in length to WT thrombi (Fig. 2.2*B*). PAD4$^{-/-}$ mice also maintained normal platelet counts compared to control sham-operated animals and after stenosis had significantly higher platelet counts than WT mice (Fig. 2.2*C*). In contrast to the diffuse extracellular H3Cit pattern in thrombi previously described at 48 h[1], immunostaining revealed that the majority of H3Cit was nuclear rather than extracellular in the WT thrombi at this early time point (Fig. S2.1*A*), while H3Cit staining was not detected in PAD4$^{-/-}$ thrombi (Fig. S2.1*B*, WT, 28.3 ± 0.75 H3Cit^{+} cells per mm^2; PAD4$^{-/-}$, no H3Cit^{+} cells detected. n=4). The thrombi presented similar histological morphologies with comparable density of leukocytes as seen by hematoxylin and eosin staining (Fig. S2.1*C*). To see if this early protection could be a result of delayed thrombus formation in PAD4$^{-/-}$ mice, we next maintained stenosis for 48 h, when the great majority of WT mice form a thrombus[10], and found that while 90% of WT stenotic vessels thrombosed, fewer than 10% of PAD4$^{-/-}$ mice had a thrombus at this time point (p=0.0002, Fig. 2.2*D*, 2.2*E*). Thrombocytopenia was associated with thrombus formation in WT mice, while PAD4$^{-/-}$ mice retained normal platelet levels (Fig. 2.2*F*). Thus, platelets are likely consumed by the thrombus. It is important to note that at

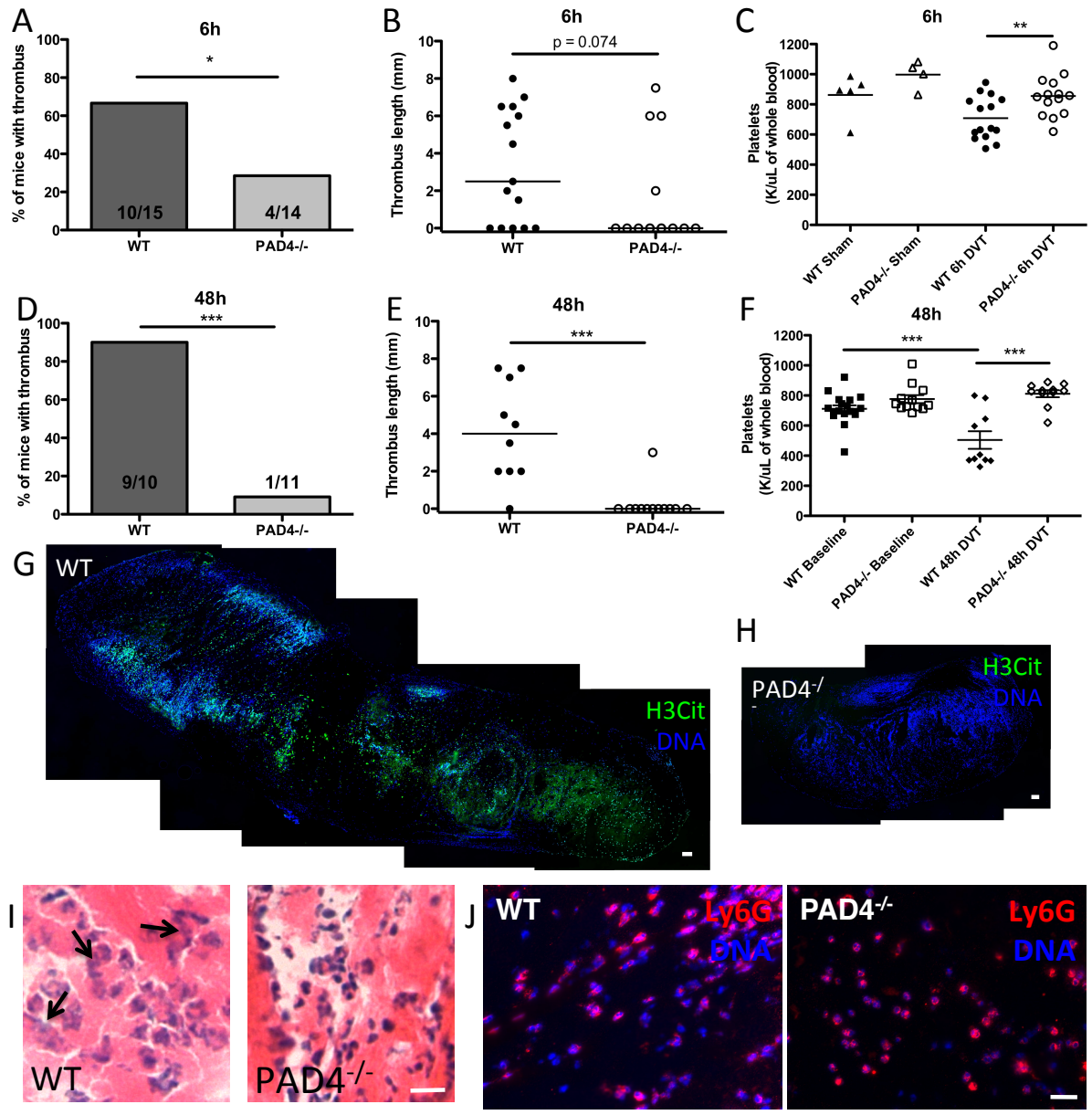

Figure 2.2. PAD4$^{-/-}$ mice are protected from DVT, especially at 48 h after stenosis. A,B. PAD4$^{-/-}$ mice were less likely to form thrombi at 6 h than WT mice. C. Platelet count is decreased in WT compared to PAD4$^{-/-}$ mice after 6 h in the venous stenosis model. D,E. At 48 h, only one small thrombus was present in a PAD4$^{-/-}$ mouse, while all but one of the WT mice had thrombi. F. WT and PAD4$^{-/-}$ mice have similar platelet counts before stenosis (Baseline). WT mice are thrombocytopenic at 48 h, while platelet counts remain stable in PAD4$^{-/-}$ mice. G,H. Composite image of a section from an entire thrombus collected at 48 h showing diffuse, extracellular H3Cit (green) staining in a WT mouse (G), which is completely absent in the sole thrombus from a PAD4$^{-/-}$ mouse (H). Hoechst staining of DNA is shown in blue and shows extensive presence of leukocytes in both thrombi. Scale bars, 100 µm. I. H&E staining of 48 h thrombi shows less dense nuclear staining and diffuse, likely extracellular, DNA (arrows) in WT

Figure 2.2 (Continued). thrombi compared to dense nuclei found in the PAD4$^{-/-}$ thrombus. Scale bar, 20 μm. J. Thrombi collected from WT mice or the PAD4$^{-/-}$ mouse that formed a thrombus 48 h after IVC stenosis showed an abundance of neutrophils by Ly6G immunostaining (red). Scale bar, 20 μm. DNA is shown in blue. *p<0.05, **p<0.01, ***p<0.001

baseline, WT and PAD4$^{-/-}$ mice had similar platelet counts (Fig. 2.2*F*). The extracellular H3Cit meshwork seen in WT thrombi at 48 h post ligation was again completely absent in the sole PAD4$^{-/-}$ thrombus, indicating that also *in vivo*, only PAD4 modifies histone H3 to produce H3Cit (Fig. 2.2*G*, 2.2*H*). Hematoxylin and eosin staining revealed many swollen neutrophil nuclei in WT thrombi, while the PAD4$^{-/-}$ thrombus contained smaller and more dense neutrophil nuclei (Fig. 2.2*I*). Neutrophils are abundantly present within WT thrombi at 48 h[1], and also in the only thrombus in the PAD4$^{-/-}$ mouse (Fig. 2.2*J*), suggesting that neutrophils are recruited to the PAD4$^{-/-}$ thrombus. NETs were absent in the single small PAD4$^{-/-}$ thrombus we obtained and analyzed by immunofluorescence staining. Thus, PAD4 deficiency was highly protective in the DVT mouse model at 48h, when in WT mice extracellular chromatin is prominently displayed[1] (Fig. 2.2*G*).

Endothelial activation and platelet function are not affected by PAD4 deficiency

Although PAD4 is highly expressed in neutrophils, it is also present at lower levels in many cell types, where citrullination of histones may regulate gene expression[17,23]. Therefore, it was important to establish in which cell type PAD4 was responsible for this prominent role in pathological thrombosis. First, we wished to investigate whether endothelial release of adhesion molecules for platelets and leukocytes, von Willebrand factor (VWF) and P-selectin, from WPBs occurs normally in PAD4$^{-/-}$ mice. Both VWF and P-selectin were determined to be important in the stenosis model of DVT[2,10]. We turned to a time point (6 h) by which WPBs have been released, resulting in massive platelet

and neutrophil adhesion to the endothelium[10]. Platelet/leukocyte adhesion and aggregate formation on the IVC vessel wall were similarly present in both WT and PAD4$^{-/-}$ IVCs 6 h after stenosis (Fig. 2.3*A*; WT 8.97 ± 0.50, PAD4$^{-/-}$ 13.56 ± 2.11 leukocytes per 200 μm of vessel wall, p=0.10, n=3).

Another way to examine the capacity of mice to release WPBs is by infusion of activated platelets, which results in systemic WPB release from endothelial cells and consequently increases leukocyte rolling in veins[24]. Leukocyte rolling occurred in both WT and PAD4$^{-/-}$ mice to a similar extent over baseline 2 h after activated platelet infusion (Fig. 2.3*B*, 2.2*C*), an interaction that is dependent on endothelial P-selectin and PSGL-1 on leukocytes[24]. Plasma VWF levels were similarly elevated in WT and PAD4$^{-/-}$ mice 2 h after platelet infusion (WT 154.6 ± 8.24%, PAD4$^{-/-}$ 140.0 ± 21.8% of control pooled plasma, n=4, p=0.56). Taken together, the protection of PAD4$^{-/-}$ mice in DVT is not due to a defect in endothelial activation leading to VWF and P-selectin release, nor in the initial leukocyte and platelet adhesion to the vessel wall which is essential for thrombus initiation in venous stenosis[2,10]. Since PAD4 could be expressed in megakaryocytes and thus affect the properties of platelets, we next evaluated the PAD4$^{-/-}$ platelets. As Fig. 2.2*F* shows, at baseline the platelet count in PAD4$^{-/-}$ mice was normal. PAD4$^{-/-}$ platelets aggregated normally in response to low and high doses of thrombin (Fig. 2.3*D*, 2.2*E*). This shows that, in general, platelet activation, granule secretion, and integrin activation are not affected in these mice. We then examined *in vivo* models in which platelets respond to injury by forming a platelet plug: tail bleeding time and the ferric chloride model of

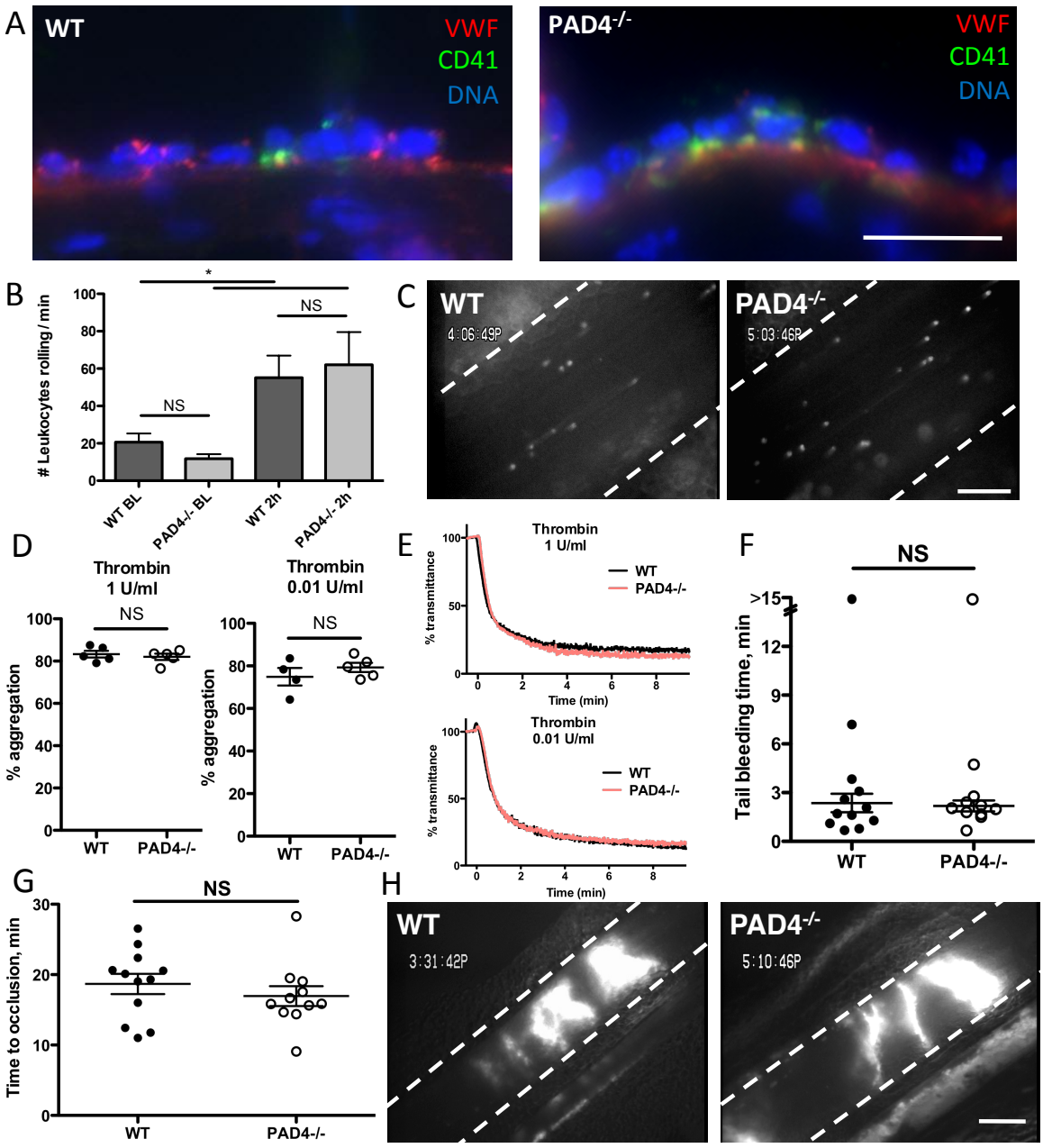

Figure 2.3. Normal adhesive interactions among platelets, leukocytes, and endothelium in PAD4$^{-/-}$ mice. A. Representative images of platelets, leukocytes, and platelet-leukocyte aggregates on endothelium in WT (left) or PAD4$^{-/-}$ (right) IVCs collected 6 h after ligation. VWF, red; CD41 (platelets), green; DNA, blue. n=3-4. Scale bar, 20 μm. B,C. Activated platelets were infused into WT or PAD4$^{-/-}$ mice. B. Leukocyte rolling was assessed in mesenteric venules by counting the number of cells crossing a defined line per minute. Baseline leukocyte rolling was determined in untreated mice. n=4-6. C. Representative still images from intravital microscopy movies showing numerous rolling leukocytes 2 h after activated

Figure 2.3 (Continued). platelet infusion in WT or PAD4$^{-/-}$ mice. Scale bar, 100 μm. D,E. Aggregometry of washed platelets stimulated with thrombin at 1 U/ml or 0.01 U/ml. D. Maximum aggregation was similar between WT and PAD4$^{-/-}$ mice. E. Representative traces showing similar kinetics of aggregation between WT and PAD4$^{-/-}$ platelets. Red line, PAD4$^{-/-}$; black line, WT. n=4-5. F. A 2 mm tail segment was transected and bleeding monitored for 15 min. The time to the first cessation in bleeding was recorded for each mouse. One mouse from each group failed to stop bleeding and these were determined to be statistical outliers using Grubb's test and excluded from means. G,H. Venous thrombosis after injury. Mesenteric venules were externalized and injured with application of 10% $FeCl_3$-soaked filter paper for 5 min. G. Time to vessel occlusion was measured and found to be similar in WT and PAD4$^{-/-}$ mice. H. Representative images of occlusive thrombi formed in WT (left) or PAD4$^{-/-}$ mice (right). n=11-12. Scale bar, 200 μm.

thrombosis. Tail tip transection results in severing of both veins and artery and the rapid cessation of blood flow depends on platelet function and coagulation. Time to cessation of bleeding was similar in WT and PAD4$^{-/-}$ mice (Fig. 2.3*F*), indicating that these mice have normal hemostatic potential. In the venous stenosis model, flow restriction leads to WPB secretion potentially due to local hypoxia[25], resulting in platelet-leukocyte interactions with the endothelium. In the ferric chloride model, by contrast, oxidative injury removes the endothelium and exposes circulating blood to the subendothelial matrix[26]. Platelets bind to the subendothelium via GPIb, integrins, and GPVI, then become activated and aggregate via integrin receptors[27]. We visualized thrombus formation in $FeCl_3$-injured mesenteric venules using intravital microscopy and found that PAD4$^{-/-}$ mice formed occlusive thrombi with similar kinetics (Fig. 2.3*G*) and thrombus morphologies (Fig. 2.3*H*) as WT mice. Thus, we have no evidence that PAD4 or NETs play a significant role in hemostasis in healthy mice. For platelet plug formation in the injured veins, coagulation is likely driven by vessel wall tissue factor and the enhancement of coagulation and thrombosis by NETs may not be necessary.

Neutrophil PAD4 is a key player in pathological thrombus formation

To assess whether the influence of PAD4 was of hematopoietic origin, we generated bone marrow (BM) chimeras by infusing WT or PAD4$^{-/-}$ BM cells into lethally irradiated WT recipients. Both groups of mice recovered body mass with similar kinetics (Fig. S2.2*A*). To test the chimerism, we stimulated leukocytes

from whole blood after red blood cell (RBC) lysis with ionomycin and found that the PAD4$^{-/-}$ BM chimeras failed to hypercitrullinate arginine residues at histone H3 (Fig. S2.2*B*, S2.2*C*). Similar to the thrombus formation frequencies in WT and PAD4$^{-/-}$ mice, a majority (6 out of 7) of WT BM chimeras produced thrombi after 48 h of stenosis, while only 1 of the 7 PAD4$^{-/-}$ BM chimeras formed a small thrombus (Fig. 2.4*A*, 2.4*B*). The H3Cit pattern within thrombi paralleled the results seen in WT and PAD4$^{-/-}$ mice, with extracellular H3Cit present in the thrombi of WT BM chimeras but H3Cit staining absent in the PAD4$^{-/-}$ BM chimera thrombus (Fig. S2.2*D*, S2.2*E*). WT BM chimeras became thrombocytopenic 48 h post stenosis, while PAD4$^{-/-}$ BM chimeras maintained normal platelet counts (Fig. 2.4*C*).

As PAD4 is expressed by other leukocytes besides neutrophils[28,29] that may enter the thrombus, we investigated whether the infusion of WT neutrophils could rescue thrombosis in PAD4$^{-/-}$ mice at 48 h. Infusing 4-5 x 10^6 isolated WT BM neutrophils into PAD4$^{-/-}$ mice restored thrombus generation (Fig. 2.4*D*, 2.4*E*). Although a significant lowering of platelet count was not achieved by neutrophil infusion (Fig. 2.4*F*), mice that had formed a thrombus in either WT and PAD4$^{-/-}$ recipients, did, however, have a significant decrease in platelet count compared to baseline levels (Fig. S2.3). Infused neutrophils were of >95% purity as assessed by Wright-Giemsa staining (Fig. S2.4*C*). The thrombi from neutrophil-infused PAD4$^{-/-}$ mice contained large numbers of Ly6G$^+$ neutrophils, while F4/80$^+$ monocytes/macrophages were rarely seen within all thrombi examined (Fig. S2.4*A*, S2.4*B*, S2.4*D*). Thrombi were analyzed by immunofluorescence and

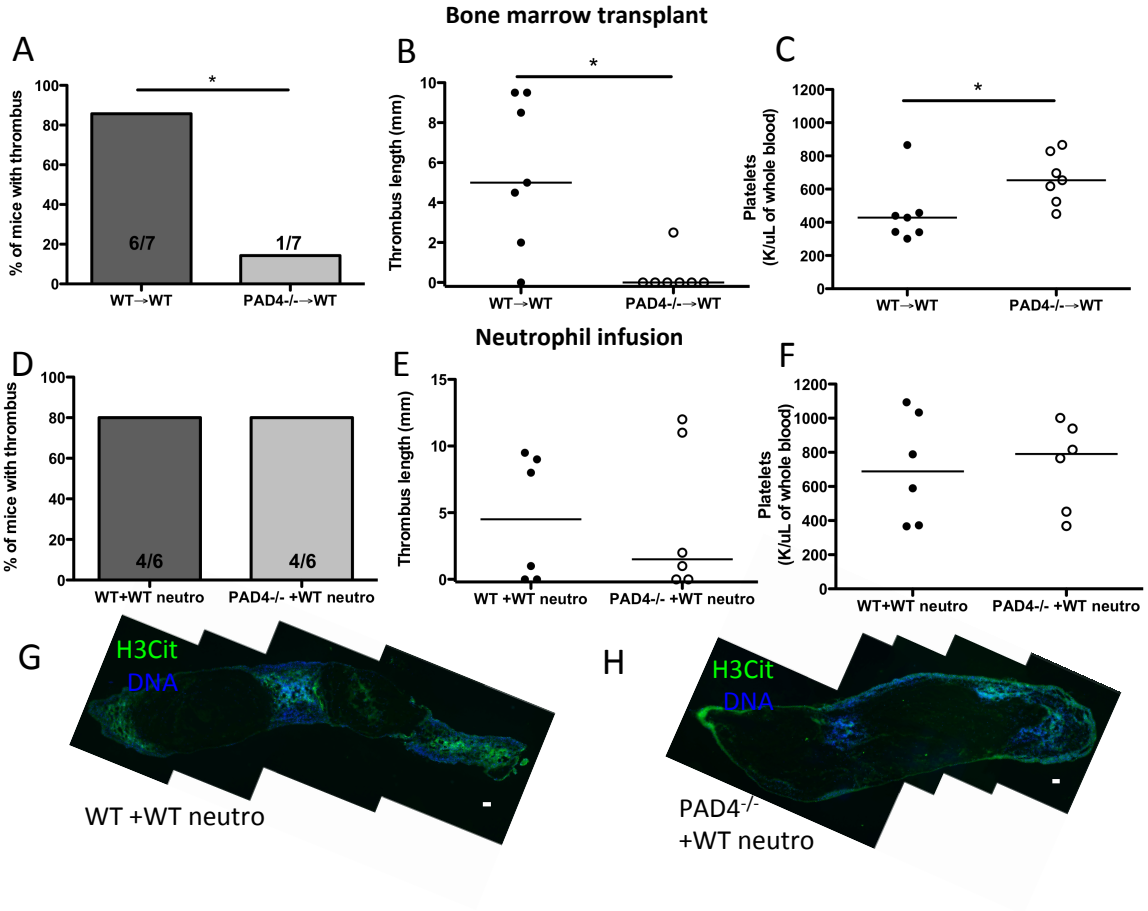

Figure 2.4. Venous thrombosis depends on the presence of PAD4 in neutrophils. A-C. Chimeric mice were generated by infusing WT or PAD4$^{-/-}$ BM cells into lethally irradiated WT recipients and later subjected to 48 h IVC stenosis. A. Percent of BM chimeras that produced thrombi. B. Length of thrombi. C. Platelet counts in BM chimeras 48 h after DVT surgery. WT→WT BM chimeras became thrombocytopenic, while PAD4$^{-/-}$→WT BM chimeras maintained normal platelet counts. D-H. WT or PAD4$^{-/-}$ mice received an *i.v.* infusion of 4-5 x 10^6 WT neutrophils immediately prior to DVT surgery and 2-2.5 x 10^6 neutrophils at 24 h. D, E. A majority (80%) of both WT and PAD4$^{-/-}$ mice formed thrombi after the infusion of WT neutrophils. F. Similar platelet counts were measured 48 h after IVC ligation in WT and PAD4$^{-/-}$ mice infused with WT neutrophils. G, H. Composite images of thrombi collected from mice infused with WT neutrophils. H3Cit-positive nuclei and extracellular staining was detected in WT (G) and PAD4$^{-/-}$ (H) thrombi, indicating that the infused WT neutrophils integrated into the PAD4$^{-/-}$ thrombus. H3Cit, green; DNA, blue. Representative of n=4. Scale bar, 100 μm. * $p<0.05$.

extracellular H3Cit staining was present within both WT and PAD4$^{-/-}$ recipient thrombi after WT neutrophil infusion (Fig. 2.4*G*, 2.4*H*), indicating that the WT neutrophils were incorporated and produced NETs in the thrombus scaffold in PAD4$^{-/-}$ recipient mice. Therefore, PAD4 within neutrophils is important for formation of stable thrombi in large veins, as the defect in thrombosis in PAD4$^{-/-}$ mice can be rescued by supplementation with WT neutrophils.

Discussion

For more than 150 years, hypercoagulable state, hypoxia due to flow disturbance such as in valves or stasis, and vascular activation were recognized as the main players in DVT[30]. Only recently has the active contribution of blood cells to DVT begun to be appreciated. First, the complex role of inflammatory cells was recognized in that they promote thrombosis, for example through production of tissue factor, and also contribute to thrombus resolution[31]. Second, the important role of platelets in DVT has been described in animal models and human trials[1,32,33]. Venous pathological thrombi were thought to be formed by fibrin and trapped RBCs and the main treatment in humans is still anti-coagulation. It is now clear that pathological thrombus formation and stabilization are much more complex, with many platelets and leukocytes present, and even the RBCs may not be trapped but rather actively recruited to the thrombus by NETs[8]. Thus, new treatment options are being revealed.

Here we present a new facet of DVT, the importance of neutrophil post-translational modification and chromatin decondensation, factors dramatically

influencing outcome of stenosis-induced DVT in mice. The enzyme PAD4 allows for dissociation of heterochromatin protein 1-β [19], affects linker histone H1[16], and reduces the positive charge of histones by arginine citrullination, thus allowing nucleosomes to unravel and chromatin to be expelled from the swollen nuclei. Absence of NETosis resulted in the formation of fewer thrombi in PAD4$^{-/-}$ mice early after the flow disturbance/hypoxia onset with almost no thrombi by 48 h. DVT represents the first non-infectious model in which the PAD4$^{-/-}$ mice are affected, and surprisingly to date this is the strongest phenotype described in these mice[18,34,35].

We have demonstrated that PAD4 deficiency does not perturb initial vessel wall activation and platelet-leukocyte adhesion. Also, platelets from PAD4 knockout mice are fully functional, and able to produce platelet plugs like WT platelets. The low incidence of DVT in PAD4$^{-/-}$ mice is largely caused by a lack of PAD4 in neutrophils as WT neutrophils could rescue the DVT process. The protection in PAD4$^{-/-}$ mice from DVT is due to the failure of neutrophils to form NETs as the PAD4$^{-/-}$ neutrophils interact properly with the vessel wall and are present in the rare thrombi that form in PAD4$^{-/-}$ veins. Our observation of less extracellular H3Cit in WT thrombi at 6 h than at 48 h (Fig S2.1, Fig. 2.2) fits well with the report of von Bruhl and colleagues[2] showing that neutrophils begin to throw NETs by 3 h in this DVT model, but the prominent diffuse staining pattern of NETs is present only later, at 48 h. Thus, NETs comprise a crucial part of the pathologic thrombus scaffold, and the lack of NETs formation results in fewer thrombi early on which appear not to be sustained over time.

Our observations help to pinpoint the importance of neutrophils and NETs in thromboembolic disease. Inhibitors of neutrophil activation in the thrombus, inhibitors of PAD4 activation or inhibitors of NET release would all impact DVT outcome. Therapeutic interventions combining both DNases and proteolytic enzymes may improve thrombolysis in patients with DVT. In addition, specific PAD4 inhibitors are not likely to impair hemostasis or neutrophil function in thrombus resolution. Thus, a better understanding of the complexity of pathological thrombosis, including the process of chromatin decondensation in neutrophils, will bring us closer to devising more effective and targeted treatments.

Materials and Methods

Mice

Experimental procedures in this study were reviewed and approved by the Institutional Animal Care and Use Committee of Boston Children's Hospital (Protocol No. 11-03-1919, 11-04-1848, 11-03-1941). WT mice were purchased from Jackson Laboratory. $PAD4^{-/-}$ mice have been recently backcrossed to C57Bl/6J for 7 or more generations.

Neutrophil isolation for in vitro NET assays.

Peripheral blood was collected via the retroorbital venous plexus and neutrophils were isolated from 6-10 week-old male or female WT, $PAD4^{+/-}$, or $PAD4^{-/-}$ mice as previously described [11]. Cells were routinely assessed to be >90% pure by

Wright-Giemsa stain. Neutrophils in RPMI/HEPES were allowed to adhere at 37°C in 5% CO_2 to glass-bottom plates for 20 min prior to stimulation with 10 μg/ml LPS from *Klebsiella pneumoniae* (Sigma) or 4 μM ionomycin (Invitrogen). After 2 h, cells were fixed in 2% PFA.

Venous stenosis model

Venous stenosis experiments were performed as previously described[10]. Mice were anesthetized with 3.5% isoflurane and anesthesia maintained at 2% in 100% oxygen. A midline laparotomy was performed and the inferior vena cava exposed. Any side branches between the renal and iliac veins were ligated with 7/0 polypropylene suture. A 30 G spacer was placed parallel to the inferior vena cava and 7/0 polypropylene suture was used to partially ligate the IVC to ~10% of its original diameter. The spacer was removed and the mouse sutured and allowed to recover. After 6 h or 48 h, mice were anesthetized with isoflurane, blood was collected via the retroorbital sinus plexus, and the IVCs exposed to allow for collection of the inferior vena cava vessel wall or thrombi formed within the IVC. Thrombus length was measured and thrombi were embedded in OCT for cryosectioning. All mice were given buprenorphine (0.1 mg/kg, s.c.) as an analgesic immediately prior to surgery and every 8-12 h subsequently.

Immunostaining and fluorescence microscopy

Fixed cells or tissue sections were washed with PBS and permeabilized (0.1% Triton X-100, 0.1% sodium citrate) for 10 min at 4°C. Samples were blocked with

3% BSA for 90 min at 37°C, rinsed, and then incubated overnight at 4°C or for 1 h at 37 °C in antibody dilution buffer containing 0.3% BSA, 0.1% Tween-20, and either rabbit anti-histone H3 (citrulline 2, 8, 17) (0.3 µg/ml, ab5103, abcam), rat anti-Gr1 (0.5 µg/ml, clone RB6-8C5, eBioscience), rat anti-Ly6G (0.5 µg/ml, clone 1A8, Biolegend, San Diego, CA), or rat anti-F4/80 (1:250, ab16911, abcam). After several washes, samples were incubated for 2 h at room temperature in antibody dilution buffer containing Alexa Fluor®-conjugated secondary antibodies in 0.3% BSA in DPBS: goat anti–rat immunoglobulin (IgG) (Alexa555, 2 µg/mL), donkey anti–rabbit IgG (Alexa488, 1.5 µg/mL), or donkey anti–sheep IgG (Alexa568, 2 µg/mL, Invitrogen). DNA was counterstained with 1 µg/ml Hoechst 33342 and slides coverslipped with Fluoromount gel (Electron Microscopy Sciences). Fluorescent images were acquired using an Axiovert 200 widefield fluorescence microscope (Zeiss) in conjunction with an Axiocam MRm monochromatic CCD camera (Zeiss) and analyzed with Zeiss Axiovision software. All channels were acquired in greyscale and pseudocolored using Zeiss Axiovision or ImageJ software (National Institutes of Health, Bethesda, MD, USA). Exposure times are identical between WT and PAD4$^{-/-}$ thrombi or neutrophils. Composite images were generated with the MosaicJ plugin[36] for ImageJ software.

Platelet counts

Whole blood was collected via the retroorbital sinus into EDTA-coated capillary tubes. Twenty-five µl of blood was analyzed by a Hemavet 950FS (Drew Scientific) for complete blood counts.

Platelet aggregation

Murine blood was collected in 10% (v/v) sodium citrate (3.2%) and centrifuged at 800g for 10 min. Platelet rich plasma was collected and PGI_2 added in Tyrode's buffer. Platelets were washed and resuspended in Tyrode's buffer and incubated at 37°C. 2.5 x 10^5 platelets per µl were analyzed using a Chronolog Platelet aggregometer. 1 U/ml or 0.01 U/ml of thrombin in the presence of calcium chloride were used as agonists for aggregation and samples were analyzed for at least 10 min.

Tail bleeding time

Six to eight-week-old male or female C57Bl/6J or PAD4$^{-/-}$ mice were anesthetized using 2.5% tribromoethanol (300 mg/kg) administered intraperitoneally. A 2-mm segment of the tail tip was transected using a single edge razor blade and the tail was immediately submersed in 37°C PBS. Tail bleeding was monitored for 15 min and the time to stop was recorded when bleeding had stopped for more than 30 sec. All mice were sacrificed immediately at the end of the observation period.

Activated platelet-induced endothelial activation

Platelets were isolated from C57Bl/6J male or female mice as previously described[24]. Washed platelets were resuspended in Tyrode's buffer containing 2 mM EDTA and 0.2 U/ml thrombin and incubated for 15 min at 37°C before addition of 1 U/ml hirudin. 1 x 10^8 platelets were injected into 4-6-week old C57Bl/6J mice via the retroorbital sinus and plasma collected after 2 h for VWF analysis. For leukocyte rolling studies, 1 x 10^8 platelets were injected into 4-week-old WT or PAD4$^{-/-}$ males. After 2 h, rhodamine 6G was injected *i.v.* in order to fluorescently label leukocytes, and mesenteric venules externalized to visualize leukocyte rolling. One venule of between 200 to 300 microns in diameter was monitored per mouse. Leukocyte rolling was quantified for 3-5 independent minutes as the average number of cells rolling past a defined line across the vessel per minute. Baseline was determined in untreated animals.

$FeCl_3$- induced mesenteric venous thrombosis

Three to four-week-old C57Bl/6J or PAD4$^{-/-}$ male mice were anesthetized using 2.5% tribromoethanol (300 mg/kg) administered *i.p.* and the level of anesthesia verified by lack of response to footpad squeeze. Rhodamine 6G was given via retroorbital injection to fluorescently label platelets and leukocytes. A midline incision was performed and the intestines externalized to reveal mesenteric vessels. A single venule of between 200-300 microns in diameter was visualized for each mouse (WT mice, 222.2 ± 20.6 μm; PAD4$^{-/-}$ mice 239.0 ± 44.6 μm). A 1-mm x 3-mm piece of filter paper was soaked in 10% ferric chloride, gently placed

on the vessel for 5 min and then removed. Occlusion time was noted for each mouse. Vessels were considered occluded when blood flow had stopped for at least 10 sec.

Bone marrow chimera preparation and validation

Four-week-old C57Bl/6J males were lethally irradiated with 1100 rad and immediately given an *i.v.* injection of at least 1 x 10^7 bone marrow cells from either WT or PAD4$^{-/-}$ mice. Mice were housed in autoclaved cages, monitored daily and weighed every other day for one month. Six weeks post-irradiation, 100 µl of blood was collected from each mouse, RBCs lysed with ACK lysis buffer (Invitrogen), and leukocytes plated and stimulated with 4 µM ionomycin for 2 h. The total leukocyte population was studied rather than isolated neutrophils in order to minimize the volume of blood being drawn from mice prior to DVT surgeries. Immunostaining for H3Cit was performed to verify successful chimerism. Following blood collection, mice were allowed to recover for 2 weeks prior to DVT surgery.

Neutrophil infusion

Neutrophil adoptive transfer studies were performed as previously described[37]. BM neutrophils were isolated from 6-8 week-old C57Bl/6J WT mice using a Percoll™ (GE Healthcare Life Sciences) gradient and rapid hypotonic lysis. Bone marrow was flushed out of tibias and femurs using a 30 G needle into cold RPMI. Cells were pelleted, resuspended in PBS, and layered onto a Percoll gradient

containing 78%/69%/52% Percoll. Cells at the 78%/69% interface were collected and subjected to hypotonic lysis. Cells were counted using a hemacytometer and resuspended in RPMI. Purity was assessed by Wright-Giemsa staining, which was determined to be >95% neutrophils. 4-5 x 10^6 cells were injected *i.v.* through the retroorbital sinus immediately prior to DVT surgery. A second *i.v*. neutrophil infusion of 2-2.5 x 10^6 neutrophils was given at 24 h. Mice were sacrificed at 48 h and any resulting thrombi harvested for analysis.

Statistics

Data are presented as means ± SEM unless otherwise noted and were analyzed using a two-sided Student's t-test or Mann-Whitney U test. Thrombus frequencies were analyzed using chi-squared tests of contingency tables. All analyses were performed using GraphPad Prism software (Version 5.0). Results were considered significant at $p<0.05$. * $p<0.05$, ** $p<0.01$, ***$p<0.001$

Acknowledgments

We thank Tanya N. Mayadas for helpful discussions and for the method of neutrophil infusion, Stephen M. Cifuni for expert technical assistance, and Lesley Cowan for assistance in manuscript preparation. This work was supported by the National Heart, Lung, and Blood Institute of the National Institutes of Health grants R01 HL095091 and R01 HL041002 (to D.D.W.) and R01CA136856 (to Y.W.) K.M. was supported in part by a research grant from GlaxoSmithKline.

Section 2.3: Bibliography

1. Brill A, Fuchs TA, Savchenko AS, et al. Neutrophil extracellular traps promote deep vein thrombosis in mice. *J Thromb Haemost*. 2012;10(1):136-144.

2. von Bruhl ML, Stark K, Steinhart A, et al. Monocytes, neutrophils, and platelets cooperate to initiate and propagate venous thrombosis in mice in vivo. *J Exp Med*. 2012;209(4):819-835.

3. Raskob GE, Silverstein R, Bratzler DW, Heit JA, White RH. Surveillance for deep vein thrombosis and pulmonary embolism: recommendations from a national workshop. *Am J Prev Med*. 2010;38(4 Suppl):S502-509.

4. Brinkmann V, Reichard U, Goosmann C, et al. Neutrophil extracellular traps kill bacteria. *Science*. 2004;303(5663):1532-1535.

5. Brinkmann V, Zychlinsky A. Neutrophil extracellular traps: is immunity the second function of chromatin? *J Cell Biol*. 2012;198(5):773-783.

6. Fuchs TA, Abed U, Goosmann C, et al. Novel cell death program leads to neutrophil extracellular traps. *J Cell Biol*. 2007;176(2):231-241.

7. Yipp BG, Petri B, Salina D, et al. Infection-induced NETosis is a dynamic process involving neutrophil multitasking in vivo. *Nat Med*. 2012;18(9):1386-1393.

8. Fuchs TA, Brill A, Duerschmied D, et al. Extracellular DNA traps promote thrombosis. *Proc Natl Acad Sci U S A*. 2010;107(36):15880-15885.

9. Massberg S, Grahl L, von Bruehl ML, et al. Reciprocal coupling of coagulation and innate immunity via neutrophil serine proteases. *Nat Med*. 2010;16(8):887-896.

10. Brill A, Fuchs TA, Chauhan AK, et al. von Willebrand factor-mediated platelet adhesion is critical for deep vein thrombosis in mouse models. *Blood*. 2011;117(4):1400-1407.

11. Demers M, Krause DS, Schatzberg D, et al. Cancers predispose neutrophils to release extracellular DNA traps that contribute to cancer-associated thrombosis. *Proc Natl Acad Sci U S A*. 2012;109(32):13076-13081.

12. Urban CF, D. E, Schmid M, et al. Neutrophil extracellular traps contain calprotectin, a cytosolic protein complex involved in host defense against Candida albicans. *PLoS Pathog*. 2009;10:e1000639.

13. Xu J, Zhang X, Pelayo R, et al. Extracellular histones are major mediators of death in sepsis. *Nat Med*. 2009;15(11):1318-1321.

14. Saffarzadeh M, Juenemann C, Queisser MA, et al. Neutrophil extracellular traps directly induce epithelial and endothelial cell death: a predominant role of histones. *PLoS One*. 2012;7(2):e32366.

15. Semeraro F, Ammollo CT, Morrissey JH, et al. Extracellular histones promote thrombin generation through platelet-dependent mechanisms: involvement of platelet TLR2 and TLR4. *Blood*. 2011;118(7):1952-1961.

16. Wang Y, Li M, Stadler S, et al. Histone hypercitrullination mediates chromatin decondensation and neutrophil extracellular trap formation. *J Cell Biol*. 2009;184(2):205-213.

17. Wang Y, Wysocka J, Sayegh J, et al. Human PAD4 regulates histone arginine methylation levels via demethylimination. *Science*. 2004;306(5694):279-283.

18. Li P, Li M, Lindberg MR, Kennett MJ, Xiong N, Wang Y. PAD4 is essential for antibacterial innate immunity mediated by neutrophil extracellular traps. *J Exp Med*. 2010;207(9):1853-1862.

19. Leshner M, Wang S, Lewis C, et al. PAD4 mediated histone hypercitrullination induces heterochromatin decondensation and chromatin unfolding to form neutrophil extracellular trap-like structures. *Front Immunol*. 2012;3:307.

20. Nakashima K, Hagiwara T, Yamada M. Nuclear localization of peptidylarginine deiminase V and histone deimination in granulocytes. *J Biol Chem*. 2002;277(51):49562-49568.

21. Darrah E, Rosen A, Giles JT, Andrade F. Peptidylarginine deiminase 2, 3 and 4 have distinct specificities against cellular substrates: novel insights into autoantigen selection in rheumatoid arthritis. *Ann Rheum Dis*. 2012;71(1):92-98.

22. Parker H, Dragunow M, Hampton MB, Kettle AJ, Winterbourn CC. Requirements for NADPH oxidase and myeloperoxidase in neutrophil extracellular trap formation differ depending on the stimulus. *J Leukoc Biol*. 2012;92(4):841-849.

23. Li P, Yao H, Zhang Z, et al. Regulation of p53 target gene expression by peptidylarginine deiminase 4. *Mol Cell Biol*. 2008;28(15):4745-4758.

24. Dole VS, Bergmeier W, Mitchell HA, Eichenberger SC, Wagner DD. Activated platelets induce Weibel-Palade-body secretion and leukocyte rolling in vivo: role of P-selectin. *Blood*. 2005;106(7):2334-2339.

25. Pinsky DJ, Naka Y, Liao H, et al. Hypoxia-induced exocytosis of endothelial cell Weibel-Palade bodies. A mechanism for rapid neutrophil recruitment after cardiac preservation. *J Clin Invest*. 1996;97(2):493-500.

26. Ni H, Denis CV, Subbarao S, et al. Persistence of platelet thrombus formation in arterioles of mice lacking both von Willebrand factor and fibrinogen. *J Clin Invest*. 2000;106(3):385-392.

27. Denis CV, Wagner DD. Platelet adhesion receptors and their ligands in mouse models of thrombosis. *Arterioscler Thromb Vasc Biol*. 2007;27(4):728-739.

28. Asaga H, Nakashima K, Senshu T, Ishigami A, Yamada M. Immunocytochemical localization of peptidylarginine deiminase in human eosinophils and neutrophils. *J Leukoc Biol*. 2001;70(1):46-51.

29. Vossenaar ER, Radstake TR, van der Heijden A, et al. Expression and activity of citrullinating peptidylarginine deiminase enzymes in monocytes and macrophages. *Ann Rheum Dis*. 2004;63(4):373-381.

30. Virchow R. Thrombosis and emboli (1846-1856). Canton, Mass: Science History Publications; 1998.

31. Wakefield TW, Henke PK. The role of inflammation in early and late venous thrombosis: Are there clinical implications? *Semin Vasc Surg*. 2005;18(3):118-129.

32. Brighton TA, Eikelboom JW, Mann K, et al. Low-dose aspirin for preventing recurrent venous thromboembolism. *N Engl J Med*. 2012;367(21):1979-1987.

33. Becattini C, Agnelli G, Schenone A, et al. Aspirin for preventing the recurrence of venous thromboembolism. *N Engl J Med*. 2012;366(21):1959-1967.

34. Rohrbach AS, Hemmers S, Arandjelovic S, Corr M, Mowen KA. PAD4 is not essential for disease in the K/BxN murine autoantibody-mediated model of arthritis. *Arthritis Res Ther*. 2012;14(3):R104.

35. Hemmers S, Teijaro JR, Arandjelovic S, Mowen KA. PAD4-mediated neutrophil extracellular trap formation is not required for immunity against influenza infection. *PloS one*. 2011;6(7):e22043.

36. Thevenaz P, Unser M. User-friendly semiautomated assembly of accurate image mosaics in microscopy. *Microsc Res Tech*. 2007;70(2):135-146.

37. Hirahashi J, Mekala D, Van Ziffle J, et al. Mac-1 signaling via Src-family and Syk kinases results in elastase-dependent thrombohemorrhagic vasculopathy. *Immunity*. 2006;25(2):271-283.

Chapter 3

PAD4-deficiency does not worsen polymicrobial sepsis mortality and ameliorates endotoxemic shock

This chapter contains one submitted manuscript:

Martinod K, Fuchs TA, Wong SL, Demers M, Gallant M, Wang Y, Wagner DD. *PAD4-deficiency does not worsen polymicrobial sepsis mortality and ameliorates endotoxemic shock.* Submitted July 10, 2014 to Blood. Major revisions August 9, 2014.

Section 3.1: Overview and Attributions

Overview

NETs were shown to trap microbes, but also fuel cardiovascular, thrombotic and autoimmune disease. In Chapter 2 I have shown that PAD4-deficient animals are protected from thrombosis, without any obvious hemostatic defects. Therefore, inhibiting NET formation could be a useful therapeutic approach for preventing pathological deep vein thrombosis and our results show that PAD4 is a very attractive target. However, according to the dogma of the literature, inhibition of NETs could come at a cost in the presence of a bacterial infection. In the case of severe systemic infection in sepsis, the balance between the antimicrobial functions of NETs and the harmful consequences of releasing histones and other cytotoxic components of NETs into the extracellular space, particularly in the vasculature, remained to be determined. NETs could be providing early protection from bacterial dissemination, but when released in excess could eventually lead to hypercoagulability and tissue damage. It was therefore important to study the $PAD4^{-/-}$ mice in a severe infection model where NETs have been previously shown to be released and where histones were shown to contribute to death in cecal ligation puncture and LPS-induced sepsis[1]. Before pursuing sepsis models, we first investigated whether $PAD4^{-/-}$ neutrophils had any defects in functions important for antimicrobial effects, such as extravasation to sites of inflammation, generation of reactive oxygen species, and the ability to degranulate. We found that $PAD4^{-/-}$ neutrophils were competent in all of these, and therefore the $PAD4^{-/-}$ mouse provides us with a model where

NETs are not being released, while neutrophils retain the ability to fight infection by other means such as phagocytosis. When we subjected the PAD4$^{-/-}$ mice to severe and mild polymicrobial sepsis, we found that the mice did not develop higher bacteremia than wild-type animals, and had similar mortality. We also wanted to compare the PAD4$^{-/-}$ animals in the absence of a live bacterial infection to study the effect of NET release on the pathogenesis of endotoxemic shock. Here we found that PAD4$^{-/-}$ animals released less nucleosomes into circulation, and that this had a protective effect by delaying mortality and diminishing signs of shock. However, there were high amounts of chromatin still detectable in the plasma and therefore NETs contribute significantly to mortality but were not the sole contributor of toxic histones. In a world of antibiotics, inhibition of NET release may in fact be beneficial, and we hope that our studies will encourage the development of specific PAD4 inhibitors.

Supplemental figures are provided in Appendix A-2.

Attributions

Preliminary experiments for optimization of the LPS model in WT mice were performed by Tobias Fuchs, including lethal dose determination. We performed the first experiments with PAD4$^{-/-}$ mice together where I learned how to assess physical signs of shock in the mice. Christine Wong and Melanie Demers provided valuable assistance with flow cytometry, plasma analysis and bacterial culture. Maureen Gallant blinded the identity of mice for survival studies and

helped with immunostainings. Our collaborator Yanming Wang at Pennsylvannia State University provided the PAD4-deficient mice which his lab generated. I performed all mouse experiments involving PAD4 knockouts, (including flow cytometry analysis of neutrophils, thioglyocollate peritonitis, LPS endotoxemia, and cecal ligation puncture surgeries), analyzed data, and wrote the paper. Denisa Wagner revised the manuscript and supervised the entire study.

I thank my dissertation advisory committee members, Tanya N. Mayadas, Ulrich H. von Andrian, and Wolfgang Junger, for helpful discussions and suggestions for experimental design. I also thank Lesley Cowan for her assistance in manuscript preparation.

Section 3.2: PAD4-deficiency does not worsen polymicrobial sepsis mortality and ameliorates endotoxemic shock

Kimberly Martinod[a,b], Tobias A. Fuchs[b,c 2], Siu Ling Wong[b,c], Melanie Demers[b,c], Maureen Gallant[b], Yanming Wang[d], Denisa D. Wagner[b,c,e,1]

[a]Immunology Graduate Program, Division of Medical Sciences, Harvard Medical School, Boston, Massachusetts, USA

[b]Program in Cellular and Molecular Medicine, Boston Children's Hospital, Boston, Massachusetts, USA

[c]Department of Pediatrics, Harvard Medical School, Boston, Massachusetts, USA

[d]Center for Eukaryotic Gene Regulation, Department of Biochemistry and Molecular Biology, Pennsylvania State University, University Park, Pennsylvania, USA

[e]Division of Hematology/Oncology, Boston Children's Hospital, Boston, Massachusetts, USA

[1]To whom correspondence should be addressed:
denisa.wagner@childrens.harvard.edu (D.D.W.)
[2]Current address: University Medical Center Hamburg-Eppendorf, Institute of Clinical Chemistry and Laboratory Medicine, Hamburg, Germany

Abstract

Neutrophil extracellular traps (NETs), consisting of nuclear DNA with histones and microbicidal proteins, are expelled from activated neutrophils during sepsis. NETs were shown to trap microbes, but also fuel cardiovascular, thrombotic and autoimmune disease. The role of NETs in sepsis, particularly the balance between their antimicrobial and cytotoxic actions, remains unclear. Neutrophils from peptidylarginine deiminase 4-deficient (*PAD4*$^{-/-}$) mice, which lack the enzyme necessary for chromatin decondensation and NET formation, were evaluated. We found that neutrophil functions involved in bacterial killing, other than NETosis, remained intact. We hypothesized therefore that prevention of NET formation might not have devastating consequences in sepsis. To test this we subjected the *PAD4*$^{-/-}$ mice to severe and mild polymicrobial sepsis produced by cecal ligation and puncture. Surprisingly, under septic conditions, *PAD4*$^{-/-}$ mice did not fare worse than wild-type mice and had comparable survival. However, *PAD4*$^{-/-}$ mice were partially protected from lipopolysaccharide-induced shock, suggesting that NETs contribute to the toxic inflammatory and procoagulant host response to endotoxin. We propose that preventing NET formation may have beneficial effects in sepsis, and that PAD4 inhibition in inflammatory or thrombotic diseases is not likely to render the host vulnerable to bacterial infections.

Introduction

Sepsis remains a significant health care problem with approximately 750,000 cases per year leading to death in 30% of patients in the U.S.[2]. The pathologies of sepsis result not only from the presence of an infection, but also from the hyperinflammatory host response[3]. The vast systemic effects seen in sepsis result in diagnostic criteria that are broad in nature[4]. Severe sepsis, characterized by organ dysfunction, and septic shock, accompanied by hypotension, can rapidly progress to an irreversible stage in which survival is not possible despite therapeutic intervention[3,4].

Neutrophil extracellular traps (NETs) are the result of a coordinated biological process whereby neutrophils release their nuclear DNA accompanied by many antimicrobial proteins including histones[5-7]. The first report identified NETs in an infected appendix[5]. Using animal models of sepsis, the release of NETs within the vasculature became evident[7-9]. NET biomarkers are elevated in septic patients[10-12]. Microbes trapped within NETs are sometimes killed[5,13] and thus NETs could represent an important mechanism of host defense, particularly in sepsis[8,14-16]. To date this has not been rigorously tested. NETs have been identified in the cecal ligation puncture (CLP) mouse model of polymicrobial sepsis[17,18] and dissolution of NETs by DNase infusion has been proposed to transiently exacerbate sepsis[17].

The release of NETs within the bloodstream has important procoagulant and prothrombotic implications[14,19]. NETs can bind platelets and red blood cells[19] and thus participate in the initiation of pathological thrombosis[20,21].

Peptidylarginine deiminase 4 (PAD4) is essential to chromatin decondensation during NETosis by modifying histone charges through citrullination[22,23]. We have seen important anti-thrombotic and cardioprotective effects in the absence of NETs[24,25] using *PAD4*$^{-/-}$ mice, which do not decondense chromatin or form NETs[22]. In our colony, these mice do not suffer from opportunistic infections.

The most abundant proteinaceous components of NETs are histones[26], which are themselves not only procoagulant[1,27-29] but also highly cytotoxic to endothelium[1,30,31]. The hypercoagulable state and organ dysfunction exacerbated by histones, some of which may originate from NETs, can quickly lead to host mortality[1]. Therefore, it is important to study sepsis in *PAD4*$^{-/-}$ mice, which do not form NETs, in order to further delineate the balance between antimicrobial host defense and the pathological consequences of NET release. Here we report that, unexpectedly, mice that cannot make NETs fared the same or better than wild-type mice in mouse models of sepsis.

Results

PAD4$^{-/-}$ mice have circulating neutrophil numbers similar to wild-type *PAD4*$^{+/+}$ mice and their bacterial killing ability by phagocytosis is not impaired[22]. *PAD4*$^{-/-}$ mice are completely unable to generate NETs, even in response to reactive oxygen species (ROS)-dependent stimuli such as PMA[22]. Exogenous H_2O_2 fails to generate NETs in vitro[22], as does calcium increase by ionophores[24]. This highlights the importance of histone citrullination-mediated chromatin decondensation during NETosis. We found that *PAD4*$^{-/-}$ cells are capable of producing ROS, as H_2O_2 generation occurs in *PAD4*$^{-/-}$ neutrophils (Figure 3.1A).

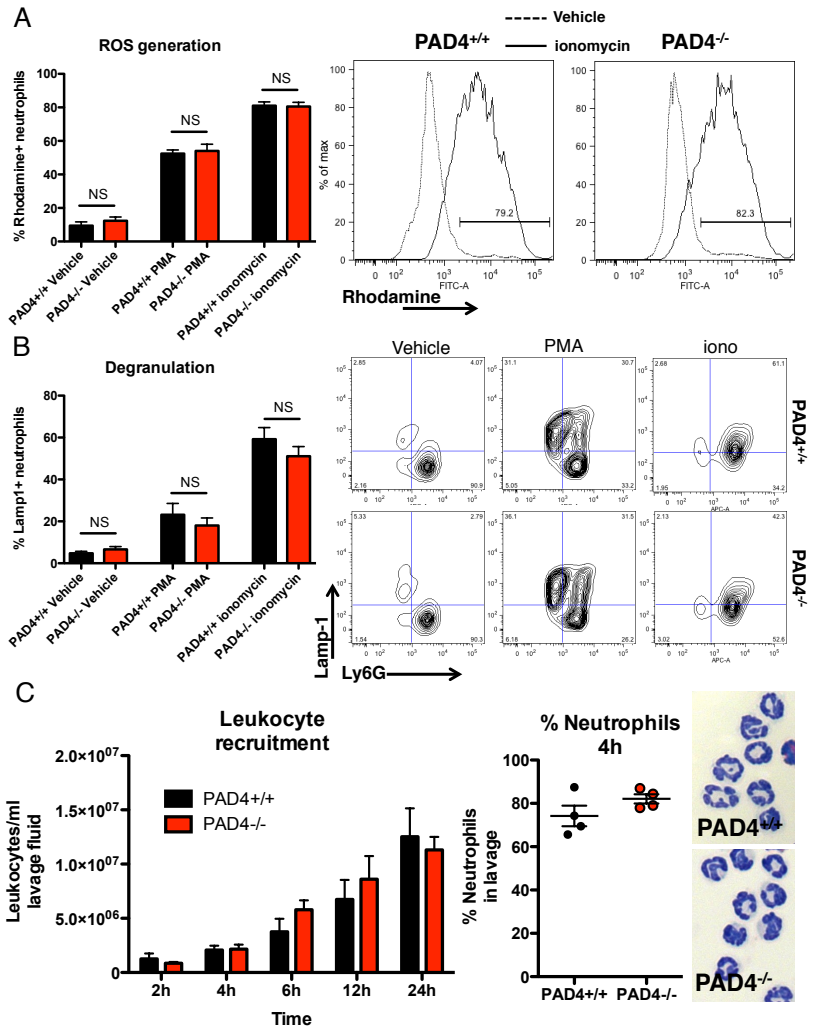

Figure 3.1. Neutrophils from *PAD4*$^{-/-}$ mice are competent in non-NET functions. A. Diluted, anticoagulated whole blood was incubated with 1 μM ionomycin, 100 nM PMA, or vehicle for 20 min at 37°C in the presence of dihydrorhodamine-123. Rhodamine^{+} ROS-generating neutrophils are quantified for each condition (left panel) and representative plots are shown (right two panels). n=4-13. B. Diluted whole blood was preincubated with 5 mM cytochalasin B for 20 min then incubated with 1 μM ionomycin, 100 nM PMA, or vehicle for 10 min at 37°C. Lamp1^{+} Ly6G^{+} degranulated cells are quantified in the left panel, with representative plots shown in the right panels. n=4-13. C. Leukocyte recruitment was assessed in vivo using thioglycollate-induced peritonitis. Infiltrating cells were counted in peritoneal lavage fluid at the indicated time points (left panel) and differential counts performed at 4h from Wright Giemsa-stained cytospins to assess neutrophil infiltration (center panel). Representative 4h cytospin images are shown in the right panels. Scale bar, 10 μm.

We also show here that the ability to degranulate is not affected by PAD4-deficiency (Figure 3.1B). Leukocyte rolling along activated endothelium occurs normally in *PAD4*$^{-/-}$ mice[24]. To investigate the ability of neutrophils to extravasate in response to an inflammatory stimulus, we quantified leukocyte recruitment to the peritoneum in a model of thioglycollate-induced peritonitis and found that *PAD4*$^{-/-}$ mice recruited similar numbers of leukocytes as *PAD4*$^{+/+}$ mice over time, and that neutrophil recruitment was also not impaired as determined by quantification of cells with characteristic neutrophil nuclear morphology (Figure 3.1C). Therefore, the use of *PAD4*$^{-/-}$ animals for sepsis studies appears to provide an ideal model in which to examine the role of NETs, because neutrophils can be recruited and are otherwise competent in non-NET microbicidal functions.

The CLP mouse model of sepsis involves ligation of the cecum followed by perforation, allowing fecal contents to be extruded into the peritoneal cavity and resulting in polymicrobial sepsis[32]. In this model, circulating cell-free DNA is elevated in plasma[17], and NETs are seen in liver sinusoids[18]. We performed CLP[32] in PAD4-deficient animals and compared them to their *PAD4*$^{+/+}$ and *PAD4*$^{+/-}$ littermates. We hypothesized that *PAD4*$^{-/-}$ mice would be the most susceptible in this model due to a reduced ability to kill bacteria via NETosis, especially in low-grade CLP where *PAD4*$^{+/+}$ mice are able to contain the infection well.

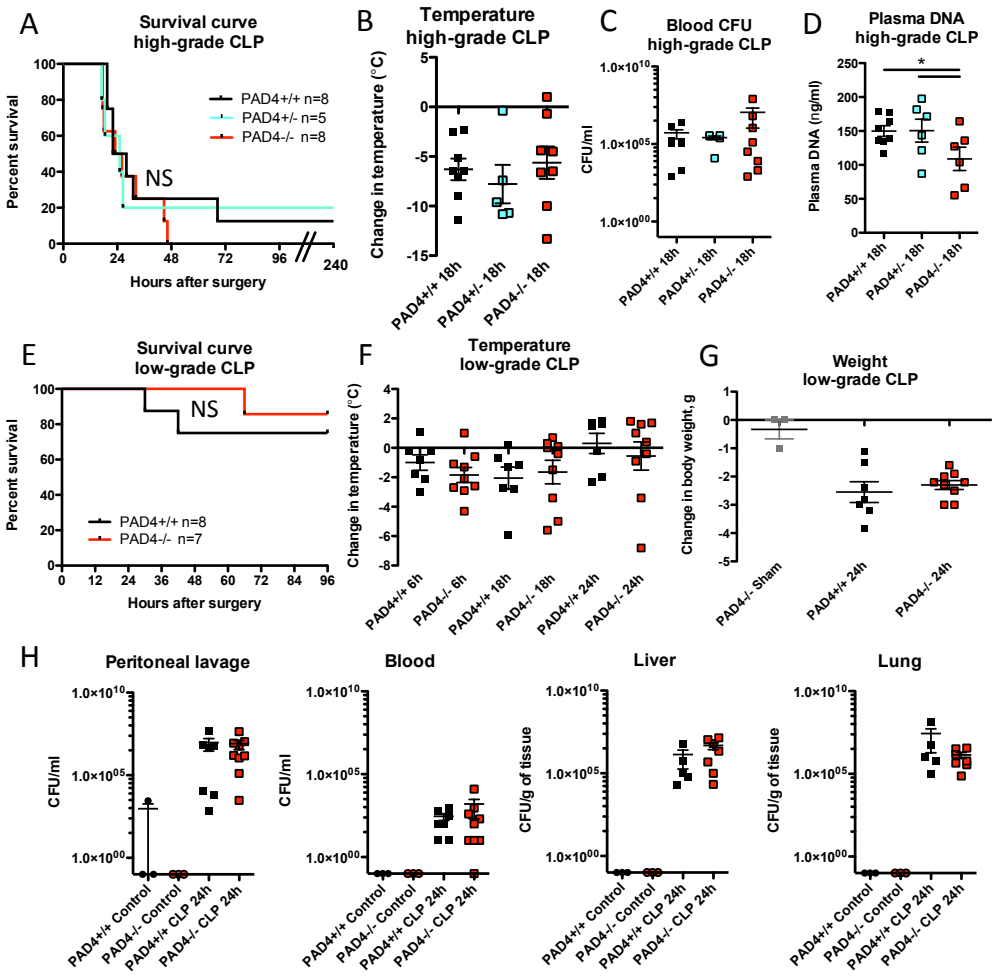

Figure 3.2. *PAD4*$^{-/-}$ mice are equally as susceptible to polymicrobial sepsis as their *PAD4*$^{+/+}$ littermates in the cecal ligation puncture model. Mice were subjected to high-grade CLP (panels A-D) or low-grade (panels E-H) CLP or sham operation (Sham). A. Survival curves indicating similar survival rates of *PAD4*$^{-/-}$ mice and their *PAD4*$^{+/-}$ or *PAD4*$^{+/+}$ littermates in high-grade CLP. B. Loss of body temperature was similar in *PAD4*$^{-/-}$ mice and their littermates. C. Bacterial colony forming units (CFU) were quantified from the blood of high-grade CLP to measure systemic bacteremia and were not significantly different between genotypes. D. High-grade CLP resulted in significant increases in circulating plasma DNA in *PAD4*$^{+/+}$ or *PAD4*$^{+/-}$ mice compared to *PAD4*$^{-/-}$ mice E, F. As with high-grade CLP, low-grade CLP resulted in similar survival (E) and body temperature changes (F). G. Weight loss was comparable in *PAD4*$^{+/+}$ vs. *PAD4*$^{-/-}$ mice, while sham-operated mice lost minimal body weight. H. Bacterial load was measured in peritoneal lavage fluid, blood, and liver and lung homogenates. Minimal CFUs were detected in control non-operated mice. Genotypes and treatments were as indicated. No statistical differences between *PAD4*$^{+/+}$ and *PAD4*$^{-/-}$ mice were detected. *PAD4*$^{+/+}$, black. *PAD4*$^{+/-}$, blue. *PAD4*$^{-/-}$, red.

However, we were surprised to see that all genotypes responded similarly to either high-grade or low-grade CLP (Figure 3.2). Mice exhibited similar mortality (Figure 3.2A, 3.2E) and clinical signs of sepsis, including hypothermia (Figure 3.2B, 3.2F) and weight loss (Figure 3.2G). As measured in a separate group of animals, blood cell counts were not statistically different between genotypes (Figure S3.1A, S3.1B, S3.1C). Leukocyte peritoneal recruitment occurred to a similar extent (Figure S3.1D, S3.1E), further demonstrating the capacity of PAD4-deficient neutrophils to transmigrate. *PAD4*$^{-/-}$ mice had lower plasma DNA levels (Figure 3.2D, S3.1F), indicating that a significant portion of circulating DNA in sepsis originates from NETs. However, the levels of circulating DNA are lower than has been reported in other NET-generating models[20,33], possibly because NETs may be consumed in microthrombi within organs. The bacterial load was similar in blood of all animals (Figure 3.2C, 3.2H) and no difference was seen in bacterial colony forming units (CFUs) in the peritoneum, liver, or lung in low-grade sepsis (Figure 3.2H). Plasma alanine aminotransferase (ALT) levels were similarly elevated in both *PAD4*$^{+/+}$ and *PAD4*$^{-/-}$ animals (Figure S3.1G), suggesting that NETs are not responsible for bacterial infection-induced liver injury. Although NETs form in the CLP model[17,18], we show that they don't influence either survival or the overall condition of the mice as *PAD4*$^{-/-}$ mice responded similarly to *PAD4*$^{+/+}$ or *PAD4*$^{+/-}$ mice. The fact that *PAD4*$^{-/-}$ mice do not succumb to low-grade CLP (Figure 3.2E), as we had anticipated, shows that they are not severely immunocompromised.

DNase I degrades NETs[5], and a recent study suggests that DNase infusion results in increased susceptibility to death in CLP[17]. However, this effect was transient and minor, with higher mortality at 24h but similar mortality at subsequent time points. While bacterial loads were elevated in DNase-treated mice 6h after CLP, by 24h CFUs were similar between treated and untreated mice[17]. Histological evidence of increased organ damage was evident by 24h[17] and could be due to liberation of NET fragments by DNase I having a cytotoxic effect on distant tissues. On the other hand, DNase I naturally facilitates clearance of NETs by macrophages[34], diminishing toxic NET effects.

There is vast evidence that aberrant NET production has pathological consequences in non-infectious conditions, including thrombosis[24], autoimmune diseases[35,36], and ischemia/reperfusion injury[25,37]. Histones are an integral part of NETs[5,26] and are cytotoxic to endothelial and epithelial cells[1,31]. In vivo, histones contribute substantially to mortality in sepsis[1] and can induce thrombocytopenia[38]. In order to study the effect of NETs and endotoxemia in mice without a live bacterial infection, we turned to established models of lipopolysaccharide-induced shock[1,39] to generate large amounts of circulating nucleosomes in vivo. While not an ideal model of human sepsis, LPS infusion allowed us to investigate the host response leading to endotoxemic shock, which has been extensively studied experimentally[1,40]. Also, we considered that while antibiotics used in patients kills pathogens, toxic products such as LPS may remain. In the LPS model, mortality is induced by the innate immune response, including cytokine storm and organ damage.

Intravenous infusion of lipopolysaccharides (LPS) from *Salmonella enterica serotype typhimurium* in *PAD4*$^{+/+}$ mice resulted in reduced platelet and leukocyte counts (Figure S3.2A) and release of cell-free nucleosomes and lactate dehydrogenase (LDH), a marker of cell lysis, into circulation in mice[1] (Figure S3.2B). Furthermore, Figure S3.2C shows histone release and fragmentation over time similarly to that reported by Esmon and colleagues[1]. Although necrotic cells can also release nucleosomes in endotoxemia[41], we saw that with increasing DNA release over time, citrullinated histone H3, a NET biomarker, became detectable in the plasma of *PAD4*$^{+/+}$ mice[39] (Figure S3.2D), indicating that NETs are formed in this model.

To investigate the role of NETs in this model, we compared *PAD4*$^{-/-}$ to *PAD4*$^{+/+}$ mice. Mortality was significantly ($p<0.007$) delayed in *PAD4*$^{-/-}$ mice after a highly lethal dose of LPS (25 mg/kg; Figure 3.3A). Similarly, an intermediate dose (10 mg/kg) resulted in 43.5% mortality in *PAD4*$^{+/+}$ mice by 24 hours compared to 4.3% mortality in *PAD4*$^{-/-}$ mice ($p<0.04$; Figure S3.2F). *PAD4*$^{-/-}$ mice became less hypothermic (Figure 3.3B) and less thrombocytopenic (Figure 3.3C) than *PAD4*$^{+/+}$ mice. This effect was similar using a non-lethal dose (Figure S3.2G, 3.3D), along with significantly higher leukocyte and neutrophil numbers in circulation (Figure 3.3D). Plasma DNA levels were significantly lower in *PAD4*$^{-/-}$ mice (Figure 3.3E), indicating again that a portion of the nucleosomes released are coming from NETs. H3Cit was not detected in any *PAD4*$^{-/-}$ mouse plasma, while it was present in *PAD4*$^{+/+}$ mice 24 hours after LPS injection (Figure 3.3F). By 48h, cell free histone H3 and DNA levels were reduced and H3Cit was no

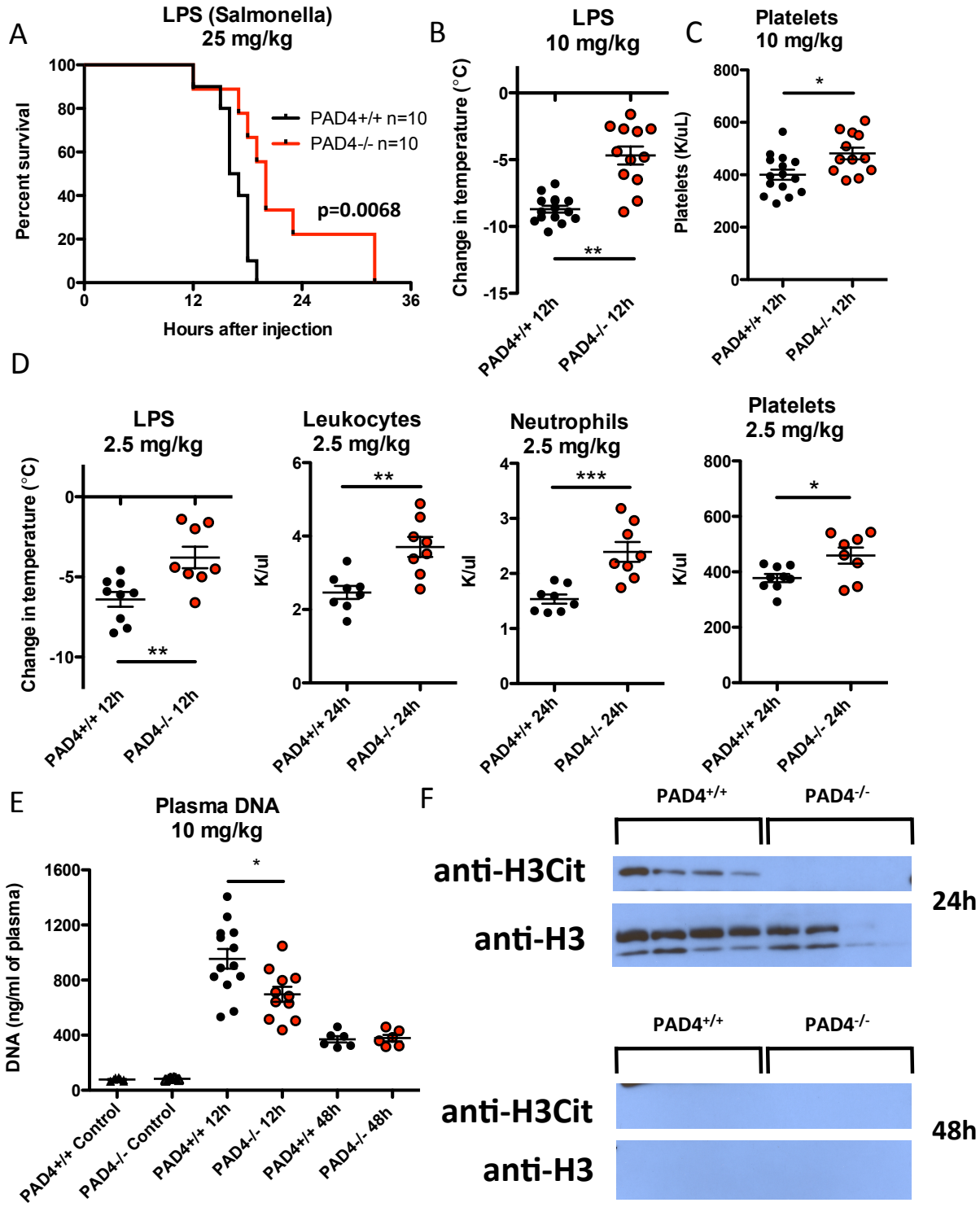

Figure 3.3. *PAD4*$^{-/-}$ mice release less extracellular DNA and are better protected than *PAD4*$^{+/+}$ mice in an LPS-induced endotoxemic shock model. A. Mice were injected i.v. with a lethal dose of LPS (25 mg/kg) and monitored every 2 hours beginning at 12h for moribundity. B,C. Mice injected i.v. with a less lethal LPS dose (10 mg/kg) were measured for signs of

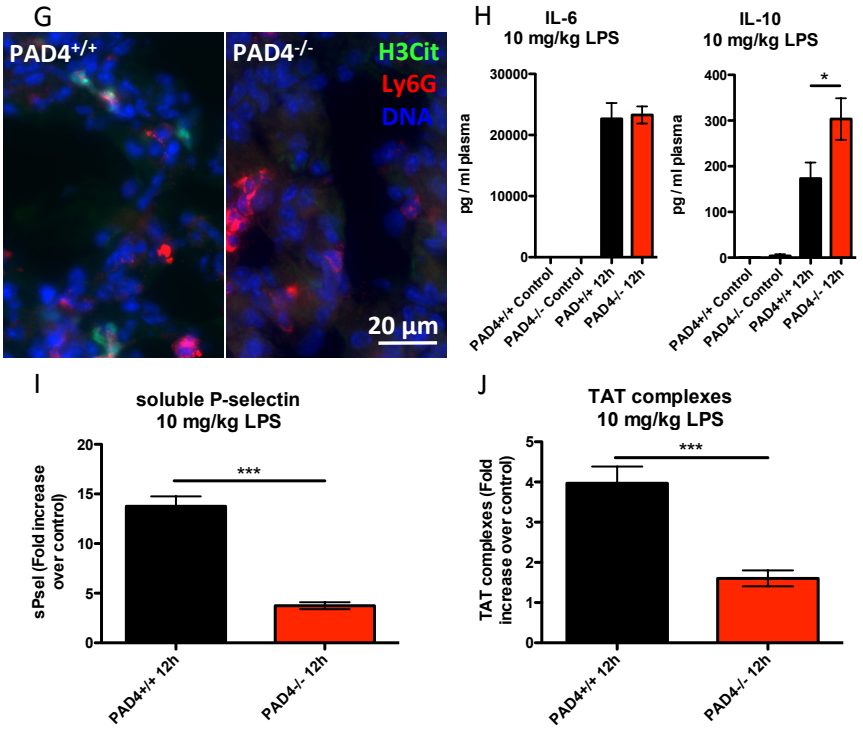

Figure 3.3 (Continued).
hypothermia. *PAD4*$^{-/-}$ mice had a milder temperature drop (B) and had higher platelet counts than *PAD4*$^{+/+}$ mice (C). D. Using a sublethal dose (2.5 mg/kg) which allowed us to follow mice surviving for 24h, similar differences in hypothermia and thrombocytopenia were observed. Total leukocyte and neutrophil levels were also higher in *PAD4*$^{-/-}$ mice. E,F. Plasma was collected at the time of sacrifice and analyzed for NET biomarkers. E. Twelve hours after LPS infusion, DNA levels were lower in *PAD4*$^{-/-}$ mice. F. Both histone H3 and citrullinated histone H3 (H3Cit) were identified in the plasma of *PAD4*$^{+/+}$ mice at 24h, and were no longer detected at 48h post-injection. H3Cit was not found in *PAD4*$^{-/-}$ mouse plasma, while histone H3 was detected. Representative of n=7 (24h) and n=6 (48h). G. H3Cit+ neutrophils were found in the lungs of *PAD4*$^{+/+}$ mice 18h after injection, while no H3Cit+ neutrophils were detected in *PAD4*$^{-/-}$ mice. Red, Ly6G. Green, H3Cit. Blue, DNA. Scale bar, 20 µm. Representative of n=5. H. IL-6 levels were similar in *PAD4*$^{+/+}$ and *PAD4*$^{-/-}$ mice at 12h, while IL-10 levels were higher in *PAD4*$^{-/-}$ mice. *PAD4*$^{+/+}$, n=13. *PAD4*$^{-/-}$ n=12. I,J. Soluble P-selectin levels (I) and thrombin anti-thrombin complexes (J) in plasma are significantly elevated in *PAD4*$^{+/+}$ mice compared to *PAD4*$^{-/-}$ mice, indicating that the presence of NETs activates platelets (increases P-selectin shedding) and induces generation of thrombin. Results are expressed as fold increase over control, untreated mice. *PAD4*$^{+/+}$, black, n=13. *PAD4*$^{-/-}$, red, n=11. *p<0.05, **p<0.01 ***p<0.001.

longer detectable in plasma (Figure 3.3E, 3.3F). Neutrophils with hypercitrullinated histone H3 are prominent in the lung 18h and 24h after LPS infusion in *PAD4*$^{+/+}$ mice (Figure 3.3G, S3.2E). Neutrophils were present in *PAD4*$^{-/-}$ mouse lungs, but they were not H3Cit-positive (Figure 3.3G). As we and others have previously shown, the formation of NETs in the lung is injurious and reduces lung function[42,43].

To further investigate the effect of PAD4-deficiency in the endotoxemia model, we measured plasma cytokine levels and found similar levels of pro-inflammatory interleukin-6 (IL-6) in *PAD4*$^{+/+}$ and *PAD4*$^{-/-}$ animals (Figure 3.3H). Interestingly, IL-10, an anti-inflammatory cytokine that is critical for reducing the progression to irreversible shock[44], was significantly higher in *PAD4*$^{-/-}$ mice (Figure 3.3H). Moreover, using soluble P-selectin (sPsel) as a biomarker of platelet and/or endothelial activation, we found that *PAD4*$^{+/+}$ mice had significantly more sPsel in circulation (Figure 3.3I). Thrombin anti-thrombin complexes were much higher in *PAD4*$^{+/+}$ mice compared with *PAD4*$^{-/-}$ mice (Figure 3.3J). The reduced inflammatory and hypercoagulable/prothrombotic state in *PAD4*$^{-/-}$ mice in response to LPS could be explained by the absence of NETs[45,46]. Thus, *PAD4*$^{-/-}$ mice exhibit reduced signs of septic shock in an endotoxemia model.

Discussion

Our study supports previously published reports that extracellular histones are highly procoagulant, prothrombotic, and injurious when released within the

vasculature, resulting in platelet-dependent thrombin generation, thrombocytopenia, endothelial cell death, and multi-organ dysfunction[1,27-29,38] We have previously shown that NETs can be dismantled by heparin[19] and that heparin inhibits histone-mediated platelet aggregation.[19,38] Wildhagen and colleagues recently reported that non-anticoagulant heparin reduces histone toxicity and thus is protective in sepsis.[47] Combined with our current results, it appears that this beneficial effect of heparin may be due in part to effects on histones released as a component of NETs. Furthermore, our genetic approach of deleting PAD4 function agrees with a new online report showing that use of Cl-amidine, a pan-PAD (PADs 1-4) inhibitor, in a similar CLP sepsis model is not immunosuppressive.[48] The pan-PAD inhibitor actually provides a survival advantage, not seen with the absence of NETs in our study using the *PAD4*$^{-/-}$ mice. This indicates that in addition to PAD4, other PADs are also involved in the negative effects of bacterial sepsis. This could be due to citrullination of additional cellular and plasma proteins.

During experimental endotoxemia, large quantities of histones are released into circulation[1] that are in complex with DNA as nucleosomes.[49] The protective effects of a complete absence of NETs are likely found both at the organ level and systemically, resulting in reduced septic shock. It is important to note that there were still prominent levels of nucleosomes in *PAD4*$^{-/-}$ animals, likely coming from necrotic cells. However, our results indicate that the contribution by NETs is substantial enough to impact mortality by increasing the inflammatory response. In the presence of a live pathogen, the balance between

the antimicrobial and host-destructive role of NETs is more complex and the benefits of reduced toxicity of NETs may be canceled out by increased bacterial impact.

Our study approach differs from previously published work using DNase infusion[15,17] in that NETs are never released in *PAD4*$^{-/-}$ mice. *PAD4*$^{+/+}$ mice administered DNase likely suffer from the reduced ability to perform other antimicrobial functions such as phagocytosis at infection sites once their neutrophils have formed NETs. Some cells may undergo "vital NETosis," and retain function as anuclear cytoplasts,[7,16] but their existence in polymicrobial sepsis remains unknown. Also, microbes amassed in NETs, upon digestion by DNase injection, may become rapidly liberated from the sites of local infection and therefore increase their dissemination.[16] Anti-NET therapy could be combined with antibiotics in settings in which an infection is suspected and direct inhibition of NETosis by PAD4 inhibitors might be most beneficial, providing both an anti-inflammatory and anti-thrombotic impact. Anti-histone treatments are effective at protecting mice from death only in the presence of antibiotics.[1] However, clinical use of activated protein C (APC), which among other functions cleaves histones, is complicated by side effects.[50] Ideally, therapeutic approaches would prevent NETs from being released in the first place and for this PAD4 is an ideal target. Because NETs are released in ischemia reperfusion injury,[25] they may be also released during the sequelae of the initial infection. Their deposition in organs and pro-thrombotic activity could lead to organ failure.[1,45,46]

PAD4-deficient mice have provided evidence of neutrophil antimicrobial activity in vivo.[22] When using a mutant, DNase-null bacteria, lesion size was reduced in WT but not *PAD4*$^{-/-}$ mice, providing in vivo evidence of the ability of NETs to kill bacteria.[22] It is, however, important to note that the use of a WT, nuclease-secreting microbe did not result in significantly larger skin lesions or higher bacterial CFU in PAD4-deficient animals in a model of necrotizing fasciitis.[22] As NETs are not sufficient to clear a bacterial infection, they may indeed cause more harm than good. Moreover, because many bacteria are able to evade NETs by secreting nucleases,[51-53] the actual physiological impact of the antimicrobial function of NETs may be minor, as seen in our study.

Our results indicate that infections are not exacerbated in the total absence of NETs and that excessive NET production contributes to the pathology of nucleosome-induced mortality. This has important implications for future development of NET-targeted therapeutics. We propose that inhibiting PAD4 would be highly beneficial and unlikely to result in drastic immunosuppressive effects. Neutrophils would remain able to reach areas of infection and have antimicrobial effects other than by NETs, and the cytotoxic impact of NETs to the host would be eliminated. No specific PAD4 inhibitors are available and there is reluctance to develop them because of fear of infection. We hope that our studies, showing that PAD4 inhibition would not render the host severely immunocompromised, will encourage such development.

Materials and Methods

Study approvals and animals

All experimental procedures involving animals were reviewed and approved by the Institutional Animal Care and Use Committee of Boston Children's Hospital (protocol numbers 11-04-1848, 14-03-2631R). All mice received food and water ad libitum; for in vivo sepsis models, mice were provided Napa Nectar enrichment gel (SE Lab Group). Mice from our *PAD4*$^{-/-}$ colony, backcrossed for 9-11 generations to C57Bl/6J background, were continually backcrossed at least once per year to C57Bl/6J mice ordered from Jackson labs. Littermates from heterozygous crosses were used in all cecal ligation puncture experiments.

Flow cytometry

Reactive oxygen species formation and degranulation analyses were performed using flow cytometry (BD FACSCanto II) and analyzed using FlowJo software (TreeStar Inc., Version 8.8.7). Whole blood was collected using heparin-coated capillary tubes via the retroorbital plexus and stimulated as previously described in the presence of dihydrorhodamine-123 (Invitrogen).[54] After stimulation, red blood cell lysis, and several washing steps, cells were stained for ROS measurements using Alexa 647-conjugated anti-Ly6G antibody (Biolegend), and for degranulation measurements using Alexa 647-conjugated anti-Ly6G antibody (Biolegend) and FITC-conjugated Lamp1 antibody (BD Pharmingen). Neutrophils were gated by forward and side scatter followed by Ly6G gating. Rhodamine^{+}

neutrophils were quantified for reactive oxygen species production, and Lamp1^{+} neutrophils were quantified for degranulation studies.

Thioglycollate peritonitis

Thioglycollate broth (3% in PBS, Sigma Aldrich) was prepared at least 2 weeks prior to use. One ml was injected intraperitoneally per mouse. At the indicated time points, mice were euthanized and a peritoneal lavage was performed using 6 ml of PBS. Total cell counts were performed using a Neubauer hemacytometer and a portion of the infiltrate was cytospun for differential cell counting using a Statspin Cytofuge II (Beckman Coulter). Differential counts were performed using at least 200 cells stained with Wright-Giemsa histologic stain.

Cecal ligation puncture

Cecal ligation puncture surgery was performed as described [32] using aseptic surgical technique. All mice in CLP experiments were obtained by heterozygous crosses and therefore were littermates on a C57Bl/6J background. Mice were anesthetized using 3.5% isoflurane in 100% oxygen and maintained at 2% isoflurane for the duration of the surgery. A midline laparotomy allowed for access to the cecum. The cecum was ligated with 4-0 silk suture located either 50% (low-grade) or 75% (high-grade) between the iliocecal junction and the distal end of the cecum. A through-and-through puncture was performed using a 21G (low-grade) or 18G (high-grade) needle. A small amount of cecal contents were extruded to ensure hole patency before returning the cecum to the abdominal cavity. The peritoneum was closed with 6-0 monofilament absorbable

vicryl suture and the skin was closed using a 6-0 nylon suture. Immediately after surgery, mice were injected with 0.9% sterile saline (500 µl, s.c.) for fluid resuscitation. Mice received buprenorphine (0.05 mg/kg s.c.) as an analgesic immediately prior to surgery and every 8-12 hours subsequently for 72 hours. Sham animals underwent the same procedure except for the ligation and puncture of the cecum. Control animals did not undergo surgery and were euthanized alongside CLP animals. All surgeries were done at similar times of the day to account for possible circadian rhythm effects on the model. Mice were observed over a 96-hour (low-grade CLP) or 10-day (high-grade CLP) time period and assessed for moribundity along with body weight and temperature. Temperatures were recorded using a handheld, non-contact infrared thermometer (Kintrex). All mice exhibited clinical sepsis symptoms (lethargy, piloerection, reduced interest in food and water, hunched posture). Any mice exhibiting loss of righting reflex when placed in a supine position were identified as moribund and immediately euthanized.

LPS endotoxemic shock

LPS from *Salmonella enterica spp typhimurium* (Sigma Aldrich, Lot number 109K4087) was injected intravenously via the retroorbital plexus at doses of either 25, 10, or 2.5 mg/kg. Lethal dosing was determined by injecting mice with increasing amounts of LPS and observing mortality over a 24 hour period. Mice were observed over a 96 hour time period and assessed for morbidity along with body weight and temperature. Mice received buprenorphine (0.05 mg/kg s.c.) as an analgesic every 12 hours. Temperatures were recorded using a handheld,

non-contact infrared thermometer (Kintrex). All mice exhibited clinical symptoms of endotoxemic shock (lethargy, piloerection, reduced interest in food and water, hunched posture). Any mice exhibiting loss of righting reflex when placed in a supine position were identified as moribund and immediately euthanized.

Complete blood counts

Blood was collected via the retroorbital plexus into EDTA-coated capillary tubes. Blood cell counts were analyzed using a Hemavet 950FS Veterinary Multi-species Hematology System (Drew Scientific).

Plasma measurements

Blood was collected into sodium citrate anticoagulant (10% v/v). After centrifugation of whole blood at 6000 rpm for 5 min, plasma was collected and centrifuged at 13200 rpm for 5 min to remove remaining cellular components. DNA was measured using the Picogreen Quant-iT dsDNA assay kit (Invitrogen). Thrombin anti-thrombin (TAT) complexes (Abcam), soluble P-selectin (R&D Systems), IL-6 (R&D Systems), IL-10 (R&D Systems), and alanine aminotransferase (Biotron) were measured according to manufacturer's instructions.

Bacterial load

All blood, lavage, and tissue collection and homogenization were performed using aseptic technique. Serial dilutions were plated onto tryptic soy agar pre-poured petri dishes supplemented with 5% sheep's blood (Hardy Diagnostics)

and incubated overnight at 37°C. Plates with 20-200 colonies were counted and CFUs were normalized per gram of tissue collected.

Circulating histone analysis

Four microliters of plasma were denatured and resolved on Tris-glycine SDS-Page gels (Lonza) or Bis-tris glycine gels (Invitrogen) under reducing conditions. After semi-dry transfer to PVDF membrane, blots were blocked with 3% BSA for 3 hours at room temperature (RT). After being incubated in primary antibody overnight at 4°C (anti-H3Cit, Abcam) or for 1 hour at RT (anti-histone H3, Abcam), membranes were washed and incubated in HRP-conjugated secondary antibody (goat anti-rabbit IgG HRP-conjugate, Bio-Rad) for 1 hour at RT. After washing, Pierce ECL (enhanced chemiluminescent) substrate (Thermo Scientific) was applied to each membrane before exposure onto film. H3Cit blots were exposed for 10 min, while histone H3 blots were exposed for 1 min.

Statistics

Data are presented as mean ± SEM and analyzed using Student's t-test or Mann-Whitney U test unless otherwise noted. Survival data were analyzed using Log-Rank tests of Kaplan-Meier curves. Data were considered significant when P-values were <0.05.

Acknowledgments

We thank Wolfgang G. Junger, Tanya N. Mayadas, and Ulrich H. von Andrian for helpful discussions and Lesley Cowan for assistance in the preparation of this

manuscript. This work was supported by the National Heart, Lung, and Blood Institute of the National Institutes of Health Grant R01HL102101 to D.D.W. and the National Cancer Institute of the National Institutes of Health Grant R01CA136856 to Y.M.W.

Author contributions

K.M. designed and performed experiments, analyzed data, and wrote the paper. T.A.F., S.L.W., M.D., and M.G. performed experiments and analyzed data. Y.M.W. provided the *PAD4*$^{-/-}$ mice, helpful advice, and contributed to discussions. D.D.W. supervised the study, designed experiments, analyzed data, and wrote the paper.

Section 3.3: Bibliography

1. Xu J, Zhang X, Pelayo R, et al. Extracellular histones are major mediators of death in sepsis. *Nat Med*. 2009;15(11):1318-1321.

2. Angus DC, Linde-Zwirble WT, Lidicker J, Clermont G, Carcillo J, Pinsky MR. Epidemiology of severe sepsis in the United States: analysis of incidence, outcome, and associated costs of care. *Crit Care Med*. 2001;29(7):1303-1310.

3. Mitchell RN. Hemodynamic Disorders, Thromboembolic Disease, and Shock. Robbins Basic Pathology, 8th Edition; 2007:81-106.

4. Angus DC, van der Poll T. Severe sepsis and septic shock. *N Engl J Med*. 2013;369(9):840-851.

5. Brinkmann V, Reichard U, Goosmann C, et al. Neutrophil extracellular traps kill bacteria. *Science*. 2004;303(5663):1532-1535.

6. Brinkmann V, Zychlinsky A. Beneficial suicide: why neutrophils die to make NETs. *Nat Rev Microbiol*. 2007;5(8):577-582.

7. Yipp BG, Kubes P. NETosis: how vital is it? *Blood*. 2013;122(16):2784-2794.

8. Clark SR, Ma AC, Tavener SA, et al. Platelet TLR4 activates neutrophil extracellular traps to ensnare bacteria in septic blood. *Nat Med*. 2007;13(4):463-469.

9. Gardiner EE, Andrews RK. Neutrophil extracellular traps (NETs) and infection-related vascular dysfunction. *Blood Rev*. 2012;26(6):255-259.

10. Margraf S, Logters T, Reipen J, Altrichter J, Scholz M, Windolf J. Neutrophil-derived circulating free DNA (cf-DNA/NETs): a potential prognostic marker for posttraumatic development of inflammatory second hit and sepsis. *Shock*. 2008;30(4):352-358.

11. Meng W, Paunel-Gorgulu A, Flohe S, et al. Deoxyribonuclease is a potential counter regulator of aberrant neutrophil extracellular traps formation after major trauma. *Mediators Inflam*. 2012;2012:149560.

12. Kambas K, Mitroulis I, Apostolidou E, et al. Autophagy mediates the delivery of thrombogenic tissue factor to neutrophil extracellular traps in human sepsis. *PloS One*. 2012;7(9):e45427.

13. Menegazzi R, Decleva E, Dri P. Killing by neutrophil extracellular traps: fact or folklore? *Blood*. 2012;119(5):1214-1216.

14. Massberg S, Grahl L, von Bruehl ML, et al. Reciprocal coupling of coagulation and innate immunity via neutrophil serine proteases. *Nat Med*. 2010;16(8):887-896.

15. McDonald B, Urrutia R, Yipp BG, Jenne CN, Kubes P. Intravascular neutrophil extracellular traps capture bacteria from the bloodstream during sepsis. *Cell Host Microbe*. 2012;12(3):324-333.

16. Yipp BG, Petri B, Salina D, et al. Infection-induced NETosis is a dynamic process involving neutrophil multitasking in vivo. *Nat Med*. 2012;18(9):1386-1393.

17. Meng W, Paunel-Gorgulu A, Flohe S, et al. Depletion of neutrophil extracellular traps in vivo results in hypersusceptibility to polymicrobial sepsis in mice. *Crit Care*. 2012;16(4):R137.

18. Cools-Lartigue J, Spicer J, McDonald B, et al. Neutrophil extracellular traps sequester circulating tumor cells and promote metastasis. *J Clin Invest*. 2013.

19. Fuchs TA, Brill A, Duerschmied D, et al. Extracellular DNA traps promote thrombosis. *Proc Natl Acad Sci U S A*. 2010;107(36):15880-15885.

20. Brill A, Fuchs TA, Savchenko AS, et al. Neutrophil extracellular traps promote deep vein thrombosis in mice. *J Thromb Haemost*. 2012;10(1):136-144.

21. von Bruhl ML, Stark K, Steinhart A, et al. Monocytes, neutrophils, and platelets cooperate to initiate and propagate venous thrombosis in mice in vivo. *J Exp Med*. 2012;209(4):819-835.

22. Li P, Li M, Lindberg MR, Kennett MJ, Xiong N, Wang Y. PAD4 is essential for antibacterial innate immunity mediated by neutrophil extracellular traps. *J Exp Med*. 2010;207(9):1853-1862.

23. Wang Y, Li M, Stadler S, et al. Histone hypercitrullination mediates chromatin decondensation and neutrophil extracellular trap formation. *J Cell Biol*. 2009;184(2):205-213.

24. Martinod K, Demers M, Fuchs TA, et al. Neutrophil histone modification by peptidylarginine deiminase 4 is critical for deep vein thrombosis in mice. *Proc Natl Acad Sci U S A*. 2013;110(21):8674-8679.

25. Savchenko AS, Borissoff JI, Martinod K, et al. VWF-mediated leukocyte recruitment with chromatin decondensation by PAD4 increases myocardial ischemia/reperfusion injury in mice. *Blood*. 2014;123(1):141-148.

26. Urban CF, Ermert D, Schmid M, et al. Neutrophil extracellular traps contain calprotectin, a cytosolic protein complex involved in host defense against Candida albicans. *PLoS Path*. 2009;5(10):e1000639.

27. Xu J, Zhang X, Monestier M, Esmon NL, Esmon CT. Extracellular histones are mediators of death through TLR2 and TLR4 in mouse fatal liver injury. *J Immunol*. 2011;187(5):2626-2631.

28. Semeraro F, Ammollo CT, Morrissey JH, et al. Extracellular histones promote thrombin generation through platelet-dependent mechanisms: involvement of platelet TLR2 and TLR4. *Blood*. 2011;118(7):1952-1961.

29. Ammollo CT, Semeraro F, Xu J, Esmon NL, Esmon CT. Extracellular histones increase plasma thrombin generation by impairing thrombomodulin-dependent protein C activation. *J Thromb Haemost*. 2011;9(9):1795-1803.

30. Gupta AK, Hasler P, Holzgreve W, Gebhardt S, Hahn S. Induction of neutrophil extracellular DNA lattices by placental microparticles and IL-8 and their presence in preeclampsia. *Hum Immunol*. 2005;66(11):1146-1154.

31. Saffarzadeh M, Juenemann C, Queisser MA, et al. Neutrophil extracellular traps directly induce epithelial and endothelial cell death: a predominant role of histones. *PLoS One*. 2012;7(2):e32366.

32. Rittirsch D, Huber-Lang MS, Flierl MA, Ward PA. Immunodesign of experimental sepsis by cecal ligation and puncture. *Nat Protoc*. 2009;4(1):31-36.

33. Demers M, Krause DS, Schatzberg D, et al. Cancers predispose neutrophils to release extracellular DNA traps that contribute to cancer-associated thrombosis. *Proc Natl Acad Sci U S A*. 2012;109(32):13076-13081.

34. Farrera C, Fadeel B. Macrophage clearance of neutrophil extracellular traps is a silent process. *J Immunol*. 2013;191(5):2647-2656.

35. Kessenbrock K, Krumbholz M, Schonermarck U, et al. Netting neutrophils in autoimmune small-vessel vasculitis. *Nat Med*. 2009;15(6):623-625.

36. Radic M, Marion TN. Neutrophil extracellular chromatin traps connect innate immune response to autoimmunity. *Semin Immunopathol*. 2013;35(4):465-480.

37. De Meyer SF, Suidan GL, Fuchs TA, Monestier M, Wagner DD. Extracellular chromatin is an important mediator of ischemic stroke in mice. *Arterioscl Thromb Vasc Biol*. 2012;32(8):1884-1891.

38. Fuchs TA, Bhandari AA, Wagner DD. Histones induce rapid and profound thrombocytopenia in mice. *Blood*. 2011;118(13):3708-3714.

39. Li Y, Liu B, Fukudome EY, et al. Identification of citrullinated histone H3 as a potential serum protein biomarker in a lethal model of lipopolysaccharide-induced shock. *Surgery*. 2011;150(3):442-451.

40. Remick DG, Newcomb DE, Bolgos GL, Call DR. Comparison of the mortality and inflammatory response of two models of sepsis: lipopolysaccharide vs. cecal ligation and puncture. *Shock*. 2000;13(2):110-116.

41. Allam R, Scherbaum CR, Darisipudi MN, et al. Histones from dying renal cells aggravate kidney injury via TLR2 and TLR4. *J Am Soc Nephrol*. 2012;23(8):1375-1388.

42. Thomas GM, Carbo C, Curtis BR, et al. Extracellular DNA traps are associated with the pathogenesis of TRALI in humans and mice. *Blood*. 2012;119(26):6335-6343.

43. Caudrillier A, Kessenbrock K, Gilliss BM, et al. Platelets induce neutrophil extracellular traps in transfusion-related acute lung injury. *J Clin Invest*. 2012;122(7):2661-2671.

44. Latifi SQ, O'Riordan MA, Levine AD. Interleukin-10 controls the onset of irreversible septic shock. *Infect Immun*. 2002;70(8):4441-4446.

45. Engelmann B, Massberg S. Thrombosis as an intravascular effector of innate immunity. *Nat Rev Immunol*. 2013;13(1):34-45.

46. Martinod K, Wagner DD. Thrombosis: tangled up in NETs. *Blood*. 2014;123(18):2768-2776.

47. Wildhagen KC, Garcia de Frutos P, Reutelingsperger CP, et al. Nonanticoagulant heparin prevents histone-mediated cytotoxicity in vitro and improves survival in sepsis. *Blood*. 2014;123(7):1098-1101.

48. Li Y, Liu Z, Liu B, et al. Citrullinated histone H3: A novel target for the treatment of sepsis. *Surgery*. 2014.

49. Esmon CT. Molecular circuits in thrombosis and inflammation. *Thromb Haemost*. 2013;109(3):416-420.

50. Bernard GR, Vincent JL, Laterre PF, et al. Efficacy and safety of recombinant human activated protein C for severe sepsis. *N Engl J Med*. 2001;344(10):699-709.

51. Sumby P, Barbian KD, Gardner DJ, et al. Extracellular deoxyribonuclease made by group A Streptococcus assists pathogenesis by enhancing evasion of the innate immune response. *Proc Natl Acad Sci U S A*. 2005;102(5):1679-1684.

52. Beiter K, Wartha F, Albiger B, Normark S, Zychlinsky A, Henriques-Normark B. An endonuclease allows Streptococcus pneumoniae to escape from neutrophil extracellular traps. *Curr Biol*. 2006;16(4):401-407.

53. Buchanan JT, Simpson AJ, Aziz RK, et al. DNase expression allows the pathogen group A Streptococcus to escape killing in neutrophil extracellular traps. *Curr Biol*. 2006;16(4):396-400.

54. Chen Y, Junger WG. Measurement of oxidative burst in neutrophils. *Methods Mol Biol*. 2012;844:115-124.

Chapter 4

Discussion

Section 4.1: Discussion

The molecular events leading to NET formation are incompletely defined, as are their consequences. The process of NET formation (NETosis) after initial stimulation involves the decondensation of chromatin, dissolution of the nuclear membrane, and expulsion of chromatin into the extracellular environment[1]. This initial stimulus still remains incompletely characterized in terms of receptor binding and downstream signaling events but there have been key findings in recent years that help us to better understand mediators that are regulating the process. Also, a novel form of NET formation was described where a neutrophil can release only a portion of its nucleus, termed vital NETosis[2,3]. Here neutrophils can retain phagocytic function even after releasing their entire nuclear contents as NETs[3]. This intriguing form of NET formation without cell death has opened up a whole new avenue of study in disease processes where NETs are involved. Parsing out which factors lead to which type of NETosis in non-infectious diseases such as thrombosis is an interesting future direction of the work presented in this dissertation.

PAD4 function and regulation

Here I have focused on one essential aspect of NETosis: chromatin decondensation. This was shown to be mediated by the enzyme peptidylarginine deiminase 4 (PAD4), which modifies arginine residues on proteins to citrulline via a deimination reaction[4]. This was first shown to occur in histones using HL-60 cells, a human promyelocytic leukemia cell line that can be differentiated to

granulocyte-like cells[5], and later in primary human neutrophils that had been challenged with inflammatory insults such as LPS or TNFα[6]. The Neeli et al. paper also first identified citrullinated histones as a component of NETs. Shortly thereafter, it was shown that this histone citrullination was responsible for driving chromatin decondensation during NETosis[7]. The generation of PAD4-deficient mice has been a big driving force in the study of NETs in vivo, as these are to date the only mice that have a complete lack of NET formation[8].

There is still much to be explored in the cell biology of PAD4 function and regulation. The crystal structure of PAD4 has been published, and from this we know that PAD4 is a calcium dependent enzyme that requires calcium binding to 5 sites in order for the active site to be conformationally available[9]. I have seen that upon calcium chelation by EDTA, histone citrullination and NET formation are completely abrogated in a fashion similar to the neutrophils of $PAD4^{-/-}$ mice. It has been shown that both intracellular and extracellular calcium stores are needed during NET formation[10].

PAD4 is the only PAD family member to have a nuclear localization signal[9], and thus is the only PAD able to enter the nucleus and citrullinate histones[11]. PAD4 activity and therefore NET formation may be regulated by its subcellular localization, either outside of the nucleus or intranuclear. It has been reported in other cell types that PAD4 translocates from the cytoplasm into the nucleus upon stimulation of the cell[12]; however, in neutrophils this has not been established and PAD4 is presumed to reside in the nucleus[13]. Unfortunately, PAD4 antibodies that recognize mouse PAD4 are not commercially available so

studying PAD4 translocation has not yet been possible in primary mouse neutrophils where I would like to investigate what happens to PAD4 during various inflammatory insults such as LPS challenge. My preliminary data with human neutrophils indicates that PAD4 is located outside of the nucleus in healthy blood donors, but that upon stimulation or in certain disease states, PAD4 becomes primarily located within the nucleus. Recently it was reported that neutrophils from rheumatoid arthritis patients had more nuclear rather than cytoplasmic PAD4[14]. However, more extensive and quantitative analyses remain to be done to support the hypothesis that PAD4 is being actively transported into the nucleus.

PAD4$^{-/-}$ mice provide an ideal model to study the role of NETs in pathological thrombosis

In this dissertation, I aimed to better understand the importance of NETs in pathological conditions involving platelets and leukocytes. PAD4$^{-/-}$ mice allowed for the study of disease models in vivo in the complete absence of NETs and thus were a critical tool for this work[8]. I have now shown that these mice are protected from pathological thrombosis (Chapter 2) and partially protected from endotoxemic shock (Chapter 3). Other than their established NET defect[8], we have not been able to identify any other major phenotype in these mice. Their neutrophils behave normally except for their lack of NET formation: they are able to be recruited to sites of inflammation, adhere and migrate towards stimuli, produce ROS, degranulate (Chapter 3), and phagocytose and kill bacteria[8].

Therefore, these mice lack many of the confounding factors present in other genetically-deficient mice that may also have a NET defect. I will discuss three other NET-deficient mice below and why ultimately they were not ideal for studying NETs in thrombosis.

Early studies identified NADPH oxidase (gp91phox) and generation of oxygen species as critical players in NET formation, and patients with chronic granulomatous disease have a defect in producing NETs that can be rescued with addition of exogenous hydrogen peroxide[15]. However, studying mice in which gp91phox has been genetically deleted posed a problem because their phenotype is much more broad than a lack of NET formation. Gp91phox is expressed other cell types than leukocytes such as platelets and endothelial[16-18], meaning that it is could be affecting functions critical for thrombus initiation. For example, platelet activation is impaired with this deficiency[19,20]. Our lab has shown that platelets are essential for the initiation of thrombus formation[21]. Mice lacking Gp1bα, which is needed for platelet binding to von Willebrand factor, fail to produce thrombi in the stenosis model[22]. This highlights the importance of maintaining fully competent platelets in order to study NETs in this model. Therefore, gp91phox$^{-/-}$ mice would not have been ideal for studying neutrophil/NET involvement in thrombosis and I did not perform any DVT experiments with these mice.

Neutrophil elastase (NE) was also thought to be critical for chromatin decondensation during NETosis. This has been proposed to occur via histone degradation, and it was shown that NE first translocates from azurophilic

granules to the nucleus[23], which occurs independently of other granule contents such as myeloperoxidase (MPO). A recently published study proposes that this mechanism of nuclear transport is independent of granule membrane fusion[23] but dependent on reactive oxygen species (ROS) and MPO[24]. Our lab has been several times asked by reviewers to perform our in vivo NET models in $NE^{-/-}$ mice in parallel to $PAD4^{-/-}$ mice to have an additional mouse model where NETs are lacking. However, I found that NE-deficient neutrophils only had a moderate reduction in NET formation and $NE^{-/-}$ mice formed NET-rich thrombi similarly to WT mice (Appendix A-7). Therefore, $NE^{-/-}$ mice proved in our hands to not be suitable for studying NET defects in mouse thrombosis models. These mice may be still be of interest for studying the in vivo impact of having NETs generated that are not containing NE on their surface, as this may have an effect on coagulation, antimicrobial function[25], and vascular permeability. These results also indicate that a more efficient reduction of NET formation (such as by targeting PAD4) is needed to have a physiological impact in DVT.

Lastly, we have studied Rac2-deficient animals because Rac2null neutrophils were shown to have a severe NET defect in response to stimuli that are ROS-dependent such as LPS or PMA[26]. Furthermore, Rac2 is important for NADPH oxidase assembly[27] and its expression is restricted to leukocytes[28]. Importantly, platelet function doesn't appear to be compromised in these mice. In collaboration with Dr. David Williams at Boston Children's Hospital, we confirmed that Rac2null neutrophils had reduced NET formation and his group is currently working on parsing out other components of the signaling cascade. I

had hoped that studying these mice in the venous stenosis model would begin to clarify the driving force behind the initiation of NETosis during thrombosis. However, while we saw a trend toward reduction in the Rac2null mice in the percentage of the mice forming thrombi compared to WT mice, the thrombi that did form in Rac2null animals were quite large. When analyzing these histologically, I saw that the thrombi from Rac2null animals were very neutrophil dense and contained $H3Cit^{+}$ NETs. The Rac2null animals have elevated neutrophil counts that reach 2.5-3 times the level of WT mice[29]. Even if the Rac2null neutrophils have substantially impaired NETosis during thrombosis, the fact that there are more of them in circulation is likely negating any effect we would see as a result of this NETosis defect. Therefore, further experiments are needed where similar numbers of neutrophils are present in circulation. This could be done by infusing neutrophils from either WT or Rac2null animals into PAD4-deficient mice. WT neutrophil supplementation was enough to initiate thrombosis in $PAD4^{-/-}$ mice, and I would hypothesize that Rac2null neutrophils would be less well able to rescue thrombosis. This would allow for the study of the importance of the NADPH oxidase-driven NETosis pathway during thrombosis.

What induces NETosis during thrombosis?

The signaling pathways and other molecular mechanisms driving NET formation during thrombosis remains to be established. It has been proposed that activated platelets can induce NET formation[22,30], but the exact interaction

occurring between platelets and neutrophils leading to NETosis is unknown. In pathological thrombosis, endothelial cell activation leads to release of the contents Weibel-Palade bodies, such as von Willebrand factor (VWF) and P-selectin, which in turn help to recruit leukocytes and platelets to initialize a growing thrombus[21,31]. NETting neutrophils at this site of leukocyte/platelet accumulation may help to drive further platelet as well as red blood cell recruitment, as both were shown to bind to NETs when whole blood was perfused over pre-formed NETs in a flow chamber[32]. In addition, VWF is closely associated with NETs in thrombi produced in animal models[21,32] as well as in thrombi harvested from venous thromboembolism patients[33]. VWF is critical to the recruitment of platelets to activated endothelium[34], and VWF was also shown to be able to bind histones[35] long before NETs were discovered. The signaling pathways in the neutrophil as a result of contact with activated platelets remain to be identified; PSGL-1 is one likely candidate, as a ligand for P-selectin which drives the initial interaction between neutrophils and platelets/endothelial cells[36,37]. Also, VWF may be participating to induce NETosis either directly or indirectly via platelets.

Our lab has identified the presence of NETs in thrombi from human patients with a confirmed venous thromboembolism diagnosis: either deep vein thrombosis, pulmonary embolism, or IVC filter clots ([33], Appendix 4). NETs were identified in certain stages of thrombus development; mainly during the organizing phase when large amounts of neutrophils and platelets are present[38]. Some NETs were also found in unorganized, fresh clots. This, along with the

mouse data in Brill et al.[39] and Chapter 2, indicates that NETs are forming early during thrombus initiation, and may be in part responsible for stabilizing the clot. Again, what drives the initial trigger for neutrophils to throw NETs during thrombosis remains to be established. The role that NETs may have later in thrombus maturation is an exciting future direction for this study. NETs could be involved in thrombus organization and may affect neovascularization that occurs as the thrombus develops into an organized, tissue-like structure.

NET inhibition in sepsis

In sepsis, neutrophils were proposed to be induced by activated platelets to undergo NETosis[30]. In vitro, the combination of activated platelets and neutrophils lead to increased bacterial trapping but also to increased endothelial damage[30], highlighting that NET release has bystander effects in addition to trapping bacteria. In live bacterial sepsis mouse models, indeed neutrophil depletion can be either detrimental or highly protective depending on the timing of the depletion: depletion at the beginning of the infection leads to increased bacterial burden and mortality while depletion after the first 12 hours prevents neutrophil-associated tissue damage[40]. In fact, mice depleted 12 hours after CLP had drastically reduced bacterial loads, indicating that neutrophils may at some point be driving bacteremia. There are now conflicting reports in the literature as to the effect of removing NETs by DNase infusion: one group reported that DNase accelerated mortality and led to transiently increased bacterial burden[41], while another group recently published the opposite finding,

that DNase protected from lung injury and decreased bacterial loads systemically[42]. Again, timing may be essential here and there is likely a dual effect of DNase digestion of NETs. Locally, reducing NET concentration may be beneficial by preventing tissue injury such as in the lung. However, DNase may be systemically disseminating NET fragments into the circulation which has damaging consequences to endothelial cells and thus could also lead to organ damage.

Our approach with the PAD4$^{-/-}$ mice differs from DNase infusion in that NETs are never released so any potential effect of freeing up NET nucleosomes within the vasculature are not present. Also, using the PAD4$^{-/-}$ mice differs from neutrophil depletion experiments in that PAD4$^{-/-}$ mice have otherwise functional neutrophils other than their inability to release NETs ([8], [43], Chapter 3). They behave like WT mice in terms of recruitment to sites of inflammation, production of reactive oxygen species, phagocytosis, and degranulation. My results in Chapter 3 show that lacking NETs does not have any major impact on the outcome of cecal ligation puncture, so NETs are not likely playing a substantial role in bacterial killing in this model. The neutrophil has much more in arsenal than throwing NETs, and there may be specific settings in which NETs play a key role in preventing pathogen dissemination from a localized site, perhaps by promoting fibrin deposition. To see if NETs have a negative impact on the host in CLP, I am planning to perform the model with the administration of antibiotics 6 hours after CLP surgery to observe whether under these conditions the PAD4$^{-/-}$

mice may fare better than WT mice since the bacterial growth would be contained.

The LPS-induced sepsis model allowed me to study the host response to a bacterial insult in the absence of a live bacterial infection. Here, I demonstrated that a portion of the DNA/histones being released into the circulation came from NETs, and that the failure to release NETs in the PAD4$^{-/-}$ mice had a positive impact on the physiological responses of these mice, ultimately delaying mortality. Current therapies for septic patients include antibiotic treatment and supportive care[44]. Activated protein C, which degrades histones[45], was a promising candidate for ameliorating the negative consequences of NET formation in patients, but this treatment came with serious bleeding risk[46] and is no longer used clinically. Antibodies neutralizing histone H4 were protective in a mouse model of CLP, but mice had to be given antibiotics in order to not succumb to the infection[45]. Histone-targeted treatments also target histones being released from cells dying by other means than NETosis. Histones themselves are also bactericidal[47], and therefore anti-histone therapy may be too non-specific and could lead to increased susceptibility to infection.

Future directions

Based on the work presented in this dissertation, I propose that targeting PAD4 to prevent NET release from taking place altogether is an ideal solution, especially in a world where antibiotic use is prevalent and any potential reduced

bacterial clearance would be mitigated by their use. There is, however, still much to be learned regarding the role of NETs in inflammatory processes. I have outlined in Chapter 1 many unanswered questions that remain. Understanding what drives NET formation during pathological thrombosis will be an important next step. Also, investigating how NETs impact thrombus progression will provide valuable insight into possible therapeutic interventions that could be taken once thrombi have already formed, as a majority of patients present with an existing thrombus.

Even with all of our knowledge about risk factors associated with VTE, thrombotic events remain a frequent complication in patients that have undergone surgery or been immobilized[48]. Therefore, new risk factors continue be explored. Genome-wide association studies have identified PAD4 as a susceptibility locus for rheumatoid arthritis in Japanese and Korean populations[49-51]. However, the exact variants have not been identified[52]. It would be of great interest to perform similar analyses in venous thromboembolism patients, as mutations in PAD4 could render the enzyme more active and make these affected persons more susceptible to aberrant NET formation. This could help to identify patients who would benefit from NET-targeted therapy as a prophylactic treatment.

Currently, treatment of existing VTE is limited to months-long treatment with anticoagulants. This comes with significant bleeding risk and once anticoagulation is stopped the risk of VTE recurrence is high[53]. The best candidate for preventing recurrence available now is low-dose aspirin[54,55], and to

remove thrombi that don't naturally dissolve involves tPA infusion and mechanical disruption via a catheter[56]. Combining DNase to degrade the NET component of the thrombus scaffold in addition to tPA which targets the proteinaceous fibrin backbone may be more effective in reducing clot burden[57,58]. PAD4 inhibitors may then be useful in preventing new thrombus growth, stabilization, or recurrence.

In conclusion, I have discussed that NETs are produced under both infectious and sterile inflammatory conditions, and contribute to the pathologies of both deep vein thrombosis, and sepsis. The $PAD4^{-/-}$ mice have been an invaluable tool to study these disease processes in vivo. I hope that the work presented in this dissertation will help to drive the development of anti-NET targeted therapeutics. I propose that PAD4 is an ideal target, both in pathological thrombosis as an anti-thrombotic that wouldn't impact normal hemostasis, and perhaps even in sepsis where its use could be combined with antibiotics.

Section 4.2: Bibliography

1. Brinkmann V, Zychlinsky A. Beneficial suicide: why neutrophils die to make NETs. *Nat Rev Microbiol*. 2007;5(8):577-582.

2. Yipp BG, Kubes P. NETosis: how vital is it? *Blood*. 2013;122(16):2784-2794.

3. Yipp BG, Petri B, Salina D, et al. Infection-induced NETosis is a dynamic process involving neutrophil multitasking in vivo. *Nat Med*. 2012;18(9):1386-1393.

4. Nakashima K, Hagiwara T, Ishigami A, et al. Molecular characterization of peptidylarginine deiminase in HL-60 cells induced by retinoic acid and 1alpha,25-dihydroxyvitamin D(3). *J Biol Chem*. 1999;274(39):27786-27792.

5. Hagiwara T, Nakashima K, Hirano H, Senshu T, Yamada M. Deimination of arginine residues in nucleophosmin/B23 and histones in HL-60 granulocytes. *Biochem Biophys Res Commun*. 2002;290(3):979-983.

6. Neeli I, Khan SN, Radic M. Histone deimination as a response to inflammatory stimuli in neutrophils. *J Immunol*. 2008;180(3):1895-1902.

7. Wang Y, Li M, Stadler S, et al. Histone hypercitrullination mediates chromatin decondensation and neutrophil extracellular trap formation. *J Cell Biol*. 2009;184(2):205-213.

8. Li P, Li M, Lindberg MR, Kennett MJ, Xiong N, Wang Y. PAD4 is essential for antibacterial innate immunity mediated by neutrophil extracellular traps. *J Exp Med*. 2010;207(9):1853-1862.

9. Arita K, Hashimoto H, Shimizu T, Nakashima K, Yamada M, Sato M. Structural basis for Ca(2+)-induced activation of human PAD4. *Nat Struct Mol Biol*. 2004;11(8):777-783.

10. Gupta AK, Giaglis S, Hasler P, Hahn S. Efficient neutrophil extracellular trap induction requires mobilization of both intracellular and extracellular calcium pools and is modulated by cyclosporine A. *PLoS One*. 2014;9(5):e97088.

11. Darrah E, Rosen A, Giles JT, Andrade F. Peptidylarginine deiminase 2, 3 and 4 have distinct specificities against cellular substrates: novel insights into autoantigen selection in rheumatoid arthritis. *Ann Rheum Dis*. 2012;71(1):92-98.

12. Mastronardi FG, Wood DD, Mei J, et al. Increased citrullination of histone H3 in multiple sclerosis brain and animal models of demyelination: a role for tumor necrosis factor-induced peptidylarginine deiminase 4 translocation. *J Neurosci*. 2006;26(44):11387-11396.

13. Nakashima K, Hagiwara T, Yamada M. Nuclear localization of peptidylarginine deiminase V and histone deimination in granulocytes. *J Biol Chem*. 2002;277(51):49562-49568.

14. Sur Chowdhury C, Giaglis S, Walker UA, Buser A, Hahn S, Hasler P. Enhanced neutrophil extracellular trap generation in rheumatoid arthritis: analysis of underlying signal transduction pathways and potential diagnostic utility. *Arthritis Res Ther*. 2014;16(3):R122.

15. Fuchs TA, Abed U, Goosmann C, et al. Novel cell death program leads to neutrophil extracellular traps. *J Cell Biol*. 2007;176(2):231-241.

16. Gorlach A, Brandes RP, Nguyen K, Amidi M, Dehghani F, Busse R. A gp91phox containing NADPH oxidase selectively expressed in endothelial cells is a major source of oxygen radical generation in the arterial wall. *Circ Res*. 2000;87(1):26-32.

17. Carnevale R, Pignatelli P, Lenti L, et al. LDL are oxidatively modified by platelets via GP91(phox) and accumulate in human monocytes. *FASEB J*. 2007;21(3):927-934.

18. Krotz F, Sohn HY, Gloe T, et al. NAD(P)H oxidase-dependent platelet superoxide anion release increases platelet recruitment. *Blood*. 2002;100(3):917-924.

19. Pignatelli P, Carnevale R, Di Santo S, et al. Inherited human gp91phox deficiency is associated with impaired isoprostane formation and platelet dysfunction. *Arterioscler Thromb Vasc Biol*. 2011;31(2):423-434.

20. Pignatelli P, Sanguigni V, Lenti L, et al. gp91phox-dependent expression of platelet CD40 ligand. *Circulation*. 2004;110(10):1326-1329.

21. Brill A, Fuchs TA, Chauhan AK, et al. von Willebrand factor-mediated platelet adhesion is critical for deep vein thrombosis in mouse models. *Blood*. 2011;117(4):1400-1407.

22. von Bruhl ML, Stark K, Steinhart A, et al. Monocytes, neutrophils, and platelets cooperate to initiate and propagate venous thrombosis in mice in vivo. *J Exp Med*. 2012;209(4):819-835.

23. Papayannopoulos V, Metzler KD, Hakkim A, Zychlinsky A. Neutrophil elastase and myeloperoxidase regulate the formation of neutrophil extracellular traps. *J Cell Biol*. 2010;191(3):677-691.

24. Metzler KD, Goosmann C, Lubojemska A, Zychlinsky A, Papayannopoulos V. A Myeloperoxidase-Containing Complex Regulates Neutrophil Elastase Release and Actin Dynamics during NETosis. *Cell Rep*. 2014.

25. Massberg S, Grahl L, von Bruehl ML, et al. Reciprocal coupling of coagulation and innate immunity via neutrophil serine proteases. *Nat Med*. 2010;16(8):887-896.

26. Lim MB, Kuiper JW, Katchky A, Goldberg H, Glogauer M. Rac2 is required for the formation of neutrophil extracellular traps. *Journal of Leukocyte Biology*. 2011;90(4):771-776.

27. Knaus UG, Heyworth PG, Evans T, Curnutte JT, Bokoch GM. Regulation of phagocyte oxygen radical production by the GTP-binding protein Rac 2. *Science*. 1991;254(5037):1512-1515.

28. Shirsat NV, Pignolo RJ, Kreider BL, Rovera G. A member of the ras gene superfamily is expressed specifically in T, B and myeloid hemopoietic cells. *Oncogene*. 1990;5(5):769-772.

29. Roberts AW, Kim C, Zhen L, et al. Deficiency of the hematopoietic cell-specific Rho family GTPase Rac2 is characterized by abnormalities in neutrophil function and host defense. *Immunity*. 1999;10(2):183-196.

30. Clark SR, Ma AC, Tavener SA, et al. Platelet TLR4 activates neutrophil extracellular traps to ensnare bacteria in septic blood. *Nat Med*. 2007;13(4):463-469.

31. Wagner DD, Frenette PS. The vessel wall and its interactions. *Blood*. 2008;111(11):5271-5281.

32. Fuchs TA, Brill A, Duerschmied D, et al. Extracellular DNA traps promote thrombosis. *Proc Natl Acad Sci U S A*. 2010;107(36):15880-15885.

33. Savchenko AS, Martinod K, Seidman MA, et al. Neutrophil extracellular traps form predominantly during the organizing stage of human venous thromboembolism development. *J Thromb Haemost*. 2014.

34. Andre P, Hartwell D, Hrachovinova I, Saffaripour S, Wagner DD. Pro-coagulant state resulting from high levels of soluble P-selectin in blood. *Proc Natl Acad Sci U S A*. 2000;97(25):13835-13840.

35. Ward CM, Tetaz TJ, Andrews RK, Berndt MC. Binding of the von Willebrand factor A1 domain to histone. *Thrombosis Research*. 1997;86(6):469-477.

36. Palabrica T, Lobb R, Furie BC, et al. Leukocyte accumulation promoting fibrin deposition is mediated in vivo by P-selectin on adherent platelets. *Nature*. 1992;359(6398):848-851.

37. Moore KL, Stults NL, Diaz S, et al. Identification of a specific glycoprotein ligand for P-selectin (CD62) on myeloid cells. *J Cell Biol*. 1992;118(2):445-456.

38. Seidman MA MR. Surgical pathology of small- and medium-sized vessels. *Surgical Pathology Clinics*. 2012;5(2):435-451.

39. Brill A, Fuchs TA, Savchenko AS, et al. Neutrophil extracellular traps promote deep vein thrombosis in mice. *J Thromb Haemost*. 2012;10(1):136-144.

40. Hoesel LM, Neff TA, Neff SB, et al. Harmful and protective roles of neutrophils in sepsis. *Shock*. 2005;24(1):40-47.

41. Meng W, Paunel-Gorgulu A, Flohe S, et al. Depletion of neutrophil extracellular traps in vivo results in hypersusceptibility to polymicrobial sepsis in mice. *Crit Care*. 2012;16(4):R137.

42. Luo L, Zhang S, Wang Y, et al. Pro-inflammatory role of neutrophil extracellular traps in abdominal sepsis. *Am J Physiol Lung Cell Mol Physiol*. 2014.

43. Martinod K, Demers M, Fuchs TA, et al. Neutrophil histone modification by peptidylarginine deiminase 4 is critical for deep vein thrombosis in mice. *Proc Natl Acad Sci U S A*. 2013;110(21):8674-8679.

44. Angus DC, van der Poll T. Severe sepsis and septic shock. *N Engl J Med*. 2013;369(9):840-851.

45. Xu J, Zhang X, Pelayo R, et al. Extracellular histones are major mediators of death in sepsis. *Nat Med*. 2009;15(11):1318-1321.

46. Bernard GR, Vincent JL, Laterre PF, et al. Efficacy and safety of recombinant human activated protein C for severe sepsis. *N Engl J Med*. 2001;344(10):699-709.

47. Hirsch JG. Bactericidal action of histone. *J Exp Med*. 1958;108(6):925-944.

48. Heit JA. Venous thromboembolism: disease burden, outcomes and risk factors. *J Thromb Haemost*. 2005;3(8):1611-1617.

49. van der Helm-van Mil AH, Huizinga TW. Advances in the genetics of rheumatoid arthritis point to subclassification into distinct disease subsets. *Arthritis Res Ther*. 2008;10(2):205.

50. Suzuki A, Yamada R, Chang X, et al. Functional haplotypes of PADI4, encoding citrullinating enzyme peptidylarginine deiminase 4, are associated with rheumatoid arthritis. *Nat Genet*. 2003;34(4):395-402.

51. Kang CP, Lee HS, Ju H, Cho H, Kang C, Bae SC. A functional haplotype of the PADI4 gene associated with increased rheumatoid arthritis susceptibility in Koreans. *Arthritis Rheum*. 2006;54(1):90-96.

52. Hoppe B, Haupl T, Gruber R, et al. Detailed analysis of the variability of peptidylarginine deiminase type 4 in German patients with rheumatoid arthritis: a case-control study. *Arthritis Res Ther*. 2006;8(2):R34.

53. Prandoni P, Noventa F, Ghirarduzzi A, et al. The risk of recurrent venous thromboembolism after discontinuing anticoagulation in patients with acute proximal deep vein thrombosis or pulmonary embolism. A prospective cohort study in 1,626 patients. *Haematologica*. 2007;92(2):199-205.

54. Becattini C, Agnelli G, Schenone A, et al. Aspirin for preventing the recurrence of venous thromboembolism. *N Engl J Med*. 2012;366(21):1959-1967.

55. Brighton TA, Eikelboom JW, Mann K, et al. Low-dose aspirin for preventing recurrent venous thromboembolism. *N Engl J Med*. 2012;367(21):1979-1987.

56. Sharifi M, Bay C, Nowroozi S, Bentz S, Valeros G, Memari S. Catheter-directed thrombolysis with argatroban and tPA for massive iliac and femoropopliteal vein thrombosis. *Cardiovasc Intervent Radiol*. 2013;36(6):1586-1590.

57. Fuchs TA, Brill A, Wagner DD. Neutrophil extracellular trap (NET) impact on deep vein thrombosis. *Arterioscler Thromb Vasc Biol*. 2012;32(8):1777-1783.

58. Martinod K, Wagner DD. Thrombosis: tangled up in NETs. *Blood*. 2014;123(18):2768-2776.

Appendix A-1

Supplemental Figures for Chapter 2

This appendix contains supplemental figures from:

Martinod K, Demers M, Fuchs TA, Wong SL, Brill A, Gallant M, Hu J, Wang Y, Wagner DD. *Neutrophil histone modification by peptidylarginine deiminase 4 is critical for deep vein thrombosis in mice*. Proc Natl Acad Sci. 2013 May 21; 110 (21): 8674-9. Epub 2013 May 6. PMCID: 3666755.

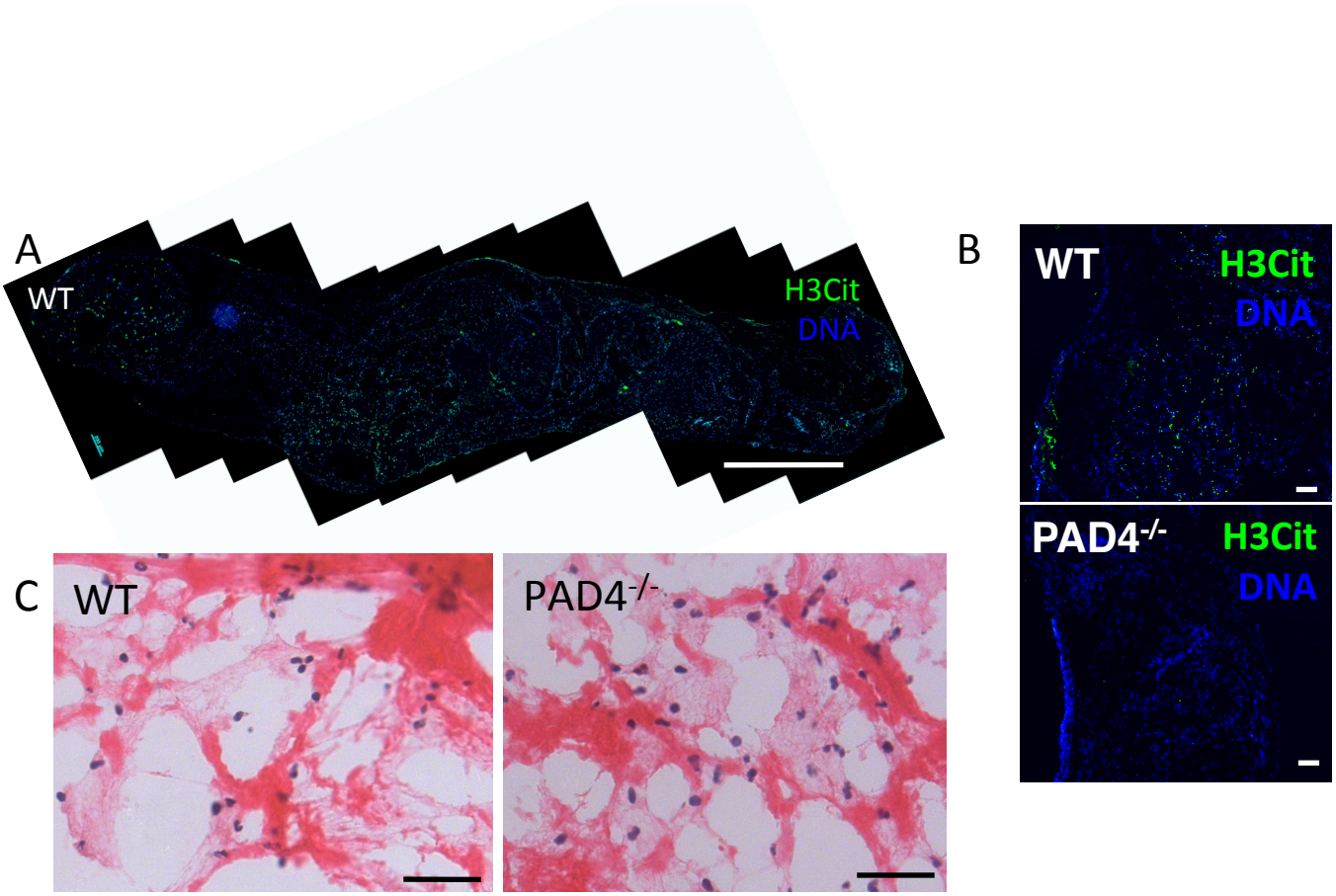

Figure S2.1. Characterization of thrombi formed 6 h after IVC stenosis. A. Composite image of a thrombus collected from a WT mouse 6 h after IVC ligation and immunostained for H3Cit and DNA. In contrast to 48 h where extracellular H3Cit is present in abundance, thrombi at 6 h contained mostly nuclear H3Cit staining. H3Cit, green; DNA, blue. Scale bar, 1 mm. B. In contrast to WT, H3Cit staining is completely absent in PAD4$^{-/-}$ thrombi collected 6 h after IVC ligation. Representative of n=3, scale bar, 100 μm. C. Hematoxylin and eosin staining shows similar leukocyte densities at 6 h between WT and PAD4$^{-/-}$ thrombi. n=3-4. Scale bar, 20 μm.

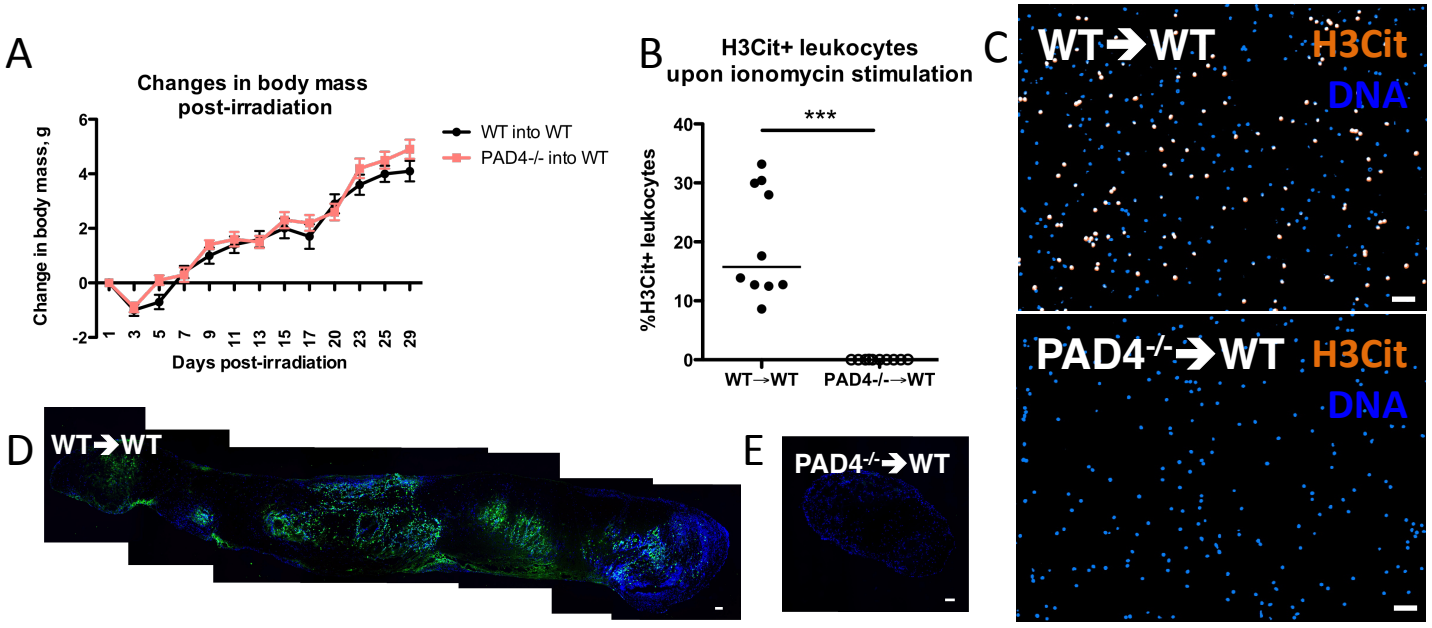

Figure S2.2. Characterization of bone marrow chimeras generated for IVC stenosis experiments. A. Bone marrow chimeras were generated by lethally irradiating WT mice and immediately transfusing at least 1 x 10^7 WT or PAD4$^{-/-}$ BM cells. Both animals groups had similar recoveries as seen by body weight gain over time. Black line, WT donor; red line, PAD4$^{-/-}$ donor. B. The success of the chimerism was tested by stimulating blood leukocytes with ionomycin for 2 h and immunostaining for H3Cit. The total leukocyte population was studied rather than isolated neutrophils in order to minimize the volume of blood being drawn from mice prior to DVT surgeries. Leukocytes from PAD4$^{-/-}$ bone marrow chimeras failed to hypercitrullinate histone H3 as determined by quantification of immunostained leukocytes. C. Representative images of H3Cit immunostaining used to evaluate chimerism. Scale bar, 100 μm. D, E. Recipients of WT bone marrow (D) produced thrombi containing H3Cit-positive extracellular staining, while the thrombus formed in a PAD4$^{-/-}$ bone marrow chimera (E) showed no H3Cit staining, similar to the PAD4$^{-/-}$ thrombus in Fig. 2.2H. Scale bar, 100 μm.

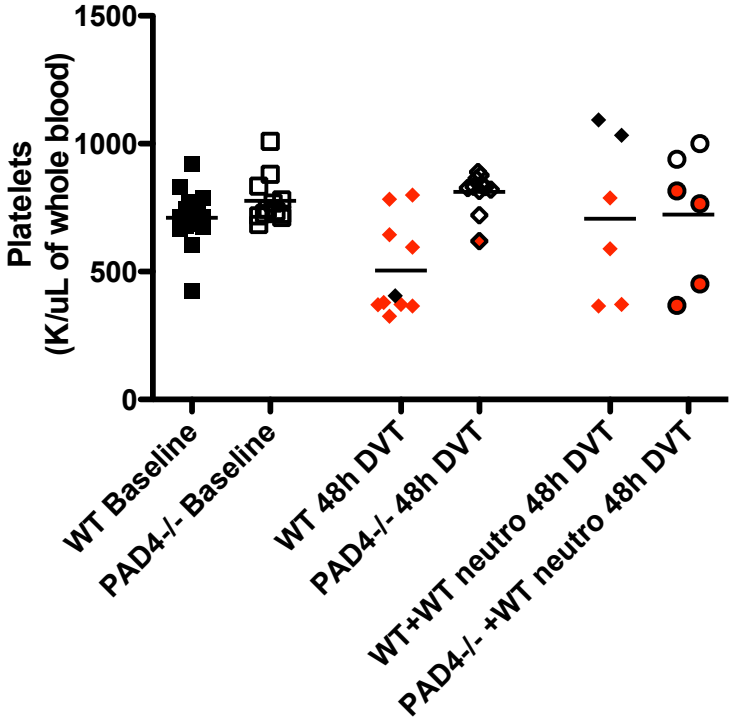

Figure S2.3. Platelet counts from 48 h venous stenosis experiments. Red color indicates mice that formed thrombi and black represents mice with no thrombi. WT baseline control compared to WT+WT neutrophil infusion 48 h DVT with thrombi, $p<0.02$, PAD4 baseline control compared to PAD4$^{-/-}$+WT neutrophil infusion 48 h DVT with thrombi, $p<0.04$).

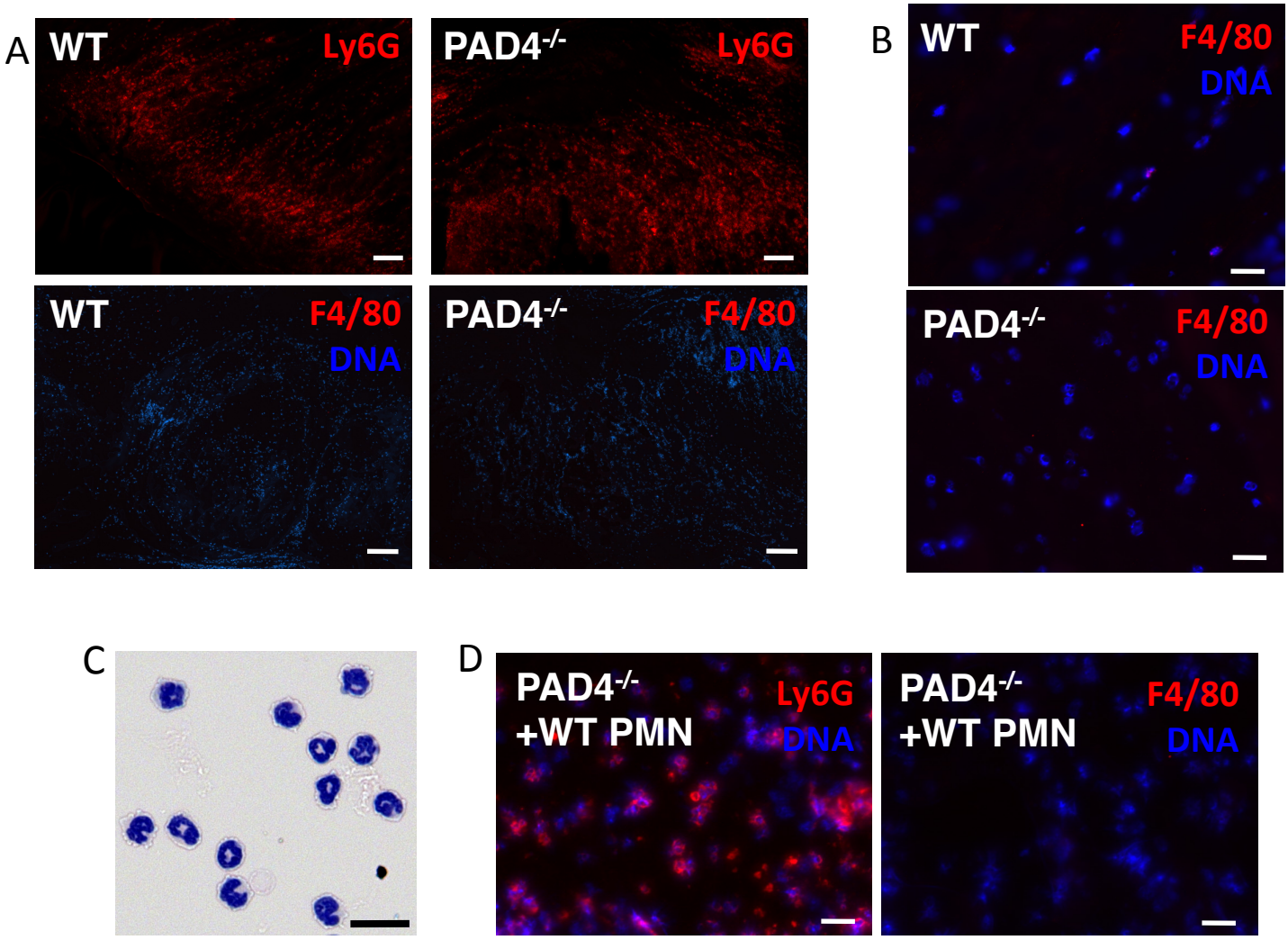

Figure S2.4. Histological analyses of thrombi collected from WT or PAD4$^{-/-}$ mice after IVC stenosis. A. Thrombi collected from WT mice or the PAD4$^{-/-}$ mouse that formed a thrombus 48 h after IVC stenosis showed an abundance of neutrophils by Ly6G immunostaining (upper panels, red) and few monocytes by F4/80 staining (lower panels, red). Scale bar, 100 μm. DNA is shown in blue. B. Thrombi from WT or PAD4$^{-/-}$ mice 48 h after IVC stenosis contained very few F4/80^{+} monocytes/macrophages. Scale bar, 20 μm. C. Isolated bone marrow neutrophils used for *in vivo* infusions were >95% pure as assessed by Wright-Giemsa staining of cytospins. Scale bar, 20 μm. D. Neutrophils were present in the thrombi of WT neutrophil-infused PAD4$^{-/-}$ mice at 48 h after ligation while few F4/80^{+} cells were detected, as is the case in thrombi produced in WT animals. Left panel, Ly6G (red); right panel, F4/80 (red). Scale bar, 20 μm.

Appendix A-2

Supplemental Figures for Chapter 3

This appendix contains supplemental figures from:

Martinod K, Fuchs TA, Wong SL, Demers M, Gallant M, Wang Y, Wagner DD. *PAD4-deficiency does not worsen polymicrobial sepsis mortality and ameliorates endotoxemic shock.* Submitted July 10, 2014 to Blood.

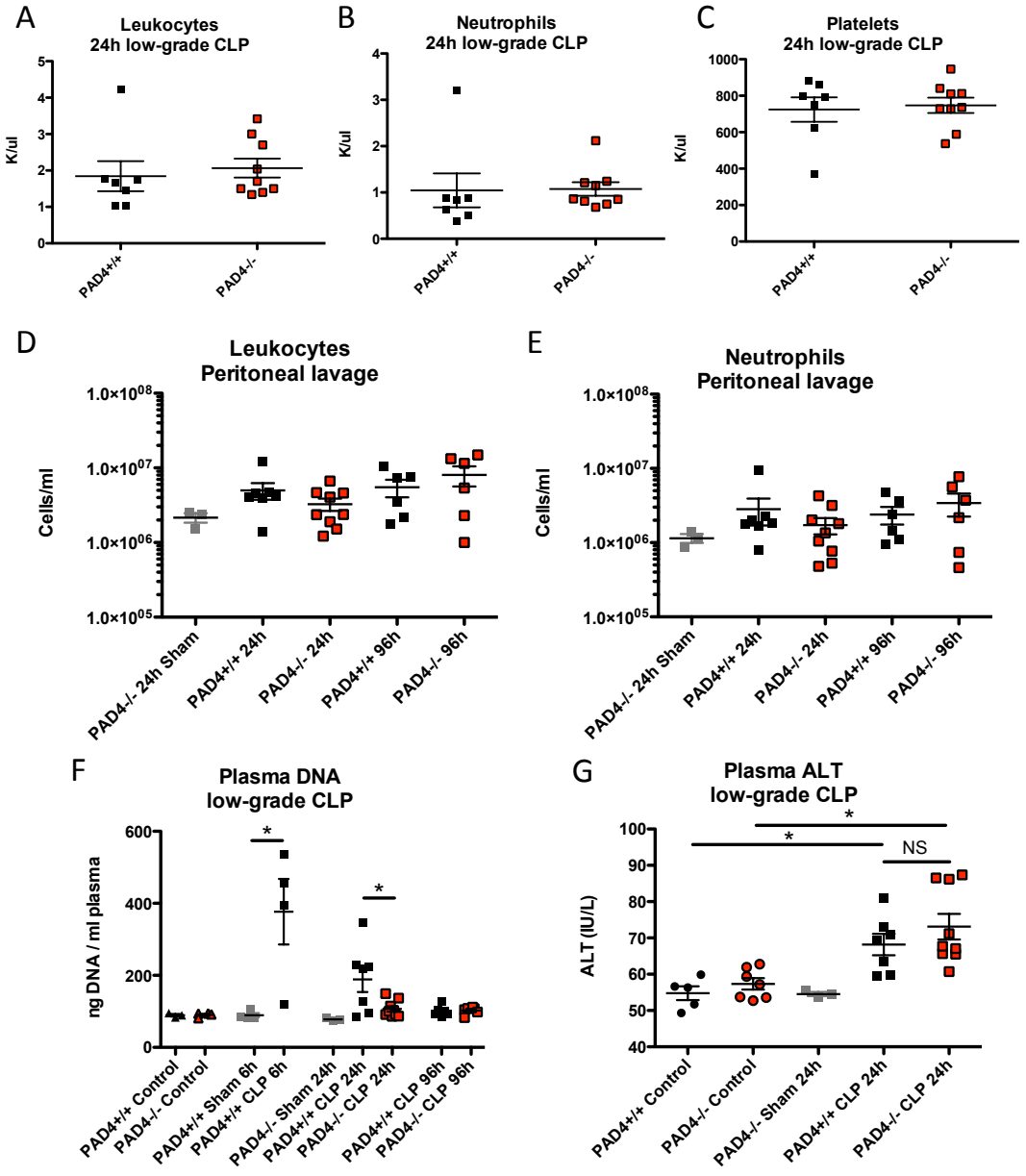

Figure S3.1. Additional blood cell parameters measured in low-grade CLP model. Leukocyte and neutrophil counts were similar between *PAD4*$^{+/+}$ and *PAD4*$^{-/-}$ CLP-operated mice in blood (A, B) and peritoneal lavage fluid (D, E). Blood platelet counts were also similar (C). F. Low-grade CLP resulted in significant increases in circulating plasma DNA in *PAD4*$^{+/+}$ compared to *PAD4*$^{-/-}$ mice. G. Plasma alanine aminotransferase (ALT), a marker of liver injury, was similarly increased in low-grade CLP mice in both *PAD4*$^{+/+}$ and *PAD4*$^{-/-}$ mice. *p<0.05.

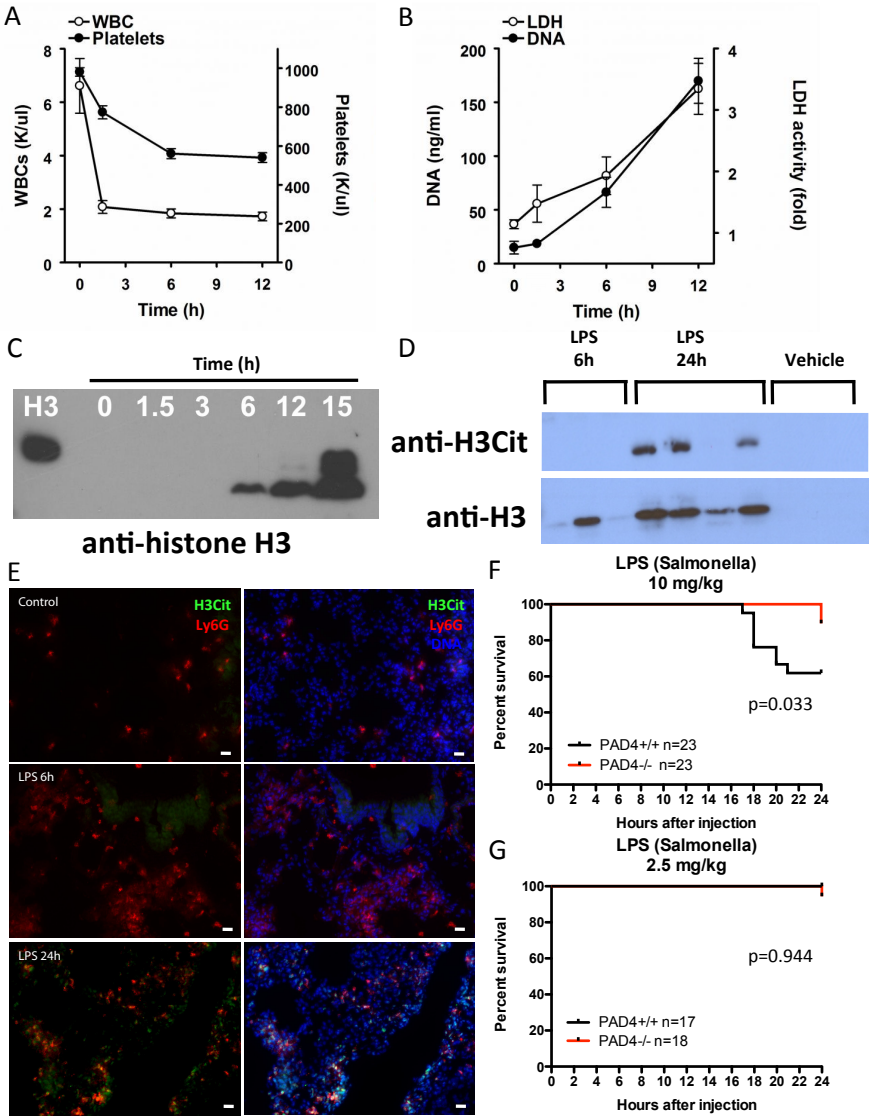

Figure S3.2. Characterization of endotoxemia induced by LPS from *Salmonella spp typhimurium*. Infusion of 10 mg/kg LPS i.v. in *PAD4*$^{+/+}$ mice resulted in a drop in platelet and leukocyte numbers in circulation (A) and increasing plasma DNA and LDH levels (B). By 6h after 10 mg/kg LPS infusion, fragmented histone H3 was detected in plasma of *PAD4*$^{+/+}$ mice by Western blot (C). At this same time point, H3Cit was not yet detected, but by 24h H3Cit was found in a majority of *PAD4*$^{+/+}$ mice (D). Vehicle-infused mice did not have significant levels of histone H3 or H3Cit in plasma. n=3-7. E. H3Cit-positive staining in neutrophils was present in the lung 24h, but not 6h after LPS infusion in *PAD4*$^{+/+}$ mice. No H3Cit+ staining was identified in liver, spleen, or kidney at the same time points (data not shown). n=3-4. F,G. Survival curves indicating degree of mortality in *PAD4*$^{+/+}$ (black line) vs *PAD4*$^{-/-}$ (red line) mice injected with 10 mg/kg LPS (F) or 2.5 mg/kg LPS (G). More *PAD4*$^{+/+}$ mice died with the 10 mg/kg LPS dose (F), while a great majority of mice survived the 2.5 mg/kg LPS dose (G).

Appendix A-3

Neutrophil Extracellular Traps Promote Deep Vein Thrombosis in Mice

This chapter contains the following publication:

Brill A, Fuchs TA, Savchenko AS, Thomas GM, Martinod K, De Meyer SF, Bhandari AA, Wagner DD. *Neutrophil extracellular traps promote deep vein thrombosis in mice*. J Thromb Haemost. 2012 Jan; 10 (1): 136-44. PMCID: 3319651.

Attributions:

Alexander Brill wrote the entirety of this manuscript. I performed immunostainings of IVC cross-sections and critically read the manuscript.

IN FOCUS

Neutrophil extracellular traps promote deep vein thrombosis in mice

A. BRILL,*† T. A. FUCHS,*† A. S. SAVCHENKO,*† G. M. THOMAS,*† K. MARTINOD,*‡ S. F. DE MEYER,*†§ A. A. BHANDARI* and D. D. WAGNER*†

*Immune Disease Institute, Program in Cellular and Molecular Medicine, Children's Hospital Boston, Boston, MA; †Department of Pediatrics, Harvard Medical School, Boston, MA; ‡Graduate Program in Immunology, Division of Medical Sciences, Harvard Medical School, Boston, MA, USA; and §Laboratory for Thrombosis Research, KULeuven Campus Kortrijk, Kortrijk, Belgium

To cite this article: Brill A, Fuchs TA, Savchenko AS, Thomas GM, Martinod K, De Meyer SF, Bhandari AA, Wagner DD. Neutrophil extracellular traps promote deep vein thrombosis in mice. *J Thromb Haemost* 2012; **10**: 136–44.

See also Gardiner EE, Ward CM, Andrews RK. The NET effect of clot formation. This issue, pp 133–5.

Summary. *Background:* Upon activation, neutrophils can release nuclear material known as neutrophil extracellular traps (NETs), which were initially described as a part of antimicrobial defense. Extracellular chromatin was recently reported to be prothrombotic *in vitro* and to accumulate in plasma and thrombi of baboons with experimental deep vein thrombosis (DVT). *Objective:* To explore the source and role of extracellular chromatin in DVT. *Methods:* We used an established murine model of DVT induced by flow restriction (stenosis) in the inferior vena cava (IVC). *Results:* We demonstrate that the levels of extracellular DNA increase in plasma after 6 h IVC stenosis, compared with sham-operated mice. Immunohistochemical staining revealed the presence of Gr-1-positive neutrophils in both red (RBC-rich) and white (platelet-rich) parts of thrombi. Citrullinated histone H3 (CitH3), an element of NETs' structure, was present only in the red part of thrombi and was frequently associated with the Gr-1 antigen. Immunofluorescent staining of thrombi showed proximity of extracellular CitH3 and von Willebrand factor (VWF), a platelet adhesion molecule crucial for thrombus development in this model. Infusion of Deoxyribonuclease 1 (DNase 1) protected mice from DVT after 6 h and also 48 h IVC stenosis. Infusion of an unfractionated mixture of calf thymus histones increased plasma VWF and promoted DVT early after stenosis application. *Conclusions:* Extracellular chromatin, likely originating from neutrophils, is a structural part of a venous thrombus and both the DNA scaffold and histones appear to contribute to the pathogenesis of DVT in mice. NETs may provide new targets for DVT drug development.

Correspondence: Denisa D. Wagner, Immune Disease Institute, 3 Blackfan Circle, 3rd floor, Boston, MA 02115, USA.
Tel.: +1 617 713 8300; fax: +1 617 713 8333.
E-mail: wagner@idi.harvard.edu

Received 26 September 2011, accepted 21 October 2011

Keywords: citrullination, deep vein thrombosis, histones, neutrophil extracellular traps, von Willebrand factor.

Introduction

Neutrophils stimulated with microbes or proinflammatory agents, reactive oxygen species (ROS) or activated platelets, release their nuclear material, forming a web-like extracellular network. These webs, formed by DNA, histones and neutrophil granule constituents [1], are designated as neutrophil extracellular traps (NETs) and are implicated in antimicrobial defense [2]. NETs are present in blood under septic conditions and platelets play a role in NETs production in a process involving binding of LPS to platelet toll-like receptor-4 (TLR4) [3]. In *in vitro* studies, NETs were shown to be prothrombotic and procoagulant [4,5]. Histones have also been reported to stimulate platelet aggregation [4,6] and promote platelet-dependent thrombin generation [7].

In addition to neutrophils, mast cells, monocytes and eosinophils have also been reported to liberate such extracellular DNA traps [8–10]. NETs can result not only from the presence of microbes but also accompany sterile inflammation, for example, in small-vessel vasculitis or pre-eclampsia [11,12]. Formation of NETs is a step-wise process characterized by nuclear membrane dissolution, chromatin decondensation and cytolysis [13]. Histone citrullination is a hallmark of chromatin decondensation in neutrophils [14]. It is a post-translational modification (conversion of arginine to a non-conventional amino acid citrulline) mediated by peptidylarginine deiminase 4 (PAD4), an enzyme expressed highly in granulocytes [15,16]. Inactivation of PAD4 results in suppression of NETs formation [16]. $PAD4^{-/-}$ neutrophils have a profound defect in their ability to kill bacteria and $PAD4^{-/-}$ mice are less protected against bacterial infection than wild-type mice [16].

Deep vein thrombosis (DVT) is diagnosed in approximately 900 000 cases in the US annually [17]. We have recently demonstrated that extracellular DNA accumulates

in plasma in experimental DVT in baboons and the presence of DNA and histones in venous thrombi [4]. The ability of histones to upregulate thrombin generation in plasma by suppressing protein C activation [18] may have direct implications on DVT as deficiency in protein C or resistance to activated protein C, due to factor V Leiden mutation, are risk factors for DVT in humans [19–21]. In this study, we explore the role of extracellular chromatin and histones in a murine model of flow restriction-induced DVT [22]. Venous thrombi developed in this model are structurally similar to human thrombi with white (platelet-rich) and red (RBC-rich) parts [22,23]. We show that venous thrombi contain large amounts of extracellular citrullinated histone H3 (CitH3), often in proximity to von Willebrand factor (VWF), an important molecule in the initiation of DVT [22]. We also demonstrate that intravenously administered histones exacerbate DVT, whereas Deoxyribonuclease 1 (DNase 1), which degrades NETs [4], protects mice from venous thrombosis.

Material and methods

Mice

Wild-type C57BL/6J (WT) mice were from Jackson Laboratory (Bar Harbor, ME, USA). All mice were 7–9-week-old males weighing 22–26 g. All experimental procedures involving mice were approved by the Animal Care and Use Committee of the Immune Disease Institute.

Flow restriction model

The murine model of DVT was performed as described [22]. In brief, mice were anesthetized by isoflurane-oxygen, intestines were exteriorized and the inferior vena cava (IVC) was diligently separated from aorta. A suture was placed on the IVC just below the renal veins over a spacer (diameter of 0.26 mm) and then the spacer was removed. This procedure has been shown to decrease vascular lumen by about 90% and avoid endothelial injury. All visible IVC side branches were also sutured. Thereafter, peritoneum and skin were closed, mice were sacrificed after 1–48 h and thrombi formed in the IVC were harvested. Sham-operated mice were opened and IVC sutured similarly to the experimental mice, but the suture was removed immediately after ligation.

Histone infusion

A mixture of all histones isolated from calf thymus (Worthington, Lakewood, NJ, USA) was dissolved in sterile saline and infused intravenously in mice immediately before IVC stenosis application. The dose used (10 mg kg^{-1}) is known to produce a 25% decrease in platelet count 10 min after infusion [6]. The infused solution of histone mix was essentially endotoxin-free (< 0.025 EU mL^{-1}; measured using the endotoxin detection kit [Lonza, Walkersville, MD, USA] according to the manufacturer's instructions). Control mice received infusion of sterile saline. Mice were sacrificed 1 h after surgery and thrombus formation was examined.

DNase 1 infusion

DNase 1 (Pulmozyme®, Genentech, San Francisco, CA, USA) was diluted in sterile saline and injected immediately after surgery (50 μg intraperitoneally and 10 μg intravenously). In experiments with 48 h IVC stenosis, injections were repeated three more times after every 12 h. Control mice were injected with the Pulmozyme vehicle buffer (8.77 mg mL^{-1} sodium chloride and 0.15 mg mL^{-1} calcium chloride) diluted in sterile saline.

Determination of extracellular DNA in plasma

Blood (100 μL) was drawn from the periorbital eye plexus and stabilized with 5 μL of 0.5 M EDTA. Time points for blood drawing were: 24 h before (all mice) and then either 6, 24 and 48 h after DVT (three mice) or sham surgery (four mice), or 6 and 48 h after DVT (three mice) or sham surgery (four mice). Plasma was obtained by centrifugation at 2300 *g*, diluted 50-fold with PBS containing 0.1% BSA, mixed with an equal volume of 1 μM of the fluorescent DNA dye SytoxGreen (Invitrogen, Carlsbad, CA, USA) and fluorescence of dye bound to DNA was immediately determined by a fluorescence microplate reader (Fluoroskan, Thermo Scientific, Waltham, MA, USA) as described [4]. Background fluorescence of PBS-plasma mixture (without SytoxGreen) was subtracted from all samples.

Frozen sections

Thrombi with or without the surrounding IVC wall or sham IVC (IVC fragment of 6–8 mm ligated at both ends with blood remaining inside) were harvested, embedded in Optimal Cutting Temperature (OCT) compound (Sakura Finetek, Torrance, CA, USA) and then cryosectioned into 10-μm sections.

Immunohistochemistry

Immunohistochemistry was performed as previously described [24]. Briefly, anti-mouse Gr-1 antibody (dilution 1:500, clone RB6-8C5; BD Pharmingen, Franklin Lakes, NJ, USA) and rabbit polyclonal [CitH3] antibody to citrullinated histone H3 (dilution 1:300, citrulline 2 + 8 + 17; ab5103, Abcam, Cambridge, MA, USA) were used as first antibodies. Histofine Simple Stain Mouse MAX PO for rat (414311F) and rabbit (414351F), respectively, purchased from Nichirei Corporation (Tokyo, Japan), were used as secondary antibodies. Diaminobenzidine (DAB) substrate kit (Vector Laboratories, Burlingame, CA, USA), containing DAB and DAB-Ni, was used for visualization of staining. Finally, sections were counterstained with Nuclear Fast Red (Sigma-Aldrich, St Louis, MO, USA). No first antibodies were applied in control sections.

Immunofluorescent staining

Sections were incubated with zinc fixative for 15 min, washed in PBS, and permeabilized with 0.1% Triton X-100, 0.1% sodium citrate on ice. After washing and blocking with 3% bovine serum albumin (BSA, Sigma-Aldrich), the sections were incubated for 16 h at 4 °C in 0.3% BSA in PBS with 0.3 μg mL^{-1} rabbit polyclonal anti-CitH3 (citrulline 2 + 8 + 17; ab5103, Abcam), and sheep polyclonal anti-VWF (1:50 dilution of IgG fraction; ab11713, Abcam). For longitudinal sections of isolated thrombi, anti-CitH3 Ab was applied overnight and anti-VWF Ab for 90 min. After washing, sections were incubated with the following Alexa Fluor-conjugated secondary antibodies (all from Invitrogen) in 0.3% BSA in PBS: Alexa Fluor 488 donkey anti-rabbit IgG and Alexa Fluor 568 donkey anti-sheep IgG (2 μg mL^{-1} for all Abs) for 2 h at room temperature. DNA was labeled with 1 μg mL^{-1} Hoechst 33342 (Invitrogen). Fluorescent images for cross-sections were acquired using an Axiovert 200 inverted widefield fluorescence microscope (Zeiss, Thornwood, NY, USA) in conjunction with a Zeiss Axiocam MRm monochromatic CCD camera. Mosaic reconstruction of entire cross-sections was performed with MosaicJ [25] for ImageJ software (National Institutes of Health, Bethesda, MD, USA; http://rsbrreb/nih/gov/iji) and consists of two to six fields of view per image shown. Images for longitudinal sections were obtained by a widefield fluorescence microscope using an Axioplan microscope (Zeiss) with color HRc Zeiss camera. Images were analyzed with Axiovision software (Zeiss).

Plasma VWF measurement

The assay was performed as described [22]. The level of VWF in pooled plasma of 20 C57BL/6J WT mice was used as a reference standard.

Statistics

Results obtained on the same animal at different time points (difference in plasma DNA levels between baseline and 6 h and plasma VWF content) were compared using paired Student's *t*-test. Plasma DNA levels in mice with IVC stenosis and sham-operated animals were compared by Mann–Whitney test. Difference in thrombi prevalence between different groups of mice was compared using a contingency table and the chi-square test. Differences were considered significant at $P < 0.05$.

Results

Flow restriction in the IVC promotes plasma DNA accumulation

We performed IVC stenosis in WT mice. Blood was drawn 24 h before and 6, 24 and 48 h after surgery and plasma DNA levels were measured. Plasma of non-operated mice contained 284 ± 18.9 ng mL^{-1} DNA. Stenosis of the IVC led to an increase in plasma DNA levels 6 h post surgery (Fig. 1) to 515 ± 34.7 ng mL^{-1} ($P < 0.003$ vs. baseline and $P < 0.03$ vs. sham-operated mice). This effect did not result from the surgical procedure because sham-operated mice had plasma DNA levels similar to non-operated animals (326 ± 47.4 ng mL^{-1}, $P = 0.9$). The concentration of DNA in plasma 48 h after surgery returned to baseline and was not different in DVT- and sham-operated mice. Appearance of DNA in plasma 6 h after stenosis application, when about half of the mice form visible thrombi (as described in the text), indicates that chromatin release occurs early in the thrombotic process.

Venous thrombi contain CitH3 located predominantly in the red part of the thrombus

Besides neutrophils, other cell types can release chromatin [8–10]. Histone citrullination by PAD4 occurs in activated granulocytes and is necessary for the formation and release of NETs [14–16,26]. To assess the presence of NETs in venous thrombi, we stained thrombi developed in mice after 48 h IVC stenosis, for CitH3. The white part of the thrombus (the platelet-rich part remote from the suture) contained numerous Gr-1-positive cells but was essentially devoid of CitH3 (Figures 2A,B and 3A). Gr-1 is an antigen present on polymorphonuclear leukocytes and also on plasmacytoid dendritic cells and a small subset of monocytes (reviewed in [27]). The large red part of the thrombus (the RBC-rich part proximal to the suture) contained loci heavily stained for either Gr-1 only (Fig. 2C, yellow arrowhead) or both Gr-1 and CitH3 with substantial overlap of the two antigens (Fig. 2C, red arrowhead). Some Gr-1-positive cells formed extracellular fiber-like structures that strongly stained for CitH3, probably representing NETs (Fig. 2D, red arrowheads; Fig. 3B).

We have previously reported an important role of VWF in venous thrombosis initiation [22]. In baboon DVT thrombi, extracellular DNA was shown to co-localize with VWF [4]. Immunofluorescent staining for VWF in murine venous thrombi was often associated with extracellular CitH3 staining in the red part of thrombi (Fig. 3A,B,E,F). Multiple

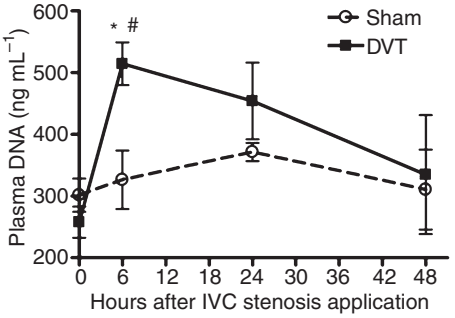

Fig. 1. Plasma DNA level is elevated 6 h after IVC stenosis application. Blood was drawn from wild-type mice before and 6, 24 and/or 48 h after IVC stenosis application (DVT) or sham surgery. Plasma was prepared and DNA levels determined by SytoxGreen dye; $n = 3$–8 per time point. *$P < 0.003$ vs. the same mice at baseline (paired *t*-test). $P < 0.03$, 6 h DVT vs. sham-operated mice (Mann–Whitney test). Error bars represent SEM.

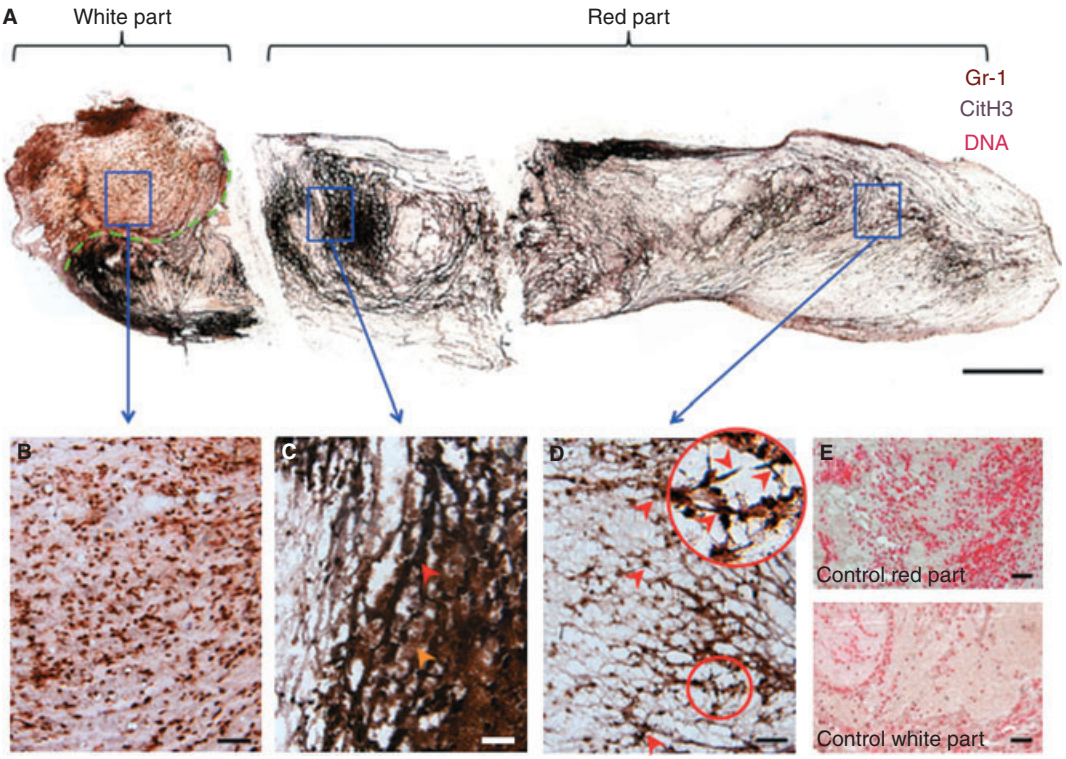

Fig. 2. Neutrophils expressing citrullinated histone H3 are present in deep vein thrombi. Frozen sections of a thrombus formed in the mouse IVC after 48 h IVC stenosis were stained for Gr-1 (brown) and CitH3 (grey-black), and counterstained for DNA (pink). (A) Composite of photographs of a stained longitudinal section of the entire thrombus with white (remote from the suture towards the tail) platelet-rich and red (adjacent to the suture) RBC-rich parts designated (dotted green line approximately delineates the white part of the thrombus). (B) High magnification of the white thrombus part. Note abundant Gr-1-positive neutrophil staining and absent CitH3 staining. (C, D) High magnification of the red part of the thrombus. (C) Orange arrowhead indicates single Gr-1 staining; red arrowhead designates double Gr-1/CitH3 staining. (D) Red arrowheads indicate NETs-like CitH3-positive structures. Inset represents high magnification of the circled area with NETs-like structures. (E) Negative control without first antibody from the red (upper panel) and white (lower panel) parts of the thrombus. (A) bar 500 μm; (B–E) bar 50 μm.

CitH3-positive cells were also revealed by the immunofluorescent staining in the core of the red part of thrombi (Fig. 3A), confirming our immunohistochemical data (Fig. 2C,D). No substantial CitH3 staining was observed in the white part of thrombi (Fig. 3A asterisk), IVC wall (Fig. 3E), sham-operated IVC (Fig. 3G) and in control sections stained without first antibody (Fig. 3C,D,H). Thus, histones present in murine IVC thrombi are likely to originate from neutrophils releasing NETs predominantly in the red part of thrombi. In mice, similar to baboon [4], thrombi extracellular chromatin frequently co-distributes with VWF.

Histones increase plasma VWF levels and promote DVT

Extracellular histones are cytotoxic to endothelial cells and activate platelets *in vitro*; histone infusion at a high dose of 75 mg kg^{-1} is lethal to mice [4,28]. We therefore used a lower dose (10 mg kg^{-1}) of histone mix, a dose that produces only mild thrombocytopenia [6], to test whether it renders mice more prone to venous thrombosis. Only two of 14 vehicle-treated mice (14%) produced thrombi after 1 h IVC stenosis (Fig. 4), while five of nine mice that received histones prior to the surgery (55%) developed a thrombus ($P < 0.04$).

Histones have been shown to cause Ca^{2+} influx in different cell types [6,29,30]. Increase in intracellular Ca^{2+} level triggers VWF secretion from endothelial cells and platelets, with some of the VWF remaining associated with the plasma membrane of these cells [31]. Platelet recruitment mediated by VWF is a key step in the initiation of venous thrombosis in this model of DVT [22]. Therefore stimulation of VWF secretion could be one of the mechanisms responsible for the prothrombotic effect of histones. Indeed, histone infusion increased plasma VWF levels compared with baseline (Table 1). In contrast, VWF plasma levels in vehicle-treated mice remained unchanged. Thus, histone infusion increases plasma concentration of VWF, which could contribute to the effect of histones on DVT in the flow restriction setting.

DNase 1 infusion protects mice from DVT

Based on the presence of histones, DNA and NET-like structures in deep vein thrombi in baboons [4] and mice (this report) and on the ability of DNase 1 to disassemble NET-induced thrombi in a flow chamber [4], we hypothesized that

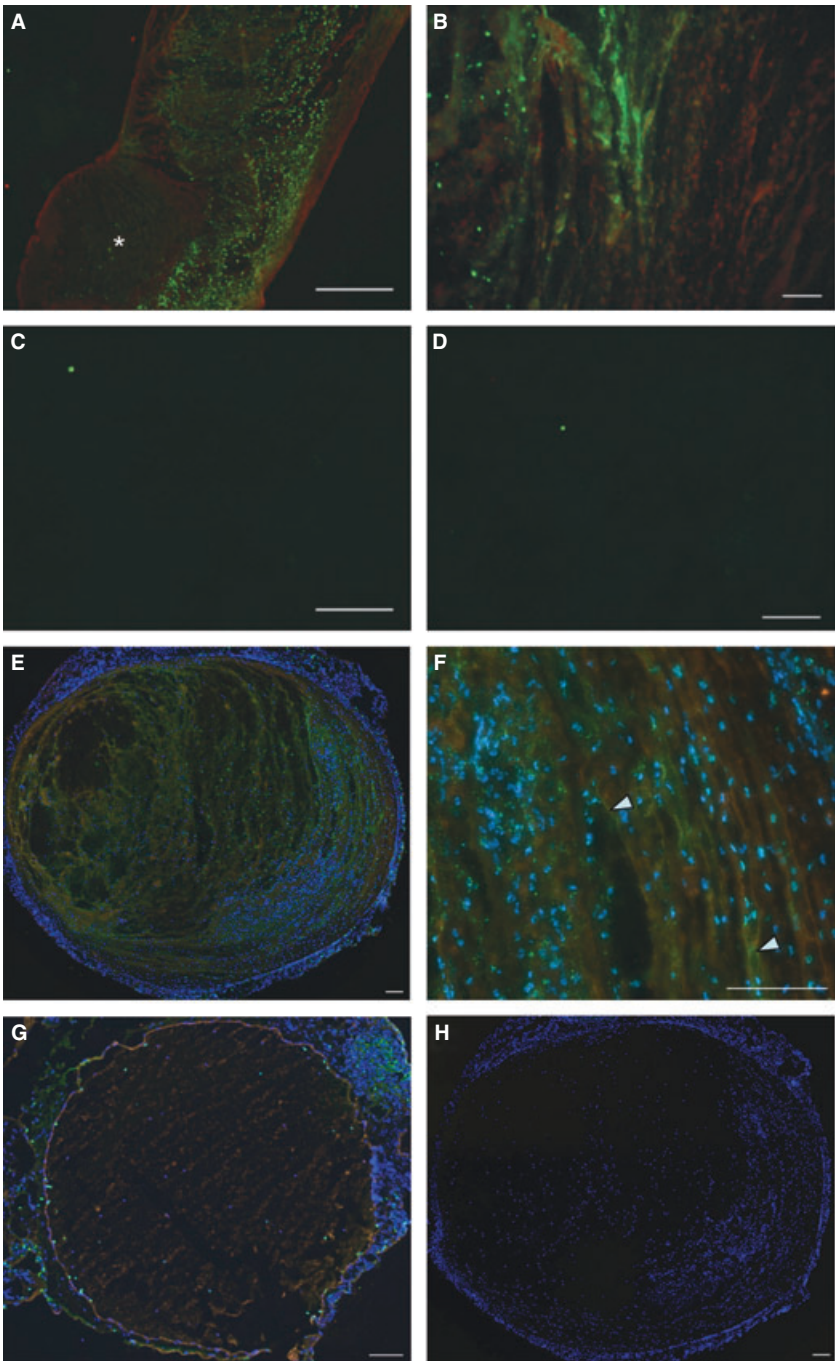

Fig. 3. Extracellular citrullinated histone H3 is partially associated with VWF in murine deep vein thrombi. (A–D) Widefield fluorescence microscopy analysis of longitudinal sections of a thrombus developed in the IVC after 48 h stenosis. Sections were immunostained for VWF (red) and for CitH3 (green) (upper panels). Incubation with only secondary antibodies served as a negative control (lower panels). (A) The 'white part' of the thrombus (*) was positive for VWF but negative for citrullinated histone H3, whereas the 'red part' of the thrombus was positive for both VWF and CitH3. The red part-associated CitH3 could be observed as a punctiform (intracellular) or diffuse (extracellular) staining. (A, C) Scale bars, 500 μm. (B) Higher magnification images show frequent co-distribution of extracellular CitH3 with VWF within the red part of thrombus as indicated by the arrowheads. (B, D) Scale bars, 50 μm. (E, F, H) Widefield fluorescence microscopy analysis of cross-sections of the red part of a thrombus developed in the IVC after 48 h stenosis and including vessel wall. (E, F, G) Sections were immunostained for VWF (red) and CitH3 (green) and counterstained for DNA (Hoechst 33342, blue); (H) control staining without first antibody. (E, F) Prominent CitH3 staining could be found within the thrombus and was often in proximity to VWF (F, arrowheads). No extracellular CitH3 could be detected in a sham-operated vessel containing only blood (G). (E–H) Scale bars, 100 μm.

DNase 1 might prevent DVT *in vivo*. To test this possibility, we infused DNase 1 in mice immediately after surgery and examined thrombosis after 6 or 48 h of IVC stenosis (in 48-h DVT experiments, infusions were repeated every 12 h). In the 6-h model, half (seven of 14) of the vehicle-treated mice produced a thrombus (Fig. 5), whereas in mice that received

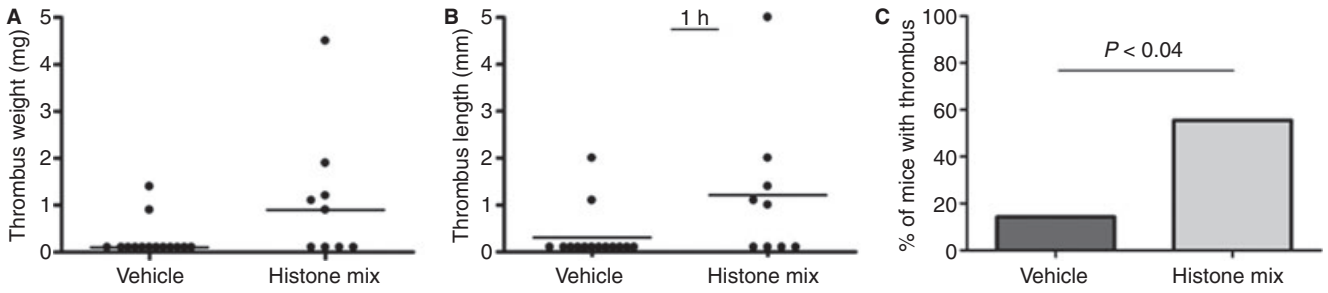

Fig. 4. Histone infusion promotes flow restriction-induced thrombosis in mice. Histone mix (10 mg kg^{-1}) was infused into WT mice immediately before DVT surgery. Mice were sacrificed after 1 h stenosis and thrombi developed in the IVC were examined and harvested. Values for weight (A) and length (B) of the thrombi are shown with medians (horizontal bars). (C) Percentage of mice that developed a thrombus. Vehicle-treated mice, $n = 14$; histone-treated mice, $n = 9$.

Table 1 Histone infusion elevates plasma VWF levels. Blood was drawn 24 h before and 1 h after infusion of saline or histone mix (10 mg kg^{-1}). *P* value was calculated by the paired *t*-test. Saline-injected mice, $n = 8$; histone-injected mice, $n = 6$

Saline		Histone mix	
Baseline	1 h after infusion	Baseline	1 h after infusion
83 ± 2.7%	78 ± 5.2%	78 ± 4.2%	94 ± 6.7%
–	$P = 0.43$	–	$P < 0.003$

DNase 1, only one mouse of 10 formed a thrombus ($P < 0.05$). In the 48-h IVC stenosis model, mice treated with control buffer developed a thrombus in 63% of cases (five of eight), whereas thrombus prevalence in mice treated with DNase 1 was 17% (two of 12, $P < 0.04$). These data suggest that extracellular chromatin may play a role in flow restriction-induced thrombosis and DNase 1 infusion is protective against thrombosis in this model.

Discussion

Several cell types have been shown to release extracellular chromatin upon activation. The role of the nuclear material originating from neutrophils, NETs, in antimicrobial defense has been convincingly demonstrated [2]. We recently published evidence that extracellular chromatin could be implicated in thrombosis because NETs can form a scaffold able to recruit both platelets and RBCs *in vitro* [4]. Perfusion of blood over NETs in a flow chamber results in the formation of a red thrombus, which was entirely NET-dependent as DNase 1, which destroys NETs, prevented recruitment of both cell types. This suggested a mechanistic link between NETs and DVT because (i) recruitment of platelets is one of the early events

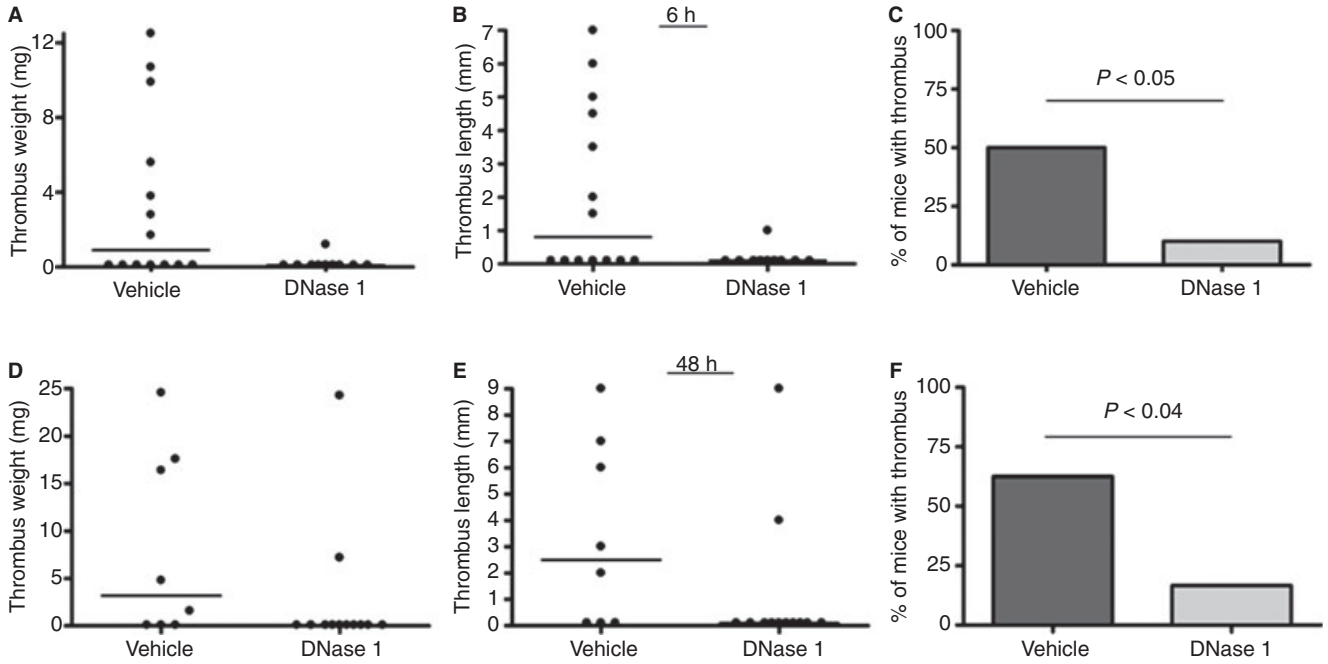

Fig. 5. DNase 1 infusion protects mice from flow restriction-induced thrombosis. Wild-type mice underwent IVC stenosis for 6 h (A–C) or 48 h (D–F). Mice received infusion of either vehicle or DNase 1 (50 μg ip and 10 μg iv) before the surgery (A–F) and every 12 h thereafter (D–F). (A, D) Thrombus weight and (B, E) thrombus length are presented; horizontal lines represent median. (C, F) Percentage of mice with a thrombus; 6 h vehicle, $n = 14$; 6 h DNase 1, $n = 10$; 48 h vehicle, $n = 8$; 48 h DNase 1, $n = 12$.

pivotal for thrombus initiation in mice [22] and (ii) DVT thrombi are rich in RBCs [23]. Thrombi developed in the murine flow restriction model of DVT also consist of a large RBC-rich red part and a smaller platelet-rich white part with both parts containing fibrin [22]. Thus, thrombi formed in this murine model share close morphological similarity to human DVT thrombi, which also include white and red parts [23].

Thrombi obtained in an experimental DVT model in baboons have been shown to contain extracellular DNA, H3 and DNA/H2A/H2B complex [4]. Here we demonstrate that histone H3 was also abundantly present in murine DVT thrombi. We show that histone H3 was citrullinated, suggesting that it is likely to have originated from neutrophils forming NETs. PAD4, the enzyme responsible for arginine conversion to citrulline, is abundantly expressed in granulocytes [15,16]. Staining for Gr-1, a neutrophil marker, revealed neutrophil presence in both red and white parts of the murine venous thrombi. Neutrophil-specific staining in the red part of thrombi was frequently associated with CitH3, with CitH3 being either confined to nuclei or localized extracellularly. This suggests that here neutrophils are at different stages of NETosis (Figures 2 and 3). Interestingly, little CitH3-positive staining was observed in the white part of thrombi despite abundant presence of Gr-1-positive cells. As NETosis is an irreversible process, one may speculate that neutrophils in the white part have spent less time in the thrombus compared with the red part neutrophils. This may suggest that the white part, originally adjacent to the stenosis site where thrombus growth begins, has a role in recruiting neutrophils from the surrounding blood. This is likely to be through binding to the activated platelets. Later on, these neutrophils may also become activated and form NETs, which in turn would contribute to recruitment of RBCs and the formation of red thrombus.

This model corroborates the reported ability of stimulated platelets to bind neutrophils and induce formation and release of NETs [3,5]. In addition, flow restriction may create hypoxic conditions in the vessel wall and cells buried inside a thrombus are exposed to even more severe hypoxia due to isolation from the blood stream. Hypoxia potentiates the release of ROS [32]. Besides neutrophils, platelets also can generate ROS, such as superoxide [33]. It has been shown that ROS not only directly contribute to thrombosis [34] but also can trigger formation of NETs [13,35]. Therefore, the adherent neutrophils exposed to two major triggers of NETs production, activated platelets and ROS, release extracellular chromatin, which then contributes to further thrombus development.

At the early stages of flow restriction, massive recruitment of both platelets and leukocytes to the endothelium occurs simultaneously [22]. It has recently been reported that co-culture of neutrophils with activated endothelial cells can also induce NET formation, which in turn promotes endothelial damage [36]. As the activation state of the endothelium is critical for DVT initiation [22], it is possible that NETs-endothelial interactions could be involved in thrombus initiation. This fits with our observation that NETs biomarkers accumulate in plasma within hours after flow restriction induction and that histones cause an increase in plasma VWF levels, probably from the activated endothelium.

As NETs are generated during the early stage of thrombus initiation and are also abundantly present in mature thrombi, it would be reasonable to hypothesize that NETs degradation might affect thrombosis. DNase 1 has been shown to degrade NETs *in vitro* [2]; a lesser ability of DNase 1 to dismantle NETs in plasma of patients with systemic lupus erythematosus correlates with severity of kidney dysfunction [37]. Here, infusion of DNase 1 protected mice from flow restriction-induced DVT regardless of the length of stenosis (6 or 48 h, Fig. 5). As no visible thrombus was detected in most DNase 1-treated mice, DNase 1 apparently cleaves NETs early, disrupting the pathways of cellular activation and preventing the cascade of events leading to thrombosis. The anti-thrombotic effect of DNase 1 is likely to be mediated by removal of NETs generated locally at the site of stenosis, similar to cleavage of endothelium-bound VWF by ADAMTS13. Similar to ADAMTS13, DNase 1 infusion may not reduce the amount of circulating DNA but rather affect its size and local concentration.

It is known that blood coagulation contributes to DVT and hypercoagulable states are considered risk factors for the disease [19–21]. The murine DVT model used in our study recapitulates this feature of human DVT because fibrin could be detected throughout the thrombus [22]. Although anticoagulants have not been tested in this model, a procoagulant state, such as in mice with high plasma levels of soluble P-selectin [38], is associated with increased DVT induced by stasis in the IVC [39]. It remains unclear whether DNase 1 infusion attenuates, directly or indirectly, blood coagulation and a potential off-target effect of DNase 1 on some components of the coagulation cascade cannot be fully ruled out.

We observed that strings of extracellular CitH3 frequently co-localized with VWF in the thrombi produced by IVC stenosis. This finding corroborates *in vitro* observations that histone [40] and NETs bind VWF [4]. Secretion of VWF from Weibel–Palade bodies (WPBs) to the surface of endothelial cells appears required for the development of DVT in mice [22].

Interestingly, VWF expression is downregulated in the venous valvular sinus, which experiences stasis and hypoxia, likely to maintain a thromboresistant phenotype at this thrombosis-susceptible site [41]. In thrombi, VWF may originate not only from endothelium but also from platelets, in which it is stored in alpha-granules. It is tempting to speculate that VWF and NETs form a mutually supportive network that contributes to VWF A1 domain activation [31] and to growth and stabilization of a venous thrombus.

Histones also are likely to participate in the process of thrombus initiation. Infusion of histone mix facilitated thrombosis in mice (Fig. 4). This may result from the observed deleterious effect of histones on endothelium *in vitro* [28], which at a lower dose *in vivo* might activate endothelium and

stimulate the release of VWF as we observed (Table 1). Another prothrombotic effect of histones could result from activation of platelets [4,6]. Activated platelets can stimulate NETs production [3,5] and promote release of WPBs [42], leading to further recruitment of platelets and leukocytes. In either case, histones would contribute to the process of thrombus initiation and propagation.

In conclusion, our study demonstrates an important functional role of NETs in DVT induced by flow restriction and provides possible new targets for drug development.

Acknowledgements

This work was supported by National Heart, Lung, and Blood Institute of the National Institutes of Health grants R01 HL041002, R01 HL095091 and R01 HL102101 (to D.D.W.). S. F. De Meyer is a postdoctoral fellow of the 'Fond voor Wetenschappelijk Onderzoek Vlaanderen' (FWO). We thank L. Cowan for help in preparing the manuscript.

Disclosure of Conflict of Interests

The authors state that they have no conflict of interest.

References

1 Brinkmann V, Zychlinsky A. Beneficial suicide: why neutrophils die to make NETs. *Nat Rev Microbiol* 2007; **5**: 577–82.
2 Brinkmann V, Reichard U, Goosmann C, Fauler B, Uhlemann Y, Weiss DS, Weinrauch Y, Zychlinsky A. Neutrophil extracellular traps kill bacteria. *Science* 2004; **303**: 1532–5.
3 Clark SR, Ma AC, Tavener SA, McDonald B, Goodarzi Z, Kelly MM, Patel KD, Chakrabarti S, McAvoy E, Sinclair GD, Keys EM, Allen-Vercoe E, Devinney R, Doig CJ, Green FH, Kubes P. Platelet TLR4 activates neutrophil extracellular traps to ensnare bacteria in septic blood. *Nat Med* 2007; **13**: 463–9.
4 Fuchs TA, Brill A, Duerschmied D, Schatzberg D, Monestier M, Myers DD Jr, Wrobleski SK, Wakefield TW, Hartwig JH, Wagner DD. Extracellular DNA traps promote thrombosis. *Proc Natl Acad Sci U S A* 2010; **107**: 15880–5
5 Massberg S, Grahl L, von Bruehl ML, Manukyan D, Pfeiler S, Goosmann C, Brinkmann V, Lorenz M, Bidzhekov K, Khandagale AB, Konrad I, Kennerknecht E, Reges K, Holdenrieder S, Braun S, Reinhardt C, Spannagl M, Preissner KT, Engelmann B. Reciprocal coupling of coagulation and innate immunity via neutrophil serine proteases. *Nat Med* 2010; **16**: 887–96
6 Fuchs TA, Bhandari AA, Wagner DD. Histones induce rapid and profound thrombocytopenia in mice. *Blood* 2011; **118**: 3708–14
7 Semeraro F, Ammollo CT, Morrissey JH, Dale GL, Friese P, Esmon NL, Esmon CT. Extracellular histones promote thrombin generation through platelet-dependent mechanisms: involvement of platelet TLR2 and TLR4. *Blood* 2011; **118**: 1952–61
8 von Kockritz-Blickwede M, Goldmann O, Thulin P, Heinemann K, Norrby-Teglund A, Rohde M, Medina E. Phagocytosis-independent antimicrobial activity of mast cells by means of extracellular trap formation. *Blood* 2008; **111**: 3070–80
9 Chow OA, von Kockritz-Blickwede M, Bright AT, Hensler ME, Zinkernagel AS, Cogen AL, Gallo RL, Monestier M, Wang Y, Glass CK, Nizet V. Statins enhance formation of phagocyte extracellular traps. *Cell Host Microbe* 2010; **8**: 445–54
10 Yousefi S, Gold JA, Andina N, Lee JJ, Kelly AM, Kozlowski E, Schmid I, Straumann A, Reichenbach J, Gleich GJ, Simon HU. Catapult-like release of mitochondrial DNA by eosinophils contributes to antibacterial defense. *Nat Med* 2008; **14**: 949–53
11 Gupta AK, Hasler P, Holzgreve W, Gebhardt S, Hahn S. Induction of neutrophil extracellular DNA lattices by placental microparticles and IL-8 and their presence in preeclampsia. *Hum Immunol* 2005; **66**: 1146–54
12 Kessenbrock K, Krumbholz M, Schonermarck U, Back W, Gross WL, Werb Z, Grone HJ, Brinkmann V, Jenne DE. Netting neutrophils in autoimmune small-vessel vasculitis. *Nat Med* 2009; **15**: 623–5
13 Fuchs TA, Abed U, Goosmann C, Hurwitz R, Schulze I, Wahn V, Weinrauch Y, Brinkmann V, Zychlinsky A. Novel cell death program leads to neutrophil extracellular traps. *J Cell Biol* 2007; **176**: 231–41
14 Wang Y, Li M, Stadler S, Correll S, Li P, Wang D, Hayama R, Leonelli L, Han H, Grigoryev SA, Allis CD, Coonrod SA. Histone hypercitrullination mediates chromatin decondensation and neutrophil extracellular trap formation. *J Cell Biol* 2009; **184**: 205–13
15 Nakashima K, Hagiwara T, Yamada M. Nuclear localization of peptidylarginine deiminase V and histone deimination in granulocytes. *J Biol Chem* 2002; **277**: 49562–8
16 Li P, Li M, Lindberg MR, Kennett MJ, Xiong N, Wang Y. PAD4 is essential for antibacterial innate immunity mediated by neutrophil extracellular traps. *J Exp Med* 2010; **207**: 1853–62
17 Heit JA. The epidemiology of venous thromboembolism in the community. *Arterioscler Thromb Vasc Biol* 2008; **28**: 370–2
18 Ammollo CT, Semeraro F, Xu J, Esmon NL, Esmon CT. Extracellular histones increase plasma thrombin generation by impairing thrombomodulin-dependent protein C activation. *J Thromb Haemost* 2011; **9**: 1795–803
19 Griffin JH, Evatt B, Zimmerman TS, Kleiss AJ, Wideman C. Deficiency of protein C in congenital thrombotic disease. *J Clin Invest* 1981; **68**: 1370–3
20 Dahlback B, Carlsson M, Svensson PJ. Familial thrombophilia due to a previously unrecognized mechanism characterized by poor anticoagulant response to activated protein C: prediction of a cofactor to activated protein C. *Proc Natl Acad Sci USA* 1993; **90**: 1004–8
21 Bertina RM, Koeleman BP, Koster T, Rosendaal FR, Dirven RJ, de Ronde H, van der Velden PA, Reitsma PH. Mutation in blood coagulation factor V associated with resistance to activated protein C. *Nature* 1994; **369**: 64–7
22 Brill A, Fuchs TA, Chauhan AK, Yang JJ, De Meyer SF, Kollnberger M, Wakefield TW, Lammle B, Massberg S, Wagner DD. von Willebrand factor-mediated platelet adhesion is critical for deep vein thrombosis in mouse models. *Blood* 2011; **117**: 1400–7
23 Sevitt S. The structure and growth of valve-pocket thrombi in femoral veins. *J Clin Pathol* 1974; **27**: 517–28
24 Savchenko AS, Hasegawa G, Naito M. Development and maturation of thymic dendritic cells during human ontogeny. *Cell Tissue Res* 2006; **325**: 455–60
25 Thevenaz P, Unser M. User-friendly semiautomated assembly of accurate image mosaics in microscopy. *Microsc Res Tech* 2007; **70**: 135–46
26 Neeli I, Khan SN, Radic M. Histone deimination as a response to inflammatory stimuli in neutrophils. *J Immunol* 2008; **180**: 1895–902
27 Egan CE, Sukhumavasi W, Bierly AL, Denkers EY. Understanding the multiple functions of Gr-1(+) cell subpopulations during microbial infection. *Immunol Res* 2008; **40**: 35–48
28 Xu J, Zhang X, Pelayo R, Monestier M, Ammollo CT, Semeraro F, Taylor FB, Esmon NL, Lupu F, Esmon CT. Extracellular histones are major mediators of death in sepsis. *Nat Med* 2009; **15**: 1318–21
29 Gamberucci A, Fulceri R, Marcolongo P, Pralong WF, Benedetti A. Histones and basic polypeptides activate Ca^{2+}/cation influx in various cell types. *Biochem J* 1998; **331** (Pt 2): 623–30
30 Kleine TJ, Lewis PN, Lewis SA. Histone-induced damage of a mammalian epithelium: the role of protein and membrane structure. *Am J Physiol* 1997; **273**: C1925–36
31 Wagner DD. Cell biology of von Willebrand factor. *Annu Rev Cell Biol* 1990; **6**: 217–46

32 Guzy RD, Schumacker PT. Oxygen sensing by mitochondria at complex III: the paradox of increased reactive oxygen species during hypoxia. *Exp Physiol* 2006; **91**: 807–19
33 Marcus AJ, Silk ST, Safier LB, Ullman HL. Superoxide production and reducing activity in human platelets. *J Clin Invest* 1977; **59**: 149–58
34 Jin RC, Mahoney CE, Coleman Anderson L, Ottaviano F, Croce K, Leopold JA, Zhang YY, Tang SS, Handy DE, Loscalzo J. Glutathione peroxidase-3 deficiency promotes platelet-dependent thrombosis in vivo. *Circulation* 2011; **123**: 1963–73
35 Nishinaka Y, Arai T, Adachi S, Takaori-Kondo A, Yamashita K. Singlet oxygen is essential for neutrophil extracellular trap formation. *Biochem Biophys Res Commun* 2011; **413**: 75–9
36 Gupta AK, Joshi MB, Philippova M, Erne P, Hasler P, Hahn S, Resink TJ. Activated endothelial cells induce neutrophil extracellular traps and are susceptible to NETosis-mediated cell death. *FEBS Lett* 2010; **584**: 3193–7
37 Hakkim A, Furnrohr BG, Amann K, Laube B, Abed UA, Brinkmann V, Herrmann M, Voll RE, Zychlinsky A. Impairment of neutrophil extracellular trap degradation is associated with lupus nephritis. *Proc Natl Acad Sci U S A* 2010; **107**: 9813–8
38 Andre P, Hartwell D, Hrachovinova I, Saffaripour S, Wagner DD. Pro-coagulant state resulting from high levels of soluble P-selectin in blood. *Proc Natl Acad Sci U S A* 2000; **97**: 13835–40
39 Myers DD, Hawley AE, Farris DM, Wrobleski SK, Thanaporn P, Schaub RG, Wagner DD, Kumar A, Wakefield TW. P-selectin and leukocyte microparticles are associated with venous thrombogenesis. *J Vasc Surg* 2003; **38**: 1075–89
40 Ward CM, Tetaz TJ, Andrews RK, Berndt MC. Binding of the von Willebrand factor A1 domain to histone. *Thromb Res* 1997; **86**: 469–77
41 Brooks EG, Trotman W, Wadsworth MP, Taatjes DJ, Evans MF, Ittleman FP, Callas PW, Esmon CT, Bovill EG. Valves of the deep venous system: an overlooked risk factor. *Blood* 2009; **114**: 1276–9
42 Dole VS, Bergmeier W, Mitchell HA, Eichenberger SC, Wagner DD. Activated platelets induce Weibel–Palade-body secretion and leukocyte rolling in vivo: role of P-selectin. *Blood* 2005; **106**: 2334–9

Appendix A-4

Neutrophil extracellular traps form predominantly during the organizing stage of human venous thromboembolism development

This chapter contains the following publication:

Savchenko AS, Martinod K, Seidman MA, Wong SL, Borissoff JI, Piazza G, Libby P, Goldhaber SZ, Mitchell RN, Wagner DD. *Neutrophil extracellular traps form predominantly during the organizing stage of human venous thromboembolism development.* J Thromb Haemost. 2014 Jun; 12 (6): 860-70. Epub ahead of print 2014 Mar 27. PMCID: 4055516.

Attributions:

Alexander Savchenko wrote the entirety of this manuscript. I performed immunofluorescent stainings of thrombi, quantified H3Cit in thrombi, and critically read the manuscript.

Journal of Thrombosis and Haemostasis, **12**: 860–870 DOI: 10.1111/jth.12571

ORIGINAL ARTICLE

Neutrophil extracellular traps form predominantly during the organizing stage of human venous thromboembolism development

A. S. SAVCHENKO,*† K. MARTINOD,*‡ M. A. SEIDMAN,§ S. L. WONG,*† J. I. BORISSOFF,*† G. PIAZZA,¶ P. LIBBY,¶ S. Z. GOLDHABER,¶ R. N. MITCHELL§ and D. D. WAGNER*†**

**Program in Cellular and Molecular Medicine, Boston Children's Hospital; †Department of Pediatrics, Harvard Medical School; ‡Immunology Graduate Program, Division of Medical Sciences, Harvard Medical School; §Department of Pathology and Laboratory Medicine, Brigham and Women's Hospital, Harvard Medical School; ¶Cardiovascular Medicine Division, Brigham and Women's Hospital, Harvard Medical School; and **Division of Hematology/Oncology, Boston Children's Hospital, Boston, MA, USA*

To cite this article: Savchenko AS, Martinod K, Seidman MA, Wong SL, Borissoff JI, Piazza G, Libby P, Goldhaber SZ, Mitchell RN, Wagner DD. Neutrophil extracellular traps form predominantly during the organizing stage of human venous thromboembolism development. *J Thromb Haemost* 2014; **12**: 860–70.

Summary. *Background:* A growing health problem, venous thromboembolism (VTE), including pulmonary embolism (PE) and deep vein thrombosis (DVT), requires refined diagnostic and therapeutic approaches. Neutrophils contribute to thrombus initiation and development in experimental DVT. Recent animal studies recognized neutrophil extracellular traps (NETs) as an important scaffold supporting thrombus stability. However, the hypothesis that human venous thrombi involve NETs has not undergone rigorous testing. *Objective:* To explore the cellular composition and the presence of NETs within human venous thrombi at different stages of development. *Patients and Methods:* We examined 16 thrombi obtained from 11 patients during surgery or at autopsy using histomorphological, immunohistochemical and immunofluorescence analyses. *Results:* We classified thrombus regions as unorganized, organizing and organized according to their morphological characteristics. We then evaluated them, focusing on neutrophil and platelet deposition as well as micro-vascularization of the thrombus body. We observed evidence of NET accumulation, including the presence of citrullinated histone H3 (H3Cit)-positive cells. NETs, defined as extracellular diffuse H3Cit areas associated with myeloperoxidase and DNA, localized predominantly during the phase of organization in human venous thrombi. *Conclusions:* NETs are present in organizing thrombi in patients with VTE. They are associated with thrombus maturation in humans. Dissolution of NETs might thus facilitate thrombolysis. This finding provides new insights into the clinical development and pathology of thrombosis and provides new perspectives for therapeutic advances.

Correspondence: Denisa D. Wagner, Boston Children's Hospital, 3 Blackfan Circle, 3rd Floor, Boston, MA 02115, USA.
Tel.: +1 617 713 8300; fax: +1 617 713 8333.
E-mail: Denisa.Wagner@childrens.harvard.edu

Received 15 January 2014
Manuscript handled by: P. H. Reitsma
Final decision: P. H. Reitsma, 21 March 2014

Keywords: blood platelets; clinical pathology; histones; neutrophils; venous thromboembolism.

Introduction

Venous thromboembolism (VTE), which includes both deep vein thrombosis (DVT) and pulmonary embolism (PE), is the most common cardiovascular disease after myocardial infarction (MI) and ischemic stroke [1]. In animals, neutrophils contribute importantly to the pathogenesis of venous thrombosis [2–5]. Neutrophil-related pro-coagulant mechanisms might contribute to large-vessel thrombosis in various types of cardiovascular diseases [6]. Our group has previously reported that neutrophil extracellular traps (NETs) provide a scaffold for experimental thrombus formation by binding erythrocytes and platelets [7]. NETs consist of released nuclear DNA containing histones and neutrophil granule proteins, such as elastase, myeloperoxidase (MPO) and cathepsin G [8,9]. NETs localize in experimental DVT in baboons [7] and extracellular chromatin comprises part of the structure of venous thrombi in mice [10,11]. Treatment with deoxyribonuclease I (DNase I), an enzyme that degrades DNA, protects mice from flow restriction-induced DVT [10,11]. Our recent experimental study indicates that neutrophil chromatin decondensation

mediated by peptidylarginine deiminase 4 (PAD4), an enzyme required for NET formation (NETosis) [12], participates crucially in venous thrombosis in mice [13], thus emphasizing the impact of NETs on DVT. Increased levels of circulating nucleosomes and markers of neutrophil activation are associated with a 3-fold higher risk of DVT in humans [14]. An elevated plasma DNA concentration correlates with biomarkers of DVT [15] and with a prothrombotic state in patients with severe atherosclerosis [16].

Thrombus evolution generally proceeds through three distinct phases [17]. Initially, thrombi are unorganized. If formed under conditions of continued blood flow, roughly alternating layers of platelets and red cells generate laminae, denoted as lines of Zahn; if formed in a static environment, the thrombus has a more uniform appearance. After a few days, the thrombus begins to organize, with inflammatory cells (initially neutrophils and later lymphocytes and monocytes) infiltrating the edges of the thrombus in association with fibroblasts, collagen deposition and neovascularization. Over weeks or more, an organized thrombus assumes a more ordered fibrotic appearance with associated hemosiderin-laden macrophages, but an otherwise sparse inflammatory infiltrate. The times suggested are approximate minimums, and should not be taken as absolutes; the progress of thrombus organization can vary significantly. Numerous factors, including host immune status, degree of residual blood flow at the thrombus site and medication use, can all affect the process to varying degrees. Additionally, at any given time, a single thrombus will often display multiple stages of development; typically, the periphery adjacent to a vessel wall exhibits the greatest organization, with the center of the thrombus showing the least.

Few reports have sought NETs in thrombi from humans. Extensive histone citrullination was observed in the thrombus of a patient with microscopic polyangiitis complicated by pneumonia and DVT [18]. Also, coronary thrombi removed from patients with acute MI contain NETs [19], as do intraluminal thrombi from abdominal aortic aneurysm patients [20]. Histone proteins H2A/H2B with DNA are found in human arterial thrombi removed from acutely (age 1–3 days) thrombosed grafts and in chronic (more than 1 year) aortic hematoma samples [21].

NETs furnish an important new link between innate immunity, inflammation, hemostasis and thrombosis [2,3,22,23]. Their recognition provides an opportunity to develop biomarker(s) based on NET components for human VTE diagnosis and to design new therapeutic approaches to improve the efficacy of thrombolysis. The current study aimed to establish the presence of NETs during the different stages of thrombus development in humans with VTE.

Materials and methods

Sample acquisition

Specimens were identified through a search of the electronic records of the Department of Pathology and Laboratory Medicine at Brigham and Women's Hospital by a cardiovascular pathologist who had full access to the origin of the samples and selected the specimens based on the prespecified inclusion criteria below. Search parameters included any one of the text strings containing 'deep vein thrombosis', 'deep vein thrombus', 'pulmonary embolus' or 'pulmonary embolism', being identified as an embolectomy specimen during accessioning, or being identified as a leg amputation and containing the text 'thrombus' or 'thrombosis'. Reports for cases meeting these criteria were manually reviewed to identify cases where deep vein thrombi, inferior vena cava (IVC) filter clots and/or pulmonary emboli were sampled and processed as formalin-fixed paraffin-embedded (FFPE) specimens. Those specimens meeting such criteria were then retrieved from the archives of the Department, and de-identified sections were generated for study. These procedures were reviewed and approved by the Human Research Committee (HRC) of Partners HealthCare, and conform to current national and international standards for ethical conduct of human subjects research.

Histology

FFPE tissue sections cut at 4-μm thickness were stained with either hematoxylin and eosin (H&E) or Masson's trichrome. A cardiovascular pathologist categorized the specimens using histomorphological features as unorganized (lack of collagen deposition, interspersed regions of fibrin/platelets and red blood cells), organizing (poorly organized collagen and/or neovasculature, and/or granulation tissue-like appearance) or organized (well-organized collagen with intermixed hemosiderin-laden macrophages, with or without a well-formed neovasculature) [17].

Immunohistochemistry

Following deparaffinization, microwave antigen retrieval used citrate buffer (pH 6.7) for 8 min, followed by the incubation of slides in heated buffer for an additional 20 min. After endogenous peroxidase activity blocking in methanol/H_2O_2 (100 : 1) for 30 min at room temperature, single immunohistochemical staining used an anti-H3Cit antibody (ab5103, 1 : 250 dilution, Abcam, Cambridge, MA, USA). Histofine Simple Stain MAX PO (MULTI) (414152F, ready to use, Nichirei Corporation, Tokyo, Japan) served as a secondary antibody.

The Diaminobenzidine (DAB) substrate kit (415192F, Nichirei) enabled visualization of staining by H3Cit antibody. Finally, sections were counterstained with hematoxylin. Isotype-matched IgG was used instead of primary antibody as a negative control of the staining. Because of differences observed in the amount of H3Cit staining, we performed a blinded semi-quantitative analysis using an H3Cit scoring system based on the proportion of H3Cit-positive cells across an entire sample. The regions with a majority of H3Cit-positive staining among the entire population of cells (observed with counterstaining) were defined as positive (+, or high H3Cit score). Those cases where H3Cit-positive signals were observed in less than half of the region's cells were classified as (±) and areas without or with very few H3Cit-positive cells were scored as negative (−). All specimens were characterized blindly by a co-investigator who did not have knowledge of the nature of the specimens at the time of scoring.

A rabbit monoclonal anti-CD11b (ab52478, 1 : 250 dilution, Abcam) served to identify leukocytes and mouse monoclonal anti-CD42b (ab74449, ready to use, Abcam) to visualize platelets. Also, the combination of anti-CD11b and mouse monoclonal anti-MPO (ab24467, 1 : 250 dilution, Abcam) antibodies was used to specify the origin of CD11b-positive cells. Histofine Simple Stain MAX PO (MULTI) was used as a secondary antibody for anti-CD11b, the first primary agent. Alkaline Phosphatase (AP)-goat anti-mouse IgG (H+L) (No. 626522, 1 : 500 dilution, Invitrogen, Carlsbad, CA, USA) was applied as a secondary antibody for anti-MPO, the second primary agent. The DAB substrate kit (SK-4100, Vector Laboratories, Burlingame, CA, USA) was used for visualization of double immunohistochemical staining. Finally, sections were counterstained with Nuclear Fast Red (Sigma-Aldrich, St Louis, MO, USA). Images were captured using Axiovision software (Zeiss, Thornwood, NY, USA) and a Zeiss Axioplan microscope coupled with a Zeiss AxioCam HRc camera. Individual images were manually aligned to generate composite images of entire thrombus sections.

Immunofluorescence analysis

Antigen retrieval was performed after deparaffinization. The slides were briefly boiled in sodium citrate buffer (10 mM, pH 6.0) in a microwave and then incubated in heated buffer for an additional 15 min. The slides were washed twice in PBS and then permeabilized with 0.1% Triton X-100 for 10 min on ice. After blocking with 3% bovine serum albumin for 1 h at 37 °C or 10% normal goat serum for 2 h at room temperature, slides were incubated overnight in antibody dilution buffer (0.3% BSA, 0.05% Tween-20) containing one of the following: rabbit polyclonal anti-citrullinated histone H3 (ab5103, 0.5 μg mL^{-1}, Abcam), mouse monoclonal anti-myeloperoxidase (MPO) (ab25989, 0.67 μg mL^{-1}, Abcam), mouse monoclonal anti-peptidylarginine deiminase 4 (PAD4) (ab128086, 4 μg mL^{-1}, Abcam), sheep polyclonal anti-von Willebrand factor (VWF) (ab11713, IgG fraction 1 : 250 dilution, Abcam), rabbit polyclonal anti-citrulline (panCit) (ab6464, whole antiserum, 1 : 1500 dilution, Abcam) or mouse monoclonal anti-CD31 (ab9498, 2 μg mL^{-1}, Abcam). For each staining, an IgG used at the same concentrations as the primary antibody served as the negative control. After thorough washing with PBS, slides were incubated in antibody dilution buffer containing 1.5 μg mL^{-1} Alexa488-conjugated rabbit IgG, 1.5 μg mL^{-1} Alexa568-conjugated sheep IgG or 1.5 μg mL^{-1} Alexa555-conjugated mouse IgG (all from Invitrogen) for 2 h at room temperature. After thorough washing, DNA was counterstained using 1 μg mL^{-1} Hoechst 33342 (Invitrogen) and cover-slipped using Fluorogel mounting medium. Images were acquired using a Zeiss Axiovert widefield fluorescence microscope in conjunction with a Zeiss MRm monochromatic CCD camera and Axiovision software.

Results

Clinical specimen characteristics

This analysis is based on 16 thrombi collected from 11 individuals (mean age 52.0 ± 17.9 years; three men and eight women, Table 1.) Six thrombus samples were derived from three autopsy cases (all within 24 h of

Table 1 Patient clinical data and thrombus samples included in the study

No. of patient	Age	Gender	Diagnosis	Tissue
Surgical				
Patient 1	36	F	CTEPH	PE IVC clot
Patient 2	47	F	CTEPH	PE
Patient 3	72	F	Metastatic endometrial adenocarcinoma	DVT
Patient 4	69	F	s/p lung transplant for UIP	PE IVC clot
Patient 5	16	M	CTEPH	PE
Patient 6	60	M	s/p hernia repair	PE
Patient 7	44	F	CTEPH	PE
Patient 8	53	M	Idiopathic recurrent VTE	IVC clot
Autopsy				
Patient 9	74	F	s/p aortic valve replacement	PE DVT
Patient 10	38	F	Obesity, recurrent VTE	DVT PE
Patient 11	63	F	Lung adenocarcinoma	PE DVT

CTEPH, chronic thromboembolic pulmonary hypertension; s/p, status post; UIP, usual interstitial pneumonia; VTE, venous thromboembolism.

death), and 10 from eight surgical cases. Clinical diagnoses included: chronic thromboembolic pulmonary hypertension ($n = 4$), recurrent venous thromboembolism ($n = 2$), cancer (one case of metastatic endometrial adenocarcinoma and one of lung adenocarcinoma) and one case each of hernia, aortic valve replacement and status post-lung transplant. Six thrombus specimens were obtained from three patients with PE and DVT; PE and IVC clot samples ($n = 4$) were collected from another two patients. Four thrombi were derived from patients with PE as a main diagnosis and two from patients with either DVT or IVC clot.

According to the morphological criteria described above, based on the results of hemotoxylin and eosin and of trichrome staining, thrombus regions fell into three major stages of thrombus development [17]: unorganized (16 regions from 11 patients), organizing (13 regions from 11 patients) and organized (eight regions from seven patients).

We then used immunohistochemical analysis to determine the distribution of platelets and leukocytes in the human thrombi during each stage of maturation, as well as the presence of H3Cit as a marker of NETosis. At least two regions corresponding to different stages of thrombus organization were identified in 15 out of 16 specimen samples.

Unorganized thrombi harbor rare H3Cit-positive cells, while these cells and NETs abound in the organizing stage of thrombus development

Figure 1 shows a representative thrombus from a PE patient with both unorganized (square box 2) and organizing (square box 1) regions. We observed platelet- and fibrin/erythrocyte-rich zones, defined by the presence of lines of Zahn (white arrows, Fig. 1A). The organizing part of a thrombus mainly contained leukocytes positive for CD11b (brown, Fig. 1A). The majority of CD11b-positive cells (brown) were identified as neutrophils by double staining with MPO (blue), showing that most CD11b-expressing cells are also MPO positive (dark blue). Prominent H3Cit-positive staining (brown, Fig. 1A, last panel) localized only within the organizing, but not the unorganized, part of the thrombus. This observation suggests that NETosis occurs in human thrombi during the organizing stage of maturation.

To clarify the composition of the human thrombus samples observed in this study, Fig. 1(B) presents larger images of the organizing region at higher magnification (areas indicated as oval 1 in Fig. 1A). We also performed immunofluorescence staining (Fig. 1C). We observed both intracellular (H3Cit-positive nuclei, green arrow in Fig. 1C) and diffuse extracellular H3Cit-positive staining patterns (green asterisk in Fig. 1C), suggesting ongoing NETosis and the prominent presence of NETs in this inflammatory stage of thrombus development.

We have previously shown that NETs bind VWF [7] and that VWF co-distributes with NET biomarkers in thrombi from baboons and mice [7,10]. Here we found platelets stained strongly positive for VWF. In addition, we observed regions with diffuse VWF staining (white asterisk) associated with H3Cit extracellular staining (Fig. 1C, lower left panel), indicating the interaction of VWF with NETs. Single channels showing VWF (diffuse VWF staining is indicated by white asterisk) and H3Cit expression patterns are presented in Figure S1. We also stained thrombus samples for PAD4, the enzyme required for NETosis [12,24,25], and found PAD4-positive cells in corresponding areas of neutrophil infiltration and NETosis (Fig. 1C, lower middle panel). Also, panCit antibody, which recognizes citrulline modifications on proteins, visualized an intracellular and a diffuse extracellular staining pattern (Fig. 1C, lower middle panel), again indicating that protein citrullination occurs in human thrombi. IgG-isotype control staining showed no positive signal by either immunohistochemical (Fig. 1B, far right panel) or immunofluorescence (Fig. 1C, second row, far right panel) analyses.

We also observed the presence of lines of Zahn (Fig. 2A) with platelet aggregates (Fig. 2B) and neutrophil infiltrates (Fig. 2B and 2C) in an organizing deep vein thrombus. Of interest, H3Cit-positive cells (Fig. 2D and 2E) originating from neutrophils (Fig. 2F) localized predominantly in the immediate vicinity of VWF-positive (Fig. 2H) platelet-rich zones (Fig. 2E and 2H), suggesting a possible involvement of NETs in the process of platelet recruitment during human thrombus organization. We further found PAD4 and panCit staining in these areas (Fig. 2G), whereas isotype-control staining displayed no specific signal (Fig. 2I). Thus, the intensity of H3Cit staining was varied throughout the different stages of thrombus development.

Organized thrombi contain multiple microvessels while NETs are rare at this stage

Organized thrombi contained microvessels, observed by trichrome staining (Fig. 3A, blue square is magnified in Fig. 3C) and confirmed by immunofluorescence analysis using an anti-CD31 antibody (Fig. 3B). The negative control staining using isotype-matched IgG showed no specific signal. A few microvessels were observed in only one case of an organizing thrombus surgically removed from a PE patient (Figure S2).

We observed areas of collagen-rich connective tissue in organized regions of thrombi (Fig. 4A, blue square box indicates a representative region), which were leukocyte deficient (Fig. 4B–C and Fig. 4F) with only a few neutrophils found in the thrombus body (Fig. 4C). Both immunohistochemical (Fig. 4D and 4E) and immunofluorescence (Fig. 4F and 4G) analyses showed the lack of prominent H3Cit-positive staining, with many completely

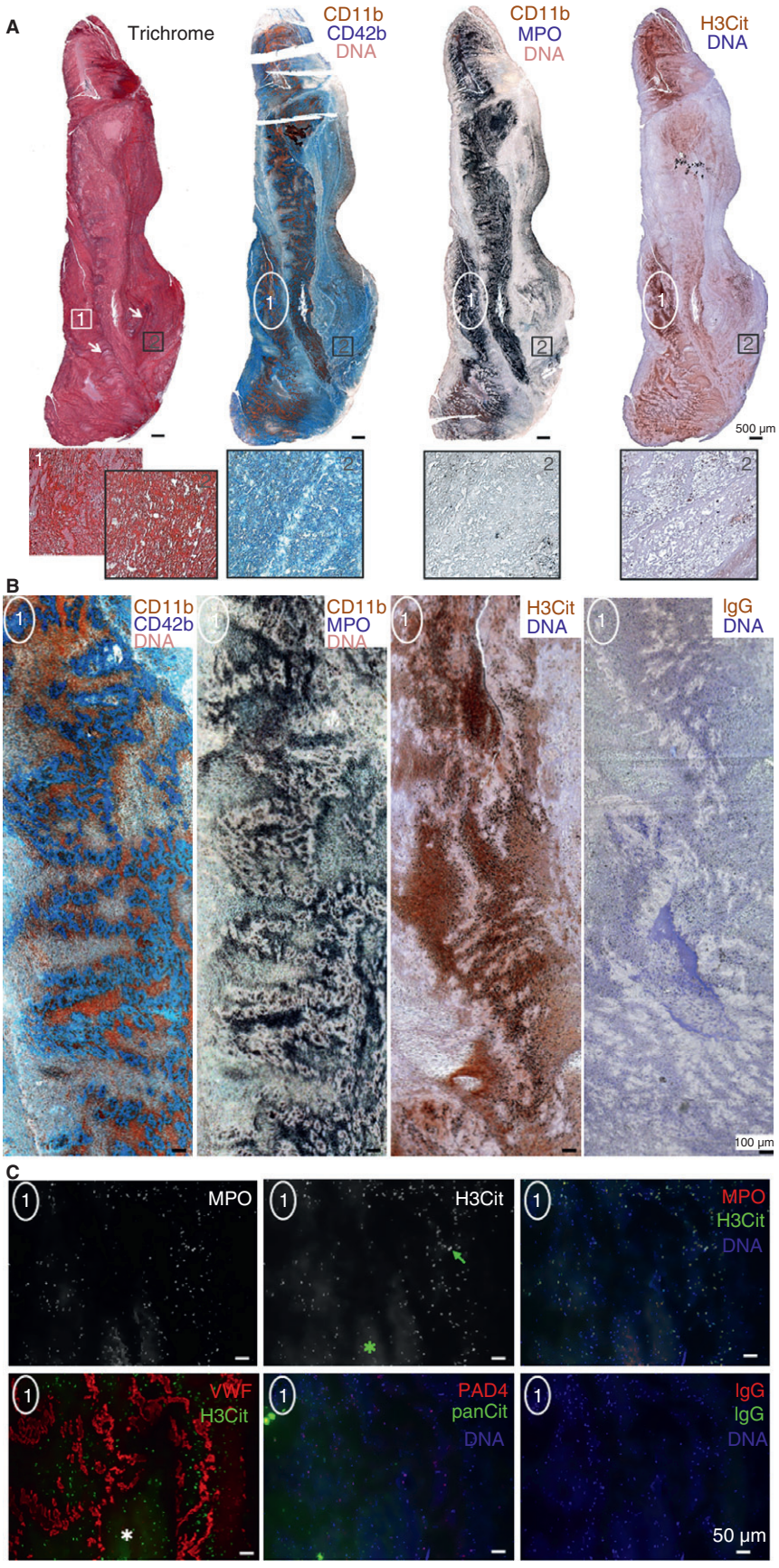

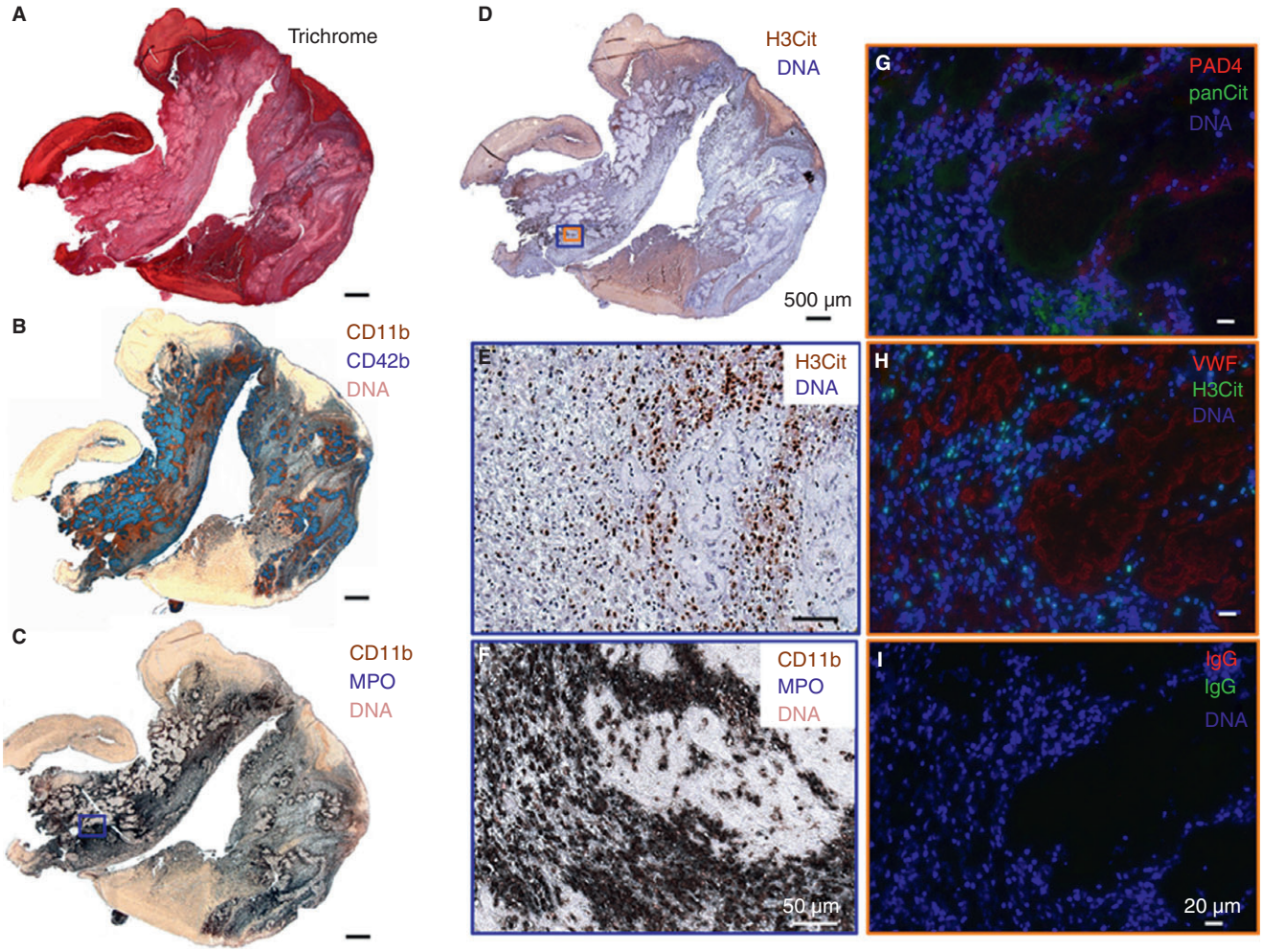

Fig. 2. Platelet-rich zones are often surrounded by MPO and H3Cit-positive staining in the organizing deep vein thrombus. Representative images from a DVT sample collected during autopsy. (A–C) Thrombus was classified as organizing based on the presence of minimal collagen deposition, early neovascularization and/or granulation-like tissue (A), CD42b-positive platelet aggregates (blue, B) and infiltrating CD11b-positive neutrophils (brown, B), co-stained with MPO (dark blue, C). (D) H3Cit-positive cells were detected in neutrophil-rich zones. Images A–D are composites of photographs of stained sections of the entire thrombus. The area indicated by the blue square is shown at a higher magnification in E and F and the area indicated by the orange square in G, H and I. Platelet-rich zones stained for VWF (red) and were surrounded by H3Cit-positive cells (H). PAD4 (red) and panCit (green) were seen primarily in neutrophil-rich areas surrounding platelet islands (G). Negative control staining was performed using isotype-matched non-specific IgG (I). Scale bars, 500 μm (A–D), 50 μm (E and F), 20 μm (G–I).

Fig. 1. Evidence of prominent NETosis observed in the organizing, but not unorganized, portions of a pulmonary embolism thrombus. Representative composite images from analysis of a pulmonary embolism (PE) sample obtained from autopsy. Consecutive sections of the thrombus were stained. (A) Trichrome stain revealed organizing (square 1) and unorganized (square 2) regions of the thrombus and the presence of lines of Zahn (white arrows). Double immunohistochemical staining for CD11b (brown, leukocytes) and CD42b (blue, platelets) showed both platelets and leukocytes within the organizing stage of the thrombus (oval 1), whereas the unorganized part contained mostly platelets (square 2). H3Cit-positive cells (brown) were observed mostly in the CD11b/MPO-double positive (dark blue) region of the organizing area. Higher magnification images from the organizing part of a thrombus (indicated as oval 1) are shown in B and C. (B) Punctiform (intracellular) and diffuse (extracellular) H3Cit staining (brown) was observed together with MPO (dark blue) within platelet/neutrophil-rich zones. Negative control staining was performed using isotype-matched IgG. Images in A and B are composites of photographs of stained sections of the entire thrombus (A) and its organizing portion (B). (C) Upper panel confirmed the close localization of the intra- (green arrow) and extracellular (green asterisk) H3Cit with MPO (single channels and merge are shown). Platelet islands stained for VWF (red), and diffuse VWF (white asterisk) were present in areas containing H3Cit. A positive staining pattern for PAD4 (red) was seen in regions with neutrophil infiltration. Citrullinated proteins were detected using anti-panCit antibody (green). IgG isotype control served as a negative control. Sections were counterstained for DNA as indicated (Hoechst 33342, blue). Scale bars, 500 μm (A), 100 μm (B), 50 μm (C).

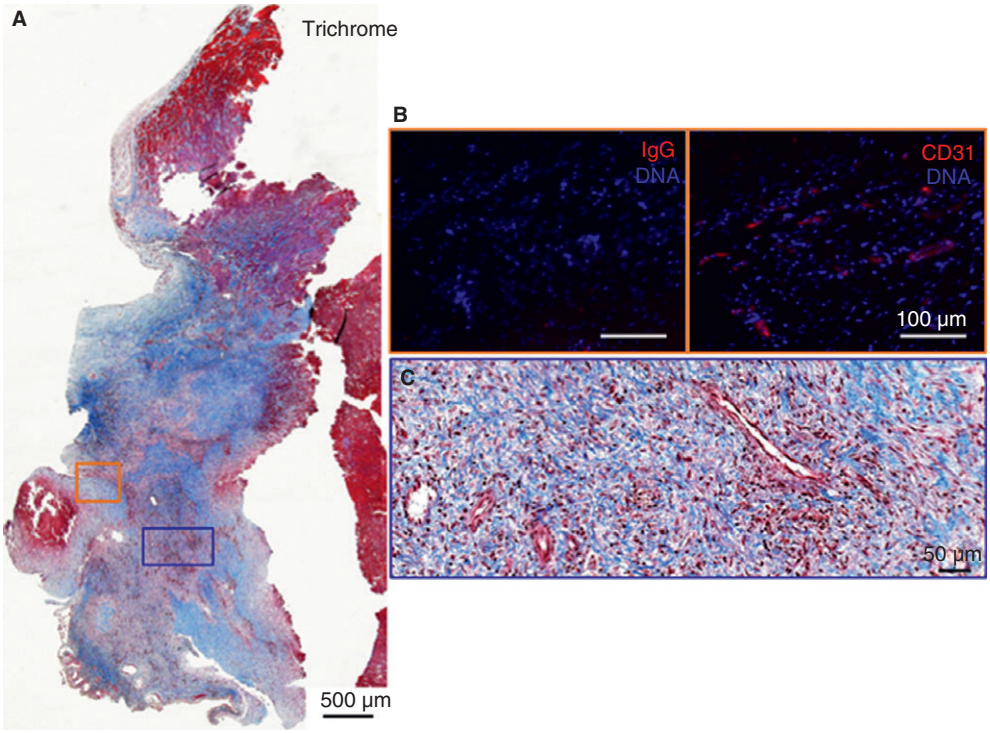

Fig. 3. Accumulation of microvessels within the organized region of a pulmonary embolism thrombus. (A,C) Trichrome stain indicated organized regions of a thrombus with micro-vascularization (area within blue square is magnified in C). (B) CD31-positive vascular endothelial cells were found in the area with newly formed blood vessels. Negative staining with non-specific IgG showed no specific pattern and nuclei are observed as distinct round shapes in this cell-rich region stained for DNA. Images A and C are composites of photographs of a stained section. Scale bars, 500 μm (A), 100 μm (B), 50 μm (C).

negative sections, indicating that NETosis does not characterize mature regions of organized thrombi. Control staining with isotype-matched IgG showed no positive signal (Fig. 4H).

Quantification confirms that excessive H3Cit staining was observed only in the organizing stage of thrombus development

Semi-quantitative analysis of H3Cit-positive cells was performed in a blinded fashion. We developed an H3Cit scoring system based on the frequency of positive staining for H3Cit (Material and Methods). This scoring system classified the specimens with predominant H3Cit-positive cells as H3Cit score (+), the specimens with less than half H3Cit-positive cells as H3Cit score (±), and specimens with no or very minor positive staining for anti-H3Cit antibody as negative H3Cit score (−).

Only organizing thrombi received a high H3Cit (+) score (Fig. 5A and 5B). Thrombus samples from PE and DVT patients revealed a similar distribution of H3Cit scores, whereas no IVC clot samples had a high H3Cit score (Fig. 5A). Of interest, an H3Cit (+) score was seen in 54% of all organizing thrombi and in the remaining 46% a score of (±) was seen (Fig. 5B). No H3Cit (−) cases were identified in regions of early organization, whereas 56% of unorganized and 50% of organized thrombi had a (−) H3Cit score (Fig. 5B). These data showed that NETosis occurs almost exclusively within the organizing stage of thrombus development.

Discussion

This study evaluated the composition of venous thromboemboli obtained either surgically or from autopsy specimens. The results show accumulation of NETs during the organizing stage of pathological venous thrombus development and thus support the participation of NETs in the organization of human thrombi.

Histomorphological and immunological assays using cell marker-specific antibodies showed differences in platelet and neutrophil deposition as well as micro-vascularization within the unorganized, organizing and organized stages of thrombus development. These findings suggest that immunohistological analysis could become a useful adjunct for the pathological description of human thrombi.

The process of leukocyte infiltration and monocyte recruitment during thrombus formation and the impact of NETs have received previous attention in experimental DVT [10,11,13,26]. This study shows evidence of ongoing NETosis in the organizing stage of human thrombus development, including both intra- and extracellular H3Cit closely associated with MPO, as well as extracellular DNA

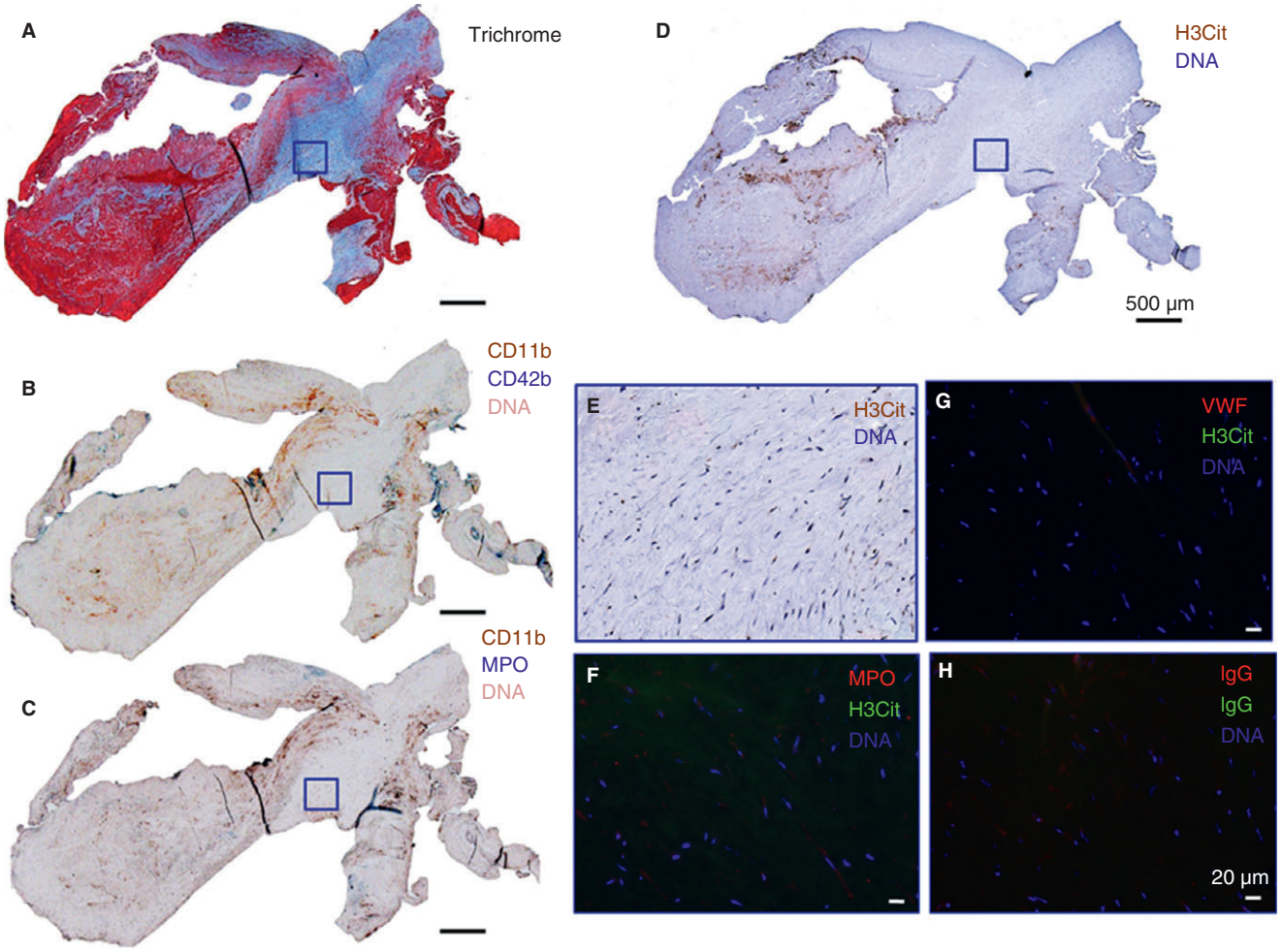

Fig. 4. H3Cit is rare in the organized regions of thrombi. Analyses of a surgically removed IVC clot. (A) Collagen-rich connective tissue (blue) was present within the organized part of the thrombus and is indicated with a blue square. (B–C) Cell-specific immunohistochemical analyses revealed few platelets and neutrophils within the entire thrombus body and their absence in the organized part of the thrombus. (D) Immunohistochemical staining for H3Cit antibody (brown) displayed a negative reactivity (area indicated as a blue square). Images A–D are composites of photographs of stained sections of the entire thrombus. (E–H) High magnification images of the organized part from the area indicated with a blue square in A–D. No staining was detected using anti-H3Cit (E–G), MPO (F) and VWF (G) antibodies in this thrombus. Negative control using IgG isotype showed a non-specific staining pattern (H). Scale bars, 500 μm (A–D).

in H3Cit-rich areas. Thrombus composition did not differ between patients with PE and DVT. Thus, NETs appear to form as part of the inflammatory response and organization in human thrombus development.

NETs' DNA and histones provide a scaffold for thrombi by binding RBCs and promoting platelet aggregation *in vitro* and in mice [6,7]. The results of this study suggest that this concept could apply to human thrombogenesis as well. Murine venous thrombi contain H3Cit, a marker of NETs, co-distributing with VWF predominantly in the red blood cell (RBC)-rich portion of the thrombus [10], and VWF-platelet interaction contributes substantially to VTE development in animals [27,28]. Plasma VWF secreted from activated vascular endothelium is induced by histone infusion, which also promotes DVT in mice [10]. This finding could result from the enhancement of thrombin generation by extracellular histones that occurs via a platelet-dependent mechanism [29,30]. We observed that H3Cit-positive cells surrounded VWF-positive platelet islands in human DVT samples and that diffuse VWF-positive staining was associated with diffuse H3Cit patterns in the organizing regions of thrombi. This observation supports the notion that NETs together with VWF could enhance thrombus formation/stability in humans.

Of interest, we found that diffuse extracellular H3Cit-positive areas in the organizing part of thrombi also contained PAD4, an enzyme required for chromatin decondensation during NETosis. PAD4-deficient mice, which cannot produce NETs [12], exhibit protection from DVT [13] and MI [31]. Thus, these data show NETting neutrophils in human venous thrombosis and identify PAD4 as a potential target for future drug development.

A

No. of patient	Diagnosis	Tissue	Regions of thrombus			Thrombus morphology		H3Cit score		
			Unorganized	Organizing	Organized	Presence of PMN	Presence of Lines of Zahn	Unorganized	Organizing	Organized
Patient 1	CTEPH	PE	+	+	+	few	–	–	±	–
		IVC clot	+	NP	+	focal	focal	–	NP	±
Patient 2	CTEPH	PE	+	+	+	few	+	±	+	–
Patient 3	metastatic endomentrial adenocarcinoma	DVT	+	+	NP	+	+	–	±	NP
Patient 4	s/p lung transplant for UIP	PE	+	+	NP	+	+	±	+	NP
		IVC clot	+	NP	+	–	–	±	NP	–
Patient 5	CTEPH	PE	+	+	+	few	+	–	+	±
Patient 6	s/p hernia repair	PE	+	+	NP	+	+	–	±	NP
Patient 7	CTEPH	PE	+	+	+	few	+	–	±	–
Patient 8	Idiopathic recurrent VTE	IVC clot	+	+	+	+	+	–	±	±
Patient 9	s/p aortic value replacement	PE	+	+	NP	few	+	±	+	NP
		DVT	+	+	NP	+	+	–	±	NP
Patient 10	obesity, recurrent VTE	DVT	+	+	NP	+	+	±	+	NP
		PE	+	+	NP	+	+	±	+	NP
Patient 11	lung adenocarcinoma	PE	+	NP	NP	few	focal	–	NP	NP
		DVT	+	+	+	+	+	±	+	±

Abbreviations: NP, not present; CTEPH, chronic thromboembolic pulmonary hypertension; UIP, usual interstitial pneumonia; VTE, venous thromboembolism

B

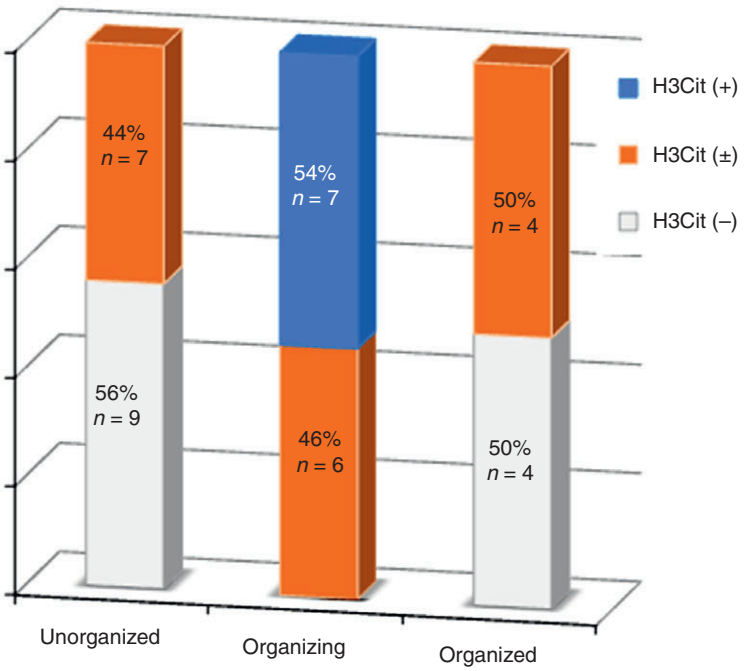

Fig. 5. Summary of clinical, histomorphological and immunological analyses performed for all thrombus samples. (A) Table summarizes clinical data from patients included in this study as well as results of histopathological validation. H3Cit score is presented for each of the cases. H3Cit scoring system: + (highlighted in blue), strongly positive with the majority of H3Cit-positive cells throughout the entire thrombus body; ±, focally positive with a few H3Cit-positive cells in the population; –, negative with mostly H3Cit-negative cells. (B) Graph shows the distribution of H3Cit score (percentage and number (*n*) of corresponding thrombus regions) between the different stages of thrombus organization.

Targeting NET components may also provide a foundation for molecular imaging to identify patients with thromboembolic disease that may respond optimally to thrombolytic therapy. Molecular imaging techniques using magnetic resonance and radionuclide scanning have been shown to distinguish fresh from chronic thrombi but have not yet reached widespread clinical use [32,33].

Fibrin clots containing DNA and histones have prolonged resistance to fibrinolysis that is reversed by DNase [7,34]. Our observations support targeting NETs, in addition to fibrin, as an approach to facilitate thrombolytic therapy in patients. DNase I has decreased the incidence of thrombosis in experimental DVT in mice [10,11]. Furthermore, we have recently reported that DNase I also has an anti-inflammatory effect when administered to mice with experimental myocardial infarction [31]. The anticoagulant heparin can also dissociate NETs [7] and prevent histone interactions with platelets, thus protecting mice from histone-induced thrombocytopenia [35]. Aspirin, a known anti-thrombotic, can inhibit NETosis *in vitro* [36] as well as reduce the incidence of recurrent VTE [37,38]. The combined approach of heparin or aspirin with DNase I or PAD4 inhibitors might enhance venous thrombus prevention. Co-administration of DNase I with a fibrinolytic might facilitate thrombolysis, particularly during the organizing stage of thrombus development.

In conclusion, this study demonstrates the presence of NETs during the process of thrombus organization in human VTE. NETs can provide a scaffold for human thrombus stability during its maturation and could become a diagnostic or therapeutic target to improve the effectiveness of thrombolytic therapy in patients with thromboembolic diseases.

Addendum

A. S. Savchenko performed experiments, analyzed data, designed research and wrote the paper; K. Martinod, S. L. Wong and J. I. Borissoff performed experiments and analyzed data; M. A. Seidman collected thrombus samples and performed histological examination; G. Piazza, P. Libby, S. Z. Goldhaber, R. N. Mitchell and D. D. Wagner designed research, provided essential expertise on cardiovascular and clinical pathology, analyzed data and co-wrote the manuscript.

Acknowledgements

The authors thank L. Cowan for help with the preparation of the manuscript. This research was supported by National Heart, Lung, and Blood Institute of the National Institutes of Health grant R01HL102101 (DDW). JIB is a recipient of a Rubicon fellowship (825.11.019) from the Netherlands Organization for Scientific Research.

Disclosure of Conflict of Interests

The authors state that they have no conflict of interests.

Supporting Information

Additional Supporting Information may be found in the online version of this article:

Fig. S1. High magnification images from the organizing region (indicated as oval 1 in Figure 1A) of a pulmonary embolism thrombus document the expression pattern for VWF and H3Cit. Left panel shows the bright VWF staining for platelet-rich zones and diffuse staining (white asterisk) was observed in areas with H3Cit-positive cells and H3Cit diffuse staining (single channel, middle panel). Right panel displays the merged image. Scale bars, 50 μm.

Fig. S2. Evidence of blood vessel formation within an organizing part of a pulmonary embolism thrombus. CD31-positive microvessels were observed only within one organizing region (region 1) and were not detected in any other organizing portions of thrombi. Left image is a composite of photographs of a stained section of the entire thrombus. Anti-CD31 antibody also stained platelet islands (region 2). Negative control staining was performed using non-specific IgG isotype control. Scale bars, 500 μm (trichrome stain), 50 μm (immunofluorescence analyses).

References

1 Go AS, Mozaffarian D, Roger VL, Benjamin EJ, Berry JD, Borden WB, Bravata DM, Dai S, Ford ES, Fox CS, Franco S, Fullerton HJ, Gillespie C, Hailpern SM, Heit JA, Howard VJ, Huffman MD, Kissela BM, Kittner SJ, Lackland DT. Heart disease and stroke statistics–2013 update: a report from the American Heart Association. *Circulation* 2013; **127**: e6–245.

2 Schulz C, Engelmann B, Massberg S. Crossroads of coagulation and innate immunity: the case of deep vein thrombosis. *J Thromb Haemost* 2013; **11**(Suppl 1): 233–41.

3 Martinod K, Wagner DD. Thrombosis: tangled up in NETs. *Blood*. 2014; **123**: 2768–76.

4 Saha P, Humphries J, Modarai B, Mattock K, Waltham M, Evans CE, Ahmad A, Patel AS, Premaratne S, Lyons OT, Smith A. Leukocytes and the natural history of deep vein thrombosis: current concepts and future directions. *Arterioscler Thromb Vasc Biol* 2011; **31**: 506–12.

5 Wakefield TW, Henke PK. The role of inflammation in early and late venous thrombosis: are there clinical implications? *Semin Vasc Surg* 2005; **18**: 118–29.

6 Massberg S, Grahl L, von Bruehl ML, Manukyan D, Pfeiler S, Goosmann C, Brinkmann V, Lorenz M, Bidzhekov K, Khandagale AB, Konrad I, Kennerknecht E, Reges K, Holdenrieder S, Braun S, Reinhardt C, Spannagl M, Preissner KT, Engelmann B. Reciprocal coupling of coagulation and innate immunity via neutrophil serine proteases. *Nat Med* 2010; **16**: 887–96.

7 Fuchs TA, Brill A, Duerschmied D, Schatzberg D, Monestier M, Myers DD Jr, Wrobleski SK, Wakefield TW, Hartwig JH, Wagner DD. Extracellular DNA traps promote thrombosis. *Proc Natl Acad Sci U S A* 2010; **107**: 15880–5.

8 Brinkmann V, Reichard U, Goosmann C, Fauler B, Uhlemann Y, Weiss DS, Weinrauch Y, Zychlinsky A. Neutrophil extracellular traps kill bacteria. *Science* 2004; **303**: 1532–5.

9 Fuchs TA, Abed U, Goosmann C, Hurwitz R, Schulze I, Wahn V, Weinrauch Y, Brinkmann V, Zychlinsky A. Novel cell death program leads to neutrophil extracellular traps. *J Cell Biol* 2007; **176**: 231–41.

10 Brill A, Fuchs TA, Savchenko AS, Thomas GM, Martinod K, De Meyer SF, Bhandari AA, Wagner DD. Neutrophil extracellular traps promote deep vein thrombosis in mice. *J Thromb Haemost* 2012; **10**: 136–44.

11 von Bruhl ML, Stark K, Steinhart A, Chandraratne S, Konrad I, Lorenz M, Khandoga A, Tirniceriu A, Coletti R, Kollnberger M, Byrne RA, Laitinen I, Walch A, Brill A, Pfeiler S, Manukyan D, Braun S, Lange P, Riegger J, Ware J. Monocytes, neutrophils, and platelets cooperate to initiate and propagate venous thrombosis in mice in vivo. *J Exp Med* 2012; **209**: 819–35.

12 Li P, Li M, Lindberg MR, Kennett MJ, Xiong N, Wang Y. PAD4 is essential for antibacterial innate immunity mediated by neutrophil extracellular traps. *J Exp Med* 2010; **207**: 1853–62.

13 Martinod K, Demers M, Fuchs TA, Wong SL, Brill A, Gallant M, Hu J, Wang Y, Wagner DD. Neutrophil histone modification by peptidylarginine deiminase 4 is critical for deep vein thrombosis in mice. *Proc Natl Acad Sci U S A* 2013; **110**: 8674–9.

14 van Montfoort ML, Stephan F, Lauw MN, Hutten BA, van Mierlo GJ, Solati S, Middeldorp S, Meijers JC, Zeerleder S. Circulating nucleosomes and neutrophil activation as risk factors for deep vein thrombosis. *Arterioscler Thromb Vasc Biol* 2013; **33**: 147–51.

15 Diaz JA, Fuchs TA, Jackson TO, Hovinga JA, Lammle B, Henke PK, Myers DD Jr, Wagner DD, Wakefield TW. Plasma DNA is elevated in patients with deep vein thrombosis. *J Vasc Surg Venous Lymphat Disord* 2013; **1**: 341–348.

16 Borissoff JI, Joosen IA, Versteylen MO, Brill A, Fuchs TA, Savchenko AS, Gallant M, Martinod K, Ten Cate H, Hofstra L, Crijns HJ, Wagner DD, Kietselaer BL. Elevated levels of circulating DNA and chromatin are independently associated with severe coronary atherosclerosis and a prothrombotic state. *Arterioscler Thromb Vasc Biol* 2013; **33**: 2032–40.

17 Seidman MA, Mitchell RN. Surgical pathology of small- and medium-sized vessels. *Surg Pathol Clin* 2012; **5**: 431–51.

18 Nakazawa D, Tomaru U, Yamamoto C, Jodo S, Ishizu A. Abundant neutrophil extracellular traps in thrombus of patient with microscopic polyangiitis. *Front Immunol* 2012; **3**: 333.

19 de Boer OJ, Li X, Teeling P, Mackaay C, Ploegmakers HJ, van der Loos CM, Daemen MJ, de Winter RJ, van der Wal AC. Neutrophils, neutrophil extracellular traps and interleukin-17 associate with the organisation of thrombi in acute myocardial infarction. *Thromb Haemost* 2013; **109**: 290–7.

20 Delbosc S, Alsac JM, Journe C, Louedec L, Castier Y, Bonnaure-Mallet M, Ruimy R, Rossignol P, Bouchard P, Michel JB, Meilhac O. Porphyromonas gingivalis participates in pathogenesis of human abdominal aortic aneurysm by neutrophil activation. Proof of concept in rats. *PLoS One* 2011; **6**: e18679.

21 Oklu R, Albadawi H, Watkins MT, Monestier M, Sillesen M, Wicky S. Detection of extracellular genomic DNA scaffold in human thrombus: implications for the use of deoxyribonuclease enzymes in thrombolysis. *J Vasc Interv Radiol* 2012; **23**: 712–8.

22 Fuchs TA, Brill A, Wagner DD. Neutrophil extracellular trap (NET) impact on deep vein thrombosis. *Arterioscler Thromb Vasc Biol* 2012; **32**: 1777–83.

23 Engelmann B, Massberg S. Thrombosis as an intravascular effector of innate immunity. *Nat Rev Immunol* 2013; **13**: 34–45.

24 Wang Y, Li M, Stadler S, Correll S, Li P, Wang D, Hayama R, Leonelli L, Han H, Grigoryev SA, Allis CD, Coonrod SA. Histone hypercitrullination mediates chromatin decondensation and neutrophil extracellular trap formation. *J Cell Biol* 2009; **184**: 205–13.

25 Leshner M, Wang S, Lewis C, Zheng H, Chen XA, Santy L, Wang Y. PAD4 mediated histone hypercitrullination induces heterochromatin decondensation and chromatin unfolding to form neutrophil extracellular trap-like structures. *Front Immunol* 2012; **3**: 307.

26 Diaz JA, Hawley AE, Alvarado CM, Berguer AM, Baker NK, Wrobleski SK, Wakefield TW, Lucchesi BR, Myers DD Jr. Thrombogenesis with continuous blood flow in the inferior vena cava. A novel mouse model. *Thromb Haemost* 2010; **104**: 366–75.

27 Takahashi M, Yamashita A, Moriguchi-Goto S, Marutsuka K, Sato Y, Yamamoto H, Koshimoto C, Asada Y. Critical role of von Willebrand factor and platelet interaction in venous thromboembolism. *Histol Histopathol* 2009; **24**: 1391–8.

28 Brill A, Fuchs TA, Chauhan AK, Yang JJ, De Meyer SF, Kollnberger M, Wakefield TW, Lammle B, Massberg S, Wagner DD. von Willebrand factor-mediated platelet adhesion is critical for deep vein thrombosis in mouse models. *Blood* 2011; **117**: 1400–7.

29 Ammollo CT, Semeraro F, Xu J, Esmon NL, Esmon CT. Extracellular histones increase plasma thrombin generation by impairing thrombomodulin-dependent protein C activation. *J Thromb Haemost* 2011; **9**: 1795–803.

30 Semeraro F, Ammollo CT, Morrissey JH, Dale GL, Friese P, Esmon NL, Esmon CT. Extracellular histones promote thrombin generation through platelet-dependent mechanisms: involvement of platelet TLR2 and TLR4. *Blood* 2011; **118**: 1952–61.

31 Savchenko AS, Borissoff JI, Martinod K, De Meyer SF, Gallant M, Erpenbeck L, Brill A, Wang Y, Wagner DD. VWF-mediated leukocyte recruitment with chromatin decondensation by PAD4 increases myocardial ischemia/reperfusion injury in mice. *Blood* 2014; **123**: 141–8.

32 Saha P, Andia ME, Modarai B, Blume U, Humphries J, Patel AS, Phinikaridou A, Evans CE, Mattock K, Grover SP, Ahmad A, Lyons OT, Attia RQ, Renne T, Premaratne S, Wiethoff AJ, Botnar RM, Schaeffter T, Waltham M, Smith A. Magnetic resonance T1 relaxation time of venous thrombus is determined by iron processing and predicts susceptibility to lysis. *Circulation* 2013; **128**: 729–36.

33 Brighton T, Janssen J, Butler SP. Aging of acute deep vein thrombosis measured by radiolabeled 99mTc-rt-PA. *J Nucl Med* 2007; **48**: 873–8.

34 Longstaff C, Varju I, Sotonyi P, Szabo L, Krumrey M, Hoell A, Bota A, Varga Z, Komorowicz E, Kolev K. Mechanical stability and fibrinolytic resistance of clots containing fibrin, DNA, and histones. *J Biol Chem* 2013; **288**: 6946–56.

35 Fuchs TA, Bhandari AA, Wagner DD. Histones induce rapid and profound thrombocytopenia in mice. *Blood* 2011; **118**: 3708–14.

36 Lapponi MJ, Carestia A, Landoni VI, Rivadeneyra L, Etulain J, Negrotto S, Pozner RG, Schattner M. Regulation of neutrophil extracellular trap formation by anti-inflammatory drugs. *J Pharmacol Exp Ther* 2013; **345**: 430–7.

37 Brighton TA, Eikelboom JW, Mann K, Mister R, Gallus A, Ockelford P, Gibbs H, Hague W, Xavier D, Diaz R, Kirby A, Simes J. Low-dose aspirin for preventing recurrent venous thromboembolism. *N Engl J Med* 2012; **367**: 1979–87.

38 Becattini C, Agnelli G, Schenone A, Eichinger S, Bucherini E, Silingardi M, Bianchi M, Moia M, Ageno W, Vandelli MR, Grandone E, Prandoni P. Aspirin for preventing the recurrence of venous thromboembolism. *N Engl J Med* 2012; **366**: 1959–67.

Appendix A-5

Cancers Predispose Neutrophils to Release Extracellular DNA Traps that Contribute to Cancer-Associated Thrombosis

This chapter contains the following publication:

Demers M, Krause DS, Schatzberg D, Martinod K, Voorhees JR, Fuchs TA, Scadden DT, Wagner DD. *Cancers predispose neutrophils to release extracellular DNA traps that contribute to cancer-associated thrombosis*. Proc Natl Acad Sci U S A. 2012 Aug 7; 109 (32): 13076-81. Epub 2012 Jul 23. PMCID: 3420209.

Attributions:

Melanie Demers wrote the entirety of this manuscript. I performed analyses of H3Cit in isolated neutrophils and plasma critically read the manuscript.

Cancers predispose neutrophils to release extracellular DNA traps that contribute to cancer-associated thrombosis

Mélanie Demers[a,b,c], Daniela S. Krause[d,e], Daphne Schatzberg[a,b], Kimberly Martinod[a,b,f], Jaymie R. Voorhees[a,b], Tobias A. Fuchs[a,b,c], David T. Scadden[d], and Denisa D. Wagner[a,b,c,1]

[a]Immune Disease Institute, Boston, MA 02115; [b]Program in Cellular and Molecular Medicine, Boston Children's Hospital, Boston, MA 02115; [c]Department of Pediatrics, Harvard Medical School, Boston, MA 02115; [e]Department of Pathology and [d]Center for Regenerative Medicine, Massachusetts General Hospital, Boston, MA 02114; and [f]Graduate Program in Immunology, Division of Medical Sciences, Harvard Medical School, Boston, MA 02115

Edited by Napoleone Ferrara, Genentech, Inc., South San Francisco, CA, and approved June 28, 2012 (received for review January 10, 2012)

Cancer-associated thrombosis often lacks a clear etiology. However, it is linked to a poor prognosis and represents the second-leading cause of death in cancer patients. Recent studies have shown that chromatin released into blood, through the generation of neutrophil extracellular traps (NETs), is procoagulant and prothrombotic. Using a murine model of chronic myelogenous leukemia, we show that malignant and nonmalignant neutrophils are more prone to NET formation. This increased sensitivity toward NET generation is also observed in mammary and lung carcinoma models, suggesting that cancers, through a systemic effect on the host, can induce an increase in peripheral blood neutrophils, which are predisposed to NET formation. In addition, in the late stages of the breast carcinoma model, NETosis occurs concomitant with the appearance of venous thrombi in the lung. Moreover, simulation of a minor systemic infection in tumor-bearing, but not control, mice results in the release of large quantities of chromatin and a prothrombotic state. The increase in neutrophil count and their priming is mediated by granulocyte colony-stimulating factor (G-CSF), which accumulates in the blood of tumor-bearing mice. The prothrombotic state in cancer can be reproduced by treating mice with G-CSF combined with low-dose LPS and leads to thrombocytopenia and microthrombosis. Taken together, our results identify extracellular chromatin released through NET formation as a cause for cancer-associated thrombosis and unveil a target in the effort to decrease the incidence of thrombosis in cancer patients.

Thrombosis is the second most common cause of death in cancer patients. Even in the absence of obvious thrombosis, cancer patients commonly have a hypercoagulable condition without a clear etiology (1). Cancer frequently induces a systemic effect similar to infection and/or inflammatory disease, including changes in cell numbers in peripheral blood and levels of inflammatory cytokines (2). A feature of chronic myelogenous leukemia (CML) is the excess of granulocytic myeloid cells of varying maturation stages (3). In murine models of solid tumors and a variety of human cancers, an increase in myeloid cells is observed (4, 5). Granulocyte colony-stimulating factor (G-CSF) is a cytokine produced by leukocytes and endothelium and is often associated with leukocytosis and neutrophilia. G-CSF is also produced by various tumors and cancer cells (6), including leukemic cells of CML patients in chronic phase (7). Its concentration can be elevated in the blood of cancer patients and has been associated with poor clinical outcome (8–10). G-CSF activates neutrophils, stimulates oxidative metabolism (11), and increases agonist-induced platelet aggregation ex vivo (12). Despite these effects of G-CSF, only a few cases of thrombotic events have been associated with G-CSF treatment in healthy donors (13).

The release of neutrophils extracellular traps (NETs) has been identified as a mechanism of bacterial killing (14). Recently, NETs were found to promote thrombosis (15, 16) and coagulation (17). Upon contact with bacteria, neutrophils become activated, and their primary response is the engulfment of pathogens into phagosomes. At later time points, in vitro experiments suggest that NET-mediated entrapment and/or killing becomes predominant (18). Furthermore, in vitro activation of human neutrophils with a strong stimulus such as phorbol-12-myristate-13-acetate or hydrogen peroxide leads to NET generation (18). The same effect is observed with a combination of weaker stimuli such as GM-CSF and LPS or C5a (19). This suggests that priming of neutrophils predisposes them to NET formation upon secondary stimulation. Because an increase in neutrophils is a hallmark of CML, we hypothesized that malignant neutrophils may be more prone to NET formation. To our surprise, not only the transformed neutrophils but also normal neutrophils from mice with CML-like myeloproliferative neoplasia (MPN) were primed to generate extracellular DNA traps. In addition, using solid tumor models, we show that cancers can induce an increase in peripheral blood neutrophils that are sensitized toward NET formation and that spontaneous thrombosis is associated with NET generation in vivo. We also show that cancer-associated G-CSF predisposes the host to an exacerbated innate immune response that results in a prothrombotic state. Our findings may further explain the association of cancer with thrombosis.

Results

Peripheral Blood Neutrophils from Mice with CML-Like MPN Are Prone to Generate Extracellular DNA Traps. To determine whether malignant transformation promotes NET formation, we first assessed the ability of neutrophils from mice with CML-like MPN to form NETs. In this model, engraftment of bone marrow cells coexpressing breakpoint cluster region–Abelson (BCR-ABL1) and green fluorescent protein (GFP) occurs around 14 d after bone marrow transplant (20) and produces an increase in BCR-ABL1$^+$ peripheral blood neutrophils without a significant increase in platelet count compared with control mice (Fig. S1). Coexistence of normal BCR-ABL1$^-$ (GFP$^-$) and BCR-ABL1$^+$ (GFP$^+$) myeloid cells was observed at day 20 posttransplant when 29.49% ± 10.39% of cells were GFP$^+$ (n = 8). Plasma analysis revealed a greater level of plasma DNA in the CML-like mice compared with controls, suggesting a possible generation of NETs in vivo (Fig. 1*A*). Isolation of peripheral blood neutrophils from control or leukemic mice routinely yielded a purity of greater than 90% (Fig. 1*B*). Platelet-activating factor (PAF) stimulation of isolated neutrophils from mice with CML-like MPN induced a significant increase in NET formation in a dose-dependent manner compared with neutrophils from control bone marrow recipients (Fig. 1*C* and Fig. S2*A*). Interestingly, at a high dose of PAF, the majority of

Author contributions: M.D., D.S.K., D.T.S., and D.D.W. designed research; M.D., D.S.K., D.S., K.M., J.R.V., and T.A.F. performed research; M.D., D.S.K., D.S., K.M., J.R.V., and D.D.W. analyzed data; and M.D. and D.D.W. wrote the paper.

The authors declare no conflict of interest.

This article is a PNAS Direct Submission.

[1]To whom correspondence should be addressed. E-mail: wagner@idi.harvard.edu.

This article contains supporting information online at www.pnas.org/lookup/suppl/doi:10.1073/pnas.1200419109/-/DCSupplemental.

isolated neutrophils from CML-like mice generated NETs, whereas only about 30% of them were BCR-ABL1$^+$. This suggested that it was not only the BCR-ABL1$^+$ neutrophils that were more sensitive to NET formation but rather the entire population. To address this more rigorously, we used FACS sorting to separate the GFP$^+$ BCR-ABL1$^+$ neutrophils from the GFP$^-$ neutrophils and evaluated their NETosis potential. Again, the majority of both GFP$^+$ and GFP$^-$ neutrophils from CML-like mice generated extracellular DNA traps (Fig. 1*D*). Normal C57BL/6 neutrophils, which had been sorted by flow cytometry, acted as controls and were shown to make NETs far less efficiently, indicating that the isolation of neutrophils through FACS sorting did not stimulate NET formation (Fig. S2*B*). In accordance with these results, in vitro pretreatment with imatinib or dasatinib, two abl-specific tyrosine kinase inhibitors (21), had no effect on NET formation (Fig. S2*C*). Although the leukemic cells underwent apoptosis in response to treatment, normal neutrophils were not affected. Thus, NETs were still being made more efficiently by the nonmalignant neutrophils from CML-like animals than by neutrophils from control mice. These results show that CML predisposes BCR-ABL1$^+$ and also BCR-ABL1$^-$ neutrophils to generate extracellular DNA traps, suggesting that a systemically acting factor may be stimulating NET formation.

Solid Tumors Generate a Leukemoid Reaction and Predispose Neutrophils to Extracellular DNA Trap Formation. Because all neutrophils from mice with CML-like MPN are more prone to generating NETs, we asked whether neutrophils from mice bearing solid tumors would also be more sensitive to NET formation. As described previously by DuPré et al. (22), injection of the 4T1 mammary carcinoma cell line into BALB/c mice induced a large increase in peripheral blood neutrophils (Fig. 2*A*) that correlated with tumor growth (Fig. S3*A*). Plasma analysis also revealed a significant increase in plasma DNA at the later stages of the disease, day 21 postinjection, which drastically increased by day 28 (Fig. 2*A*). Regression analysis performed with plasma DNA (μg/mL) as the dependent variable suggests that the increase in plasma DNA could be better determined by the number of circulating neutrophils than by tumor size (Fig. S3*B*). This suggests that NETs could be the source of the plasma DNA. Isolation of peripheral blood Gr-1$^+$ neutrophils from tumor-bearing mice and control mice showed similar purity and morphology (Fig. 2*B*). As in the leukemia model, PAF-mediated induction of NET formation by neutrophils from tumor-bearing mice revealed a tumor-age dependence in the susceptibility, reaching almost 100% NET formation 14-d after tumor implantation (Fig. 2*C* and Fig. S3*C*). Interestingly, a significant increase in NET formation was observed in isolated neutrophils from 28-d tumor-bearing mice without any additional stimulus, again suggesting that NET formation is occurring in these mice. An increase in peripheral blood neutrophils and enhanced NET formation was also observed after s.c. inoculation of Lewis lung carcinoma (LLC) cells in C57BL/6 mice (Fig. S4 *A* and *B*). The susceptibility of mice bearing different types of tumors to produce NETs suggests that priming or activation of the neutrophils occurred in these animals. Immunofluorescence staining for DNA and histone H3 of neutrophils treated with PAF from tumor-free mice showed slight decondensation of the chromatin, whereas neutrophils from 7- and 14-d tumor-bearing mice showed complete destruction of the nuclear shape and, ultimately, a spider web-like pattern, with only a few distinguishable nuclei (Fig. 2*D*). Moreover, extracellular histone H3 staining was observed along with DNA. Together, these results suggest that in murine models of CML, breast, and lung cancer, a systemic environment is created that sensitizes neutrophils to generate extracellular DNA traps.

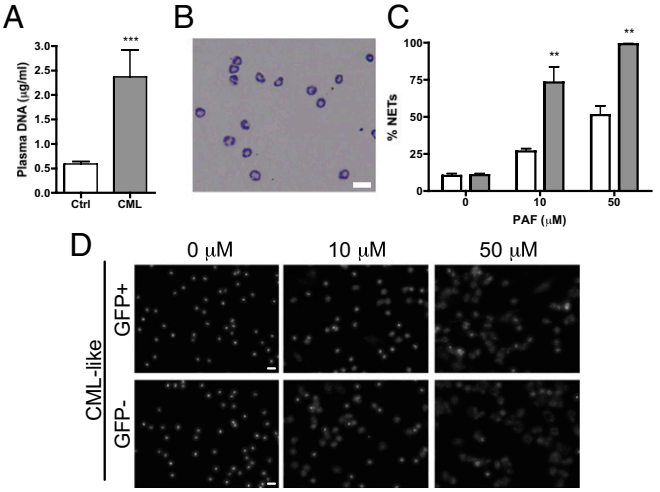

Fig. 1. Neutrophils from mice with chronic myelogenous leukemia are more prone to generate extracellular DNA traps. (*A*) Plasma analysis showed a higher level of DNA in CML mice compared with control mice ($n = 6$; $^{***}P < 0.001$). (*B*) Wright–Giemsa staining showing the purity of the neutrophil isolation from C57BL/6 mice. (Scale bar: 20 μm.) (*C*) Quantification of NETs after PAF stimulation of isolated neutrophils from CML mice (gray) shows a significant increase compared with control vector–transduced bone marrow recipients (white) ($n = 6$; $^{**}P < 0.01$). (*D*) Fluorescent images of NET formation after PAF stimulation and Hoechst staining of fluorescence-activated cell–sorted GFP$^+$ leukemic cells or control GFP$^-$ cells showed no difference in the numbers of NETs ($n = 4$). (Scale bar: 20 μm.) Graph presents means ± SEM.

Spontaneous NET Formation in Cancer Is Associated with the Presence of Lung Thrombosis. We demonstrated previously that NETs are prothrombotic (15, 16). Our mammary carcinoma model showed signs of a prothrombotic state with increasing levels of plasma von Willebrand factor (VWF), soluble P-selectin, and fibrinogen (23–26) during tumor progression (Fig. S3*D*). Immunostaining of the lungs of tumor-bearing mice showed VWF- and fibrin-rich thrombi in veins of four out of four lungs evaluated at 28-d post implantation, whereas no indication of thrombi was observed in control mice or at earlier stages of the disease (Fig. 2*E*). Moreover, citrullinated histone H3 (H3Cit), a histone modification necessary for NET production (27, 28), was present in the plasma at a late stage of the disease when plasma DNA is high, consistent with a drop in the number of hypercitrullinated neutrophils in peripheral blood (Fig. 2*F*). Thus, our results suggest that at 28-d after mammary tumor implantation, NETosis occurs and is associated with thrombosis. Together, these results suggest that NETs are implicated in cancer-associated thrombosis.

Exacerbated Effect of Low-Dose LPS in Mammary Tumor–Bearing Mice on NET Formation and Induction of a Prothrombotic State. NETosis has been defined previously as part of the innate immune defense against infection (14, 18). We, thus, evaluated the effect of LPS in vitro on neutrophils isolated from tumor-free and 14-d mammary tumor–bearing mice. As observed with PAF stimulation, LPS-treated neutrophils from tumor-bearing mice showed a significant increase in NET formation (Fig. 3*A*), suggesting that a minor infection in a tumor-bearing host would generate a larger quantity of NETs than in tumor-free mice. To test this, we injected tumor-free and tumor-bearing mice with low doses of LPS and assessed whether the predisposition of the neutrophils to form NETs would materialize in vivo and generate a procoagulant state. Two hours after injection of LPS, the neutrophil count in the blood was reduced by more than 15,000 neutrophils/μL in tumor-bearing mice and by only about 1,000 in tumor-free mice (Fig. 3*B*). This large decrease in neutrophil count in tumor-bearing LPS-treated mice was associated with a significant reduction in platelet count that was not observed in mice free of tumors (Fig. 3*C*). To determine if these effects could be related to NET formation in vivo, we evaluated NET biomarkers in blood. Plasma analysis revealed an increase in DNA and in histone H3 only in the tumor-bearing LPS-treated mice

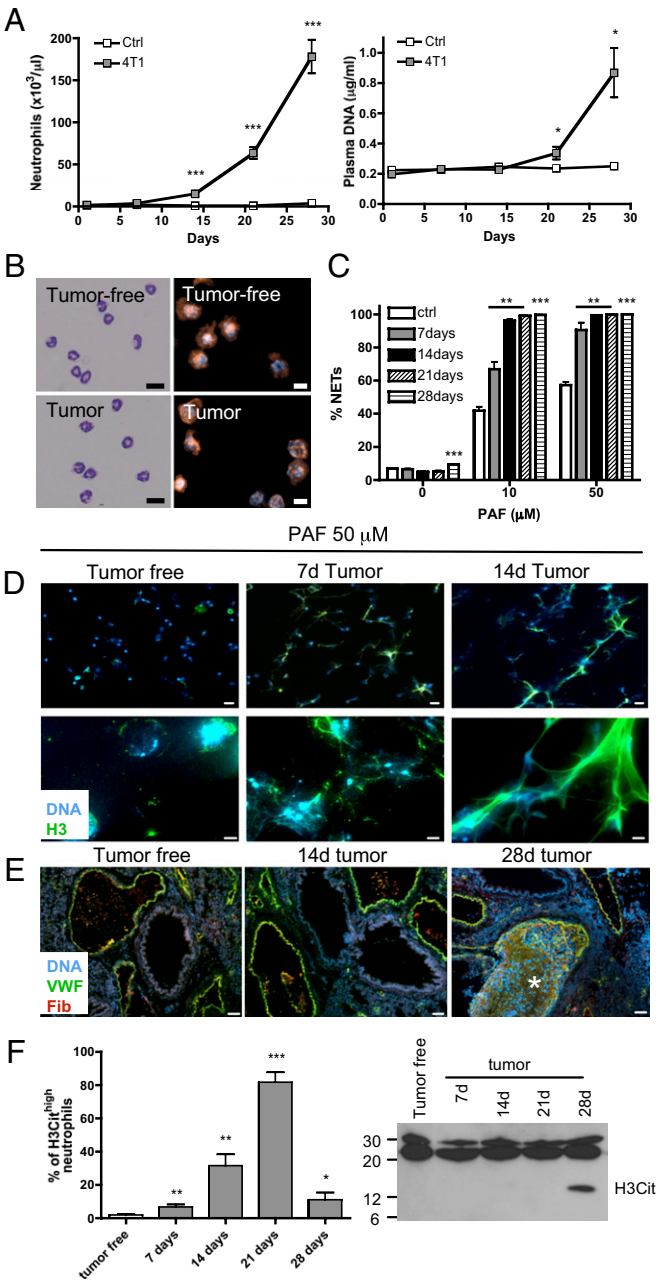

Fig. 2. Neutrophils from mammary tumor–bearing mice are more prone to NET formation and signs of spontaneous NETosis are associated with thrombosis at late stages of the disease. Tumor cells were injected in the mammary fat pad of BALB/c mice. (*A*) Neutrophil counts and plasma DNA were evaluated every 7 d (n = 6–10; $*P < 0.05$; $***P < 0.001$). (*B*) Wright–Giemsa staining (scale bar: 20 µm) and Gr-1 (red) immunostaining with Hoechst (blue) counterstaining (scale bar: 10 µm) showing the purity of the neutrophil isolation of tumor-free and 14-d 4T1 tumor–bearing BALB/c mice. (*C*) Quantification of NETs after PAF stimulation of isolated neutrophils from tumor-bearing mice at different times after tumor cell injections shows a significant increase in NET production compared with tumor-free mice (n = 6–7; $**P < 0.01$; $***P < 0.001$). (*D*) Histone H3 (green) combined with Hoechst staining (blue) of neutrophils stimulated with 50 µM PAF for 1 h at low (*Upper*) and high (*Lower*) magnification. [Scale bars: 20 µm (*Upper*); 5 µm (*Lower*).] (*E*) VWF (green) and fibrinogen/fibrin (red) immunostaining with Hoechst staining (blue) of lungs of tumor-bearing mice and tumor-free mice. VWF- and fibrin-rich thrombi (asterisk) were detected only 28 d after tumor injection (n = 4). (Scale bar: 50 µm.) (*F*) Percentage of hypercitrullinated neutrophils obtained following H3Cit immunostaining of isolated neutrophils from tumor-bearing-mice. At day 21 after tumor injection, most of the neutrophils are hypercitrullinated. At day 28, only some hypercitrullinated neutrophils remain. A minimum of 10 fields (at least 300 cells) were evaluated for hypercitrullination of histone H3 in the nucleus. Similar observations were made in four different animals. Western blot analysis of H3Cit in the plasma of tumor-bearing mice revealed the presence of H3Cit at day 28. A distinct band was observed in four out of seven plasma from 28-d tumor-bearing mice. Data shown in *A*, *C*, and *F* are means ± SEM.

(Fig. 3 *D* and *E*). No increase was observed in the tumor-bearing mice treated with vehicle or in the tumor-free mice treated with LPS, suggesting a stronger effect of LPS on chromatin release in the tumor-bearing mice. To assess whether DNA originated from NETs, we evaluated the presence of cathelicidin-related antimicrobial peptide (CRAMP), the murine homolog of human cathelicidin, a protein highly expressed in neutrophils and shown to be associated with NETs (29), and H3Cit in the plasma. Whereas a small increase in CRAMP was observed in the plasma of LPS-treated tumor-free mice, a higher level was observed in the plasma of LPS-treated tumor-bearing mice (Fig. 3*E*), likely indicating greater formation of NETs. H3Cit was detected only in the plasma of tumor-bearing mice treated with LPS. These results suggest that although low-dose LPS injection activates neutrophils and probably generates small quantities of NETs in the vasculature of tumor-free mice, as observed by the presence of CRAMP in plasma, NET formation was strongly enhanced only in the presence of cancer. Moreover, low-dose LPS treatment reduced the bleeding time of tumor-bearing mice without affecting that of tumor-free mice, a sign of a powerful effect of LPS on hemostasis in tumor-bearing mice (Fig. 3*F*). Administration of DNase1, which digests NETs, to tumor-bearing mice prevented the reduction of bleeding time associated with LPS injection. This suggests that the presence of undigested circulating extracellular DNA may promote platelet plug formation. DNase1 pretreatment did not affect neutrophil counts or prevent the reduction in the number of platelets (Fig. S5). These results show that mice with cancer develop a systemic environment that increases the ability of neutrophils to generate NETs, which contribute to the prothrombotic state of the host.

G-CSF Potentiates Neutrophils to Generate NETs. G-CSF increases neutrophil numbers in the circulation and activates them. The 4T1 tumor cells produce G-CSF, and its presence in the serum of tumor-bearing mice is associated with a leukemoid-like reaction (22). Elevated G-CSF levels were observed in the plasma of the CML-like mice and both the mammary and lung carcinoma models compared with control mice (Fig. 4*A*). To assess whether G-CSF could be responsible for the increased predisposition of peripheral blood neutrophils to form NETs, we treated healthy mice with recombinant human (rh)G-CSF. A 4-d treatment led to an increase in neutrophil count and a decrease in platelet count (Fig. S6*A*). PAF stimulation resulted in a dose-dependent increase in NET formation in isolated neutrophils similar to what we observed with the three cancer models (Fig. 4*B*). Moreover, treatment of 4T1 tumor–bearing mice with a G-CSF–neutralizing antibody prevented accumulation of neutrophils in the blood (6) and reduced their sensitization toward NET generation in vitro (Fig. 4 *C* and *D*). Similar to the mammary carcinoma model, immunostaining of isolated neutrophils revealed hypercitrullination of histone H3, corroborating their predisposition to form NETs (Fig. 4*E*).

Combination of G-CSF and Low-Dose LPS Induces NETs, and This Leads to Thrombocytopenia and Microthrombosis. As with the tumor-bearing mice, injection of low-dose LPS in the rhG-CSF–treated mice decreased neutrophil and platelet counts and increased plasma DNA (Fig. 5*A*). Similarly, reduction in tail-bleeding time was observed in the rhG-CSF–treated mice that received low-dose LPS for 1 h (Fig. 5*A*). Interestingly, 24 h after LPS challenge, DNA was still present in the plasma of rhG-CSF–treated mice, but an increase in tail-bleeding time was observed. This correlated with marked thrombocytopenia, suggesting platelet

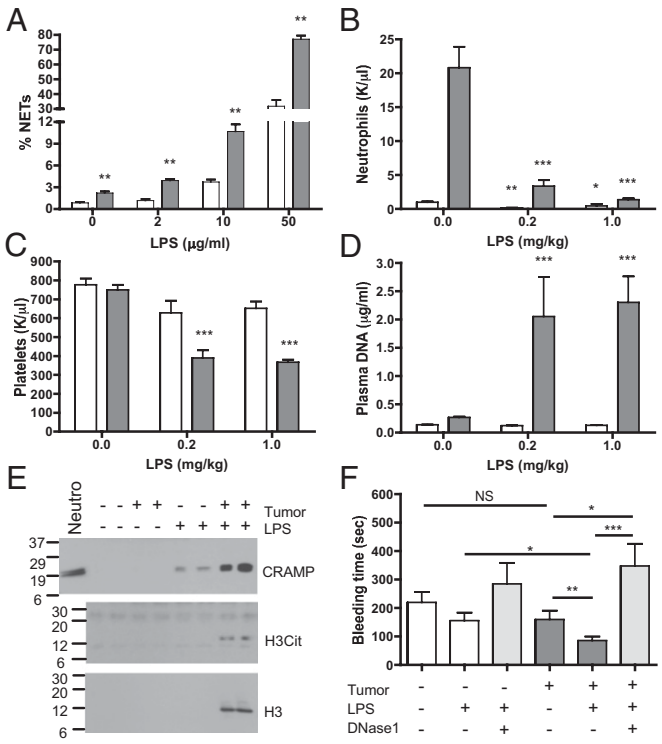

Fig. 3. Low-dose LPS induces extracellular DNA trap formation in mammary tumor–bearing mice. (*A*) Quantification of NET formation by isolated neutrophils from tumor-free (white) or 14-d 4T1 tumor–bearing (gray) mice after stimulation with low doses (as indicated) of LPS ($n = 6$; $^{**}P < 0.01$). (*B–F*) Fourteen-day tumor-bearing mice (gray) or tumor-free mice (white) were injected with low doses of LPS. Significant decreases in peripheral blood neutrophil counts (*B*) and platelet counts (*C*) were observed in tumor-bearing mice. Plasma analysis of DNA (*D*) and Western blot analysis for histone H3, histone H3Cit and CRAMP (*E*) showed much higher levels of these NET biomarkers in tumor-bearing mice than in tumor-free mice when treated with LPS (1 mg/kg). (*F*) Tail-bleeding time 1 h after LPS injections was significantly reduced in tumor-bearing mice, indicating increased prothrombotic activity. Pretreatment with DNase1 before LPS injections prevent the reduction in tail bleeding ($n = 9–17$; $^{*}P < 0.05$; $^{**}P < 0.01$; $^{***}P < 0.001$). Data shown are means ± SEM.

consumption possibly by microthrombosis. In control mice, the 24 h LPS challenge did not affect tail-bleeding time; however, it increased plasma DNA and decreased platelet numbers to a lesser extent than in rhG-CSF–treated mice. This suggests that NET formation occurs in control mice but is strongly enhanced by rhG-CSF treatment. After 24 h, in both groups, the number of blood neutrophils rebounded, likely because of the up-regulation of G-CSF after LPS injection (30). To determine whether the rhG-CSF–treated mice challenged with LPS for 24 h showed signs of thrombosis, we measured the level of thrombin–antithrombin (TAT) complexes, a marker of thrombin generation, in the plasma and analyzed the lungs for signs of fibrosis. As has been reported in healthy donors receiving rhG-CSF (31), a higher level of TAT was observed in mice treated with rhG-CSF compared with control mice at baseline (Fig. 5*B*). Whereas no significant change was observed in control mice 24 h after LPS challenge, TAT levels were significantly reduced in rhG-CSF–treated mice, suggesting a consumption of coagulation factors. Histology and immunofluorescence analysis revealed signs of fibrosis and fibrinogen-/fibrin-rich microthrombi in the lungs of both rhG-CSF–treated and untreated mice after LPS challenge. However, the effect was greatly enhanced in rhG-CSF–treated mice (Fig. 5*C*). No signs of fibrosis were observed in mice that had not received LPS. A greater accumulation of fibrinogen/fibrin deposits was also found in the renal glomeruli of the rhG-CSF–treated group after LPS challenge (Fig. 5*C*). These results suggest that in rhG-CSF–treated mice, NETs are formed early after LPS injection and induce a prothrombotic state. Such a state could lead, in the extreme, to the consumption of platelets and coagulation factors and microthrombosis. Taken together, our results indicate that increased levels of G-CSF, which are generated in different types of cancers, can produce a systemic environment that primes peripheral blood neutrophils to generate NETs more readily. This effect may contribute, at least in part, to the prothrombotic state observed in cancer.

Discussion

Cancers are known to elevate the risk of thrombosis. Leukocytosis, thrombocytosis, microparticles, cytokines, tissue factor, soluble P-selectin, and elevation in coagulation factors could all be partially responsible for the prothrombotic state (32). Here, we report that cancer induces a systemic environment that primes neutrophils to release NETs, thereby further promoting a prothrombotic state. Our results show that (*i*) peripheral blood neutrophils from leukemic mice and solid tumor–bearing mice are more prone to NET formation ex vivo; (*ii*) NETosis is associated with lung thrombosis in the breast carcinoma model; (*iii*) injection of a low dose of LPS in tumor-bearing mice

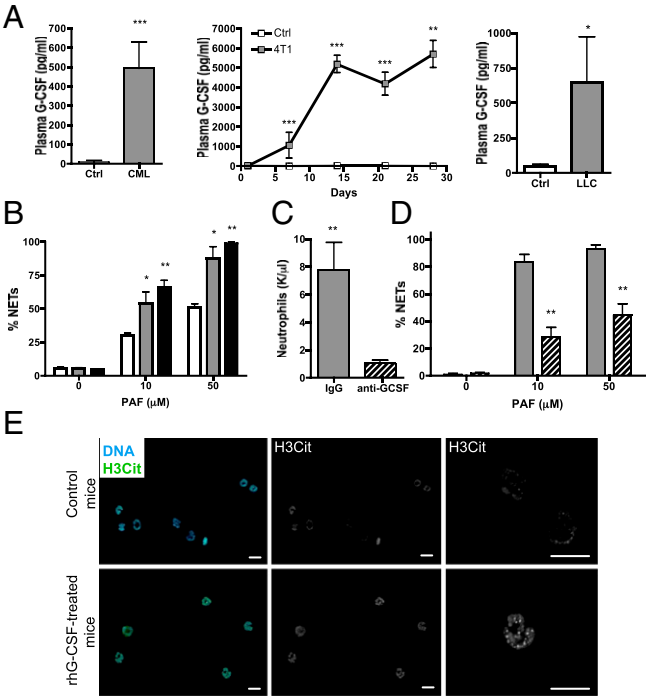

Fig. 4. Tumors produce G-CSF, which elevates blood neutrophil count and predisposes neutrophils to generate NETs. (*A*) Increased quantities of G-CSF were observed in the plasma of CML (*Left*), mammary carcinoma (*Center*), and lung carcinoma (*Right*) tumor–bearing mice compared with tumor-free mice (white) ($n = 5–9$; $^{*}P < 0.05$). (*B*) BALB/c mice were treated in vivo with 2.5 μg (gray) or 10 μg (black) rhG-CSF, neutrophils were isolated, and PAF-mediated induction of NETs was evaluated and compared with neutrophils from control mice (white). rhG-CSF significantly increased the percentage of cells forming NETs ($n = 4–5$; $^{*}P < 0.05$; $^{**}P < 0.01$). (*C*) Mice bearing 4T1 tumors were treated daily with neutralizing anti–G-CSF antibody starting 2 d after tumor cell injection. The anti–G-CSF treatment reduced the number of peripheral blood neutrophils in 4T1 tumor–bearing mice (hashed) ($n = 5$). (*D*) The anti–G-CSF treatment significantly diminished the ability of neutrophils to form NETs ex vivo upon PAF stimulation compared with control isotype–treated 4T1 tumor–bearing mice (gray) ($n = 5$). $^{**}P < 0.05$. (*E*) Citrullinated histone H3 (green) immunostaining with Hoechst (blue) counterstain revealed an increase in citrullination in isolated neutrophils from rhG-CSF–treated mice (*Left*). (*Center* and *Right*) H3Cit alone (*Center*) and higher magnification (*Right*). (Scale bar: 10μm). Data shown in *A–D* represent means ± SEM.

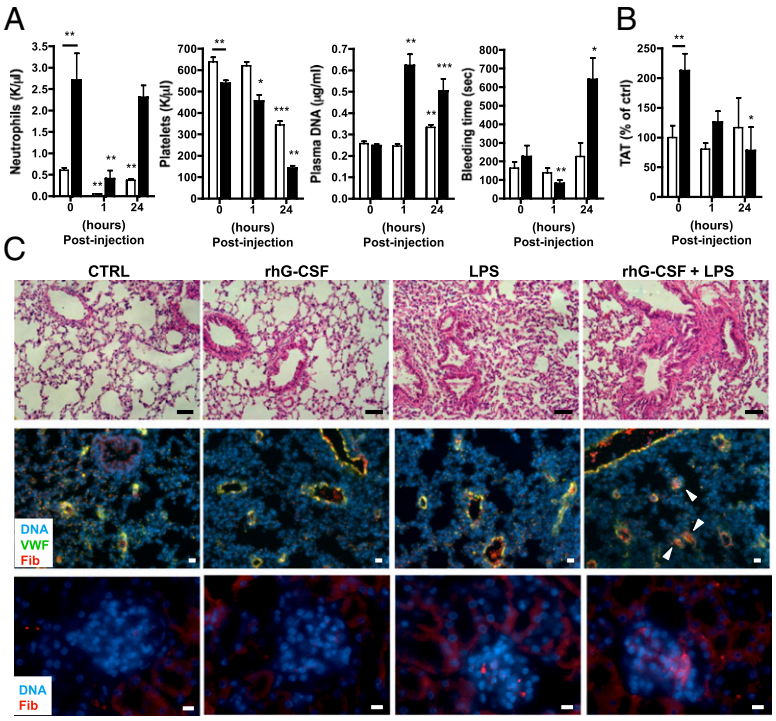

Fig. 5. Low-dose LPS injection induces a prothrombotic state in rhG-CSF–treated mice. Mice were treated with vehicle (control; white) or rhG-CSF (black) and challenged with low-dose LPS (1 mg/kg) for 1 or 24 h. (*A*) One hour after LPS injection, the blood counts showed a significant reduction in neutrophils and platelets, which corresponded to an increase in plasma DNA and a reduction in tail-bleeding time only in rhG-CSF–treated mice. Only the neutrophil count was reduced in control mice. Twenty-four hours after LPS treatment, decreased platelet counts and increased DNA levels were also observed in control mice without modulation of tail-bleeding time. In contrast, 24 h after LPS injection the tail-bleeding time was prolonged in rhG-CSF–treated mice (n = 5–9; *$P < 0.05$; **$P < 0.01$; ***$P < 0.001$ compared with no LPS treatment). (*B*) Twenty-four hours after LPS challenge, a decrease in TAT complexes was observed in rhG-CSF–treated compared with control mice (n = 5–9; *$P < 0.05$; **$P < 0.01$). (*C*) Hematoxylin and eosin staining (top images) of the lungs of mice 24 h after LPS challenge showed some signs of fibrosis in mice treated with LPS, but fibrosis was strongly enhanced in rhG-CSF–treated mice. (Scale bar: 50 μm.) Anti-fibrinogen staining (red) revealed an enhanced presence of fibrinogen-/fibrin-rich microthrombi (arrows) in the lungs (middle images) and the glomeruli of the kidneys (bottom images) of rhG-CSF–treated mice challenged with LPS for 24 h. [Scale bar: 20 μm (*Middle*) and 10 μm (*Lower*)]. Hoechst, blue. Data in *A* and *B* represent means ± SEM.

increases plasma NET biomarkers and induces a prothrombotic state; and (*iv*) the increased predisposition of neutrophils to NET formation could be attributable to elevated G-CSF in the plasma of mice with cancer. Thus, by generating G-CSF, cancers prime neutrophils to undergo NETosis.

NETs were originally described as a defense mechanism against infection (14). Recently, our group showed that NETs activate platelets and trigger thrombosis (15) and are implicated in the pathogenesis of deep vein thrombosis (DVT) in mice (16). An increased risk of thrombosis is associated with many cancers, and such cancers may even be diagnosed only following a thrombotic event such as DVT. Therefore, one may hypothesize that the predisposition to generate extracellular DNA traps in cancer patients could increase the risk of thrombosis. DNA, histones, and neutrophil granular proteins have been shown to promote coagulation and to be injurious to tissues (17, 33–35). NETs' products and histones also induce platelet activation and aggregation, red blood cell accumulation, and VWF release, hallmarks of venous thrombus formation (15–17, 36).

Although CML is not associated with a high risk of thrombosis (37), our results show that the neutrophils from mice with CML-like MPN are primed to NET formation, and plasma DNA is observed. It is conceivable that neutrophil activation and NET generation are important players in cancer-associated thrombosis but are not sufficient. Production of tissue factor by various tumors (38), for example, could further potentiate the prothrombotic state. In addition, our results indicate that a further activation of the innate immune system in a cancer patient could precipitate a thrombotic event and organ damage through NET-/histone-induced injury. Given the close interaction of platelets and neutrophils during infection and the implication of platelet activation in the generation of NETs (39, 40), their potential contribution in the cancer models should be addressed.

NET induction by LPS in the solid tumor model rapidly generates a large quantity of injurious products in the bloodstream with the onset of a prothrombotic state, leading to pulmonary microthrombosis. This latter effect has also been observed in mice after an injection of large quantities of histones, leading to sepsis-like disease (34). Moreover, our laboratory showed that injection of a sublethal dose of histones in healthy mice results in thrombocytopenia (36). In mice with late-stage cancer, we observed thrombi in the lung, even in the absence of additional stimulation. This correlated with the presence of a high quantity of plasma DNA. Interestingly, our laboratory in collaboration with that of Bernhard Lämmle recently reported increased levels of DNA and neutrophil markers in plasma from cancer patients with acute thrombotic microangiopathies (41).

Similar to the solid cancer mouse models, in humans, elevated serum G-CSF levels (8–10, 42) and extreme leukocytosis (>40,000/μL) related to a paraneoplastic leukemoid reaction have been reported for a variety of solid tumor types (43). Although initially clinically stable, the vast majority of patients with a neutrophilic predominance have poor clinical outcomes, with 76% dying within 12 wk of development of extreme leukocytosis (43). It is, thus, possible that NETs are generated in late-stage cancer patients and play a role in the critical outcome. Determination of DNA levels in the plasma of these patients in relation to leukocytosis would assess this further.

G-CSF is broadly used to treat neutropenia or for hematopoietic stem cell mobilization in patients and healthy donors. Studies have reported endothelial cell dysfunction, clotting activation, an increase in blood oxidative status, platelet aggregation, and neutrophil activation in healthy donors during treatment with G-CSF (31, 44). Despite this, most of the G-CSF–treated healthy subjects do not experience thrombotic events (13, 44, 45), and G-CSF is considered a safe mobilizing agent. The prothrombotic effects that have been associated with G-CSF have been linked to its use in the treatment of inflammatory or already-prothrombotic states, such as acute myocardial infarction, through mobilization of autologous stem cells (45, 46). This is in accordance with our results suggesting that, in the presence of G-CSF, neutrophils may be more sensitive to NET formation, in particular, upon encountering a "second hit," such as low-grade infection.

In conclusion, we have uncovered an important role for extracellular chromatin that is generated in animals with cancer, predisposing them to thrombosis. Release of large quantities of DNA in the blood occurs at late stages of the disease or upon a "second hit," such as a minor infection, and could be detrimental to the host. It will be important to determine whether

agents neutralizing G-CSF and/or NETs can decrease the incidence of thrombosis in cancer patients.

Materials and Methods

For a full description of all methods, see *SI Materials and Methods*.

Animals. Experimental procedures were approved by the Institutional Animal Care and Use Committee of the Immune Disease Institute and Massachusetts General Hospital. Experiments are described in *SI Materials and Methods*.

Stainings and Plasma Analysis. Neutrophils/NETs were stained with anti–Gr-1 and anti–histone H3 antibodies. Lung sections were stained with hematoxylin and eosin or anti-fibrinogen antibody and anti-VWF. Hoechst-33342 was used as a counterstain. ELISAs are described in *SI Materials and Methods*. DNA was quantified with a Quant-iT Picogreen assay (Invitrogen). For Western blot analysis, equal amounts of plasma were analyzed using anti-CRAMP, anti–histone H3 or anti–histone H3 (citrulline 2, 8, 17) antibodies.

Peripheral Blood Neutrophil Isolation and NET Induction. Peripheral blood neutrophils were isolated on a Percoll gradient, followed by hypotonic lysis and stimulated with PAF or LPS. DNA was stained with Hoechst-33342, and cells were fixed before visualization. NETs were counted from six different fields in triplicate wells and expressed as percentage of NET-forming cells per total number of cells in the field.

Statistical Analysis. Data are represented as means ± SEM and were analyzed by a two-sided Mann–Whitney test performed between groups. All *P* values were considered significant at or below 0.05.

ACKNOWLEDGMENTS. We thank Lesley Cowan for help with manuscript preparation, Myriam Armant for help with G-CSF studies, and Julian I. Borissoff for help with regression analysis and thoughtful discussions. This work was supported by the National Heart, Lung, and Blood Institute of the National Institutes of Health Grant R01 HL102101 (to D.D.W.), Terry Fox Foundation Grant TF-018748 through the Canadian Cancer Society (to M.D.), and National Cancer Institute Grant 5K08CA138916-02 (to D.S.K.).

1. Rickles FR, Levine M, Edwards RL (1992) Hemostatic alterations in cancer patients. *Cancer Metastasis Rev* 11:237–248.
2. Chechlinska M, Kowalewska M, Nowak R (2010) Systemic inflammation as a confounding factor in cancer biomarker discovery and validation. *Nat Rev Cancer* 10:2–3.
3. Champlin RE, Golde DW (1985) Chronic myelogenous leukemia: Recent advances. *Blood* 65:1039–1047.
4. Youn JI, Gabrilovich DI (2010) The biology of myeloid-derived suppressor cells: The blessing and the curse of morphological and functional heterogeneity. *Eur J Immunol* 40:2969–2975.
5. Ueha S, Shand FH, Matsushima K (2011) Myeloid cell population dynamics in healthy and tumor-bearing mice. *Int Immunopharmacol* 11:783–788.
6. Kowanetz M, et al. (2010) Granulocyte-colony stimulating factor promotes lung metastasis through mobilization of Ly6G+Ly6C+ granulocytes. *Proc Natl Acad Sci USA* 107:21248–21255.
7. Jiang X, Lopez A, Holyoake T, Eaves A, Eaves C (1999) Autocrine production and action of IL-3 and granulocyte colony-stimulating factor in chronic myeloid leukemia. *Proc Natl Acad Sci USA* 96:12804–12809.
8. Joshita S, et al. (2009) Granulocyte-colony stimulating factor-producing pancreatic adenosquamous carcinoma showing aggressive clinical course. *Intern Med* 48: 687–691.
9. Kaira K, et al. (2008) Lung cancer producing granulocyte colony-stimulating factor and rapid spreading to peritoneal cavity. *J Thorac Oncol* 3:1054–1055.
10. Kawaguchi M, et al. (2010) Aggressive recurrence of gastric cancer as a granulocyte-colony-stimulating factor-producing tumor. *Int J Clin Oncol* 15:191–195.
11. Avalos BR, et al. (1990) Human granulocyte colony-stimulating factor: Biologic activities and receptor characterization on hematopoietic cells and small cell lung cancer cell lines. *Blood* 75:851–857.
12. Spiel AO, et al. (2011) Increased platelet aggregation and in vivo platelet activation after granulocyte colony-stimulating factor administration. A randomised controlled trial. *Thromb Haemost* 105:655–662.
13. Quillen K, Byrne P, Yau YY, Leitman SF (2009) Ten-year follow-up of unrelated volunteer granulocyte donors who have received multiple cycles of granulocyte-colony-stimulating factor and dexamethasone. *Transfusion* 49:513–518.
14. Brinkmann V, et al. (2004) Neutrophil extracellular traps kill bacteria. *Science* 303: 1532–1535.
15. Fuchs TA, et al. (2010) Extracellular DNA traps promote thrombosis. *Proc Natl Acad Sci USA* 107:15880–15885.
16. Brill A, et al. (2011) Neutrophil extracellular traps promote deep vein thrombosis in mice. *J Thromb Haemost* 10:136–144.
17. Massberg S, et al. (2010) Reciprocal coupling of coagulation and innate immunity via neutrophil serine proteases. *Nat Med* 16:887–896.
18. Fuchs TA, et al. (2007) Novel cell death program leads to neutrophil extracellular traps. *J Cell Biol* 176:231–241.
19. Yousefi S, Mihalache C, Kozlowski E, Schmid I, Simon HU (2009) Viable neutrophils release mitochondrial DNA to form neutrophil extracellular traps. *Cell Death Differ* 16:1438–1444.
20. Li S, Ilaria RL, Jr., Million RP, Daley GQ, Van Etten RA (1999) The P190, P210, and P230 forms of the BCR/ABL oncogene induce a similar chronic myeloid leukemia-like syndrome in mice but have different lymphoid leukemogenic activity. *J Exp Med* 189: 1399–1412.
21. Druker BJ, et al. (2001) Activity of a specific inhibitor of the BCR-ABL tyrosine kinase in the blast crisis of chronic myeloid leukemia and acute lymphoblastic leukemia with the Philadelphia chromosome. *N Engl J Med* 344:1038–1042.
22. DuPré SA, Hunter KW, Jr. (2007) Murine mammary carcinoma 4T1 induces a leukemoid reaction with splenomegaly: Association with tumor-derived growth factors. *Exp Mol Pathol* 82:12–24.
23. André P, Hartwell D, Hrachovinová I, Saffaripour S, Wagner DD (2000) Pro-coagulant state resulting from high levels of soluble P-selectin in blood. *Proc Natl Acad Sci USA* 97:13835–13840.
24. Koster T, Blann AD, Briët E, Vandenbroucke JP, Rosendaal FR (1995) Role of clotting factor VIII in effect of von Willebrand factor on occurrence of deep-vein thrombosis. *Lancet* 345:152–155.
25. van Hylckama Vlieg A, Rosendaal FR (2003) High levels of fibrinogen are associated with the risk of deep venous thrombosis mainly in the elderly. *J Thromb Haemost* 1: 2677–2678.
26. Myers DD, et al. (2003) P-selectin and leukocyte microparticles are associated with venous thrombogenesis. *J Vasc Surg* 38:1075–1089.
27. Neeli I, Dwivedi N, Khan S, Radic M (2009) Regulation of extracellular chromatin release from neutrophils. *J Innate Immun* 1:194–201.
28. Li P, et al. (2010) PAD4 is essential for antibacterial innate immunity mediated by neutrophil extracellular traps. *J Exp Med* 207:1853–1862.
29. Jann NJ, et al. (2009) Neutrophil antimicrobial defense against Staphylococcus aureus is mediated by phagolysosomal but not extracellular trap-associated cathelicidin. *J Leukoc Biol* 86:1159–1169.
30. Barsig J, et al. (1995) Lipopolysaccharide-induced interleukin-10 in mice: Role of endogenous tumor necrosis factor-alpha. *Eur J Immunol* 25:2888–2893.
31. Falanga A, et al. (1999) Neutrophil activation and hemostatic changes in healthy donors receiving granulocyte colony-stimulating factor. *Blood* 93:2506–2514.
32. Connolly GC, Khorana AA (2010) Emerging risk stratification approaches to cancer-associated thrombosis: Risk factors, biomarkers and a risk score. *Thromb Res* 125 (Suppl 2):S1–S7.
33. Hirahashi J, et al. (2009) Mac-1 (CD11b/CD18) links inflammation and thrombosis after glomerular injury. *Circulation* 120:1255–1265.
34. Xu J, et al. (2009) Extracellular histones are major mediators of death in sepsis. *Nat Med* 15:1318–1321.
35. Swystun LL, Mukherjee S, Liaw PC (2011) Breast cancer chemotherapy induces the release of cell-free DNA, a novel procoagulant stimulus. *J Thromb Haemost* 9: 2313–2321.
36. Fuchs TA, Bhandari AA, Wagner DD (2011) Histones induce rapid and profound thrombocytopenia in mice. *Blood* 118:3708–3714.
37. Wehmeier A, Daum I, Jamin H, Schneider W (1991) Incidence and clinical risk factors for bleeding and thrombotic complications in myeloproliferative disorders. A retrospective analysis of 260 patients. *Ann Hematol* 63:101–106.
38. Rickles FR, Patierno S, Fernandez PM (2003) Tissue factor, thrombin, and cancer. *Chest* 124(3 Suppl):58S–68S.
39. Andonegui G, et al. (2005) Platelets express functional Toll-like receptor-4. *Blood* 106: 2417–2423.
40. Clark SR, et al. (2007) Platelet TLR4 activates neutrophil extracellular traps to ensnare bacteria in septic blood. *Nat Med* 13:463–469.
41. Fuchs TA, Kremer Hovinga JA, Schatzberg D, Wagner DD, Lämmle B (2012) Circulating DNA and myeloperoxidase indicate disease activity in patients with thrombotic microangiopathies. *Blood*, 10.1182/blood-2012-02-412197.
42. Stathopoulos GP, et al. (2011) Granulocyte colony-stimulating factor expression as a prognostic biomarker in non-small cell lung cancer. *Oncol Rep* 25:1541–1544.
43. Granger JM, Kontoyiannis DP (2009) Etiology and outcome of extreme leukocytosis in 758 nonhematologic cancer patients: A retrospective, single-institution study. *Cancer* 115:3919–3923.
44. Cella G, et al. (2006) Blood oxidative status and selectins plasma levels in healthy donors receiving granulocyte-colony stimulating factor. *Leukemia* 20:1430–1434.
45. Hill JM, et al. (2005) Outcomes and risks of granulocyte colony-stimulating factor in patients with coronary artery disease. *J Am Coll Cardiol* 46:1643–1648.
46. Kuroiwa M, et al. (1996) Effects of granulocyte colony-stimulating factor on the hemostatic system in healthy volunteers. *Int J Hematol* 63:311–316.

Supporting Information

Demers et al. 10.1073/pnas.1200419109

SI Materials and Methods

Cell Lines and Reagents. The 4T1 and LLC cell lines were purchased from ATCC and maintained in high-glucose Dulbecco's modified Eagle medium (DMEM) plus L-GlutaMAX-1 [supplemented with 10% (vol/vol) FCS, 10 mM Hepes buffer, 10 mM sodium carbonate (4T1 cells)]. The 4T1 cell line was originally isolated from a spontaneously arising mammary tumor in a BALB/c mouse (1), whereas LLC cells originated from C57BL/6 mice. The 4T1 and LLC cells were injected in mice after less than 4 and 10 serial passages in vitro, respectively. All cell culture products were purchased from Life Technologies/Invitrogen.

Animals. All animal procedures were performed using 6- to 8-wk-old BALB/c female or C57BL/6 female mice (Jackson Laboratory). All experimental procedures involving mice were approved by the Animal Care and Use Committee of the Immune Disease Institute. All transplantation experiments were approved by the Institutional Animal Use and Care Committee of Massachusetts General Hospital.

Bone Marrow Transduction and Transplantation. Transduction/transplantation experiments were performed as described (2, 3). Briefly, ecotropic replication-defective retrovirus was generated by cotransfection of MSCV-IRES-GFP-p210-BCR-ABL or MSCV-IRES-GFP (vector control) and the *kat* packaging plasmids into 293 cells. The retrovirus was harvested and used to infect the bone marrow of 5-fluorouracil–pretreated C57BL/6 mice twice. Consequently, the bone marrow was transplanted into lethally irradiated (900 cGy) C57BL/6 mice in a dose of 3–5 $\times$ 10^5 cells/mouse by tail vein injection. Disease induction was monitored by weekly full blood count analyses by using a Vetscan 5 HM (Abaxis) and by flow cytometry of peripheral blood after red blood cell lysis (ACK lysing buffer; Lonza) and staining of leukocytes with a phycoerythrin (PE)-conjugated antibody to CD11b (clone M1/70; BioLegend). Disease burden was measured by percentage of GFP^+ $CD11b^+$ cells in peripheral blood. Necropsies were performed on euthanized mice, and spleen weights were recorded to confirm establishment of CML at the time the NET experiments were performed.

Induction of Solid Tumors. The 4T1 cells (4×10^5) were inoculated in the mammary fat pad of 6- to 8-wk-old BALB/c mice. For the LLC model, 5×10^5 cells were inoculated in the right flank of 6- to 8-wk-old C57BL/6 mice. Animals were monitored twice a week, at which time tumors were carefully measured using calipers. The tumor volume was calculated using the formula $V = lw^2 \times 0.4$, where l is the length and w the width (4). Mice were killed at the indicated time or when tumor volume reached 2,500 mm^3 or animals were moribund. For peripheral blood cell count, blood was collected using EDTA-coated capillaries and analyzed with a Hemavet hematology analyzer (Drew Scientific). At sacrifice, blood was collected through the retroorbital sinus into Tyrode's buffer containing 10 mM EDTA, centrifuged at 3,300 $\times g$ for plasma collection, and centrifuged again at 13,400 $\times g$ to remove any contaminating cells.

Injection of Low-Dose LPS. Fourteen-day tumor-bearing mice or rhG-CSF–treated mice were injected intraperitoneally with LPS (Sigma-Aldrich) at the indicated concentration. The mice were killed at different time points (as indicated) and bled into 3.2% (wt/vol) sodium citrate for plasma collection. A drop of blood was also collected in EDTA-coated capillaries for blood cell count.

DNase1 Treatment. Fourteen-day tumor-bearing or tumor-free mice were injected intraperitoneally with 50 μg of DNase1 (Pulmozyme; Genentech) or saline (APP Pharmaceuticals) 3 h before LPS injections for 1 h before tail-bleeding experiments.

Tail-Bleeding Time. Mice were anesthetized with 2.5% tribromoethanol, and tail-bleeding time was determined by removing 2 mm of the distal mouse tail and immediately immersing the tail in PBS at 37 °C. A complete cessation of bleeding for more than 120 s was defined as the bleeding time.

rhG-CSF Treatment. Mice received s.c. injections between the scapulae with 2.5 or 10 μg of rhG-CSF (Neupogen; Amgen) once daily for 4 d to stimulate durable granulopoiesis (5). Control mice received vehicle [5% (wt/vol) dextrose] following the same injection schedule. On day 5, plasma was collected, and peripheral blood neutrophils were isolated.

Anti–G-CSF Treatment. Mice were injected with 4×10^5 4T1 cells in the mammary fat pad. After 2 d, mice were injected intraperitoneally with 10 μg of mouse neutralizing monoclonal antibody to G-CSF (R&D Systems) or with a matching isotype control IgG (R&D Systems) daily for 12 d. On day 14, plasma was collected, and peripheral blood neutrophils were isolated.

Peripheral Blood Neutrophil Isolation. Mice were exsanguinated into PBS containing 1% (wt/vol) BSA and 15 mM EDTA. After centrifugation, blood cells were resuspended and layered onto a Percoll gradient of 78%, 69%, and 52% in PBS (vol/vol), centrifuged and cells at the 69%/78% interface were collected. Red blood cell contamination was eliminated by hypotonic lysis, and final cell concentration was determined by hemacytometer. Neutrophil purity was established to be routinely >90%, as assessed by Wright–Giemsa staining on cytospin.

Cell Sorting by Flow Cytometry. Flow cytometry–based cell sorting of GFP^+ or control GFP^- cells was performed after drawing of a leukocyte-specific and, consequently, a myeloid cell–specific gate by an SORP 7-laser LSR-II (BD Biosciences).

Induction of Extracellular DNA Traps in Vitro. Isolated peripheral blood neutrophils (1.5×10^4) were seeded into 96 wells and allowed to adhere at 37 °C and 5% CO_2 for 15 min before stimulation with PAF or LPS at the indicated concentrations for 1 or 2-1/2 h, respectively. DNA was stained with Hoechst-33342 (Invitrogen), and cells were fixed with 2% (vol/vol) paraformaldehyde before visualization using an epifluorescent Axiovert microscope (Zeiss). For quantification, NETs were counted from six different fields in triplicate wells for each condition and expressed as percentage of NET-forming cells per total number of cells in the field.

Quantification of Plasma VWF, Soluble P-Selectin, Fibrinogen, G-CSF, and DNA. The VWF ELISA was performed as described (6) using the level of VWF in pooled plasma of 20 C57BL/6J WT mice as a reference standard [normal mouse plasma (nmp)]. Plasma-soluble P-selectin, fibrinogen, G-CSF, TAT, and DNA levels were determined using the mouse sP-Selectin/CD62P Quantikine ELISA (R&D Systems), the mouse fibrinogen ELISA (Genway Biotech), the Quantikine mouse or human G-CSF ELISA (R&D Systems), human TAT ELISA (Affinity Biologicals), and Quant-iT Picogreen assay (Invitrogen) according to the instructions of the manufacturers.

Immunostaining of Neutrophils and NETs. Isolated neutrophils were plated on a cell culture slide and stimulated as described above. After stimulation, cells were fixed in 2% paraformaldehyde and permeabilized, and neutrophils were stained with a rat anti–Gr-1 antibody (BD Bioscience) and NETs with a rabbit anti–histone H3 antibody (Abcam). Alexa 555–conjugated goat anti-rat IgG or Alexa 488–conjugated goat anti-rabbit IgG were used as secondary antibodies (Invitrogen). For H3Cit staining, isolated neutrophil cytospins were stained with a rabbit anti–histone H3 (citrulline 2, 8, 17) antibody (Abcam) and Alexa 488–conjugated goat anti-rabbit IgG (Invitrogen) used as secondary antibody. All immunostainings were counterstained with Hoechst-33342 to visualize DNA, and slides were mounted with Fluoro-gel (Electron Microscopy Sciences) and observed under an epifluorescent Axiovert microscope (Zeiss).

Western Blot Analysis. Equal amounts of plasma were analyzed on a 4–20% SDS/PAGE gel and transferred onto Immobilon PVDF membranes using a Mini-Trans Blot Electrophoretic Transfer Cell System (Bio-Rad Laboratories). The membranes were blocked with 5% milk in TBS/0.05% Tween-20 overnight and blotted for 2 h with primary antibodies. Membranes were probed with a rabbit polyclonal anti-cathelicidin (CRAMP) or anti–histone H3 and anti–histone H3 (citrulline 2, 8, 17) antibodies (Abcam). Secondary antibodies consisted of horseradish peroxidase–conjugated anti-rabbit IgG (Bio-Rad Laboratories). Detection was carried out with a Pierce ECL Western Blotting Substrate (Thermo Scientific). After detection, membranes were stained with Coomassie blue to ensure equal loading of all wells.

Lung Histology and Immunostaining. Lungs were harvested from killed animals and fixed in zinc fixative (100 mM Tris-HCl containing 37 mM zinc chloride, 23 mM zinc acetate, and 3.2 mM calcium acetate). Paraffin-embedded sections were deparaffinized in xylenes and rehydrated through a graded alcohol series. Sections were stained with hematoxylin and eosin, mounted in DPX mountant (Fluka BioChemika), and observed by light microscopy. For fibrinogen/fibrin and VWF staining, the sections were stained with a sheep anti-fibrinogen antibody (ABD Biologicals) and rabbit anti–human VWF antibody (Dako) and incubated with anti-sheep Alexa-555 and anti-rabbit Alexa-488 (Invitrogen) as secondary antibodies. Sections were counterstained with Hoechst-33342 to visualize all nuclei, mounted with Fluoro-gel (Electron Microscopy Sciences), and observed under an epifluorescent Axiovert microscope (Zeiss).

Statistical Analysis. Data are represented as means ± SEM and were analyzed by a two sided Mann–Whitney test performed between groups. Regression analysis was performed with plasma DNA (μg/mL) as the dependent variable using IBM SPSS Statistics (IBM), version 19.0. For this model, the adjusted R^2 and the standardized regression coefficients (β) of the independent variables were calculated. All P values were considered significant at or below 0.05.

1. Aslakson CJ, Miller FR (1992) Selective events in the metastatic process defined by analysis of the sequential dissemination of subpopulations of a mouse mammary tumor. *Cancer Res* 52:1399–1405.
2. Krause DS, Lazarides K, von Andrian UH, Van Etten RA (2006) Requirement for CD44 in homing and engraftment of BCR-ABL-expressing leukemic stem cells. *Nat Med* 12: 1175–1180.
3. Li S, Ilaria RL, Jr., Million RP, Daley GQ, Van Etten RA (1999) The P190, P210, and P230 forms of the BCR/ABL oncogene induce a similar chronic myeloid leukemia-like syndrome in mice but have different lymphoid leukemogenic activity. *J Exp Med* 189: 1399–1412.
4. Attia MA, Weiss DW (1966) Immunology of spontaneous mammary carcinomas in mice. V. Acquired tumor resistance and enhancement in strain A mice infected with mammary tumor virus. *Cancer Res* 26:1787–1800.
5. Scholz M, et al. (2009) A pharmacokinetic model of filgrastim and pegfilgrastim application in normal mice and those with cyclophosphamide-induced granulocytopaenia. *Cell Prolif* 42:813–822.
6. Brill A, et al. (2011) von Willebrand factor-mediated platelet adhesion is critical for deep vein thrombosis in mouse models. *Blood* 117:1400–1407.

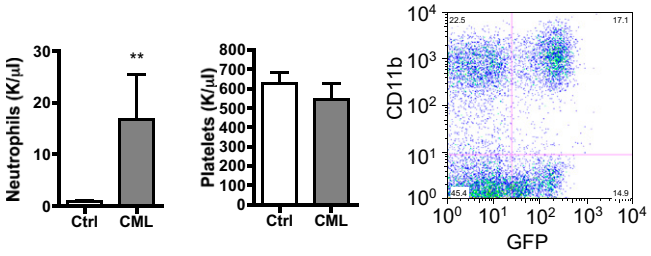

Fig. S1. Induction of CML-like disease increases neutrophils without affecting platelets. Bone marrow transduced with a retrovirus encoding BCR/ABL and GFP was transplanted into lethally irradiated C57BL/6 mice to induce CML. Control mice were transplanted with bone marrow transduced with a vector encoding only GFP (Ctrl). At days 18–20 posttransplantation, peripheral blood was collected, and numbers of neutrophils and platelets were evaluated in the blood of CML-like (gray) and control (white) mice ($n = 6$; $^{**}P < 0.01$). Representative flow cytometry dot plot showing the percentage of leukemic (BCR-ABL$^+$) cells in the peripheral blood assessed by the expression of CD11b and GFP. Data shown are means ± SEM.

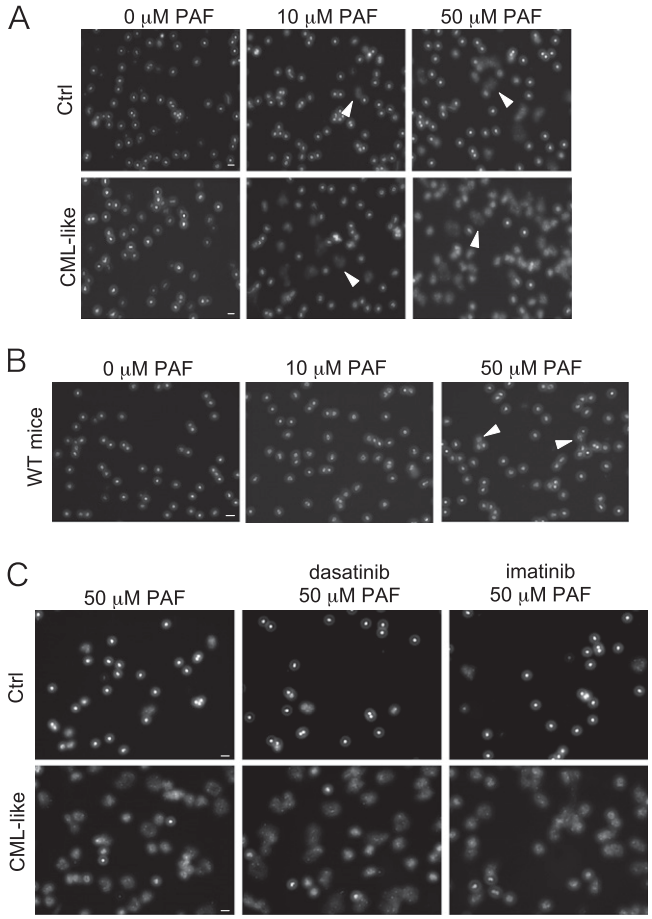

Fig. S2. Malignant and nonmalignant neutrophils from CML-like mice generate extracellular DNA traps. Representative fluorescent images of Hoechst staining after PAF stimulation (*A*) Nuclear decondensation of isolated neutrophils from CML-like mice shows a significant increase compared with control vector–transduced bone marrow recipients (Ctrl). Arrow, NET-forming cells. (Scale bar: 20 μm.) (*B*) NET formation of fluorescence-activated cell–sorted WT neutrophils (control for Fig. 1*D*). Arrow, NET-forming cells. (Scale bar: 20 μm.) (*C*) Neutrophils were isolated from CML-like or control mice and pretreated in vitro with dasatinib or imatinib, abl-specific tyrosine kinase inhibitors, at 10 μM for 4 h before PAF stimulation. This treatment induces apoptosis of leukemic cells but does not affect normal neutrophils. PAF stimulation showed that even after destruction of the malignant neutrophils, normal neutrophils from CML-like mice form NETs. (Scale bar: 20 μm.)

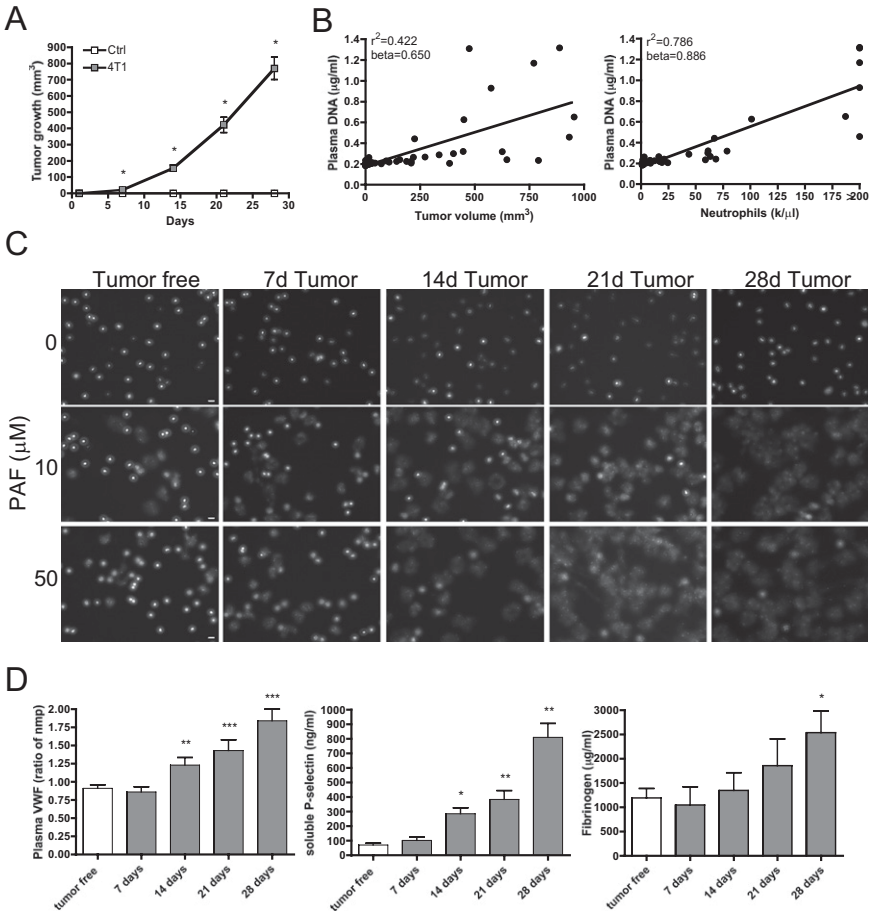

Fig. S3. The increase in plasma DNA in the 4T1 mammary carcinoma model is associated with NET formation and thrombosis markers. Tumor cells were injected in the mammary fat pad of BALB/c mice. (*A*) Tumor growth was measured every 7 d. (*B*) Plasma DNA was assessed as the dependent variable in a regression analysis. For this, the adjusted r^2 and the standardized regression coefficients (β) of the independent variables were calculated. The β indicates the change of the dependent variable, expressed in SD, when the independent variable increases 1 SD and all other variables in the model remain unchanged. The increase in plasma DNA is determined more by the number of neutrophils than by tumor size. (*C*) Representative fluorescent images showing chromatin decondensation after PAF stimulation and Hoechst staining of isolated neutrophils from tumor-bearing mice at different times after tumor cell injections show increased sensitivity to NET formation. (*D*) Plasma VWF, soluble P-selectin, and fibrinogen levels were determined by ELISA. Graphs represent means ± SEM (n = 6–10; *$P < 0.05$; **$P < 0.01$; ***$P < 0.001$).

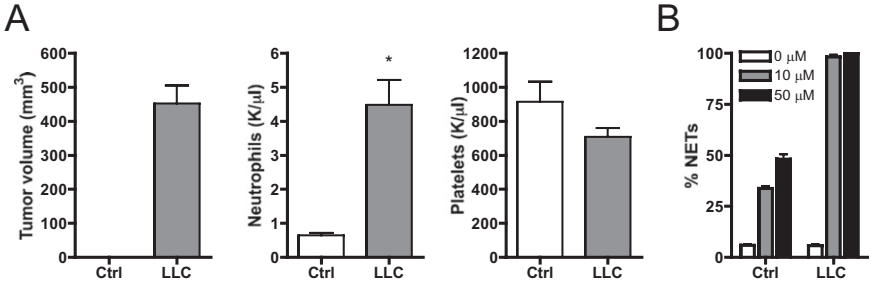

Fig. S4. Increased peripheral blood neutrophils in LLC tumor–bearing mice are more prone to NET formation. LLC tumor cells were injected in the right flank of C57BL/6 mice. (*A*) When tumor volume reached ~500 mm^3, peripheral blood neutrophil and platelet counts were determined (n = 4; *$P < 0.05$). (*B*) Quantification of NETs after PAF stimulation of isolated neutrophils from tumor-bearing mice showed a significant increase of NETosis compared with tumor-free mice. Data shown are means ± SEM.

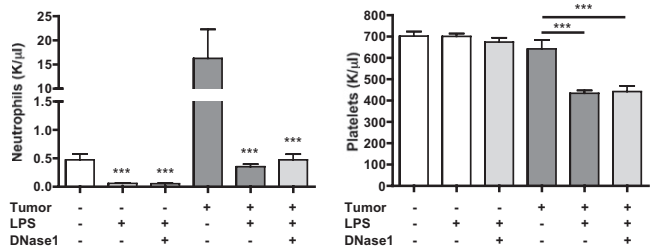

Fig. S5. DNase1 treatment of tumor-bearing mice does not prevent the reduction in neutrophil and platelet counts after LPS challenge. Fourteen-day tumor-bearing mice or tumor-free mice were injected with 50 μg of DNase1 or saline for 3 h before injection of LPS (1 mg/mL). The pretreatment with DNase1 did not prevent the reduction in the number of neutrophils and platelets observed 1 h after LPS injection (n = 5–9; ***P < 0.001). Data shown are means ± SEM.

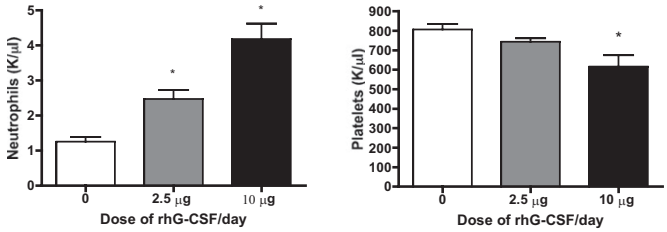

Fig. S6. rhG-CSF injection in WT mice results in an increase in peripheral neutrophils. rhG-CSF was injected s.c. daily at the indicated concentrations for 4 d. A dose-dependent increase in neutrophil counts and a reduction in platelet counts was observed (n = 4–5; *P < 0.05).

Appendix A-6

Diabetes Primes Neutrophils to Undergo NETosis which Severely Impairs Wound Healing

This chapter contains the following manuscript in preparation:

Wong SL, Martinod K, Demers M, Gallant M, Wang Y, Kahn CR, Wagner DD. *Diabetes primes neutrophils to undergo NETosis which severely impairs wound healing.*

Attributions:

Siu Ling Wong wrote the entirety of this manuscript. I performed initial in vitro NET assays and flow cytometry experiments for measurement of reactive oxygen species, and critically read the manuscript.

Diabetes primes neutrophils to undergo NETosis which severely impairs wound healing

Siu Ling Wong[1,2], Kimberly Martinod[1,3], Melanie Demers[1,2], Maureen Gallant[1], Yanming Wang[4], C. Ronald Kahn[5] & Denisa D. Wagner[1,2,6]

[1]Program in Cellular and Molecular Medicine, Boston Children's Hospital, Boston, Massachusetts, USA. [2]Department of Pediatrics, Harvard Medical School, Boston, Massachusetts, USA. [3]Immunology Graduate Program, Division of Medical Sciences, Harvard Medical School, Boston, Massachusetts, USA. [4]Center for Eukaryotic Gene Regulation, Department of Biochemistry and Molecular Biology, Pennsylvania State University, University Park, Pennsylvania, USA. [5]Section on Integrative Physiology and Metabolism, Joslin Diabetes Center, Harvard Medical School, Boston, Massachusetts, USA. [6]Division of Hematology/Oncology, Boston Children's Hospital, Boston, Massachusetts, USA.

Correspondence should be addressed to D.D.W. (Denisa.Wagner@childrens.harvard.edu).

Word count: (Introductory paragraph) 198 **(Main text)** 1874
Figures: 4
References: 40
Supplementary material: 1

Diabetes impairs wound healing which results in significant health problems. Neutrophils are the main leukocytes involved in the early phase of healing. As part of their anti-microbial defense, neutrophils form extracellular traps (NETs) by releasing nuclear chromatin lined with cytotoxic proteins. NETs, with their histones and enzymes such as neutrophil elastase and myeloperoxidase, can also induce tissue damage. Here we show that neutrophils isolated from diabetic mice and neutrophils from healthy subjects exposed to high glucose in vitro are primed to form NETs. When subjected to excisional skin wounds, wild-type (WT) mice produced large quantities of NETs at the wound site, but this did not happen in mice lacking peptidylarginine deiminase 4 (*PAD4*$^{-/-}$) which cannot decondense chromatin to form NETs. Impressively, *PAD4*$^{-/-}$ mice healed faster than WT mice, and their wound healing was not affected by diabetes. Furthermore, treatment with DNase 1, which disrupts NETs, significantly accelerated wound healing in both normoglycemic and diabetic mice. We conclude that NETs impair wound healing, especially in diabetes where neutrophils are more susceptible to NET production. Inhibiting NET formation or facilitating their clearance may be a new therapeutic strategy to improve wound healing and reduce the NET-driven chronic inflammation in diabetes.

NETs were originally recognized as a host defense mechanism in which neutrophils release their nuclear and granular contents to contain and kill pathogens[1]. Bacterial endotoxins, such as lipopolysaccharides (LPS), stimulate the release of NETs[1] that form extensive webs of DNA coated with cytotoxic histones and microbicidal proteases[1,2]. A prerequisite for NET formation (NETosis) is modification of arginine residues of histones to citrulline by PAD4, which changes the charge of the histones, leading to massive chromatin decondensation[3,4]. Recently it became

evident that NETs also form during sterile inflammation[5]. NETs are a key scaffold in pathologic thrombi and fuel cardiovascular, inflammatory and thrombotic diseases in mice and humans[5,6].

Under diabetic conditions, neutrophils produce more superoxide[7,8] and cytokines[9]. Tumor necrosis factor-α, which primes neutrophils for NETosis[10,11], is increased in diabetic patients[12]. To test whether diabetes predisposes neutrophils to NETosis, we first investigated whether diabetic neutrophils are primed towards this process. In agreement with previous observations in humans[7,8], we found that circulating neutrophils from mice made diabetic with streptozotocin (STZ) (**Supplementary Fig. 1a-c**) produced more reactive oxygen species (ROS) upon stimulation with phorbol 12-myristate 13-acetate (PMA) compared to controls (**Fig. 1a**). Immunostaining of fresh blood cells showed that diabetic mice had ~4 fold more neutrophils positive for citrullinated histone H3 (H3Cit), a biomarker of NETosis, than normoglycemic mice (**Fig. 1b**). About 4.5 fold more isolated neutrophils from diabetic mice were $H3Cit^{high}$ (**Fig. 1c**) and ~2% produced NETs after incubation in vitro without stimulation, while <0.2% of NETs were seen in the normoglycemic controls (**Fig. 1d**). LPS further stimulated more neutrophils from diabetic mice to hypercitrullinate histones (**Fig 1c,e**) and form NETs (**Fig. 1d,e**) compared to vehicle-treated normoglycemic mice. Thus, diabetes has inflammatory or metabolic components that predispose neutrophils to NETosis. Neutrophil priming in diabetes is due to the increased PAD4 activity as indicated by the elevated H3Cit levels[4] (**Fig. 1b**). This occurred without an increase in PAD4 mRNA levels (**Supplementary Fig. 2**). Increased neutrophil ROS production (**Fig. 1a**), which is known to induce NETosis[13] via a PAD4-dependent pathway[14], may contribute to the increased susceptibility to NETosis in diabetes. Plasma DNA levels of STZ-treated mice were not different from vehicle-treated controls (data not shown), indicating that the primed neutrophils in diabetes are not spontaneously producing NETs in vivo.

To examine whether high glucose levels in diabetic mice (**Supplementary Fig. 1b**) prime neutrophils, we isolated neutrophils from normoglycemic mice and pre-incubated them in media with normal or high glucose concentrations prior to LPS stimulation. LPS stimulated more of the high glucose-exposed neutrophils to hypercitrullinate histone H3 (**Fig. 1f**) and produce NETs (**Fig. 1g**). Thus, the increased susceptibility of diabetic neutrophils to NETosis is at least partly due to elevated blood glucose. Importantly, similar observations were obtained in neutrophils isolated from healthy subjects and exposed to high glucose in vitro (**Fig. 1h**). Pre-incubation of human neutrophils with high glucose medium also increased NETosis following stimulation by ionomycin (**Fig. 1h**, **Supplementary Fig. 3a**) or PMA (**Fig. 1h**, **Supplementary Fig. 3b**) compared to pre-incubation with normal glucose or equal concentrations of the non-metabolizable sugar alcohol, mannitol. Our observations differ from earlier reports[15,16] which showed that high glucose or diabetes does not affect or may impair NETosis. This is likely due to the pre-activation of human neutrophils during isolation with dextran sedimentation, a method that can induce ROS production and NET formation[13,17] prior to culture, which could result in the loss of the primed neutrophil population during the preparatory process in the previous studies. Using minimally activating Histopaque/Percoll gradients for human neutrophil isolation[18], we found a clear priming effect of high glucose to NETosis.

Depletion of neutrophils in mice was previously shown to accelerate re-epithelialization of uninfected diabetic wounds[19]. Because NETs can be injurious to tissues[20], we asked whether NETs form in wounds and impact healing. We examined excisional wounds[21] from normoglycemic WT mice. H&E staining confirmed that neutrophil recruitment overlaps with the keratinocyte proliferation stage that leads to re-epithelialization (**Supplementary Fig. 4**). Therefore, neutrophils or NETs could interfere with healing. Analysis of wound proteins by

Western blotting showed a progressively increasing level of H3Cit that peaked from 3 to 7 days after wounding (**Fig. 2a**). Immunofluorescence images of 3-day wounds showed that hypercitrullinated neutrophils were present in the wound bed immediately beneath the scab (**Fig. 2b**; **Supplementary Fig. 5**). Confocal microscopy substantiated the presence of NETs in skin wounds. Externalized DNA colocalized with H3Cit in areas associated with intense staining of the neutrophil membrane marker, Ly6G (**Fig. 2c**). Of note, H3Cit and neutrophils were absent in the surface layers of unwounded skin (**Supplementary Fig. 5**). Skin expresses PAD isoforms 1-3[22] which could citrullinate extracellular proteins in the scab. To verify the cellular source of H3Cit, we subjected CD18 (β2 integrin)-deficient (*CD18*$^{-/-}$) mice, which are defective in leukocyte recruitment, to wounding. In these mice, both H3Cit and Ly6G were undetectable by Western blotting in 3-day wounds (**Fig. 2d**, left panels), a time when H3Cit was maximal in the WT wounds (**Fig. 2a**), indicating that H3Cit is of leukocyte origin. H&E staining and immunofluorescence microscopy showed that the few *CD18*$^{-/-}$ neutrophils present in these wounds had H3Cit and produced NETs (**Supplementary Fig. 6a,b**). Indeed, isolated *CD18*$^{-/-}$ neutrophils produced NETs as efficiently as WT (**Supplementary Fig. 6c**), showing that β2 integrins are not required for NETosis. Wounds from WT mice with depleted neutrophils showed markedly reduced H3Cit (**Fig. 2d**, right panels). Thus, our data indicate that neutrophils are the source of the H3Cit and extracellular chromatin present in the wounds.

To establish the role of NETs in wound healing, we compared wounds of WT to *PAD4*$^{-/-}$ mice. Unlike neutrophil recruitment-defective P-/E-selectin double mutants that have opportunistic infections[23] and impaired wound healing[21], wounds of the *PAD4*$^{-/-}$ mice did not show overt signs of infection (**Fig. 3a**) and healed faster than WT (**Fig. 3a,b**). This is likely because other neutrophil functions such as phagocytosis[14], degranulation and ROS production (our

unpublished observations) are intact in *PAD4*$^{-/-}$ neutrophils. About 80% of *PAD4*$^{-/-}$ mice had all wounds healed on day 14 compared to only 25% of WT controls (**Fig. 3c**). The beneficial effect of PAD4 deficiency on wound healing was observed very early after injury (**Fig. 3b**), indicating that NETs might impair the onset of initial healing processes such as keratinocyte proliferation/migration. In line with this hypothesis, re-epithelialization progressed 3-fold faster in *PAD4*$^{-/-}$ mice compared to WT (**Fig. 3d**). In contrast to the robust H3Cit signals in WT wounds, no H3Cit was detected in wounds from *PAD4*$^{-/-}$ mice despite normal neutrophil recruitment (**Fig. 3e**; **Supplementary Fig. 7**). Prominent extracellular DNA structures observed by H&E were absent in *PAD4*$^{-/-}$ scabs (**Fig. 3f**, upper panels), as were the H3Cit and extracellular chromatin patterns seen in WT mice by confocal microscopy (**Fig. 3f**, lower panels). Although WT and *PAD4*$^{-/-}$ neutrophils also express PAD2 and PAD3[14], our data demonstrate that PAD4, the only nuclear PAD, is essential for histone H3 citrullination and NETosis in skin wounds. Coudane et al.[24] reported that PAD4 is the main PAD isoform detected in scabs of wounds from WT mice, and that PAD2 is unnecessary for citrullination of scab proteins as observed in PAD2-deficient mice, further strengthening the unique deimination role of PAD4 in the wounds.

We next examined whether NETs interfere with diabetic wound healing. Diabetes was induced in WT and *PAD4*$^{-/-}$ mice and 8 weeks later these mice were subjected to wounding. Changes in body weight, fed blood glucose and induction rate were similar between the two genotypes (**Supplementary Fig. 1d-f**). As expected, diabetic WT mice healed more slowly than normoglycemic controls (**Fig. 4a**). All normoglycemic WT mice healed by day 16, while ~20% of diabetic mice still had open wounds on day 19 (**Fig. 4d**). Diabetic *PAD4*$^{-/-}$ mice healed >35% faster than diabetic WT mice on day 7 (**Fig. 4b**) and had all wounds closed by day 15 (**Fig. 4e**). Notably, diabetes did not impair wound healing in *PAD4*$^{-/-}$ mice (**Fig. 4c,f**), which underscores

NETs as the major determinant delaying healing in the diabetic mice. Antibiotics, provided to mimic the medical regimen of diabetic patients with chronic wounds, did not abolish the beneficial effect of PAD4 deficiency (**Supplementary Fig. 8**).

Enhanced wound healing in *PAD4*$^{-/-}$ mice suggests that NETs may be a redundant host defense mechanism that compromises wound repair. NETs and histones can directly induce epithelial and endothelial cell death in vitro[20]. Histones disrupt cell membranes and induce calcium influx, resulting in cytotoxicity in vitro and in vivo[25]. High neutrophil elastase concentration, a component of NETs[1,2], can cause degradation of the wound matrix and delay healing[26]. Such a cytotoxic environment produced by NETs may explain the slower keratinocyte repopulation in the wound beds of WT. Because PAD4 is not expressed in the skin[22], its negative effect on wound healing is most likely due to infiltrating neutrophils. In fact, using NETs to defend against microbes may not be very effective during wound healing. *Staphylococcus* species are very abundant in diabetic wounds[27], and *Staphylococcus aureu*s expresses nucleases to degrade NETs and thus escape trapping[28]. Staphylococcal nuclease and adenosine synthase A can degrade and convert NETs into 2'-deoxyadenosine which promotes macrophage apoptosis[29]. Macrophages are the source of vascular endothelial growth factor and transforming growth factor-β1, important cytokines for wound healing[30]. Thus, the non-selective cytotoxicity of NETs and/or their degradation products by bacteria can profoundly delay wound healing.

Farrera and Fadeel reported that pre-digestion of NETs with DNase 1 accelerated their clearance by macrophages in vitro [31]. Facilitated clearance of NETs in wounds may reduce their toxicity and diminish wound matrix degradation that is essential for the directional migration of keratinocytes[32]. We thus tested whether DNase 1 could accelerate wound healing. Three days

post wounding, wound areas in normoglycemic mice treated with DNase 1 were smaller than in those treated with vehicle (**Fig. 4g**, left). Re-epithelialization was also enhanced by ~54% in the DNase 1-treated group (**Fig. 4g**, right), while neutrophil recruitment was not affected (data not shown). Similar beneficial effects of DNase 1 were observed in diabetic WT mice maintained on antibiotics. DNase 1 promoted wound area reduction by >20% (**Fig. 4h**, left) and enhanced re-epithelialization by >75% (**Fig. 4h**, right), an extent similar to that of DNase 1-treated normoglycemic mice (**Fig. 4h**). These results demonstrate the beneficial effect of extracellular chromatin cleavage in wound repair and tissue regeneration. Our current findings also corroborate positive results from pilot clinical trials with activated protein C (APC), which cleaves and reduces the cytotoxicity of histones[33] and facilitates healing of chronic wounds[34] and diabetic ulcers[35]. Topical treatment with an ointment containing fibrinolysin and DNase (Elase) is used clinically for wound debridement. In addition to removing necrotic tissue, our findings suggest the DNase component may also cleave NETs to enhance wound recovery.

In summary, our data demonstrate that diabetes activates neutrophils to overproduce NETs and identify NETs as a key factor delaying wound healing. PAD4 inhibition and facilitated clearance of NETs by DNase could be novel therapeutic approaches to wound resolution, not only to diabetic wounds, but also wounds resulting from aseptic procedures such as surgeries of normoglycemic patients. Because PAD4 and NET formation contribute to inflammatory and thrombotic diseases[6] that are prominent in diabetics[36,37], such therapy could have additional benefits. The increased NETosis in diabetes suggests that NETs may fuel these disorders and inhibiting NETosis or cleavage of NETs may lessen them.

METHODS

Methods and associated references are available in the online version of the paper.

Note: Supplementary information is available in the online version of the paper.

ACKNOWLEDGMENTS

We thank Heather Ferris, Joslin Diabetes Center, for advice on diabetes protocols, Jessica E. Cabral and Lesley Cowan, Boston Children's Hospital, for valuable technical and manuscript preparation assistance, respectively. This study was supported by the American Diabetes Association (Innovation Award 7-13-IN-44, D.D.W.), National Heart, Lung, and Blood Institute of the National Institutes of Health (R01HL102101, D.D.W.), National Cancer Institute (R01CA136856, Y.W.), National Institute of Diabetes and Digestive and Kidney Diseases (R01DK031036, C.R.K) and a GlaxoSmithKline/Immune Disease Institute Alliance Fellowship (S.L.W.).

AUTHOR CONTRIBUTIONS

S.L.W. designed the study, performed the majority of the experiments, analyzed the data and wrote the manuscript; K.M. and M.D. performed experiments and analyzed data; M.G. provided expert technical assistance; Y.W. and C.R.K. provided helpful suggestions on experimental design and critical reading of the manuscript; D.D.W. designed the study, supervised the project and co-wrote the manuscript.

COMPETING FINANCIAL INTERESTS

The authors declare no competing financial interests.

REFERENCES

1. Brinkmann, V.*, et al.* Neutrophil extracellular traps kill bacteria. *Science* **303**, 1532-1535 (2004).
2. Urban, C.F.*, et al.* Neutrophil extracellular traps contain calprotectin, a cytosolic protein complex involved in host defense against Candida albicans. *PLoS Pathog* **5**, e1000639 (2009).
3. Wang, Y.*, et al.* Histone hypercitrullination mediates chromatin decondensation and neutrophil extracellular trap formation. *J Cell Biol* **184**, 205-213 (2009).
4. Wang, Y.*, et al.* Human PAD4 regulates histone arginine methylation levels via demethylimination. *Science* **306**, 279-283 (2004).
5. Yipp, B.G. & Kubes, P. NETosis: how vital is it? *Blood* **122**, 2784-2794 (2013).
6. Martinod, K. & Wagner, D.D. Thrombosis: tangled up in NETs. *Blood* **123**, 2768-2776 (2014).
7. Ayilavarapu, S.*, et al.* Diabetes-induced oxidative stress is mediated by Ca2+-independent phospholipase A2 in neutrophils. *J Immunol* **184**, 1507-1515 (2010).
8. Karima, M.*, et al.* Enhanced superoxide release and elevated protein kinase C activity in neutrophils from diabetic patients: association with periodontitis. *J Leukoc Biol* **78**, 862-870 (2005).
9. Hanses, F., Park, S., Rich, J. & Lee, J.C. Reduced neutrophil apoptosis in diabetic mice during staphylococcal infection leads to prolonged TNF-α production and reduced neutrophil clearance. *PLoS One* **6**, e23633 (2011).
10. Khandpur, R.*, et al.* NETs are a source of citrullinated autoantigens and stimulate inflammatory responses in rheumatoid arthritis. *Sci Transl Med* **5**, 178ra140 (2013).
11. Thomas, G.M.*, et al.* Extracellular DNA traps are associated with the pathogenesis of TRALI in humans and mice. *Blood* **119**, 6335-6343 (2012).
12. Alexandraki, K.I.*, et al.* Cytokine secretion in long-standing diabetes mellitus type 1 and 2: associations with low-grade systemic inflammation. *J Clin Immunol* **28**, 314-321 (2008).
13. Fuchs, T.A.*, et al.* Novel cell death program leads to neutrophil extracellular traps. *J Cell Biol* **176**, 231-241 (2007).
14. Li, P.*, et al.* PAD4 is essential for antibacterial innate immunity mediated by neutrophil extracellular traps. *J Exp Med* **207**, 1853-1862 (2010).
15. Joshi, M.B.*, et al.* High glucose modulates IL-6 mediated immune homeostasis through impeding neutrophil extracellular trap formation. *FEBS Lett* **587**, 2241-2246 (2013).

16. Riyapa, D.*, et al.* Neutrophil extracellular traps exhibit antibacterial activity against burkholderia pseudomallei and are influenced by bacterial and host factors. *Infect Immun* **80**, 3921-3929 (2012).
17. Rebecchi, I.M., Ferreira Novo, N., Julian, Y. & Campa, A. Oxidative metabolism and release of myeloperoxidase from polymorphonuclear leukocytes obtained from blood sedimentation in a Ficoll-Hypaque gradient. *Cell Biochem Funct* **18**, 127-132 (2000).
18. Brinkmann, V., Laube, B., Abu Abed, U., Goosmann, C. & Zychlinsky, A. Neutrophil extracellular traps: how to generate and visualize them. *J Vis Exp* (2010).
19. Dovi, J.V., He, L.K. & DiPietro, L.A. Accelerated wound closure in neutrophil-depleted mice. *J Leukoc Biol* **73**, 448-455 (2003).
20. Saffarzadeh, M.*, et al.* Neutrophil extracellular traps directly induce epithelial and endothelial cell death: a predominant role of histones. *PLoS One* **7**, e32366 (2012).
21. Subramaniam, M.*, et al.* Role of endothelial selectins in wound repair. *Am J Pathol* **150**, 1701-1709 (1997).
22. Nachat, R.*, et al.* Peptidylarginine deiminase isoforms 1-3 are expressed in the epidermis and involved in the deimination of K1 and filaggrin. *J Invest Dermatol* **124**, 384-393 (2005).
23. Frenette, P.S., Mayadas, T.N., Rayburn, H., Hynes, R.O. & Wagner, D.D. Susceptibility to infection and altered hematopoiesis in mice deficient in both P- and E-selectins. *Cell* **84**, 563-574 (1996).
24. Coudane, F.*, et al.* Deimination and expression of peptidylarginine deiminases during cutaneous wound healing in mice. *Eur J Dermatol* **21**, 376-384 (2011).
25. Abrams, S.T.*, et al.* Circulating histones are mediators of trauma-associated lung injury. *Am J Respir Crit Care Med* **187**, 160-169 (2013).
26. Herrick, S.*, et al.* Up-regulation of elastase in acute wounds of healthy aged humans and chronic venous leg ulcers are associated with matrix degradation. *Lab Invest* **77**, 281-288 (1997).
27. Grice, E.A.*, et al.* Longitudinal shift in diabetic wound microbiota correlates with prolonged skin defense response. *Proc Natl Acad Sci U S A* **107**, 14799-14804 (2010).
28. Berends, E.T.*, et al.* Nuclease expression by Staphylococcus aureus facilitates escape from neutrophil extracellular traps. *J Innate Immun* **2**, 576-586 (2010).
29. Thammavongsa, V., Missiakas, D.M. & Schneewind, O. Staphylococcus aureus degrades neutrophil extracellular traps to promote immune cell death. *Science* **342**, 863-866 (2013).

30. Ishida, Y., Gao, J.L. & Murphy, P.M. Chemokine receptor CX3CR1 mediates skin wound healing by promoting macrophage and fibroblast accumulation and function. *J Immunol* **180**, 569-579 (2008).
31. Farrera, C. & Fadeel, B. Macrophage clearance of neutrophil extracellular traps is a silent process. *J Immunol* **191**, 2647-2656 (2013).
32. Pilcher, B.K.*, et al.* The activity of collagenase-1 is required for keratinocyte migration on a type I collagen matrix. *J Cell Biol* **137**, 1445-1457 (1997).
33. Xu, J.*, et al.* Extracellular histones are major mediators of death in sepsis. *Nat Med* **15**, 1318-1321 (2009).
34. Whitmont, K.*, et al.* Treatment of chronic leg ulcers with topical activated protein C. *Arch Dermatol* **144**, 1479-1483 (2008).
35. Whitmont, K.*, et al.* Treatment of chronic diabetic lower leg ulcers with activated protein C: a randomised placebo-controlled, double-blind pilot clinical trial. *Int Wound J* (2013).
36. Laakso, M. & Kuusisto, J. Insulin resistance and hyperglycaemia in cardiovascular disease development. *Nat Rev Endocrinol* **10**, 293-302 (2014).
37. Morel, O., Jesel, L., Abbas, M. & Morel, N. Prothrombotic changes in diabetes mellitus. *Semin Thromb Hemost* **39**, 477-488 (2013).

Figure legends

Figure 1. Diabetes or high glucose concentration in vitro primes neutrophils to undergo NETosis. (**a**) Whole blood from vehicle-treated or STZ-induced diabetic mice was either incubated with 100 nM PMA or left unstimulated for 20 min. Flow cytometry using the ROS-sensitive dye dihydrorhodamine 123 revealed a larger increase in respiratory burst in neutrophils from diabetic mice. Ly6G+ neutrophils were gated during analysis. ***P<0.001, $^{\#\#}$P<0.01; n = 10 for Vehicle, n = 8 for STZ. (**b**) Blood cytospin was performed and cells were stained for H3Cit and Ly6G. More circulating neutrophils with elevated basal H3Cit level were detected in STZ-treated mice. ***P<0.001. (**c**-**e**) Neutrophils were isolated and stimulated with LPS from *Klebsiella pneumoniae* at indicated concentrations for 2.5 h. More neutrophils from STZ-induced diabetic mice were H3Cit^{high} (**c**) and formed NETs (**d**). US, unstimulated. *P<0.05, **P<0.01, ***P<0.001; n = 12 for Vehicle, n = 10 for STZ. (**e**) Representative images of isolated neutrophils from in vitro NETosis experiments. Neutrophils were exposed to LPS (25 μg/mL) for 2.5 h. Green, H3Cit; Blue, DNA stained with Hoechst 33342. Yellow arrows indicate NETs. Scale, 50 μm. (**f**,**g**) Neutrophils were isolated from normoglycemic mice and pre-incubated for 1 h in media with normal (5.5 mM) or high (22 mM) glucose concentration. Twenty-two mM corresponds to 396 mg/dL, which is similar to the fed blood glucose level in STZ-induced mice 8 weeks post-induction (376.3 ± 26.9 mg/dL). Mannitol (16.5 mM added into medium with 5.5 mM glucose) was employed as an osmotic control. LPS (10 μg/mL, in respective medium) was added and neutrophils were further incubated for 2.5 h. More neutrophils in high glucose medium were H3Cit^{high} (**f**) and produced NETs (**g**). *P<0.05, **P<0.01; n = 10 per medium condition. (**h**) High glucose experiments, similar to those in (**g**), were performed on isolated neutrophils from healthy subjects using ionomycin (4 μM) or PMA (100 nM) as stimuli.

Consistent for every subject, more high glucose (HG)-treated neutrophils produced NETs compared to those in normal glucose (NG) or mannitol (M). Each color and symbol represents one individual. *P<0.05, **P<0.01.

Figure 2. Neutrophil H3Cit and extracellular chromatin are observed in the wounds of WT mice, indicating the formation of NETs. (**a**) Western blots showing the time course of H3Cit appearance after skin injury. Wounds were generated with biopsy punches at the dorsal skin of the mice. Scab and the surrounding 0.5 mm skin were collected at the time indicated. H3Cit was detectable starting day 1 post wounding and peaked from day 3 to 7. H3Cit was absent in the control unwounded skin (Ctrl). **P<0.01 versus Ctrl, n = 3-5. (**b**) Immunofluorescence images of a 3-day wound bed immediately beneath scab. Cells were mostly positive for Ly6G and H3Cit. (**c**) Representative images of a 3-day wound using confocal microscopy. Area enclosed by the yellow box is magnified and shown on the right. H3Cit (green) co-localized with extracellular DNA (blue) in the Ly6G (red)-positive area in the scab. (**d**) Western blots of 3-day wounds collected from mice with defective leukocyte recruitment (*CD18*$^{-/-}$, left) and mice depleted of neutrophils using an anti-Ly6G antibody (right, representative of n = 7). H3Cit was markedly reduced in these wounds.

Figure 3. PAD4 deficiency facilitates wound repair in normoglycemic mice. (**a**) Photographs of wounds of WT and *PAD4*$^{-/-}$ mice. Wounds of *PAD4*$^{-/-}$ healed faster and both healed without apparent signs of infection. Scale, 5 mm. (**b**) Changes in wound area compared to day 0. Wound area reduced faster in *PAD4*$^{-/-}$ mice starting day 1 post wounding. *P<0.05, **P<0.01, ***P<0.001 versus WT; n = 9-16. (**c**) Significantly more *PAD4*$^{-/-}$ mice had wounds completely closed by day 14. **P<0.01. (**d**) Hematoxylin and eosin (H&E) staining of 3-day wounds from

WT and *PAD4*$^{-/-}$ mice. Re-epithelialization was determined by the distance that keratinocytes migrated into the wound area from the shoulder of the wounds (indicated by blue dotted lines and arrows). Re-epithelialization occurred faster in *PAD4*$^{-/-}$ mice. ***P<0.001, n = 6-9. (**e**) Representative Western blots of wounds from WT (+/+) and *PAD4*$^{-/-}$ (-/-) mice. H3Cit was absent in the wounds from *PAD4*$^{-/-}$ mice. Ly6G levels in wounds were similar in both genotypes. (**f**) Images of H&E staining and confocal microscopy of 3-day wounds from WT and *PAD4*$^{-/-}$ mice. H&E (upper panels) revealed the presence of extracellular DNA (blue streaks, indicated by yellow arrows) in the scab of WT mice, while neutrophils appeared intact (ring-shaped, indicated by yellow arrowheads) in *PAD4*$^{-/-}$ scabs. Confocal immunofluorescence images (lower panels) showed intact neutrophil morphology and an absence of H3Cit in the scabs of *PAD4*$^{-/-}$ mice compared to the NETs in the scabs of WT mice.

Figure 4. PAD4 deficiency or DNase 1 treatment enhances wound healing in diabetic mice. WT and *PAD4*$^{-/-}$ mice were treated with vehicle or STZ. Wounding was performed 8 weeks after diabetic induction. (**a-f, h**) All mice were provided with antibiotics (2.5% Sulfatrim) in the drinking water immediately after wounding. (**a-f**) Data from all groups were obtained simultaneously in multiple experiments but split into three graphs (**a**-**c** and **d**-**f**) to facilitate comparison. n = 6-9; *P<0.05, **P<0.01, ***P<0.001 between groups on respective post-wounding day (**a**-**c**) or between curves (**d**-**f**). (**a**) Wound healing was impaired in STZ-induced diabetic WT mice compared to normoglycemic mice (vehicle). (**b**) *PAD4*$^{-/-}$ mice had much faster wound repair than WT under diabetic conditions. (**c**) Diabetes did not impair wound repair in *PAD4*$^{-/-}$ mice. (**d**) STZ-induced diabetic WT mice had delayed wound closure compared to normoglycemic mice (vehicle). (**e**) STZ-treated *PAD4*$^{-/-}$ mice reached total wound closure earlier than STZ-treated WT mice. (**f**) Wound closure was not significantly different (NS) between normoglycemic

(vehicle) and diabetic (STZ) *PAD4*$^{-/-}$ mice. (**g**) Normoglycemic or (**h**) diabetic WT mice were treated with DNase 1 (dornase alfa) immediately before wounding and subsequently until wound harvest 3 days post wounding. DNase 1 treatment facilitated wound area reduction (left) and re-epithelialization (right) in both (**g**) normoglycemic and (**h**) diabetic WT mice. *P<0.05 ***P<0.001; n = 6-10.

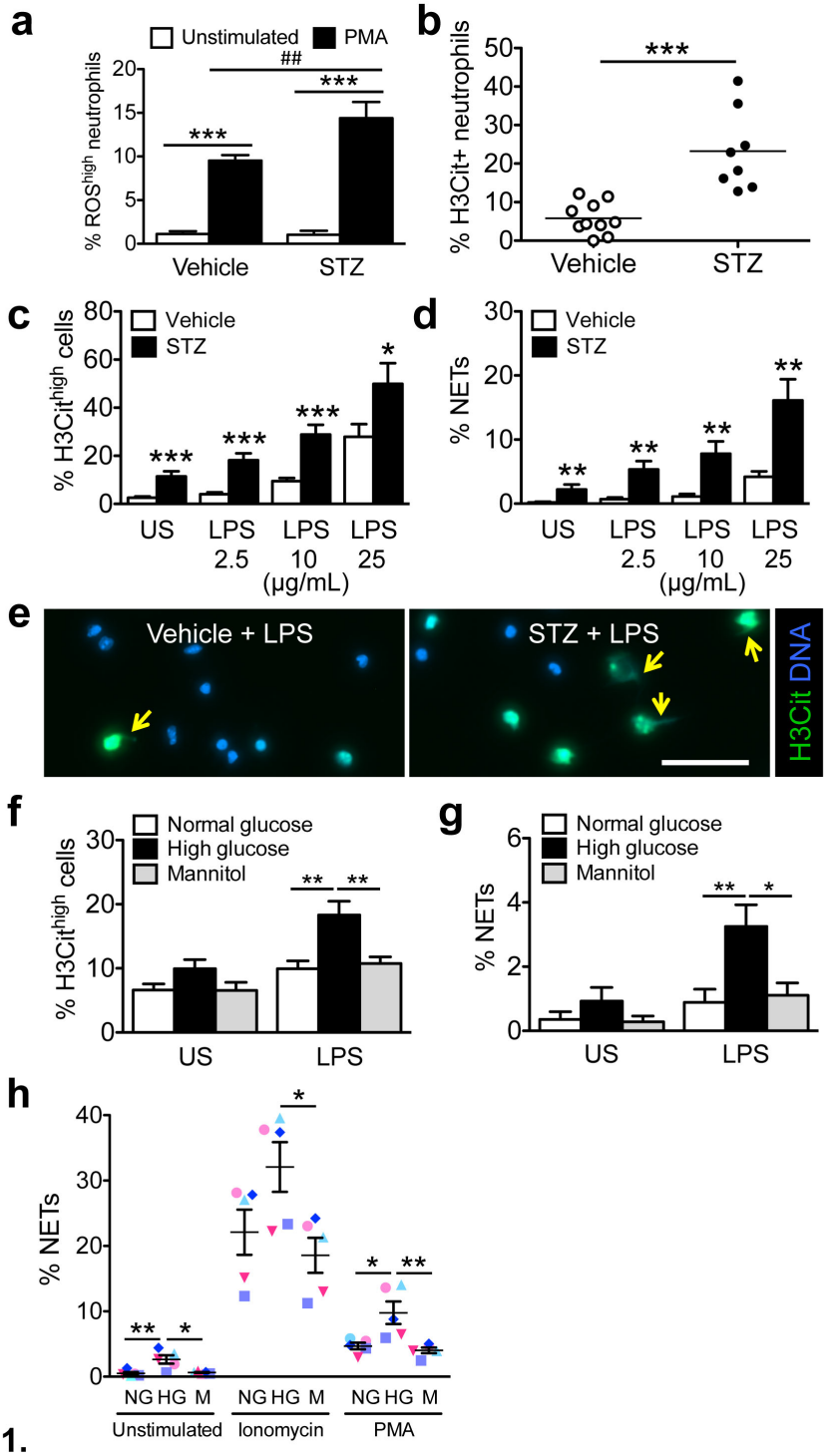
a
Unstimulated
PMA
% ROS^high neutrophils
Vehicle
STZ
b
% H3Cit+ neutrophils
Vehicle
STZ
c
Vehicle
STZ
% H3Cit^high cells
US
LPS 2.5
LPS 10
LPS 25
(μg/mL)
d
Vehicle
STZ
% NETs
US
LPS 2.5
LPS 10
LPS 25
(μg/mL)
e
Vehicle + LPS
STZ + LPS
H3Cit DNA
f
Normal glucose
High glucose
Mannitol
% H3Cit^high cells
US
LPS
g
Normal glucose
High glucose
Mannitol
% NETs
US
LPS
h
% NETs
NG HG M
Unstimulated
Ionomycin
PMA

Figure 1.

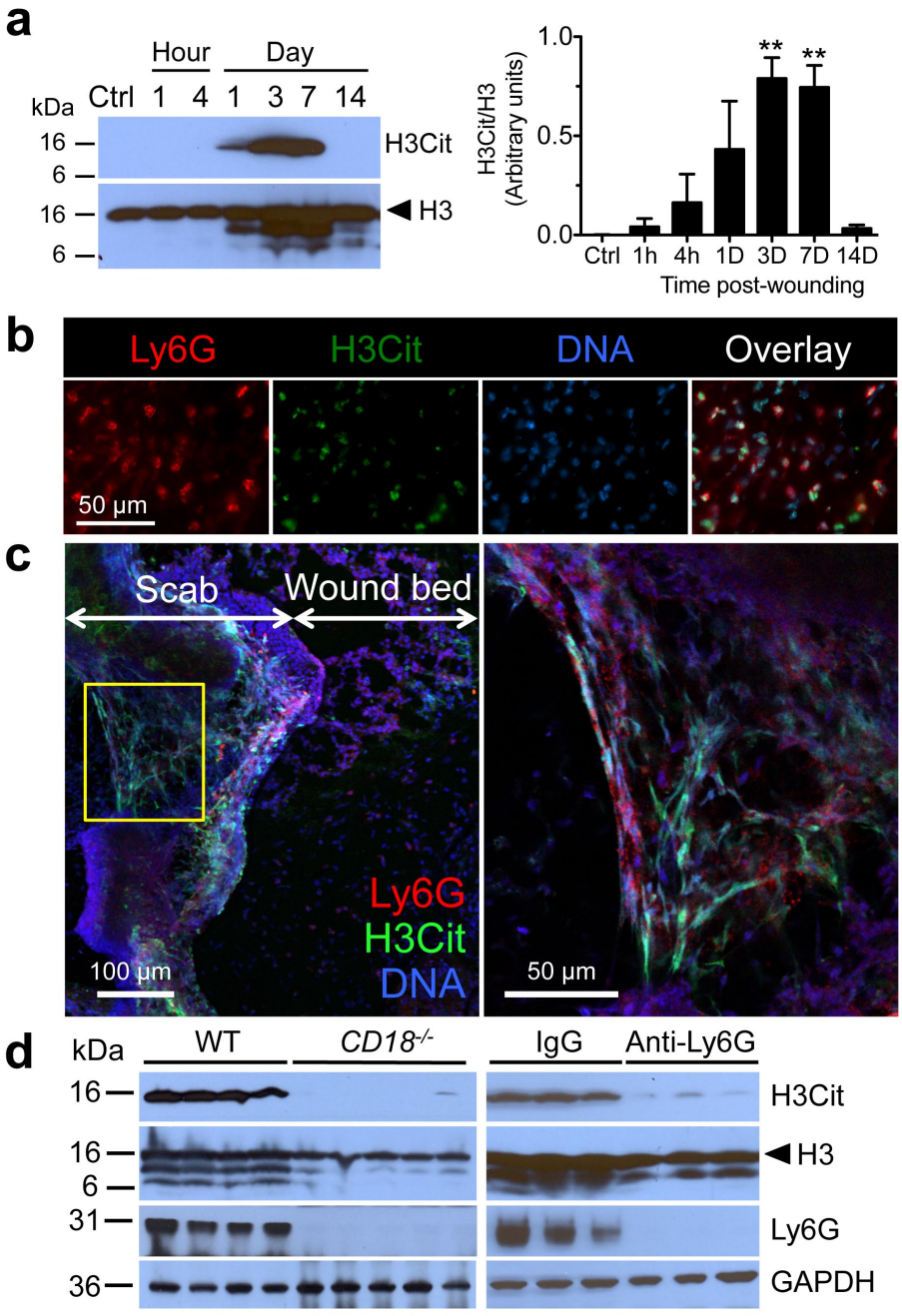
a
Hour
Day
kDa
Ctrl 1 4 1 3 7 14
16
6
H3Cit
16
6
H3
H3Cit/H3 (Arbitrary units)
1.0
0.5
0.0
**
**
Ctrl 1h 4h 1D 3D 7D 14D
Time post-wounding
b
Ly6G
H3Cit
DNA
Overlay
50 μm
c
Scab
Wound bed
Ly6G
H3Cit
DNA
100 μm
50 μm
d
kDa
WT
CD18-/-
IgG
Anti-Ly6G
16
H3Cit
16
6
H3
31
Ly6G
36
GAPDH

Figure 2.

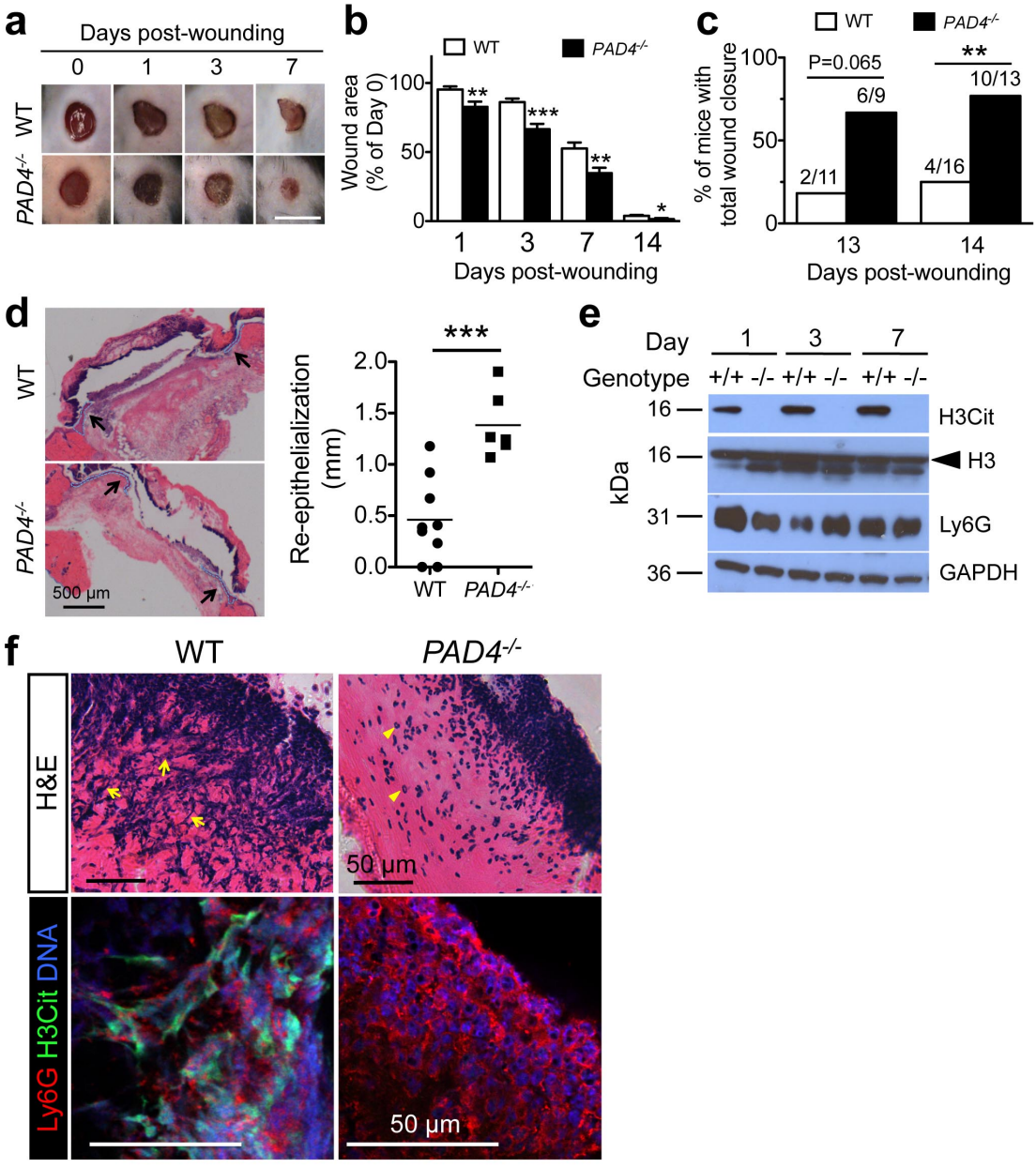
a
Days post-wounding
0
1
3
7
WT
PAD4-/-
b
WT
PAD4-/-
Wound area (% of Day 0)
100
50
0
**
***
**
*
1
3
7
14
Days post-wounding
c
WT
PAD4-/-
% of mice with total wound closure
100
50
0
P=0.065
**
6/9
10/13
2/11
4/16
13
14
Days post-wounding
d
WT
PAD4-/-
500 µm
***
Re-epithelialization (mm)
2.0
1.5
1.0
0.5
0.0
WT
PAD4-/-
e
Day
1
3
7
Genotype
+/+ -/- +/+ -/- +/+ -/-
kDa
16
H3Cit
16
H3
31
Ly6G
36
GAPDH
f
WT
PAD4-/-
H&E
50 µm
Ly6G H3Cit DNA
50 µm

Figure 3.

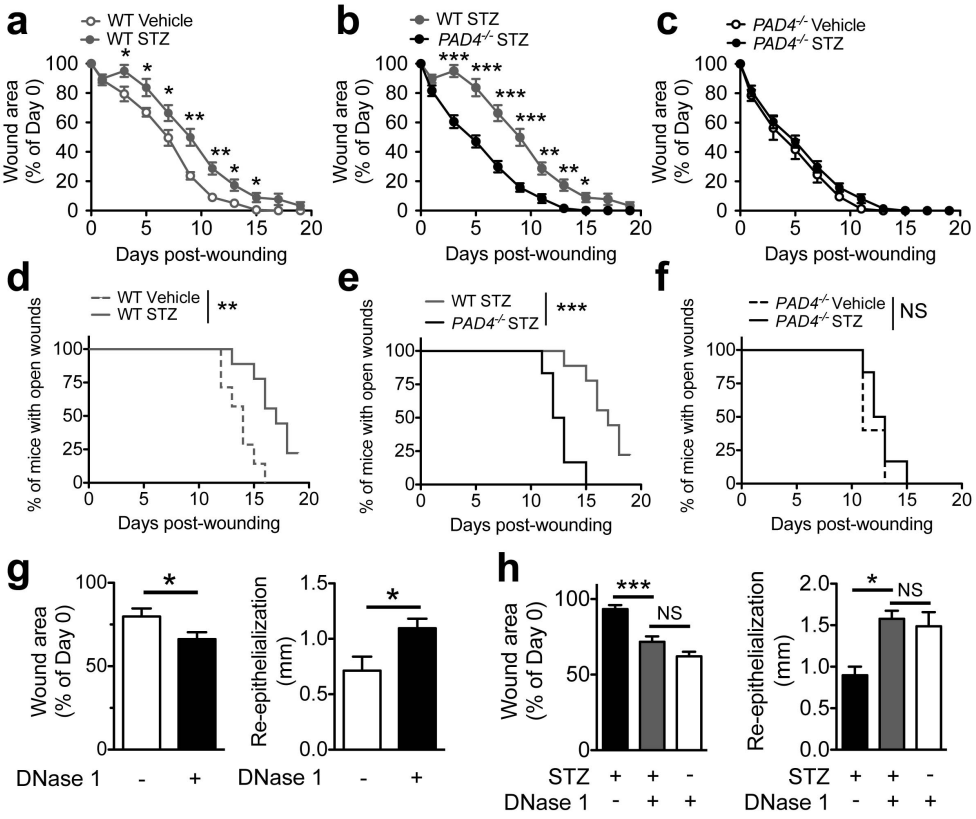
a
WT Vehicle
WT STZ
Wound area (% of Day 0)
Days post-wounding
b
WT STZ
PAD4-/- STZ
Wound area (% of Day 0)
Days post-wounding
c
PAD4-/- Vehicle
PAD4-/- STZ
Wound area (% of Day 0)
Days post-wounding
d
WT Vehicle
WT STZ
**
% of mice with open wounds
Days post-wounding
e
WT STZ
PAD4-/- STZ
***
% of mice with open wounds
Days post-wounding
f
PAD4-/- Vehicle
PAD4-/- STZ
NS
% of mice with open wounds
Days post-wounding
g
Wound area (% of Day 0)
DNase 1 - +
Re-epithelialization (mm)
DNase 1 - +
h
Wound area (% of Day 0)
STZ + + -
DNase 1 - + +
Re-epithelialization (mm)
STZ + + -
DNase 1 - + +
NS

Figure 4.

Appendix A-7

Neutrophil elastase-deficient mice form neutrophil extracellular traps in experimental models of deep vein thrombosis and wound healing

This chapter contains one manuscript in preparation:

Martinod K, Wong SL, Gallant M, Wagner DD. *Neutrophil elastase-deficient mice form neutrophil extracellular traps in experimental models of deep vein thrombosis and wound healing*. In preparation for submission to the Journal of Leukocyte Biology.

Appendix A-7: Overview and Attributions

Overview

Our results in Chapter 2 and Appendix A-3[1] revealed that NETs comprise a crucial part of the thrombus scaffold. We were interested in seeing if neutrophil elastase (NE) was also contributing to NET formation in thrombosis. NE has been shown to degrade histones and thus aid in chromatin decondensation during NETosis in human neutrophils[2]. However, mouse studies quantitatively evaluating NET formation remained to be performed and we were frequently asked to perform our in vivo NET models in $NE^{-/-}$ mice in parallel to $PAD4^{-/-}$ mice to have two mouse models where NETs are lacking. However, we found that NE-deficiency only slightly inhibited NET production in mouse neutrophils. This study is important as it shows that while a complete lack of NETs in the $PAD4^{-/-}$ mice resulted in fewer thrombi (Chapter 2) and improved wound healing (Appendix A-6), a slight reduction in NET formation in the NE-deficient mice had no effect on thrombus generation or rate of wound closure which is affected by NETs. This highlights that NET-targeted therapies would need to be highly effective in order to have a substantial impact in vivo.

Attributions

For this manuscript, I performed all in vitro NET assays and deep vein thrombosis surgeries and analyses. Siu Ling Wong performed all wound healing studies and analyses. We share first authorship and I wrote a majority of the paper. Maureen Gallant prepared cryosections of thrombi for immunostaining.

Denisa Wagner supervised the study, designed experiments, and revised the paper.

Neutrophil elastase-deficient mice form neutrophil extracellular traps in experimental models of deep vein thrombosis and wound healing

Kimberly Martinod[1,2,a], Siu Ling Wong[2,3,a], Maureen Gallant[2], Denisa D. Wagner[2,3,4*]

[1]Immunology Graduate Program, Division of Medical Sciences, Harvard Medical School, Boston, Massachusetts, USA

[2]Program in Cellular and Molecular Medicine, Boston Children's Hospital, Boston, Massachusetts, USA

[3]Department of Pediatrics, Harvard Medical School, Boston, Massachusetts, USA

[4]Division of Hematology/Oncology, Boston Children's Hospital, Boston, Massachusetts, USA

[a]These authors contributed equally to this work

*Correspondence: Denisa D. Wagner, Boston Children's Hospital, 3 Blackfan Circle, Third Floor, Boston, MA, 02115, USA. Ph. 617-713-8300, Fax 617-713-8333, denisa.wagner@childrens.harvard.edu

Abstract

Neutrophil elastase was proposed to be involved in chromatin decondensation via its ability to translocate into the nucleus and degrade histones. It has been hypothesized that neutrophil elastase-deficient ($NE^{-/-}$) mice are unable to decondense chromatin or release NETs in response to a microbial stimulus. We wished to establish if neutrophils from $NE^{-/-}$ mice would not produce NETs during sterile inflammation and to examine whether this would impact venous thrombosis and/or wound healing, two models in which we see abundant NET release in the absence of infection, with serious pathological consequences. What we found, however, is that NE-deficiency only resulted in a slight reduction in NET formation in vitro and that this had no effect on NET formation in vivo or outcome in models of thrombosis and wound repair. Therefore, $NE^{-/-}$ mice do not phenocopy $PAD4^{-/-}$ mice, which remain the best model of studying lack of NET release in vivo. Experiments using NE inhibitors with the goal of inhibiting NET formation in vivo are therefore not recommended.

Introduction

The serine protease function neutrophil elastase (NE) plays a crucial role in host defense[3] and is present on neutrophil extracellular traps that are released from activated neutrophils[4,5]. In addition to being present on NETs, NE has also been implicated in chromatin decondensation in the process of forming NETs by cleaving histones. Indeed, NE translocates from azurophilic granules to the nucleus[2], which occurs before translocation of other granule contents such as

myeloperoxidase (MPO). This occurs by a recently described mechanism independent of granule membrane fusion[2] but dependent on reactive oxygen species (ROS) and MPO[6]. In the Papayannopoulos et al. study, an elegant series of in vitro experiments was performed using isolated primary human neutrophils to show that NE, and not other serine proteases in the neutrophil such Cathepsin G or proteinase 3, aids in chromatin decondensation during NETosis[2]. NE inhibitors greatly diminished NE entry into the nucleus, chromatin decondensation and NET formation in response to PMA. The effect of NE was also tested in mice, where intranasal instillation of *Klebsiella pneumoniae* in WT mice led to extensive fiber formation in the alveolar space, whereas $NE^{-/-}$ mouse lungs remained free of such NET-like fibers. While nuclear decondensation was shown to be decreased in the knockout using a cell-free assay in which the nuclei from thioglycollate-elicited peritoneal neutrophils are extruded, a quantitative in vitro NET assay remains to be performed using peripheral blood neutrophils which have not been activated in an inflammatory model. In addition, the role of NE in non-infectious disease models strongly affected by NET production was not studied.

Results/Discussion

Neutrophils from $NE^{-/-}$ mice present only a small reduction in NET production

We examined neutrophil elastase-deficient neutrophils for their ability to form NETs in response to several non-microbial stimuli (Figure 1). We isolated WT and NE/- neutrophils from mouse peripheral blood and stimulated them in parallel

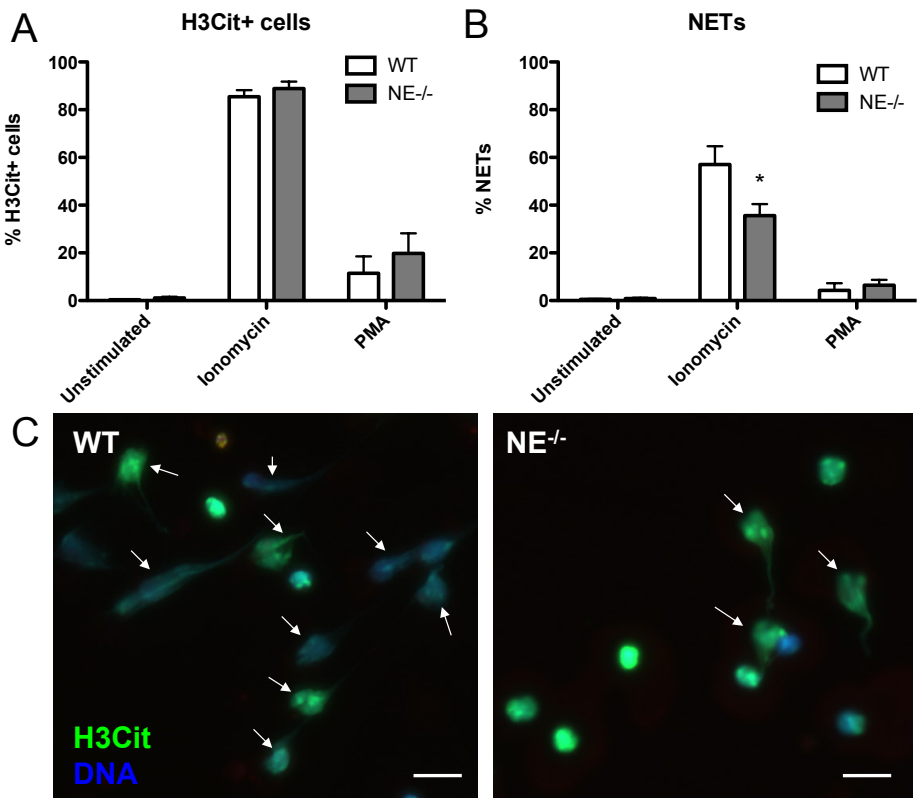

Figure 1. Neutrophil elastase-deficient neutrophils form fewer NETs in response to calcium ionophore but citrullination is unaffected. A. Neutrophils isolated from WT and $NE^{-/-}$ mice became hypercitrullinated at histone H3 to a similar degree in response to stimulation with PMA or ionomycin for 3.5 h. n=5-10. B. NET formation was similar between WT and $NE^{-/-}$ neutrophils in response to PMA, but was reduced by about 40% in $NE^{-/-}$ neutrophils in response to ionomycin. n=5-10. C. Representative micrographs of ionomycin-stimulated cells showing H3Cit-positive NETs forming both in WT and $NE^{-/-}$ neutrophils. White arrows indicate NETs. H3Cit, green; DNA, blue. Representative of n=10, scale bar, 20 μm. *$p<0.05$.

with PMA or ionomycin for 3.5 hours. The percentage of cells becoming hypercitrullinated at histone H3 was similar (Figure 1A), indicating the PAD4 is functional in these cells and that NE is not required for its nuclear transloation or activity. NET release is thought to be impaired in the $NE^{-/-}$ mice as shown by electron microscopy of *Klebsiella pneumonia* infected lungs. Although we also did find that $NE^{-/-}$ neutrophils formed less NETs at the same time point as WT mice, this reduction was only slight and a substantial portion of $NE^{-/-}$ neutrophils still released NETs (Figure 1B). This can be seen in the representative images in Figure 1C which show staining for H3Cit+ NETs in response to ionomycin as indicated by white arrows.

$NE^{-/-}$ mice form NET-rich thrombi in the IVC stenosis model

Venous thrombosis in the IVC stenosis model is highly NET dependent[7-9]. DVT is therefore an interesting setting in which to study the role of NE in NETosis and thrombosis. NET formation should be slightly reduced in the $NE^{-/-}$ animals and any NETs being released would be devoid of neutrophil elastase. NE can cleave tissue factor pathway inhibitor[10] and therefore NETs were proposed to enhance coagulation[11]. We hypothesized that thrombus size would be reduced in $NE^{-/-}$ mice since they form less NETs and release no NE. Thrombus initiation was unaffected in $NE^{-/-}$ compared to WT mice 6 h after partial IVC ligation (Figure 2A, 2B), but circulating plasma cell-free DNA levels were reduced by about 20%

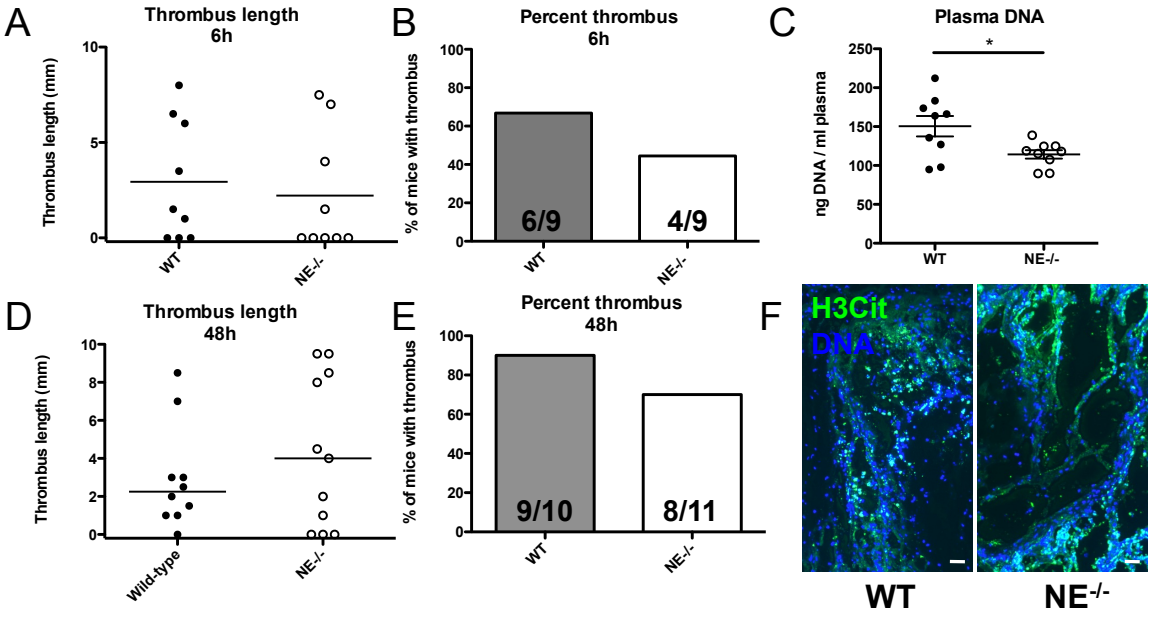

Figure 2. NE$^{-/-}$ mice form NET-containing thrombi in the venous stenosis model of DVT. A,B. NE$^{-/-}$ mice formed thrombi to a similar extent to WT mice after 6 h of IVC stenosis. C. Plasma DNA is slightly decreased after 6 h in NE$^{-/-}$ mice compared to WT mice. D,E. At 48 h, NE$^{-/-}$ mice also presented with thrombi to a similar extent to WT mice. F. Both thrombi collected from WT or NE$^{-/-}$ mice 48 h after IVC stenosis showed an abundance of NETs as seen by H3Cit immunostaining (green) and extensive diffuse extracellular DNA staining (blue). Scale bar, 25 μm. *p<0.05.

(Figure 2C), indicating that fewer NETs are being released in the $NE^{-/-}$ mice. By 48 h, thrombus frequency was again similar between WT and $NE^{-/-}$ mice (Figure 2D, 2E), and $NE^{-/-}$ mice were capable of forming thrombi that were quite large in size (Figure 2D), indicating that they don't have a major thrombotic defect and that the thrombi were stable. Thrombi from both the WT and $NE^{-/-}$ mice had a characteristic NET meshwork[1,9] within thrombi at 48 h, as seen by extracellular H3Cit staining (Figure 2F). These results greatly differ from the phenotype seen in $PAD4^{-/-}$ mice[9] or from mice treated with DNase[1,8] in the same model. In IVC stenosis, $PAD4^{-/-}$ are highly protected from thrombus initiation and the few thrombi that do form are absent of NETs[9]. Also, DNase 1, which cleaves NETs[4] significantly reduces the incidence of thrombosis[1,8].

$NE^{-/-}$ mouse wounds contain NETs and don't have accelerated wound healing

We have observed that a lack of NETosis in $PAD4^{-/-}$ mice facilitates wound healing and similar results were observed in mice treated with DNase 1 (Wong and Wagner, unpublished observation in Appendix 6). We next investigated the ability of $NE^{-/-}$ mice to produce NETs outside of the vasculature. Full thickness skin wounds were performed on mice using a skin biopsy tool and were allowed to heal over the course of 2 weeks. Similar quantities of H3Cit were detected in wound beds by Western blot in WT and $NE^{-/-}$ mice (Figure 3A), and this was not due to any differences in neutrophil infiltration as seen by analysis of Ly6G, a

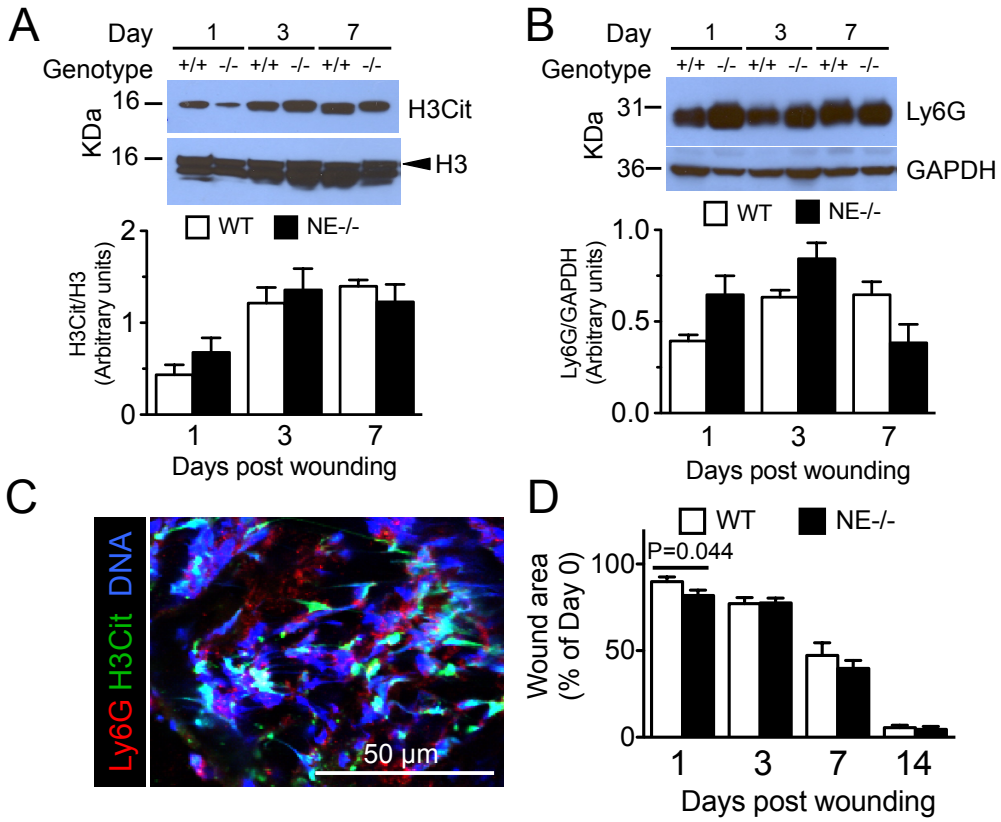

Figure 3. NETs are present in wounds of NE$^{-/-}$ mice and NE-deficiency does not offer long-term wound healing benefits. Western blots show that levels of (A) H3Cit and (B) Ly6G were similar between wild-type (WT, +/+) and NE$^{-/-}$ mice ($^{-/-}$) throughout days 1-7 after wounding. Mann-Whitney test; n=3-6. (C) Representative confocal microscopy image showing extracellular DNA (blue) positive for H3Cit (green) in Ly6G-rich areas (red) in the scab of a 3-day wound from the NE$^{-/-}$ mice. (D) Wound area reduction was faster in NE$^{-/-}$ mice only on day 1 after wounding. Their wound healing, however, became similar to that of the WT mice after 3 days. Mann-Whitney test. n= 3-25.

specific membrane marker of neutrophils, by Western blot (Figure 3B). By confocal microscopy we were able to identify NETting neutrophils with H3Cit-positive staining colocalizing with DNA within the wound scab (Figure 3C), similarly to what we see in WT mice (Appendix A-6). Lastly, we analyzed the rate of wound closure in these mice and found that while at day 1 post-wounding the $NE^{-/-}$ mice have slightly decreased wound area, perhaps due to a small reduction in NETosis. However, this difference did not persist as the rate of wound closure was later similar between the WT and $NE^{-/-}$ mice (Figure 3D). By contrast, $PAD4^{-/-}$ mice, which never generate NETs in the wound bed, show significantly accelerated wound healing rates with significantly smaller wound areas throughout the entire time course of wound closure (Appendix A-6).

Taken together, these results show that slightly reduced NET formation has little beneficial impact in vivo in non-infectious mouse models where NETs have been shown to have pathological consequences. This is in agreement with our observation that mice heterozygous for PAD4 showed no significant protection in DVT (unpublished result, Martinod and Wagner 2012). We had hypothesized that $NE^{-/-}$ mice would phenocopy $PAD4^{-/-}$ mice, which are completely unable to form NETs due to a lack of a histone-modifying enzyme required for chromatin decondensation[9,12]. While we did see less NET release in the $NE^{-/-}$ mice, this reduction was minor and not observed under stimulation with PMA. From our results, it would appear that NE inhibitors have additional activities besides inhibiting NE, as we could not reproduce their effect in the mouse genetically lacking NE. There may also be differences in the molecular

mechanisms driving NETosis in mouse vs. human neutrophils, and mouse neutrophils are may be more dependent on PAD4 than NE.

Our results have important implications for designing therapeutics targeting prevention of NET formation. We have proposed that PAD4 would be an attractive candidate for this goal, but to date highly specific and effective PAD4 inhibitors remain to be generated. Targeting NE could be beneficial in more aspects than just reducing NET formation, as protective effects have been seen using specific NE inhibitors in mouse models[13]. NE inhibition is unlikely to have major NET inhibition effects in vivo, and even partial NET release may be sufficient to drive venous thrombus formation, as neutrophils can adhere to the vessel wall, throw NETs, bind platelets and in turn initiate thrombus development[8,14]. Furthermore, when more neutrophils are recruited to inflamed and NETs accumulate, the effect of partial NET inhibition is likely to be insignificant over time. $NE^{-/-}$ mice should not be used as a method to study mouse models addressing the role of NETs. However, studying the effect of the lack of NE on NETs themselves in various disease settings remains an interesting approach and should be explored.

Materials and Methods

Mice

Experimental procedures in this study were reviewed and approved by the Institutional Animal Care and Use Committee of the Immune Disease Institute

and Boston Children's Hospital (Protocol No. 11-03-1919, 11-04-1848, 14-02-2609R, 14-03-2631R). C57Bl/6J (WT) and Elane^{tm1Sds}/J (NE$^{-/-}$) mice were purchased from The Jackson Laboratory.

In vitro NET assays

Peripheral blood was collected via the retroorbital venous plexus and neutrophils were isolated from 6-18 week-old male or female WT or NE$^{-/-}$ mice as previously described [15]. Cells were routinely assessed to be >90% pure by Wright-Giemsa stain. Neutrophils in RPMI/HEPES were incubated at 37°C in 5% CO_2 in glass-bottom plates for 20 min prior to stimulation with 100 nM phorbol 12-myristate 13-acetate (PMA, Sigma) or 4 μM ionomycin (iono, Invitrogen). After 3.5 h, cells were fixed in 2% PFA and analyzed as previously described[9].

Venous stenosis model

Venous stenosis experiments were performed as previously described under aseptic conditions[7,9], with 90% ligation of the inferior vena cava and complete ligation of side branches to minimize variation between mice. Blood was collected 6 h or 48 h after stenosis via the retroorbital sinus plexus, and thrombi harvested, measured and embedded in OCT for cryosectioning and histological analysis. All mice were given buprenorphine (0.1 mg/kg, s.c.) as an analgesic immediately before beginning surgery and every 8-12 h subsequently.

Blood cell and plasma analysis

Whole blood was collected via the retroorbital sinus into EDTA-coated capillary tubes. Twenty-five µl of whole blood collected via the retroorbital sinus plexus into EDTA-coated capillary tubes was analyzed by a Hemavet 950FS (Drew Scientific) for complete blood counts. At the time of sacrifice in DVT experiments, at least 250 µl of citrated whole blood was centrifuged to prepare platelet-poor plasma as previously described[9]. Plasma DNA concentrations were measured according to manufacturer's instructions using the Quant-iT^{TM} PicoGreen® dsDNA Assay kit (Invitrogen).

Immunostaining and fluorescence microscopy

Fixed cells or tissue sections were immunostained as described[9]. Fluorescent images were acquired using an Axiovert 200 widefield fluorescence microscope (Zeiss). All channels were acquired in greyscale with an Axiocam MRm monochromatic CCD camera (Zeiss), pseudocolored using Zeiss Axiovision software, and analyzed using ImageJ software (National Institutes of Health, Bethesda, MD, USA).

Wounding and wound area assessment

Full-thickness excisional wounding was performed on 9-10 week-old wild-type and NE$^{-/-}$ mice aseptically as described[16]. Mice were anesthetized by intraperitoneal injection of ketamine and xylazine (100 mg/kg and 10 mg/kg, respectively). Hair of the dorsal skin was removed and cleaned with 70% ethanol and betadine. Using two 4-mm disposable sterile biopsy punches (Miltex), 4

wounds were made by punching twice through the dorsal skin folded at midline. Mice were then housed individually. Area of wounds were determined using ImageJ from digital photographs taken with a Sony Camcorder on days 1, 3 and 7 post wounding, and expressed as percentages with respective to the area on day 0.

Western blot

H3Cit and Ly6G levels in the wounds were quantified with Western blotting. Wounds were snap frozen, homogenized on ice in protease inhibitor cocktail-supplemented (Sigma) RIPA buffer, and centrifuged at 20000 g for 20 min at 4^{o}C. Supernatant was collected and protein content was determined by bicinchoninic acid assay. Samples were resolved on gradient gels (4-20%, Lonza) and electroblotted on PVDF membranes, which were then incubated with primary antibodies (rabbit polyclonal anti-H3Cit, 1:1000, abcam; rabbit polyclonal anti-H3, 1:6000, abcam; rat monoclonal anti-mouse Ly6G, 1:500, BD Pharmingen) at 4^{o}C overnight. After several washes, the blots were incubated with the appropriate HRP-conjugated secondary antibodies for 2 hours at room temperature. The blots were developed with enhanced chemiluminescence substrate on film, and quantified with ImageJ. GAPDH (1:40000, Ambion) was probed to confirm equal loading.

Confocal immunofluorescence microscopy

Presence of NETs was examined by confocal microscopy. Wounds were cut into halves and immediately embedded in OCT following tissue collection. They were then cryosectioned into 20 μm sections, post-fixed in zinc fixative (100 mM Tris-HCl, 37 mM zinc chloride, 23 mM zinc acetate, 3.2 mM calcium acetate), permeabilized and incubated with primary antibodies against H3Cit (1:1000) and Ly6G (1:500) at 4^{o}C overnight. After several washes, the sections were incubated with Alexa Fluor-conjugated secondary antibodies (1:1500, Invitrogen) for 2 hours at room temperature. DNA was stained with Hoechst 33342. Images were captured with Olympus Fluoview software using an Olympus IX 81 confocal microscope.

Statistics

Data are presented as means ± SEM unless otherwise noted and were analyzed using a two-sided Student's t-test or Mann-Whitney U test. Thrombus frequencies were analyzed using chi-squared tests of contingency tables. All analyses were performed using GraphPad Prism software (Version 5.0). Results were considered significant at $p<0.05$. * $p<0.05$, ** $p<0.01$, ***$p<0.001$.

Acknowledgments

We thank Melanie Demers for helpful discussions. This work was supported by the National Heart, Lung, and Blood Institute of the National Institutes of Health grants R01HL095091 to D.D.W. and a GlaxoSmithKline/Immune Disease Institute Research Alliance Fellowship to S.L.W.

Authorship contributions

K.M. and S.L.W. designed and performed experiments, analyzed data, and wrote the paper. M.G. provided expert technical assistance. D.D.W. supervised the study, designed experiments, analyzed data, and wrote the paper.

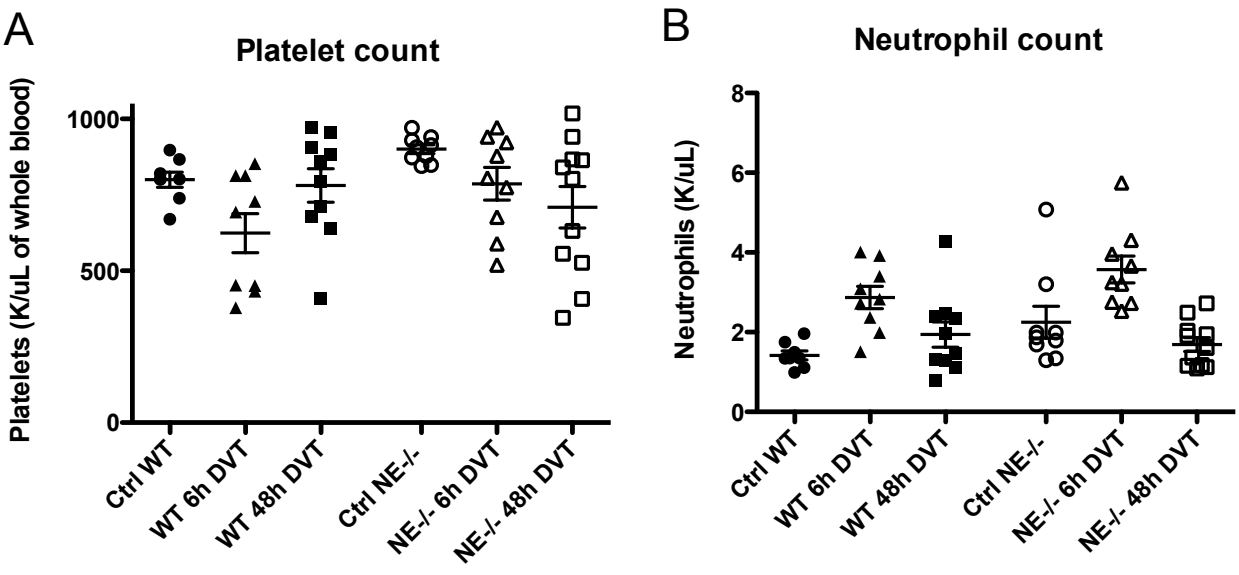

Figure S1. WT and NE-deficient mice have similar changes in platelet and neutrophil counts after IVC stenosis. A. Platelet counts dropped compared to control mice in both WT and $NE^{-/-}$ groups at 6 h. At 48 h, $NE^{-/-}$ mice remain thrombocytopenic. B. Neutrophil counts become similarly elevated 6 h after stenosis in both genotypes, and return to near normal levels by 48 h.

Appendix A-7: Bibliography

1. Brill A, Fuchs TA, Savchenko AS, et al. Neutrophil extracellular traps promote deep vein thrombosis in mice. *J Thromb Haemost*. 2012;10(1):136-144.

2. Papayannopoulos V, Metzler KD, Hakkim A, Zychlinsky A. Neutrophil elastase and myeloperoxidase regulate the formation of neutrophil extracellular traps. *J Cell Biol*. 2010;191(3):677-691.

3. Belaaouaj A, McCarthy R, Baumann M, et al. Mice lacking neutrophil elastase reveal impaired host defense against gram negative bacterial sepsis. *Nat Med*. 1998;4(5):615-618.

4. Brinkmann V, Reichard U, Goosmann C, et al. Neutrophil extracellular traps kill bacteria. *Science*. 2004;303(5663):1532-1535.

5. Urban CF, Ermert D, Schmid M, et al. Neutrophil extracellular traps contain calprotectin, a cytosolic protein complex involved in host defense against Candida albicans. *PLoS Path*. 2009;5(10):e1000639.

6. Metzler KD, Goosmann C, Lubojemska A, Zychlinsky A, Papayannopoulos V. A Myeloperoxidase-Containing Complex Regulates Neutrophil Elastase Release and Actin Dynamics during NETosis. *Cell Rep*. 2014.

7. Brill A, Fuchs TA, Chauhan AK, et al. von Willebrand factor-mediated platelet adhesion is critical for deep vein thrombosis in mouse models. *Blood*. 2011;117(4):1400-1407.

8. von Bruhl ML, Stark K, Steinhart A, et al. Monocytes, neutrophils, and platelets cooperate to initiate and propagate venous thrombosis in mice in vivo. *J Exp Med*. 2012;209(4):819-835.

9. Martinod K, Demers M, Fuchs TA, et al. Neutrophil histone modification by peptidylarginine deiminase 4 is critical for deep vein thrombosis in mice. *Proc Natl Acad Sci U S A*. 2013;110(21):8674-8679.

10. Higuchi DA, Wun TC, Likert KM, Broze GJ, Jr. The effect of leukocyte elastase on tissue factor pathway inhibitor. *Blood*. 1992;79(7):1712-1719.

11. Massberg S, Grahl L, von Bruehl ML, et al. Reciprocal coupling of coagulation and innate immunity via neutrophil serine proteases. *Nat Med*. 2010;16(8):887-896.

12. Li P, Li M, Lindberg MR, Kennett MJ, Xiong N, Wang Y. PAD4 is essential for antibacterial innate immunity mediated by neutrophil extracellular traps. *J Exp Med*. 2010;207(9):1853-1862.

13. Cools-Lartigue J, Spicer J, McDonald B, et al. Neutrophil extracellular traps sequester circulating tumor cells and promote metastasis. *J Clin Invest*. 2013.

14. Fuchs TA, Brill A, Duerschmied D, et al. Extracellular DNA traps promote thrombosis. *Proc Natl Acad Sci U S A*. 2010;107(36):15880-15885.

15. Demers M, Krause DS, Schatzberg D, et al. Cancers predispose neutrophils to release extracellular DNA traps that contribute to cancer-associated thrombosis. *Proc Natl Acad Sci U S A*. 2012;109(32):13076-13081.

16. Subramaniam M, Saffaripour S, Van De Water L, et al. Role of endothelial selectins in wound repair. *Am J Pathol*. 1997;150(5):1701-1709.